Understanding the physiological and molecular aspects of charcoal rot resistance mechanisms in sorghum and soybean

by

Afsana Noor

B.S., Bangladesh Agricultural University, 2009
M.S., North Dakota State University, 2014

AN ABSTRACT OF A DISSERTATION

submitted in partial fulfillment of the requirements for the degree

DOCTOR OF PHILOSOPHY

Department of Plant Pathology
College of Agriculture

KANSAS STATE UNIVERSITY
Manhattan, Kansas

2022

Abstract

Charcoal rot (CR) of soybean (*Glycine max* (L.) Merr.) and sorghum (*Sorghum bicolor* (L.) Moench) is caused by the hemibiotrophic soilborne fungus *Macrophomina phaseolina* (MP) and is an important pathogen in the midwestern United States. Complex molecular mechanisms underlie the interaction of MP with these two hosts, which impedes resistance breeding. To select for charcoal rot resistance, a thorough understanding of the host's physiological and molecular responses to MP along with screening of genotypes with resistance to CR is essential.

To understand MP induced host's physiological and molecular responses, first we investigated MP-induced oxidative stress-mediated senescence by using the reactive oxygen species (ROS) scavenger ascorbic acid in soybean seedlings. Three soybean isolates of MP were tested for their sensitivity to ascorbic acid using an in-vitro assay. An in-planta soybean cut-stem assay was used for the exogenous application of ascorbic acid (oxidized and reduced form) following inoculation with MP. A ROS (H_2O_2) quantification assay was used to validate H_2O_2 induced by MP and ascorbic acid pre-treatment. All three MP isolates were sensitive to ascorbic acid concentrations of ≥ 15 mM. Ascorbic acid (10mM) pre-treatment following MP inoculation reduced CR lesion length compared to inoculated treatment. MP induced a significantly higher H_2O_2 than ascorbic acid pre-treated inoculated plant. Second, through comparative transcriptomics, MP-resistant and susceptible soybean genotypes revealed contrasted responses to MP-induced senescence. Gene Ontology and pathway analysis showed MP-induced receptor kinase like genes in both genotypes while down-regulated defense related antioxidant, hormonal, and other metabolic pathways in both genotypes. Ascorbic acid pre-treatment induced a more significant number of photosynthesis genes in both genotypes. Hydrogen peroxide pre-treatment following inoculation showed up-regulation of oxidative stress responsive pathways while down-regulated photosynthesis and hormonal signal transduction pathways. Third, the NAM phenotyping for CR resistance results of location- and year-wise data showed strong genotype by environment interactions. Overall, using MP screening, charcoal rot resistance phenotyping in the NAM parental lines revealed the genotype SC1103 as the most resistant line and Segaolane and Macia as the most susceptible. The SC1103 NAM family-derived population can be used for charcoal rot resistance in association studies to map charcoal rot resistance.

Understanding the physiological and molecular aspects of charcoal rot resistance mechanisms in sorghum and soybean

by

Afsana Noor

B.S., Bangladesh Agricultural University, 2009
M.S., North Dakota State University, 2014

A DISSERTATION

submitted in partial fulfillment of the requirements for the degree

DOCTOR OF PHILOSOPHY

Department of Plant Pathology
College of Agriculture

KANSAS STATE UNIVERSITY
Manhattan, Kansas

2022

Approved by:

Major Professor
Dr. Christopher R. Little

Copyright

Abstract

Charcoal rot (CR) of soybean (*Glycine max* (L.) Merr.) and sorghum (*Sorghum bicolor* (L.) Moench) is caused by the hemibiotrophic soilborne fungus *Macrophomina phaseolina* (MP) and is an important pathogen in the midwestern United States. Complex molecular mechanisms underlie the interaction of MP with these two hosts, which impedes resistance breeding. To select for charcoal rot resistance, a thorough understanding of the host's physiological and molecular responses to MP along with screening of genotypes with resistance to CR is essential.

To understand MP induced host's physiological and molecular responses, first we investigated MP-induced oxidative stress-mediated senescence by using the reactive oxygen species (ROS) scavenger ascorbic acid in soybean seedlings. Three soybean isolates of MP were tested for their sensitivity to ascorbic acid using an in-vitro assay. An in-planta soybean cut-stem assay was used for the exogenous application of ascorbic acid (oxidized and reduced form) following inoculation with MP. A ROS (H_2O_2) quantification assay was used to validate H_2O_2 induced by MP and ascorbic acid pre-treatment. All three MP isolates were sensitive to ascorbic acid concentrations of ≥ 15 mM. Ascorbic acid (10mM) pre-treatment following MP inoculation reduced CR lesion length compared to inoculated treatment. MP induced a significantly higher H_2O_2 than ascorbic acid pre-treated inoculated plant. Second, through comparative transcriptomics, MP-resistant and susceptible soybean genotypes revealed contrasted responses to MP-induced senescence. Gene Ontology and pathway analysis showed MP-induced receptor kinase like genes in both genotypes while down-regulated defense related antioxidant, hormonal, and other metabolic pathways in both genotypes. Ascorbic acid pre-treatment induced a more significant number of photosynthesis genes in both genotypes. Hydrogen peroxide pre-treatment following inoculation showed up-regulation of oxidative stress responsive pathways while down-regulated photosynthesis and hormonal signal transduction pathways. Third, the NAM phenotyping for CR resistance results of location- and year-wise data showed strong genotype by environment interactions. Overall, using MP screening, charcoal rot resistance phenotyping in the NAM parental lines revealed the genotype SC1103 as the most resistant line and Segaolane and Macia as the most susceptible. The SC1103 NAM family-derived population can be used for charcoal rot resistance in association studies to map charcoal rot resistance.

Table of Contents

List of Figures

List of Tables

Acknowledgements

The Ph.D. is a long journey, like climbing an enormous mountain. For this challenge, one of the significant ingredients is having a knowledgeable, supportive supervisor. I am very fortunate to have had Dr. Christopher R. Little as my Ph.D. mentor. I found Dr. Little not only deep in the discipline but he also allowed me to experiment, learn from mistakes, and guided me relentlessly, and helped me think critically. I am very thankful to Dr. Little for his patience, motivation, and trust in me throughout my Ph.D. journey in the Department of Plant Pathology at Kansas State University. His vast knowledge of mycology, excellent supervision, meticulous editing, constructive suggestions, and encouragement enriched my knowledge and vision of scientific study and research. I feel proud to have had such a great mentor in my Ph.D. studies, whose positivity augmented my vision and mission for scientific endeavors.

I am very grateful to my committee, Dr. Sanzhen Liu, for his technical support, particularly for the RNA-seq analysis. His assistance was instrumental for that chapter. I learned considerably from his Bioinformatics Applications course, which paved the way for my programming background and built my interest and enthusiasm for bioinformatics. I am thankful to Dr. David Cook for his invaluable suggestions, guidance, and insights into my research. I would like to acknowledge Dr. Cook for offering the Molecular Plant-Microbe Interactions (MPMI) course, where I learned different aspects of MPMI that I wish to investigate more during my scientific career. I am also very grateful to Dr. Tesfaye Tesso for serving on my committee and for allowing me to conduct NAM phenotyping experiments in his research plots. I greatly acknowledge all the support and assistance during the field trials from Dr. Tesso's lab. I acknowledge Dr. Sunghun Park for serving as my outside chairperson and for his time and devotion.

Thanks to the Row Crops Pathology Lab (RCPL), especially lab manager Natalie Waite, whose help and organization provided technical support throughout the research. Also, I appreciate my lab mate Nathan Smith's help and assistance during the NAM phenotyping project. Thanks go to previous undergraduate students in the RCPL, especially Cori Ondrashek, Daphne Lofing, and Casinda Smith, for their research assistance.

I thank the Faculty, graduate students, and staff of the Department of Plant Pathology for their encouragement, scholastic guidance, friendship, and support throughout my studies at Kansas

State University. I would like to especially acknowledge my friend, Dr. Guifang Lin, for her incredible help and assistance with my RNA-seq data analysis.

My husband, Dr. Md. Abdullah Al Bari was beside me with his constant love, support, and inspiration throughout my studies. I am thankful to the math genius, Asnud Shah, my 3rd grade son for his understanding, sacrifices, and acceptance of my hectic schedule allowing me time to devote to research and study. I am grateful to the Almighty for gifting this precious prize in our lives. I am ever grateful to my Mother and Father for their tremendous support, advice, prayers, and counseling throughout my life. I am grateful to my brothers Md. Toslim Arif and Toufiq Anam, for their continuous encouragement for my higher study. I greatly acknowledge my Father-in-law's encouragement for my higher study and my Mother-in-law's prayers, motivation, and counseling when times were rough.

Thanks to the Kansas Grain Sorghum Commission, Kansas Soybean Commission, United Soybean Board, and Kansas Academy of Science for funding the research.

Dedication

I am dedicating this dissertation to my beloved parents- Mother and Father. My mother Tahamina Khatun, in particular for her moral and spiritual support during the entire Ph.D. journey. She is very positive towards life and always encourages me to keep going until reaching my goals.

I am dedicating this piece of work to my husband, who always inspires to be optimistic and face challenges. I often remember his quote, “if you do not face challenges, how can you overcome them to reach the next level.”

This dissertation is also dedicated to my math genius son Asnud Shah, who was with me from the beginning of my journey and bravely faced odd days and helped me conquer obstacles on the way.

Chapter 1 - Literature Review

Sorghum: Origin, distribution, and history of development

Sorghum (*Sorghum bicolor* (L.) Moench) is a C_4 cereal crop that belongs to the grass family Poaceae (Gramineae). According to anthropological evidence, sorghum was introduced by "hunter-gatherer" cultures around 8000 BC (Smith and Fredericksen, 2000). The domestication of sorghum occurred around 4000 BC in the eastern Sudanese savannah following its introduction to nearly 100 countries of diverse agroclimatic zones (Venkateswaran et al., 2019). Taxonomically and genetically resembling corn (*Zea may*s L.), sorghum belongs to the Andropogoneae subfamily. It is a diploid plant with chromosome number 2n = 20 (Huskins and Smith, 1932). Sorghum has a relatively small genome of 730 Mbp (Paterson et al., 2009). It is considered the fifth most important cereal crop as a human food and animal feed for the world's arid subtropical and tropical regions.

Sorghum has twenty-two variable species, of which only one *Sorghum bicolor* is attributed to widely cultivated sorghums, while the rest are wild or weedy types. Five interfertile races (*bicolor*, *kafir*, *caudatum*, *durra*, and *guinea*) and ten other intermediate races have been classified among all cultivated sorghums according to their floral morphology (Venkateswaran et al., 2019).

Sorghum is considered a climate-resilient crop due to its high photosynthetic ability, water use efficiency, and diverse adaptation capability in the hot and dry agro-ecological zones where adaptation of other domesticated crops is difficult. To the most food-insecure people in the semi-arid tropics (SAT) of Africa and Asia, sorghum is used as a staple food (Reddy and Reddy, 2019). Although in Africa it is mainly cultivated as a food crop, in west Africa its fodder is used for thatching, while in east Africa it is also grown as animal feed. In the United States, sorghum is mainly grown for animal feed and fodder purposes. The United States is the world's prime exporter of grain sorghum, with a 70% trade share. The total sorghum planted in the USA in 2021 was 7,340,000 acres, producing 471,125,000 bushels (USDA-NASS). There are fourteen sorghum-producing states in the USA, where Kansas, Nebraska, Missouri, Oklahoma, Texas, and New Mexico are the top producers. Kansas ranks number one among these states, with nearly 40% of U.S. grain sorghum production (Reddi and Reddi, 2019).

As a climate-smart crop, sorghum has excellent potential to be disseminated into harsher climates and can thrive under changing environmental conditions due to global warming. Not only could it perform well in resource-limited environments, but productivity increases in average and ideal environments (Rooney, 2014; Chadalavada et al., 2021). Also, along with its use as grain sorghum, food, fodder, and syrup, it is accepted as a bioenergy crop. With increased attention to sustainable bioenergy, sorghum could play a role as a model crop for bioenergy production as sorghum is already a well-accepted and established crop in the USA and other parts of the world (Rooney, 2014). Also, the genetic improvement of sorghum is indispensable as an established seed industry and a wide range of breeding techniques are available for crop improvement.

Abiotic and biotic stresses are the major constraints for all domesticated crops. As a climate-resilient crop, sorghum has been found to perform well under the most common abiotic stressors such as high temperature, drought, or water limitation (Taylor, 2019; Rooney, 2014). However, biotic constraints such as pests and diseases take advantage of abiotic stress conditions as the crop needs to spend more energy to adapt to a changing environment. There are some prevalent sorghum diseases of economic importance, of which anthracnose (*Colletotrichum graminicola*), Fusarium stalk rot (*Fusarium* spp.), charcoal rot (*Macrophomina phaseolina*), downy mildew (*Peronosclerospora sorghi*) (Tesso et al., 2012), and viral diseases due to potyviruses, e.g., Maize Dwarf Mosaic Virus (Toler, 1985), Johnsongrass Mosaic Virus, and Sugarcane Mosaic Virus (Tosic et al., 1990), are among the most important.

Soybean: Origin, distribution, and history of development

Soybean (*Glycine max* (L.) Merrill) belongs to the Fabaceae family, subfamily Papilionoidea, and tribe Phaseoleae. As a leguminous crop and considering the higher protein content, soybean is economically most important like other members of Phaseoleae (Hymowitz, 2008) for its value as an oilseed crop, food for humans, and feed for livestock. The word “soy” originated from the Japanese word “shoyu” and was published in the Japanese dictionary in 1957 (Shurtleff and Aoyagi, 1983; Hymowitz, 2008). However, the taxonomic history of the genus *Glycine* is confusing, and Linnaeus first described it in 1753. ln 1971, Merrill proposed the current scientific name *G. max* (Hymowitz, 2008). Soybean originated in Southeast Asia (Singh and Hymowitz, 1999; Singh

et al., 2001) and was first domesticated in the eastern half of northern China and later disseminated to other parts of Asia (Hymowitz, 2008).

Soybean domestication history suggests it was derived from the wild relative *Glycine soja* Sieb. & Zucc around 5000 years ago in China (Wang et al., 2016). Wang et al. (2016) constructed 355,595 SNPs and studied the genetic variation pattern of 105 wild ancestors and 265 cultivated soybeans. The population genetics analysis from this study revealed the origin of soybean from the Northern part of China and reported its dissemination to other parts of Asia with gradual increases in seed weight. Significant phenotypic transformations of soybean have been observed since domestication to local adaptation. For example, wild soybeans are prostrate plants with tiny black seeds, while modern cultivated soybeans are upright plants with improved seed weight and diverse seed coat colors (Li et al., 2013; Wang et al., 2016). In addition, modern plant breeding improved the cultivated soybean through selection for better cultivar development that could more precisely satisfy consumers' needs (Li et al., 2013; Wang et al., 2016).

Historical evidence suggests that soybeans were introduced to North America between 1767-1770 (Hymowitz, 2008). The United States produces ~33% of the world's soybeans and, in 2020, produced 4.14 billion bu, which was 16% higher than in 2019 (USDA-NASS). Soybean is a diploid species with chromosome number 2n = 40 and has a large genome (1.15 GB). Until 2010, the soybean whole-genome shotgun sequence was the largest among all sequenced plant genomes compared to all other high-quality drafts of whole shotgun-sequenced plant genomes (Schmutz et al., 2010). The availability of the soybean whole genome sequence advanced modern soybean genetic improvement research through developing genomic analysis that links phenotypic variation related to genetic variation. The advent of high-throughput sequencing technologies like next-generation sequencing (Davey et al., 2012) and DNA microarrays (Gupta et al., 2008), advanced genomic information gathering, and eased genetic improvement research (Wang et al., 2016).

Significance of charcoal rot disease in soybean

Charcoal rot was first observed in soybean in 1949 (Young, 1949) and then spread to all soybean growing areas of the USA. As a result, charcoal rot is the number one root rot-causing disease of soybean, and soybean is ranked as the most susceptible host of *M. phaseolina* among all its host crops (Wrather et al., 2010; Bressano et al., 2010; Deshmukh and Tiwari, 2021).

Eventually charcoal rot became one of the U.S.'s most economically important soybean diseases due to significant yield losses from Kansas and other southern US States (Luna et al., 2016). Charcoal rot has been considered one of the most important soybean diseases in the U.S. over the past 20 years, and disease incidence has increased over the last 30 years in the northern US States (Luna et al., 2016). In 2003 and 2012, the disease was named the second most important soybean disease, with yield losses of nearly 1.5 and 2.0 million metric tons, respectively (Wrather et al., 2010; Allen et al., 2017), and it was ranked among the top three soybean diseases of economic importance from a recent report of 28 soybean producing states in the United States (Bandara et al., 2020).

Charcoal rot of soybean and sorghum: Pathogen invasion, disease progression, molecular mechanisms of infection, and impact on crop quality

Charcoal rot is one of the top-ranked production problems in the soybean and sorghum growing regions of the USA, especially for soybean. CR ranked within the top three soybean diseases of economic importance from 1996 to 2016 (Bandara et al., 2020). *M. phaseolina* is an agronomically important pathogen of several crops in the USA, such as sorghum (*Sorghum bicolor* (L.) Moench), corn (*Zea mays* L.), soybean (*Glycine max* (L.) Merrill), and cotton (*Gossypium hirsutum* L.) (Su et al., 2000).

Charcoal rot of sorghum and soybean is one of the major fungal diseases of both commodities that cause economic losses under disease-conducive environmental conditions. Charcoal rot of sorghum is caused by the fungus *Macrophomina phaseolina* (Tassi) Goid. Charcoal rot is more prevalent when plants are stressed due to prolonged drought during the post-flowering grain-filling stages (Edmunds, 1964). Another sorghum stalk rot is caused by *Fusarium* spp., and the severity of this stalk rot manifests in the drought-stressed plant at grain filling if the crop was exposed to a wet and cool environment during physiological maturity (Zummo, 1980). Among these two stalk rot pathogens, *M. phaseolina* is more aggressive in causing infection as it exhibits larger lesions than those caused by *Fusarium* spp. (*F. proliferatum*, *F. thapsinum*, and *F. andiyazi*) when four drought-tolerant stalk rot-resistant parental lines and their inbred lines were inoculated with both fungi (Tesso et al., 2005).

A host specialization experiment from *M. phaseolina* infested root tissue and soil in a 15-year continuous cropping experiment including soybean, sorghum, corn, and cotton showed that only corn isolates were host-specific. In contract, other isolates didn't exhibit any host specificity (Su et al., 2000). In addition, genetic differentiation among the isolates of these hosts using restriction fragment length polymorphisms (RFLP) and random amplified polymorphic DNA (RAPD) revealed *M. phaseolina* as a single species since no differences were observed in the DNA restriction pattern after polymerase chain reaction (PCR) (Su et al., 2000). However, recently utilizing the multilocus phylogenetic analysis, two more species of *Macrophomina* were described as *M. pseudophaseolina* (Sarr et al., 2014) from Senegal and *M. euphorbiicola* from Brazil (Machado et al., 2019).

The charcoal rot fungus *M. phaseolina* survives and perpetuates in the soil in and among infected crop debris as melanized structures called microsclerotia (Almeida et al., 2003; Pawlowski et al., 2015). Microsclerotia function as primary inoculum and can survive in the soil for extended periods (2 to 15 years) but lose viability with time (Cook et al., 1973; Reis et al., 2014; Deshmukh and Tiwari, 2021). Microsclerotia are melanized and hydrophobic, which protects them from plant secondary metabolite-mediated degradation (Short and Wyllie, 1978; Deshmukh and Tiwari, 2021). The pathogen can infect the host irrespective of the growth stages (Gangopadhyay et al., 1970), and hot and dry environmental conditions that induce pathogenic infection in the host can lead to premature wilting and death (Deshmukh and Tiwari, 2021). Viable microsclerotia can infect younger seedlings if soil moisture conditions exist (Meyer et al., 1974). Microsclerotia germinate within a temperature range of 28 to 35˚C (Mihail, 1989) or through mechanical injury (Deshmukh and Tiwari, 2021). Germinating mycelia from the fungus on the root surface initially grows on the epidermal cells and produce a fungal appressorium on the host tissue (Ammon et al., 1975).

To enter through the host's cellulosic barrier, *M. phaseolina* uses a lectin glycoprotein, a cellulose-binding elicitor that interacts with the host cell wall for infection and host plasma membrane-mediated defense avoidance (Bhowal et al., 2010; Islam et al., 2012). Like other fungi, *M. phaseolina* also secretes phytospihngosine and phytoceramide before host entry to protect from mechanical injury during host penetration (Del Poeta et al., 2014; Magnin-Robert et al., 2015). Phytosphingosine and phytoceramide are unknown for their role in pathogenicity. Still, they are

also involved in pathogen-mediated programmed cell death (PCD), the ROS burst, germination and proliferation of fungi, and alkaline tolerance (Del Poeta et al., 2014; Magnin-Robert et al., 2015).

Fungi produce cell wall degrading enzymes (CWDE) to penetrate through the host cell wall (Gupta et al., 2012; Kaur et al., 2012). Further, *M. phaseolina* induces host susceptibility by stimulating the production of host cell wall degrading enzymes (CWDE) (Bandara et al., 2018). An RNA-Seq experiment from *M. phaseolina*-inoculated sorghum plants revealed the upregulation of CWDEs such as pectin methylesterase-, polygalacturonase-, cellulase-, endoglucanase-, and glycosyl hydrolase-encoded genes in the susceptible sorghum plant but not in the charcoal rot resistant sorghum plant (Bandara et al., 2018). Also, the functional validation assay following the RNA-seq experiment showed increased cellulose degrading enzyme activity in the *M. phaseolina* inoculated susceptible plants (Bandara et al., 2018).

A study by Abbas et al. (2019) predicted the role of the toxin (-)-botryodiplodin secretion *by M. phaseolina* in soybean root entry, and they showed that the majority of the *M. phaseolina* isolates (51.4%) produce (-)-botryodiplodin. Furthermore, most of the isolates caused charcoal rot disease in soybean, but not all, and some of the isolates produced an unknown toxin that is also related to pathogenicity. These results suggest no strong link between toxin secretion and pathogenicity in the *M. phaseolina*-soybean pathosystem.

The fungus then grows intercellularly and remains in an endophytic or latent state. The asymptomatic state of *M. phaseolina* invasion is believed to be a biotrophic phase of the fungus (Chowdhury et al., 2017). A histopathological assay using both *M. phaseolina*-resistant and -susceptible soybean cultivars revealed *M. phaseolina* remains in a biotrophic phase for nine days before switching to a necrotrophic phase (Hemmati et al., 2018). Islam et al. (2017) revealed *M. phaseolina* remain in an endophytic biotrophic phase, initially following a transition to biotrophy to necrotrophy switch (BNS) and a necrotrophic phase. The duration of these phases was dependent on the host's resistant or susceptibility status (Islam et al., 2017). Once the plants reach physiological maturity and are exposed to environmental stressors such as drought and high temperatures > 30˚C (Edmunds, 1964; Edmunds and Voigt, 1966, Odvody and Dunkle, 1979; Kaur et al., 2012)), *M. phaseolina* initiates heavy infestation by producing mycelia and microsclerotia in the

xylem and associated cells and clogs the vascular tissue of the plant that ultimately leads to wilting or stalk lodging (Kaur et al., 2012) and darkening of the collar region and root of soybean (Cummings and Bergstrom, 2013). During the BNS phase MP induce to kill the host, shortly becoming necrotroph (Chowdhury et al., 2017). However, for soybean plants, symptoms may appear in early growth stages as seedling blight, but late-stage wilting and premature senescence is more commonly observed (Mengistu et al., 2015). These transitions from an asymptomatic to a symptomatic state have been described as the biotrophy to necrotrophy switch (Islam et al., 2012).

Wilting or lodging impacts grain quality and yield. Some of the detrimental impacts of *M. phaseolina* on soybean production include high canopy temperatures and interference with stomatal gas exchange (Doubledee et al., 2012), an increase in linoleic acid content rendering poor seed quality (Bellaloui et al., 2008), and interfering with nitrogen fixation in susceptible soybean cultivars (Bellaloui et al., 2008). Bellaloui et al. (2021) also studied the impacts of charcoal rot on soybean seed composition from irrigated and non-irrigated conditions using resistant and susceptible soybean genotypes. Their study demonstrated that increased protein and oleic acid, along with decreased linolenic acid, resulted in a potential physiological mechanism of soybean to charcoal rot responses.

Bandara et al. (2017) studied the impacts of charcoal rot on the biofuel trait total soluble sugars (TSSP) from seven sweet sorghum parental lines and twelve hybrid genotypes using juice weight and sugar content (°Bx). Their study revealed that *M. phaseolina* and *Fusarium thapsinum* reduced TSSP by 22.2 to 33.3%, juice weight from 11.3 to 25.9%, and sugar content from 0.2 to 16.7 °Bx, which suggested the negative impacts of *M. phaseolina* pathogenesis on biofuel traits in sweet sorghum genotypes (Bandara et al., 2018). Bandara et al. (2018) also detected the adverse effect of charcoal rot on specific sugar attributes of sweet sorghum. They demonstrated that stalk rot induced decreased sucrose content in the sweet sorghum genotypes. Furthermore, the correlation analysis between sucrose and fructose content from this study suggested that stalk rot pathogenesis induced increased conversion from sucrose to fructose, thus negatively impacting sugar attributes in sweet sorghum (Bandara et al., 2018).

Host lipids have a significant role in plant-pathogen interactions. To detect the role of lipids in *M. phaseolina*-induced host susceptibility or resistance mechanisms from the sorghum, Bandara et al.

(2019) performed an RNA-seq and mass spectrometry assay (ESI-MS/MS) to analyze the transcriptome and lipidomes from *M. phaseolina*-inoculated resistant and susceptible sorghum genotypes. The results from this study showed *M. phaseolina* induced decreased phosphatidylserine, phytosterol, and ox-lipid content in the susceptible genotype. The transcriptome and lipidome study revealed susceptible genotype is adversely impacted by *M. phaseolina* invasion in terms of plastid and cell membrane integrity along with lipid-based signaling (Bandara et al., 2019). This study also showed enhanced oxidative stress induced by *M. phaseolina* in the susceptible genotype (Bandara et al., 2019). Bandara et al. (2017) also studied the impacts of stalk rot fungus *M. phaseolina* on the yield traits of sorghum. This study detected that growth stage (GS)-specific inoculation induced yield retardation in sorghum, where GS-1 (30 days after emergence) inoculation showed increased yield reduction compared to GS-3 (14 days after flowering) inoculation (Bandara et al., 2017).

Host-pathogen interaction biology of charcoal rot disease

Host-pathogen interaction mechanisms play an important role in understanding and deploying host resistance against the pathogen. Functional genomics studies have been conducted to investigate the interactions of *M. phaseolina* with several host cultivars through transcriptomics and proteomics (Marquez et al., 2021). Sharma et al. (2014) detected the overexpression of antifungal genes (chitinase, stilbene synthase) within the first hour of infection by *M. phaseolina* in sorghum cultivars. A similar result was observed in groundnut (*Arachis hypogea* L.) when inoculated with *M. phaseolina*. The result was enhanced expression of antifungal chitinase and β-1,3-glucanase genes (Iwuala et al., 2020).

The model plant *Medicago truncatula* has been used to study transcriptional changes induced by *M. phaseolina* (Gaige et al., 2010). Gene expression analysis using quantitative real-time PCR revealed strong upregulation of flavonoid and isoflavonoid biosynthetic pathway-related genes in the shoot but no activation of such genes in the root (Gaige et al., 2010). Also, this study did not reveal jasmonate (JA)- and ethylene (ET)-related genes upregulation in the *M. phaseolina* infected root (Gaige et al., 2010). However, treatment with methyl jasmonate and ethylene before inoculation induced partial resistance. Results from this study suggest a potential path of charcoal rot resistance activation through the modification of JA and ET pathways (Gaige et al., 2010). With

the recent advent of next-generation sequencing technology, the 50 Mb genome comprised of 15,000 genes from the jute isolate of *M. phaseolina* was sequenced. Analysis of this genome detected a redundancy of genes encoding for degradative enzymes gene for cellulose hydrolysis and lignin degradation (Islam et al., 2012).

Deshmukh and Tiwari (2021) described the roles of soybean plasma membrane-associated surface pattern recognition receptors (PRR), enzymatic degradation-related pathogen entry, host defense responses through kinase receptors, and other pathogenesis-related gene upregulation. These authors studied the soybean-*M. phaseolina* interaction using an RNA-seq gene expression assay to determine differential responses between a resistant and susceptible soybean genotype. Their experiment suggested that defense signaling genes, calcium, kinases, and pathogenesis-related genes were up-regulated in both genotypes, while leucine-rich repeat genes were differentially up-regulated only in the resistant genotype. This study also detected the up-regulation of WRKY genes contributing to the expression of phenylpropanoid pathway genes in the resistant genotype, which suggested a possible role of these genes in soybean charcoal rot resistance (Deshmukh and Tiwari, 2021). Radadiaya et al. (2021) studied a sesame-*Macrophomina phaseolina* transcriptome analysis using a resistant and susceptible genotype. Their study also revealed the up-regulation of transcription factors, including MYB, WRKY, leucine zipper protein, bHLH, bZIP, and NAC from the resistant genotype and predicted the role of these transcription factors along with metabolic (glutathione and secondary metabolites), biosynthetic (fatty acid), and phytohormonal (auxin, abscisic acid, ethylene, and gibberellic acid) pathways in host resistance against *M. phaseolina* (Radadiaya et al., 2021). A comparative transcriptome analysis by Yan et al. (2021) also revealed the co-activation of transcriptional and translational mechanisms in conferring resistance to *M. phaseolina* in sesame. Through weighted gene co-expression network analysis (WGCNA) of differentially expressed (DE) genes, they detected leucine-rich repeat receptor-like kinase (LRR-RLK) proteins as a source of sesame resistance to *M. phaseolina* (Yan et al., 2021). Along with LRR-RLKs, they detected pattern-triggered immunity (PTI), effector-triggered immunity (ETI), and hormonal signaling pathways (jasmonate/ethylene, JA/ET) and salicylic acid's role in contributing to resistance responses against *M. phaseolina* invasion in the sesame host (Yan et al., 2021).

Infection by *M. phaseolina* induces reactive oxygen species in the host, including hydrogen peroxide, superoxide, and hydroxyl radical in the host and excess ROS accumulation leads to oxidative stress-mediated host cell damage and death. Plants have cellular antioxidant machinery (superoxide dismutase, catalase, ascorbate peroxidase, and glutathione peroxidase) to overcome these oxidative stresses (Kumari et al., 2015). A study by Kumari et al. (2015) indicated that a charcoal rot tolerant sorghum cultivar, PJ-1430, induced enhanced malondialdehyde (a biomarker of oxidative stress) in the roots along with higher antioxidant activity and less oxidative damage. On the other hand, a susceptible cultivar SU-1080 resulted in enhanced oxidative damage due to lower antioxidant activity (Kumari et al., 2015).

Genetic mechanisms of charcoal rot resistance

Management of charcoal depends on cultural controls (crop rotation, no-till, irrigation) and planting moderately resistant or resistant cultivars. Complete resistance has not been detected for *M. phaseolina*. However, reports of reduced susceptibility against the fungi have been documented in soybean (Mengistu et al., 2013; Paris et al., 2006; Twizeimana et al., 2012) and sorghum (Mahmud et al., 2018; Reddy et al., 2008). Resistant cultivar development against this pathogen remains elusive due to the complex quantitative inheritance of resistance to the disease (Mukuru, 1992; Rosenow, 1992). A genome-wide association study to detect the genomic regions of charcoal rot resistance in sorghum using 300 diverse sorghum lines revealed fourteen loci and sets of candidate genes for plant defense responses (Adeyanju et al., 2015). However, the associated SNPs showed minute effects on the trait and the allele frequency; although suggested two subpopulations with representative resistance alleles, the study indicated this resulted in resistance against the pathogen as a complex molecular mechanism of resistance (Adeyanju et al., 2015).

Some earlier research in sorghum suggested a correlation between lodging resistance and stalk characteristics (stalk vigor and shorter stalk length) (Craig and Hooker, 1961; Thompson, 1963; Dodd, 1980), but other research related to this didn't find any correlation and detected the association between lodging and the incidence of charcoal rot disease (Seetharama et al., 1987). This study suggested that charcoal rot-susceptible genotypes are more lodging prone irrespective of their morphological stature and characteristics (Seetharama et al., 1987). Some researchers have suggested selecting the stay-green character to select for charcoal rot resistance (Tesso et al., 2012)

as many charcoal rot-resistant lines have stay-green germplasm (SC33, SC35, SC599) (Bramel-Cox et al., 1988; Woodfin et al., 1988). However, no attempt has been successful in selecting for charcoal rot resistance due to the complex pathogen biology, lack of an effective high throughput phenotyping protocol, and confounding environmental stressors (Tesso et al., 2012).

Charcoal rot resistance in sorghum has a direct association with the post-flowering stress response (Adeyanju et al., 2016). Adeyanju et al. (2016) investigated the relationship between stay-green (*stg*) quantitative trait loci (QTL) with charcoal. rot and stalk rot infection by both *M. phaseolina* and *Fusarium thapsinum* using14 genotyping groups of sorghum. The study revealed sorghum genotypes with stay green QTL *stg1*, *stg3*, or their combination (*stg1+3*) exhibited strong resistance reactions to *M. phaseolina* (Adeyanju et al., 2016). A recent genome-wide association (GWAS) study to dissect genetic architecture of lodging in sorghum detected 213 QTL responsible for lodging, which are associated with leaf-senescence traits and plant height (Wang et al., 2020). This study also suggested selecting for stay-green characters as a primary source of reduced lodging susceptibility in sorghum (Wang et al., 2020). The stay-green genotypes can reduce water loss during the post-anthesis period by continuing photosynthesis. In addition, it can also prevent carbohydrate metabolism. Thus, the plant could remain unstressed during the grain filling stage (Wang et al., 2020), which will indirectly select for charcoal rot disease resistance.

Therefore, understanding the host physiology behind charcoal rot progression and developing an effective phenotyping protocol is necessary to assist the breeder in producing charcoal rot-resistant sorghum lines and soybean cultivars. To assess physiological resistance against the charcoal rot pathogen *M. phaseolina*, leaf photosynthesis was measured using the chlorophyll index and photosystem II quantum yield (Fv/Fm ratio) in both susceptible and resistant sorghum genotypes after inoculation (Bandara et al., 2019). The research demonstrated that inoculation significantly reduced Fv/Fm ratios in the susceptible genotypes and across the crop's developmental stages. In contrast, chlorophyll index was reduced across genotypes and only in the inoculated plants across all developmental stages. The result also assessed some genotypes with greater photosynthetic ability despite a lower chlorophyll index due to disease pressure, which suggested a source of potential physiological resistance of the plant against the pathogen (Bandara et al., 2019).

Charcoal rot is one of the most economically important disease concern of soybean in the mid-southern states of USA. Since no commercially charcoal resistant cultivar available, an evaluation of 27 maturity groups (MG) III, 29 early MG IV, 34 late MG IV, and 59 MG V for screening charcoal rot resistance were conducted from 2006 to 2008 in a three year naturally infested soil with no irrigation and under no till conditions (Mengistu et al., 2011). The result from this study demonstrated significant disease expression among genotypes and year and no single genotypes consistently showed resistance expression for each year they were evaluated based on the colony forming unit index (CFUI) (Mengistu et al., 2011). However, this screening resulted in six (one in MG III, one in late MG IV, and four in MG V) genotypes with moderate resistant reactions (Mengistu et al., 2011).

Significant research has been conducted for screening sources for resistant genes to develop a charcoal rot-resistant soybean cultivar. Despite repeated efforts, progress has not been possible due to the complex nature of the disease and inadequate information regarding the genetic mechanisms of charcoal rot resistance in soybean. A GWAS study to detect sources of new charcoal rot resistance genes using 459 diverse plants from the USDA soybean germplasm core collection was conducted under both greenhouse and field conditions. Coser et al. (2017) detected five SNPs and candidate genes related to biotic and abiotic stress from field conditions and eight candidate genes from greenhouse conditions. Although all candidate genes from both environmental conditions were related to plant defense responses, there were no overlapping genes or markers between the two conditions. This trend suggested a complex molecular mechanism underlying charcoal rot as resistance showed variability in response to environmental variation (Coser et al., 2017).

Dissection of genomic regions responsible for charcoal rot resistance could accelerate breeding in soybean, which is the most effective means of controlling the disease. A QTL mapping analysis study using a biparental mapping population (PI 567562A (Resistant) × PI 567437 (susceptible)) detected one QTL in chromosome 15 and two more QTL in chromosome 16 that represented significant amounts of phenotypic variation for charcoal rot resistance (da Silva et al., 2019).

Detection of genomic regions responsible for charcoal rot resistance has been conducted in the field. It could be confounded due to environmental conditions such as temperature, rainfall, plant maturity stage, and uneven inoculum distribution (Pawlowski et al., 2015). A cut-stem inoculation

technique under controlled environments showed consistent charcoal rot screening in soybean seedlings (Twizeyimana et al., 2012). This cut-stem inoculation technique has been used to screen soybean genotypes from 70 ancestral types. Lesion progression caused by *M. phaseolina* has been conducted to measure lesion length and estimated percent survival rate. Both experiments revealed that PI 548302 and PI 548414 exhibited the lowest lesion length and highest survival rate, and PI 548178 had a significantly higher survival rate than the moderately resistant genotype DT97-4290 (Pawlowski et al., 2015). These three partially resistant soybean cultivars could contribute to developing charcoal rot resistance if QTL region(s) representing charcoal rot resistance could be detected and mapped in the soybean genome using marker-assisted selection (Pawlowski et al., 2015).

To understand the genetic mechanisms of charcoal rot resistance in soybean, a QTL-seq approach was used by da Silva et al. (2019), where bulk segregant analysis (BSA) was utilized to dissect charcoal rot resistance genomic regions using soybean PI 567562A. A single nucleotide polymorphism (SNP) index and Δ SNP index were estimated from the sequence of selected resistant and susceptible bulk progeny of a biparental mapping population (PI 567562A × PI 567437) that was aligned with the soybean genome of PI 567562A (da Silva et al., 2019). This study detected three genomic regions representing QTLs associated with the charcoal rot resistance in soybean (da Silva et al., 2019).

Significant research has been conducted to understand the host-pathogen interaction and genetic basis of charcoal rot resistance in soybean. Research areas include pathogenic diversity, phenotypic characterization, phytotoxin-related pathogenesis, detection of SNPs, host defense-related genes, QTL detection, and mapping (Ramezani et al., 2007; Deshmukh and Tiwari, 2021; Coser et al., 2017). To incorporate host resistance against charcoal rot disease, studies should emphasize understating the genetics behind host susceptibility and resistance, molecular signaling of host and pathogen, transcriptional changes induced by the pathogen, hormonal signaling, and host defense responses (Deshmukh and Tiwari, 2021). A soybean transcriptome analysis in response to *M. phaseolina* invasion has been conducted by Deshmukh and Tiwari (2021) to reveal the genomic architecture changes induced by the fungus (Deshmukh and Tiwari, 2021). This study detected the transcriptional changes from both resistant and susceptible soybean cultivars when inoculated with

M. phaseolina. The analysis revealed up-regulation of WRKY, LysM-RLKs, NBS-LLR, and flavonoid pathway genes, which suggests these resistance traits may be utilized in soybean breeding for charcoal rot resistance development (Tiwari et al., 2021).

Since previous studies suggest that charcoal rot resistance is a quantitative trait as no complete resistance has been screened, so introgressions of these gene families into breeding programs may assist in durable charcoal rot resistant cultivar development (Coser et al., 2017; Deshmukh and Tiwari et al., 2021).

REFERENCES

1. Abbas, H. K., Bellaloui, N., Accinelli, C., Smith, J. R., & Shier, W. T. (2019). Toxin production in soybean (*Glycine max* L.) plants with charcoal rot disease and by *Macrophomina phaseolina*, the fungus that causes the disease. *Toxins*, *11*, 645.
2. Adeyanju, A., Little, C., Yu, J., & Tesso, T. (2015). Genome-wide association study on resistance to stalk rot diseases in grain sorghum. *G3: Genes, Genomes, Genetics*, *5*, 1165-1175.
3. Adeyanju, A., Yu, J., Little, C., Rooney, W., Klein, P., Burke, J., & Tesso, T. (2016). Sorghum RILs segregating for stay-green QTL and leaf dhurrin content show differential reaction to stalk rot diseases. *Crop Science*, *56*, 2895-2903.
4. Allen, T. W., Bradley, C. A., Sisson, A. J., Byamukama, E., Chilvers, M. I., Coker, C. M., Collins, A. A., Dmicone, J. P., Dorrance, A. E. (2017). Soybean yield loss estimates due to diseases in the United States and Ontario, Canada, from 2010 to 2014. *Plant Health Progress*, *18*, 19-27.
5. Almeida, Á. M., Abdelnoor, R. V., Arias, C. A. A., Carvalho, V. P., Jacoud Filho, D. S., Marin, S. R., Benato, L. C., Pinto, M. C. & Carvalho, C. G. (2003). Genotypic diversity among Brazilian isolates of *Macrophomina phaseolina* revealed by RAPD. *Fitopatologia Brasileira*, *28*, 279-285.
6. Ammon, V., Wyllie, T. D., & Brown, M. F. (1975). Investigation of the infection process of *Macrophomina phaseolina* on the surface of soybean roots using scanning electron microscopy. *Mycopathologia*, *55*, 77-81.

7. Bandara, A. Y., Weerasooriya, D. K., Bradley, C. A., Allen, T. W., & Esker, P. D. (2020). Dissecting the economic impact of soybean diseases in the United States over two decades. *PloS One*, *15*, e0231141.
8. Bandara, A. Y., Weerasooriya, D. K., Liu, S., & Little, C. R. (2019). Host lipid alterations after *Macrophomina phaseolina* infection contribute to charcoal rot disease susceptibility in grain sorghum: Evidence from transcriptomic and lipidomic data. *bioRxiv*, 854067.
9. Bandara, A. Y., Weerasooriya, D. K., Tesso, T. T., & Little, C. R. (2019). Stalk rot resistant sorghum genotypes are resilient to pathogen-mediated photosystem II quantum yield retardation. *Crop Protection*, *124*, 104852.
10. Bandara, Y. M. A. Y., Tesso, T. T., Zhang, K., Wang, D., & Little, C. R. (2018). Charcoal rot and Fusarium stalk rot diseases influence sweet sorghum sugar attributes. *Industrial Crops and Products*, *112*, 188-195.
11. Bandara, Y. M. A. Y., Weerasooriya, D. K., Liu, S., & Little, C. R. (2018). The necrotrophic fungus *Macrophomina phaseolina* promotes charcoal rot susceptibility in grain sorghum through induced host cell-wall-degrading enzymes. *Phytopathology*, *108*, 948-956
12. Bandara, Y. M. A. Y., Weerasooriya, D. K., Tesso, T. T., & Little, C. R. (2017). Stalk rot diseases impact sweet sorghum biofuel traits. *BioEnergy Research*, *10*, 26-35.
13. Bandara, Y. M. A. Y., Weerasooriya, D. K., Tesso, T. T., Prasad, P. V. V., & Little, C. R. (2017). Stalk rot fungi affect grain sorghum yield components in an inoculation stage-specific manner. *Crop protection*, *94*, 97-105.
14. Bellaloui, N., Mengistu, A., & Paris, R. L. (2008). Soybean seed composition in cultivars differing in resistance to charcoal rot (*Macrophomina phaseolina*). *The Journal of Agricultural Science*, *146*, 667-675.
15. Bellaloui, N., Mengistu, A., Smith, J. R., Abbas, H. K., Accinelli, C., & Shier, W. T. (2021). Effects of charcoal rot on soybean seed composition in soybean genotypes that differ in charcoal rot resistance under irrigated and non-irrigated conditions. *Plants*, *10*, 1801.
16. Bhowal, J., Gosh, S., Guha, A. K., & Chatterjee, B. P. (2010). Infection of jute seedlings by the phytopathogenic fungus *Macrophomina phaseolina* mediated by endogenous lectin. *Research Journal of Microbiology*, *5*, 322-331.

17. Bramel-Cox, P. J., Stein, I. S., Rodgers, D. M., & Claflin, L. E. (1988). Inheritance of resistance to *Macrophomina phaseolina* (Tassi) Goid. and *Fusarium moniliforme* Sheldom in sorghum. *Crop Science*, *28*, 37-40.
18. Bressano, M., Giachero, M. L., Luna, C. M., & Ducasse, D. A. (2010). An in vitro method for examining infection of soybean roots by *Macrophomina phaseolina*. *Physiological and Molecular Plant Pathology*, *74*, 201-204.
19. Chadalavada, K., Kumari, B. D., & Kumar, T. S. (2021). Sorghum mitigates climate variability and change on crop yield and quality. *Planta*, *253*, 1-19.
20. Chowdhury, S., Basu, A., & Kundu, S. (2017). Biotrophy-necrotrophy switch in pathogen evoke differential response in resistant and susceptible sesame involving multiple signaling pathways at different phases. *Scientific Reports*, *7*, 1-17.
21. Cook, G. E., Boosalis, M. G., Dunkle, L. D., & Odvody, G. N. (1973). Survival of *Macrophomina phaseoli* in corn and sorghum stalk residue. *Plant Disease Reporter*, *57*, 873-875.
22. Coser, S. M., Chowda Reddy, R. V., Zhang, J., Mueller, D. S., Mengistu, A., Wise, K. A., Allen, T. W., Singh, A., & Singh, A. K. (2017). Genetic architecture of charcoal rot (*Macrophomina phaseolina*) resistance in soybean revealed using a diverse panel. *Frontiers in Plant Science*, *8*, 1626.
23. Craig, J., & Hooker, A. L. (1961). Relation of sugar trends and pith density to Diplodia stalk rot in dent corn. Diplodia root and stalk rot of dent corn. *Phytopathology*, *51*, 376-382.
24. Cummings, J. A., & Bergstrom, G. C. (2013). First report of charcoal rot caused by *Macrophomina phaseolina* in soybean in New York. *Plant Disease*, *97*, 1506.
25. da Silva, M. P., Klepadlo, M., Gbur, E. E., Pereira, A., Mason, R. E., Rupe, J. C., Bluhm, B. H., Wood, L., Mozzoni, L. A., & Chen, P. (2019). QTL mapping of charcoal rot resistance in PI 567562A soybean accession. *Crop Science*, *59*, 474-479.
26. da Silva, M. P., Zaccaron, A. Z., Bluhm, B. H., Rupe, J. C., Wood, L., Mozzoni, L. A., Mason, R. E., Yingling, S., & Pereira, A. (2020). Bulked segregant analysis using next-generation sequencing for identification of genetic loci for charcoal rot resistance in soybean. *Physiological and Molecular Plant Pathology*, *109*, 101440.

27. Davey, J. W., Hohenlohe, P. A., Etter, P. D., Boone, J. Q., Catchen, J. M., & Blaxter, M. L. (2011). Genome-wide genetic marker discovery and genotyping using next-generation sequencing. *Nature Reviews Genetics*, *12*, 499-510.
28. Del Poeta, M., Nimrichter, L., Rodrigues, M. L., & Luberto, C. (2014). Synthesis and biological properties of fungal glucosylceramide. *PLoS Pathogens*, *10*, e1003832.
29. Deshmukh, R., & Tiwari, S. (2021). Analysis of soybean transcriptome uncovers differential genomic regulations in response to charcoal rot in resistant and susceptible Genotypes. *Physiological and Molecular Plant Pathology*, *115*, 101672.
30. Deshmukh, R., & Tiwari, S. (2021). Molecular interaction of charcoal rot pathogenesis in soybean: A complex interaction. *Plant Cell Reports*, *40*, 1799-1812.
31. Dodd, J. L. (1980). The photosynthetic stress translocation balance concept of sorghum stalk rot. In *Proceedings of International Workshop of Sorghum Diseases* (pp. 300-305). Texas A&M University/ICRISAT Press Hyderabad, India.
32. Doubledee, M. D. (2012). *Effects of environment and genotype on charcoal rot development on soybeans*. M.S. thesis, University of Arkansas, Fayetteville. 114 pp.
33. Edmunds, L. K. (1964). Combined relation of plant maturity temperature+ soil moisture to charcoal stalk rot development in grain sorghum. *Phytopathology*, *54*, 514.
34. Edmunds, L. K., & Voigt, R. L. (1966). Role of seed production in predisposition of sorghum to charcoal rot. In *Phytopathology*, *56*, 876.
35. Gaige, A. R., Ayella, A., & Shuai, B. (2010). Methyl jasmonate and ethylene induce partial resistance in *Medicago truncatula* against the charcoal rot pathogen *Macrophomina phaseolina*. *Physiological and Molecular Plant Pathology*, *74*, 412-418.
36. Gangopadhyay, S., Wyllie, T. D., & Luedders, V. D. (1970). Charcoal rot disease of soybean transmitted by seeds. *Plant Disease Reporter*, *54*, 1088-1091.
37. Gupta, G. K., Sharma, S. K., & Ramteke, R. (2012). Biology, epidemiology and management of the pathogenic fungus *Macrophomina phaseolina* (Tassi) Goid with special reference to charcoal rot of soybean (*Glycine max* (L.) Merrill). *Journal of Phytopathology*, *160*, 167-180.
38. Gupta, P. K., Rustgi, S., & Mir, R. R. (2008). Array-based high-throughput DNA markers for crop improvement. *Heredity*, *101*, 5-18.

39. Hemmati, P., Zafari, D., Mahmoodi, S. B., Hashemi, M., Gholamhoseini, M., Dolatabadian, A., & Ataei, R. (2018). Histopathology of charcoal rot disease (*Macro-phomina phaseolina*) in resistant and susceptible cultivars of soybean. *Rhizosphere*, *7*, 27-34.
40. Huskins, C. L., & Smith, S. G. (1932). A cytological study of the genus Sorghum Pers. *Journal of Genetics*, *25*, 241-249.
41. Hymowitz, T. (2008). The history of the soybean. In *Soybeans* (pp. 1-31). AOCS Press.
42. Islam, M.S.; Haque, M.S.; Islam, M.M.; Emdad, E.M.; Halim, A.; Hossen, Q.M.; Hossain, M.Z.; Ahmed, B.; Rahim, S.; Rahman, M.S.; Alam, M.M.; Hou, S.; Wan, X.; Saito, J.A.; Alam M. (2012). Tools to kill: genome of one of the most destructive plant pathogenic fungi *Macrophomina phaseolina*. *BMC Genomics*, *13*, 1-16.
43. Iwuala, E., Odjegba, V., Unung, O., & Alam, A. (2020). Expression of stress responsive β-1,3-glucanase and chitinase genes in *Arachis hypogaea* seedlings against *Macrophomina phaseolina*. *Gene Reports*, *20*, 100693.
44. Jayati, B., Sumita, G., Guha, A. K., & Chatterjee, B. P. (2010). Infection of jute seedlings by the phytopathogenic fungus *Macrophomina phaseolina* mediated by endogenous lectin. *Research Journal of Microbiology*, *5*, 322-331.
45. Kaur, S., Dhillon, G. S., Brar, S. K., Vallad, G. E., Chand, R., & Chauhan, V. B. (2012). Emerging phytopathogen *Macrophomina phaseolina*: biology, economic importance and current diagnostic trends. *Critical Reviews in Microbiology*, *38*, 136-151.
46. Knogge, W. (1996). Fungal infection of plants. *The Plant Cell*, *8*, 1711.
47. Kumari, N., Sharma, I., Alam, A., & Sharma, V. (2015). Oxidative stress and role of antioxidant machinery in two cultivars of sorghum (*Sorghum bicolor* L.) to combat the damage induced by *Macrophomina phaseolina*. *European Journal of Biotechnology and Bioscience*, *3*, 5-13.
48. Li, Y. H., Zhao, S. C., Ma, J. X., Li, D., Yan, L., Li, J., Qi, X. T., Guo, X. S., Zhang, L., He, W. M., Chang, R. Z., Liang, Q. S., Guo, Y. (2013). Molecular footprints of domestication and improvement in soybean revealed by whole genome re-sequencing. *BMC Genomics*, *14*, 1-12.

49. Machado, A. R., Pinho, D. B., Soares, D. J., Gomes, A. A. M., & Pereira, O. L. (2019). Bayesian analyses of five gene regions reveal a new phylogenetic species of *Macrophomina* associated with charcoal rot on oilseed crops in Brazil. *European Journal of Plant Pathology*, *153*, 89-100.
50. Magnin-Robert, M., Le Bourse, D., Markham, J., Dorey, S., Clément, C., Baillieul, F., & Dhondt-Cordelier, S. (2015). Modifications of sphingolipid content affect tolerance to hemibiotrophic and necrotrophic pathogens by modulating plant defense responses in Arabidopsis. *Plant Physiology*, *169*, 2255-2274.
51. Mahmoud, A. F., Abou-Elwafa, S. F., & Shehzad, T. (2018). Identification of charcoal rot resistance QTLs in sorghum using association and in silico analyses. *Journal of Applied Genetics*, *59*, 243-251.
52. Marquez, N., Giachero, M. L., Declerck, S., & Ducasse, D. A. (2021). *Macrophomina phaseolina*: General characteristics of pathogenicity and methods of control. *Frontiers in Plant Science*, *12*, 634397.
53. Mengistu, A., Arelli, P. A., Bond, J. P., Shannon, G. J., Wrather, A. J., Rupe, J. B., Chen, P., Little, C.R., Canaday, C.H., Newman, M.A. and Pantalone, V.R. (2011). Evaluation of soybean genotypes for resistance to charcoal rot. *Plant Health Progress*, *12*, 6.
54. Mengistu, A., Arelli, P., Bond, J., Nelson, R., Rupe, J., Shannon, G., & Wrather, A. (2013). Identification of soybean accessions resistant to *Macrophomina phaseolina* by field screening and laboratory validation. *Plant Health Progress*, *14*, 25.
55. Mengistu, A., Wrather, A., and Rupe, J. C. 2015. Charcoal rot. In: Hartman, G. L., Rupe, J. C., Sikora, E. F., Domier, L., Davies J. A., and Steffey, K. L., (Eds.), *Compendium of Soybean Diseases*. American Phytopathological Society Press, St. Paul, MN.
56. Meyer, W. A., Sinclair, J. B., & Khare, M. N. (1974). Factors affecting charcoal rot of soybean seedlings. *Phytopathology*, *64*, 845-849.
57. Mihail, J. D. (1989). *Macrophomina phaseolina*: Spatio-Temporal Dynamics of Inoculum and of Disease in a Highly Susceptible Crop. *Phytopathology*, *79*, 848-855.
58. Mukuru, S. Z. (1992). Breeding for grain mold resistance. *Sorghum and millets disease: a second world review. ICRISAT, Patancheru, Andhra Pradesh*, *502*, 273-285.
59. Odvody, G. N., & Dunkle, L. D. (1979). Charcoal stalk rot of sorghum: Effect of Environment on Host-Parasite Relations. *Phytopathology*, *69*, 250-254.

60. Paris, R. L., Mengistu, A., Tyler, J. M., & Smith, J. R. (2006). Registration of soybean germplasm line DT97-4290 with moderate resistance to charcoal rot. *Crop Science*, *46*, 2324.
61. Paterson, A., Bowers, J., Bruggmann, R., Dubchak, I., Grimwood, J., Gundlach, H., Haberer, G., Hellsten, U., Mitros, T., Poliakov, A., Schumutz, J. (2009). *The Sorghum bicolor* genome and the diversification of grasses. *Nature*, *457*, 551-556.
62. Pawlowski, M. L., Hill, C. B., & Hartman, G. L. (2015). Resistance to charcoal rot identified in ancestral soybean germplasm. *Crop Science*, *55*, 1230-1235.
63. Radadiya, N., Mangukia, N., Antala, V., Desai, H., Chaudhari, H., Dholaria, T. L., Dholaria, D., Tomar, R. S., Golakiya, B. A., & Mahatma, M. K. (2021). Transcriptome analysis of sesame-*Macrophomina phaseolina* interactions revealing the distinct genetic components for early defense responses. *Physiology and Molecular Biology of Plants*, *27*, 1675-1693.
64. Ramezani, M., Shier, W. T., Abbas, H. K., Tonos, J. L., Baird, R. E., & Sciumbato, G. L. (2007). Soybean charcoal rot disease fungus *Macrophomina phaseolina* in Mississippi produces the phytotoxin (−)-botryodiplodin but no detectable phaseolinone. *Journal of Natural Products*, *70*, 128-129.
65. Reddy, P. S., & Reddy, B. V. (2019). History of Sorghum Improvement. In *Breeding Sorghum for Diverse End Uses* (pp. 61-75). Woodhead Publishing.
66. Reddy, P. S., Fakrudin, B., Punnuri, S. M., Arun, S. S., Kuruvinashetti, M. S., Das, I. K., & Seetharama, N. (2008). Molecular mapping of genomic regions harboring QTLs for stalk rot resistance in sorghum. *Euphytica*, *159*, 191-198.
67. Reis, E. M., Boaretto, C., & Danelli, A. L. D. (2014). *Macrophomina phaseolina*: density and longevity of microsclerotia in soybean root tissues and free on the soil, and competitive saprophytic ability. *Summa Phytopathologica*, *40*, 128-133.
68. Romero Luna, M. P., Mueller, D., Mengistu, A., Singh, A. K., Hartman, G. L., & Wise, K. A. (2017). Advancing our understanding of charcoal rot in soybeans. *Journal of Integrated Pest Management*, *8*, 1-8.
69. Rooney, W. L. (2014). Sorghum. In Karlen, D. L., (Eds.). *Cellulosic Energy Cropping Systems*, (pp.109-129). Wiley, USA.

70. Rosenow, D. T. (1992). Using germplasm from the world collection in breeding for disease resistance. *Sorghum and Millets Diseases—A second world review. ICRISAT, Patancheru, Andhra Pradesh*, *502324*, 319-324.
71. Sarr, M. P., Groenewald, J. Z., & Crous, P. W. (2014). Genetic diversity in *Macrophomina phaseolina*, the causal agent of charcoal rot. *Phytopathologia Mediterranea*, *53*(2), 250.
72. Schmutz, J., Cannon, S. B., Schlueter, J., Ma, J., Mitros, T., Nelson, W., Hyten, D. L., Song, Q., Thelen, J. J., Cheng, J., Xu, D., Hellsten, U. (2010). Genome sequence of the palaeopolyploid soybean. *Nature*, *463*, 178-183.
73. Seetharama, N., Bidinger, F. R., Rao, K. N., Gill, K. S., & Mulgund, M. (1987). Effect of pattern and severity of moisture deficit stress on stalk rot incidence in Sorghum I. Use of line source irrigation technique, and the effect of time of inoculation. *Field Crops Research*, *15*, 289-308.
74. Sharma, I., Kumari, N., & Sharma, V. (2014). Defense gene expression in Sorghum bicolor against Macrophomina phaseolina in leaves and roots of susceptible and resistant cultivars. *Journal of Plant Interactions*, *9*, 315-323.
75. Short, G. E., & Wyllie, T. D. (1978). Inoculum potential of *Macrophomina phaseolina*. *Phytopathology*, 68, 742-746.
76. Shurtleff, W., & Aoyagi, A. (1983). *The book of miso*. 2 nd Eds., Speed Press: Berkeley, California.
77. Singh, R. J., & Hymowitz, T. (1999). Soybean genetic resources and crop improvement. *Genome*, *42*, 605-616.
78. Singh, R. J., Kim, H. H., & Hymowitz, T. (2001). Distribution of rDNA loci in the genus Glycine Willd. *Theoretical and Applied Genetics*, *103*, 212-218.
79. Smith, C. W., & Frederiksen, R. A. (Eds.). (2000). *Sorghum: Origin, History, Technology, and Production* (Vol. 2). John Wiley & Sons.
80. Su, G., Suh, S. O., Schneider, R. W., & Russin, J. S. (2001). Host specialization in the charcoal rot fungus, Macrophomina phaseolina. *Phytopathology*, *91*, 120-126.
81. Taylor, J. R. (2019). Sorghum and millets: Taxonomy, history, distribution, and production. In *Sorghum and millets* (pp. 1-21). AACC International Press.
82. Tesso, T. T., Claflin, L. E., & Tuinstra, M. R. (2005). Analysis of stalk rot resistance and genetic diversity among drought tolerant sorghum genotypes. *Crop Science*, *45*, 645-652.

83. Tesso, T. T., Perumal, R., Little, C. R., Adeyanju, A., Radwan, G. L., Prom, L. K., & Magill, C. W. (2012). Sorghum pathology and biotechnology-a fungal disease perspective: Part II. Anthracnose, stalk rot, and downy mildew. *European Journal of Plant Science and Biotechnology*, *6*, 31-44.
84. Thompson, D. L. (1963). Stalk strength of corn as measured by crushing strength and rind thickness[1]. *Crop Science*, *3*, 323-329.
85. Toler, R. W. (1985). Maize dwarf mosaic, the most important virus disease of sorghum. *Plant Disease*, *69*, 1011-1015.
86. Tosic, M., Ford, R. E., Shukla, D. D., and Jilka, J. 1990. Differentiation of sugarcane, maize dwarf, johnsongrass and sorghum mosaic viruses based on reactions of oat and some sorghum cultivars. *Plant Disease*, *74*, 549-552.
87. Twizeyimana, M., Hill, C. B., Pawlowski, M., Paul, C., & Hartman, G. L. (2012). A cut-stem inoculation technique to evaluate soybean for resistance to *Macrophomina phaseolina*. *Plant Disease*, *96*, 1210-1215.
88. USDA-NASS. 2022. Available at [https://www.nass.usda.gov/Statistics_by_Subject/result.php?7CBAD13B-11BE-3F8B-8566EBFB39314A0C&sector=CROPS&group=FIELD%20CROPS&comm=SORGHUM] (Accessed on Jan. 6, 2022).
89. Venkateswaran, K., Elangovan, M., & Sivaraj, N. (2019). Origin, domestication and diffusion of *Sorghum bicolor*. In Aruna, C., Bhat, B. V., & Tonapi, V. A. (Eds.), *Breeding Sorghum for Divers End Uses*, (pp. 15-31). Woodhead publishing, USA.
90. Wang, J., Chu, S., Zhang, H., Zhu, Y., Cheng, H., & Yu, D. (2016). Development and application of a novel genome-wide SNP array reveals domestication history in soybean. *Scientific Reports*, *6*, 1-10.
91. Wang, X., Mace, E., Tao, Y., Cruickshank, A., Hunt, C., Hammer, G., & Jordan, D. (2020). Large-scale genome-wide association study reveals that drought-induced lodging in grain sorghum is associated with plant height and traits linked to carbon remobilisation. *Theoretical and Applied Genetics*, *133*, 3201-3215.
92. Woodfin, C. A., Rosenow, D. T., & Clark, L. E. (1988). Association between the stay-green trait and lodging resistance in sorghum. In *Agronomy Abstracts* (p. 102). Madison, WI: ASA.

93. Wrather, A., Shannon, G., Balardin, R., Carregal, L., Escobar, R., Gupta, G. K., ... & Tenuta, A. (2010). Effect of diseases on soybean yield in the top eight producing countries in 2006. *Plant Health Progress*, *11*, 29.
94. Yan, W., Ni, Y., Liu, X., Zhao, H., Chen, Y., Jia, M., Liu, M., Liu, H., & Tian, B. (2021). The mechanism of sesame resistance against *Macrophomina phaseolina* was revealed via a comparison of transcriptomes of resistant and susceptible sesame genotypes. *BMC Plant Biology*, *21*, 1-21.
95. Young, P. A. 1949. Charcoal rot of plants in east Texas. Bulletin Texas Agricultural Experimental Station No. 33.
96. Zummo, N. 1980. Fusarium disease complex of sorghum in West Africa. P. 297-299. In G.D. Bengtson (ed.), *Sorghum disease: A world review*. Proc. Of Int. Workshop of Sorghum Diseases, Hyderabad, India. 11-15 Dec. 1978. ICRISAT, Patancheru, Andhra Pradesh, India.

Chapter 2 - Evaluating the role of exogenously applied ascorbic acid in rescuing soybean plant health in the presence of pathogen-induced oxidative stress

ABSTRACT

Charcoal rot, caused by the soilborne hemibiotrophic fungus *Macrophomina phaseolina*, is a prevalent and economically significant plant disease. It is hypothesized that *M. phaseolina* induces oxidative stress-mediated senescence in plants. Infection by *M. phaseolina* results in the host's accumulation of reactive oxygen species (ROS) that contribute toward basal defense. However, the production of ROS could also lead to cellular damage and senescence in host tissue. This study aimed to determine if ascorbic acid, a ROS scavenging molecule, could quench *M. phaseolina*-induced hydrogen peroxide (H_2O_2) generation in a soybean-*M. phaseolina* pathosystem. In vitro sensitivity tests showed that *M. phaseolina* isolates were sensitive to L-ascorbic acid (LAA) at concentrations of 10.5 to 14.3 mM based on IC_{50} data. In planta cut-stem assays demonstrated that pre-treatment with 10 mM of either LAA (reduced form) or DHAA (dehydroascorbic acid; oxidized form) significantly decreased lesion length compared to the non-pretreated control and post-treatments with both ascorbic acid forms after *M. phaseolina* inoculation. Further, H_2O_2 quantification from ascorbic acid-pretreated tissue followed by *M. phaseolina* inoculation showed significantly less accumulation of H_2O_2 than the inoculated control or the mock-inoculated control. This result demonstrated that *M. phaseolina* not only induced H_2O_2 after host infection but also increased ROS-mediated senescence. This study shows the potential of ascorbic acid, an effective ROS scavenger, to limit ROS-mediated senescence associated with *M. phaseolina* infection.

INTRODUCTION

Charcoal rot of soybean (*Glycine max* (L.) Merr.) is caused by the ubiquitous soilborne fungus *Macrophomina phaseolina* (Tassi) Goid. *M. phaseolina* infects a wide range of plant hosts and is distributed worldwide (Hartman et al., 2015; Živanov et al., 2019; Basandrai et al., 2021; Rogers and Koehler, 2021; Masi et al., 2021). Under favorable environmental conditions, host infection begins with the germination of microscelerotia in the soil near plant roots. Then, microsclerotial hyphae penetrate the soybean plant through the root and grow intercellularly into the vascular region. Fungal colonization ultimately damages plant tissue by plugging xylem vessels and producing phytotoxins (Bowers et al., 1999; Islam et al., 2012; Twizeyimana et al., 2012; Doubledee et al., 2018). When no conspicuous disease symptoms are expressed in the plant, the fungus remains biotrophic and latent. A histopathological study using a resistant and susceptible soybean cultivar revealed that *M. phaseolina* requires a nine-day incubation or biotrophic phase in a susceptible cultivar to grow intercellularly and colonize the stele tissue. In contrast, the resistant cultivar restricted infection and disease development (Hemmati et al., 2018). However, with the onset of an environmental stressor, such as drought or high temperature, high plant populations, or nutritional deficiency during the post-flowering stages, *M. phaseolina* may induce necrotrophy (Twizeyimana et al., 2012; Marquez et al., 2021). In the necrotrophic phase, *M. phaseolina* causes disease symptoms associated with wilting as the pathogen blocks the vascular bundles, induces the production of plant degradative enzymes, and causes phytotoxin-mediated necrosis (Hartman et al., 2015; Twizeyimana et al., 2012; Hemmati et al., 2018; Bandara et al., 2018). Therefore, *M. phaseolina* functions as a hemibiotroph by taking advantage of both the biotrophic phase needed for its initial infection and development and the progression of the necrotrophic phase, which is required for pathogen survival (Hemmati et al., 2018).

Plants possess two layers of defenses against microorganisms, basal and specific. Specific defense is mediated by resistance (R) genes. It produces a hypersensitive response (HR) in incompatible interactions, whereas basal defense recognizes microbe-associated molecular patterns (MAMPs), which triggers MAMP-triggered immunity (MTI) (Boller and Felix, 2009; Chisholm et al., 2006; Jones and Dangl, 2006; Millet et al., 2010). Biotrophic pathogens depend on living hosts for nutrition and proliferation. At the same time, their growth is restricted once the host R gene recognizes the biotrophic pathogen-secreted effector, and the host induces HR-mediated cell death.

However, pathogens with necrotrophic phases, such as *M. phaseolina*, take advantage of this R gene-mediated necrotrophic effector recognition and HR-mediated built-in cell senescence as their growth, nutrition, infection, and further proliferation initiate with the R gene-mediated defense responses and host senescence. This host defense mechanism benefits pathogens with necrotrophic phases to become more infective and ultimately increases host susceptibility (Faris et al., 2010; Foley et al., 2016).

Reactive oxygen species (ROS) are generated as defense signals in plants in response to abiotic and biotic stresses (Bandara et al., 2018; Akram et al., 2017; Sarkar et al., 2014). ROS species include H_2O_2 (hydrogen peroxide), OH• (hydroxyl radical), and $•O_2–$ (superoxide radical) (Turkan, 2018). Of these, H_2O_2 is long-lived and is a REDOX (reduction-oxidation) metabolite that acts as a signaling molecule or an inducer of oxidative damage depending on its concentration (Hossain et al., 2015; Černý et al., 2018). Low and balanced levels of H_2O_2 are known to be involved in diverse signaling processes in the plant, including stress tolerance, control of enzymatic and non-enzymatic antioxidative defense systems (the plant has a built-in antioxidative defense system to mask against oxidative damage caused by these free toxic and reactive oxygen intermediates), stomatal control, cell cycle, growth regulation, and photosynthesis (Hossain et al., 2015; Černý et al., 2018; Habibi et al., 2014). However, imbalanced or excessive H_2O_2 induces toxicity and damage to biomolecules, which leads to cellular injury and cell death (Hossain et al., 2015; Černý et al., 2018).

A previous study showed that *M. phaseolina* induced ROS generation in sorghum (Bandara et al., 2018) and RNS generation in jute after inoculation (Sarkar et al., 2014). ROS could act as a defense signal-related response against the biotic stress conferred by the pathogen or insects and abiotic stress conferred by non-biotic entities if the balance between ROS generation and scavenging is maintained (Nath et al., 2016). However, if excess ROS generated by abiotic and biotic stressors are not scavenged, the cellular homeostasis will be lost, and resulting malfunctions in plant metabolic activity could lead to oxidative damage-related cell senescence (Caverzan et al., 2019). If *M. phaseolina* induces oxidative stress-mediated senescence in soybean, we hypothesize that ascorbic acid, a reactive oxygen scavenger of H_2O_2, can mitigate pathogen-mediated senescence. The specific objectives were: (i) to test the in vitro sensitivity of *M. phaseolina* isolates against inhibition by ascorbic acid; (ii) to apply ascorbic acid to wounded and inoculated soybean seedling stems in

an in-planta assay to determine its ability to reduce *M. phaseolina*-associated development; and (iii) to validate the ROS (H_2O_2) induced by *M. phaseolina* in the soybean host using a spectrophotometric absorbance assay.

MATERIALS AND METHODS

Soybean genotype and *Macrophomina phaseolina* isolates

The commonly grown soybean genotype AG3039 (Asgrow, Bayer Crop Science, Creve Coeur, Missouri, USA) was used for this experiment. Susceptibility of AG3039 to M. phaseolina was established using the seedling stem necrosis assay (Figure 2.6) (Twizeyimana et al., 2012).

Three *M. phaseolina* isolates were selected for testing in this study. These included MP110, MP154, and MP336. The isolates were obtained from soybeans grown in Rossville (in 2002), Leavenworth (in 2002), and Manhattan (Ashland Bottoms Research Farm, Kansas State University, Manhattan, KS, USA; in 2008), Kansas, respectively. MP110 and MP154 were previously characterized by Saleh et al. (Saleh et al., 2010). In addition to cultural and morphological characteristics, the rDNA-ITS region of MP336 was sequenced using the *MpKF1* and *MpKR1* primer set developed by Babu et al. (2007) to confirm its identity.

In vitro sensitivity of *M. phaseolina* to ascorbic acid

For the in vitro growth test, ¼-strength potato dextrose agar (PDA; Difco Laboratories, Detroit, Michigan, USA) media was amended with ten concentrations (0, 0.5, 5, 10, 15, 20, 25, 30, 40, and 50 mM) of ascorbic acid (L-ascorbic acid; Sigma-Aldrich Co., St. Louis, Missouri; Figure 2.7). The ascorbic acid was added once the media cooled < 55°C after autoclaving. *M. phaseolina* isolates MP336, MP154, and MP110 were plated on the media, and growth was recorded every 24 hr for 5 days. The experimental design was a RCBD with factorial (*M. phaseolina* isolates and ascorbic acid concentrations) with three replications. In addition, IC50 (inhibitory concentration) values were calculated from daily measurements using the Quest GraphTM IC50 calculator online tool [AAT Bioquest, 2021]. DHAA (dehydroascorbic acid) was not tested in the in vitro sensitivity experiment.

Soybean stem necrosis assay

These experiments were conducted in the Throckmorton Plant Sciences greenhouse facilities at Kansas State University, Manhattan, KS, USA. The experimental design was a RCBD with three replications and twelve treatments. The experiment was repeated twice.

Five soybean seeds were planted in 12.7 × 12.7 cm (5 × 5 in.) pot, and seedlings thinned to three plants per pot once they reached the cotyledonary stage (VC). The remaining seedlings were grown until the 2nd trifoliate (V2) stage.

The cut-stem inoculation method of Twizeymania et al. (2012) was followed for this experiment. The apical portions of V2 soybean seedlings were cut 25 mm above the unifoliate node. Inverted two hundred microliter (200 µl) micropipette tubes containing one of the pre-treatments and treatments listed in Table 3 were placed on the cut portion of the seedling. To apply the ascorbic acid or H_2O_2 exogenously, a small sponge piece was inserted inside the micropipette, and it was soaked with 100 µl of the respective liquid (ascorbic acid or H_2O_2). Sterile agar plugs (~5 mm diameter × ~8 mm depth) were used as the negative control. Agar plugs of the same dimensions, colonized with *M. phaseolina* (isolate MP336), were placed fungal colonized-side down on the cut-stem and used as the positive control and inoculated treatments.

H_2O_2 absorbance assay

To show that *M. phaseolina* induces the production of the reactive oxygen species (ROS), specifically H_2O_2, in the soybean stem assay, mock-inoculated, inoculated, ascorbic acid pre-treated, and inoculated soybean stems were processed using the method from Veljovic-Jovanovic et al., (2002) and Liu et al., (2014). Briefly, cut stems were collected at the 2nd trifoliate stage (including the top, middle, and bottom portion of the cotyledonary node to 25 mm above it) and immediately frozen in liquid nitrogen. The tissue was homogenized in 1.5 ml 1 M HClO4 with 100 mg polyvinylpyrrolidone (to remove phenolic compounds). The homogenate was centrifuged at 13,000 × g for 10 min at 4˚C. Following the method of Cheesseman, (2006) and Liu et al., (2014), 60 ml of centrifuged stem tissue extract was mixed with 600 ml of eFOX reagent, which contained 250 µM ferrous ammonium sulfate, 100 µM sorbitol, 100 µM xylenol orange, and 1% methanol combined

in 25 mM H_2SO_4, and 1% ethanol. Thirty minutes after mixing tissue extract with the eFOX reagents, spectrophotometric absorbance was measured at 550 and 800 nm using a plate reader (BioTek Synergy H1 Hybrid Multi-Mode Microplate Reader; BioTek Instruments, Inc., Winooski, VT, USA). Quantification of H_2O_2 was calibrated using an H_2O_2 standard curve.

Statistics

For the in vitro sensitivity assay, analysis of variance (ANOVA) was performed using the PROC GLM procedure of SAS 9.4 (SAS Institute, Cary, NC, USA). Across isolates and days post-plating (DPPL), mean separations were conducted for ascorbic acid concentration, and *M. phaseolina* isolates using the LSMEANS of SAS PROC GLM procedure. Within isolates and DPPL, the student's t-test (JMP 16.2.0; SAS Institute, Inc., Cary, NC) was used to compare growth on 0 mM ascorbic acid to each individual concentration of ascorbic acid, For the cut-stem assay, ANOVA was conducted using the PROC GLIMMIX procedure of SAS. Means separations for areas under the disease progress curve (AUDPC) values were performed using LSMEANS of the SAS GLIMMIX procedure. ANOVA for the H_2O_2 absorbance assay was carried out using the PROC GLM procedure of SAS. Means separation was performed using the Least Significant Difference (LSD) of the mean. Box plots were used for the graphical representation of AUDPC (Figure 2.3) and H_2O_2 quenching by ascorbic acid (Figure 2.5) (Krzywinski and Altman, 2014).

RESULTS

In vitro sensitivity assay

The ANOVA table (Table 2.1) shows that there is a significant difference present in isolates by ascorbic acid concentration (I×C) at $\alpha = 0.05$ level of confidence at 1-day and 3- to 4-days post-plating (DPPL). However, isolates by ascorbic acid concentration (I×C) was not significant at 5-DPPL. Also, there is significant difference present among isolates (I) and ascorbic acid concentrations (C) from 1- to 5-days post-plating (DPPL) (Table 2.1). The isolates were highly significant from 3- to 5-DPPL at $P \leq 0.001$. All ascorbic acid concentrations (C) were highly significant from 1- to 5-DPPL at $P \leq 0.001$ (Table 2.1).

The comparison of colony growth on media containing ascorbic acid with media not containing ascorbic acid (i.e., 0 mM) was significantly decreased. At 3- and 4-days post-plating (DPPL), all three isolates were grown on 5 mM ascorbic acid showed significantly decreased growth compared to control plates. However, at 1 DPPL, MP110, MP154, and MP336 differed from the control at 10 mM, 20 mM, and 25 mM, respectively. At 2 DPPL, MP110 and MP154 differed from control at 5 mM, whereas MP336 differed at 15 mM. At 5 DPPL, MP110 and MP154 differed from the control at 5 mM, whereas MP336 differed at 10 mM. Overall, MP154 and MP336 exhibited a significantly higher IC50 than MP110 ($F = 13.96$; $P < 0.0001$) (Table 2.1; Figure 2.1). At 10 to 15 mM ascorbic acid concentrations, all *M. phaseolina* isolates exhibited reduced microsclerotia production. At the same concentrations, cultures transitioned from a circular form with entire margins to an irregularly formed colony with lobate to filiform margins (Figure 2.2). Based on these results, MP336 was chosen as the test isolate for the remainder of the experiments.

Cut-stem assay

The area under disease progress curve (AUDPC) from the cut-stem assay of the two experiments showed a higher AUDPC value for the non pre-treated *M. phaseolina* inoculated control compared with the non-pretreated agar plug inoculated mock control (Figure 2.3). The *M. phaseolina* inoculated stem following treatment with both forms of ascorbic acid showed significantly higher AUDPC value than its mock control counterparts and non pre-treated *M. phaseolina* inoculated treatment (Figure 2.3). The ascorbic acid (reduced and oxidized forms) pre-treated and *M. phaseolina* inoculated treatment exhibited significantly lower AUDPC values than the non pre-treated *M. phaseolina* inoculated treatment. Ascorbic acid pre-treated inoculated treatment was not statistically significant than its mock control counterpart (ascorbic acid pre-treated following agar plug inoculated mock control); however, it was statistically significant with the *M. phaseolina* inoculated following ascorbic acid applied treatment. There was no statistical significance between non pre-treated H_2O_2 applied treatment with the H_2O_2 pre-treated *M. phaseolina* inoculated treatment. In addition, the AUDPC value was lower than the non-pretreated inoculated treatment and statistically non significant to mock-inoculated treatment (Figure 2.3).

In the cut-stem assay, *M. phaseolina*-inoculated soybean plants produced significantly longer lesions than agar alone. Furthermore, when cut stems were inoculated with *M. phaseolina* and subsequently treated with DHAA and LAA (day +0), lesion length on the stem was significantly longer than in the inoculated plants (Figure 2.4). However, when cut stems were pre-treated with DHAA and LAA (day -1), lesion length was significantly reduced compared to inoculation alone and not different than agar after ascorbic acid treatment (Figures 2.4). The non pre-treated H_2O_2 applied stem did not show any stem tissue necrosis like the inoculated control, however H_2O_2 pre-treated following *M. phaseolina* inoculated stem exhibited prominent areas of tissue senescence (Fig. 2.4).

H_2O_2 absorbance assay

To confirm that *M. phaseolina* induces the H_2O_2 generation, absorbance was measured from inoculated plants in vitro (Table 2.2; Figure 2.5). The ANOVA table for the H_2O_2 quantification assay showed all four treatments were significant at $P \leq 0.05$ (Table 2.2). *M. phaseolina* inoculation (positive control) increased H_2O_2 concentration from soybean stem tissue extracts compared to no pre-treatment and subsequent inoculation with agar (negative control). Likewise, pre-treatment with LAA or DHAA and subsequent inoculation with *M. phaseolina* after 1 day significantly reduced H_2O_2 compared to the positive control and did not differ from the negative control (Table 2.2; Figure 2.5).

DISCUSSION

To investigate pathogen-induced ROS (reactive oxygen species)-mediated senescence in soybean, reduced (L-ascorbic acid, LAA) and oxidized (dehydroascorbic acid, DHAA) forms of ascorbic acid were tested as ROS scavengers to determine their potential to minimize ROS-induced effects in planta. LAA was used to test in vitro sensitivity of *M. phaseolina*. In this study, *M. phaseolina* isolates showed sensitivity to LAA concentrations > 10 mM. Botanga et al., (2012), using a similar in vitro assay, tested the growth of the necrotrophic fungus, *Alternaria brassicicola*, against various concentrations of ascorbic acid in minimal media. Their study demonstrated that fungal growth was inhibited at 25 μM and restricted at 10 mM. Based on the current study and Botanga et al., (2012), it may be concluded that higher ascorbic acid concentrations are toxic and inhibitory to

fungal growth. However, specific levels may vary between fungal species or isolates of the same species. However, the ascorbic acid-sensitive fungal metabolic targets, whether direct or indirect via pH changes, remain unclear.

Ascorbic acid has been used in plant systems to evaluate its activity in scavenging abiotic stress-mediated ROS generation (Akram et al., 2017). For example, exogenously applied ascorbic acid actively protected lipids and proteins from drought and salt stress (Miguel et al., 2006; Ameer et al., 2010; Hira et al., 2016). Ascorbate, which is a regenerative and potent antioxidant molecule (Akram et al., 2017; Noctor and Foyer, 1998; Ye et al., 2012), has shown promising ROS neutralizing capabilities along with vitamin E through direct and indirect actions (enzyme catalysis) (Akram et al., 2017; Noctor and Foyer, 1998; Ye et al., 2012). Endogenous ascorbate has a significant role in antioxidative metabolism. Exogenous application of ascorbic acid has been found to increase endogenous ascorbic acid levels (Akram et al., 2017; Khan and Ashraf, 2008; Noctor et al., 2014). Ascorbic acid has the potential to activate antioxidant molecules, and ascorbate peroxidase (APx) is known to dismute the major ROS, H_2O_2, to water and oxygen (Akram et al., 2017; Mittler et al., 2004; Van Doorn and Ketsa, 2014). Ameer et al. (2010) assessed the role of exogenously applied ascorbic acid (0, 50, and 100 mg L-1) in attenuating the salt toxicity effect on two wheat (*Triticum aestivum* L.) cultivars (salt tolerant and moderately salt sensitive) when grown under normal conditions (0 mM NaCl) and a salt treated condition (150 mM NaCl). Their study revealed that foliar sprays of ascorbic acid shielded the photosynthetic machinery of both wheat cultivars against the toxic effect of the salt treatment and rescued plants from salt-induced chlorophyll-a content reduction. Also, exogenously applied ascorbic acid rescued okra (*Abelmoschus esculentus* (L.) Moench) plants from oxidative stress-associated electrolyte leakage and lipid peroxidation during drought stress conditions (Amin et al., 2009).

Basal defense in plants upon microbe recognition is initiated through ROS signaling. For example, ROS was generated in the initial, short-lived biotrophic phase of *M. phaseolina* upon recognition by both susceptible and resistant sesame (*Sesamum indicum* L.) plants. However, ROS generation increased significantly in susceptible sesame plants compared to the resistant host once the fungus switched from the biotrophic to the necrotrophic phase (Chowdhury et al., 2017). ROS generation is a normal plant phenomenon during any physiological or metabolic process (Boguszewska and Zagdańska, 2012; Nandini and Samir, 2016). Biotic and abiotic stressors induce excessive ROS,

which leads to redox imbalances and oxidative stress in the plant (Turkan, 2018; Nandini and Samir, 2016; Maurino and Flügge, 2008). Plants possess antioxidant machinery comprised of both enzymatic (superoxide dismutase (SOD), catalase (CAT), ascorbate peroxidase, glutathione peroxidase (GPx), glutathione-S-transferase, monodehydroascorbate reductase, and dehydroascorbate reductase) and non-enzymatic compounds (ascorbate, phenolic compounds, carotenoids, and tocopherol) to mitigate such redox imbalances (Boguszewska and Zagdańska, 2012; Nandini and Samir, 2016). Therefore, plants have an innate "immune" reaction against the oxidative damage caused by ROS through the secretion of antioxidants and other substances that can scavenge ROS (Akram et al., 2017). In susceptible plants, it is possible that excess production of ROS cannot be fully quenched by host antioxidants, which results in further accumulation of ROS and oxidative damage to cells (Gill et al., 2012).

Our results showed that 10 mM of exogenously applied ascorbic acid, whether LAA or DHAA, significantly reduced *M. phaseolina*-induced lesion development in ascorbic acid-pre-treated seedling cut-stems. The role of ascorbic acid in plant tolerance to pathogen-induced stress has been elucidated in transgenic potato plants with enhanced ascorbic acid levels when inoculated with *Phytophthora infestans* (Chung et al., 2009). Their study showed that transgenic potato lines with enhanced ascorbic acid significantly reduced late blight lesions, H_2O_2, and malondialdehyde levels, a biomarker for oxidative stress. These authors also found that increased cellular ascorbic acid in transgenic plants aided in balancing cellular antioxidant levels, PR gene expression, and defense-associated hormones such as gibberellic acid and abscisic acid, which reduced senescence caused by *P. infestans*. Further, a previous study demonstrated ascorbic acid's potential to defend against environmentally induced oxidative stress (Ameer et al., 2010). Our study that has shown the efficacy of exogenously applied ascorbic acid in scavenging H_2O_2 generated after inoculation by the necrotrophic fungus, *M. phaseolina*.

Pathogens with necrotrophic phases take advantage of induced, defense-associated ROS bursts and associated cell death for nutrition and concurrent colonization of senescent and necrotic tissue (Govrin and Levine, 2000). This phenomenon was observed in the soybean seedling cut-stem in-planta assay, where inoculated plants showed increased senescence as induced by *M. phaseolina*.

Tolerance to environmental stressors in plants such as salt stress is related to ROS scavenging. Arabidopsis mutant vst1 showed increased tolerance to salt stress due to a ROS scavenging mechanism (Tsugane et al., 1999). ROS detoxification or scavenging was performed by several antioxidants such as ascorbic acid, glutathione, thioredoxin, carotenoids, and other ROS scavenging enzymes, including SOD, GPx, and CAT (Ameer et al., 2010). Exogenous foliar application of ascorbic acid at 200 mg L-1 significantly improved the growth of flax cultivars under salt stress conditions (El Hariri et al., 2010). A study by Shao et al. (2008) demonstrated that ascorbic acid protects metabolic processes against H_2O_2 and minimizes H_2O_2-associated oxidative damage (Shao et al., 2008). Our result is also consistent with this finding, as the exogenous application of ascorbic acid showed reduced senescence induced by *M. phaseolina*. As measured by AUDPC, disease progression was significantly slowed when either LAA or DHAA was applied to cut stems, suggesting the phenotype prediction of ROS scavenging by ascorbic acid. Also, the ROS quantification assay suggested the increased concentration of ROS generation as induced by *M. phaseolina* demonstrated the oxidative stress impact in plants. Ascorbic acid pre-treatment demonstrated a significantly lower level of H_2O_2 content, supporting a ROS quenching mechanism of ascorbic acid.

Charcoal rot is a plant disease that manifests during high temperature and water-limiting conditions. These environmental stressors contribute to pre-mature plant senescence, a situation that may be exploited by the necrotrophic phase of *M. phaseolina*. Furthermore, combinations of stressors are expected to exacerbate plant productivity in the future as they do now (Rivero et al., 2022). Therefore, understanding potential mechanisms by which charcoal rot, and other stress-associated diseases, may be mitigated, including quenching ROS-mediated responses, is an area of continued research interest.

REFERENCES

1. AAT Bioquest, Inc. Quest GraphTM. IC50 calculator. 2021. [Available at https://www.aatbio.com/tools/ic50-calculator] (Accessed on Sept. 15, 2022).
2. Akram, N. A., Shafiq, F., & Ashraf, M. (2017). Ascorbic acid-a potential oxidant scavenger and its role in plant development and abiotic stress tolerance. *Frontiers in Plant Science*, 8, 613.

3. Ameer, K., Iram, I., Amin, S., Humera, N., Farooq, A., & Ibrahim, M. (2010). Alleviation of adverse effects of salt stress in brassica (Brassica campestris) by pre-sowing seed treatment with ascorbic acid. *American-Eurasian Journal of Agricultural and Environmental Science*, *7*, 557-560.
4. Amin, B., Mahleghah, G., Mahmood, H. M. R., & Hossein, M. (2009). Evaluation of interaction effect of drought stress with ascorbate and salicylic acid on some of physiological and biochemical parameters in okra (*Hibiscus esculentus* L.). *Research Journal Biological Science*, *4*, 380-387.
5. Babu, B. K., Saxena, A. K., Srivastava, A. K., & Arora, D. K. (2007). Identification and detection of *Macrophomina phaseolina* by using species-specific oligonucleotide primers and probe. *Mycologia*, *99*, 797-803.
6. Bandara, Y. M. A. Y., Weerasooriya, D. K., Liu, S., & Little, C. R. (2018). The necrotrophic fungus *Macrophomina phaseolina* promotes charcoal rot susceptibility in grain sorghum through induced host cell-wall-degrading enzymes. *Phytopathology*, *108*, 948-956.
7. Basandrai, A. K., Pandey, A. K., Somta, P., & Basandrai, D. (2021). *Macrophomina phaseolina*-host interface: Insights into an emerging dry root rot pathogen of mungbean and urdbean, and its mitigation strategies. *Plant Pathology*, *70*, 1263-1275.
8. Boguszewska, D., & Zagdańska, B. (2012). ROS as signaling molecules and enzymes of plant response to unfavorable environmental conditions. In Lushchak, V., & Semchyshyn, H. M. (Eds.), *Oxidative stress-molecular mechanisms and biological effects*. Rijeka, Croatia: InTech, 341-362.
9. Boller, T., & Felix, G. (2009). A renaissance of elicitors: perception of microbe-associated molecular patterns and danger signals by pattern-recognition. *Annual Review of Plant Biology*, *60*, 379-406.
10. Botanga, C. J., Bethke, G., Chen, Z., Gallie, D. R., Fiehn, O., & Glazebrook, J. (2012). Metabolite profiling of *Arabidopsis* inoculated with *Alternaria brassicicola* reveals that ascorbate reduces disease severity. *Molecular Plant-Microbe Interactions*, *25*, 1628-1638.
11. Bowers, G. R., Russin, J. S., Heatherly, L. G., & Hodges, H. F. (1999). Soybean disease management. In Heatherly, L. G., & Hodges, H. F. (Eds.), *Soybean production in the Mid-south* (pp. 231-271). CRC Press, FL, USA.

12. Caverzan, A., Piasecki, C., Chavarria, G., Stewart Jr, C. N., & Vargas, L. (2019). Defenses against ROS in crops and weeds: The effects of interference and herbicides. *International Journal of Molecular Sciences*, 20, 1086.
13. Černý, M., Habánová, H., Berka, M., Luklová, M., & Brzobohatý, B. (2018). Hydrogen peroxide: Its role in plant biology and crosstalk with signalling networks. *International Journal of Molecular Sciences*, *19*, 2812.
14. Cheeseman, J. M. (2006). Hydrogen peroxide concentrations in leaves under natural conditions. *Journal of Experimental Botany*, *57*, 2435-2444.
15. Chisholm, S. T., Coaker, G., Day, B., & Staskawicz, B. J. (2006). Host-microbe interactions: shaping the evolution of the plant immune response. *Cell*, *124*, 803-814.
16. Chowdhury, S., Basu, A., & Kundu, S. (2017). Biotrophy-necrotrophy switch in pathogen evoke differential response in resistant and susceptible sesame involving multiple signaling pathways at different phases. *Scientific Reports*, *7*, 1-17.
17. Chung, I. M., Venkidasamy, B., Upadhyaya, C. P., Packiaraj, G., Rajakumar, G., & Thiruvengadam, M. (2019). Alleviation of *Phytophthora infestans* mediated necrotic stress in the transgenic potato (*Solanum tuberosum* L.) with enhanced ascorbic acid accumulation. *Plants*, *8*, 365.
18. Doubledee, M. D., Rupe, J. C., Rothrock, C. S., & Bajwa, S. G. (2018). Effect of root infection by *Macrophomina phaseolina* on stomatal conductance, canopy temperature and yield of soybean. *Canadian Journal of Plant Pathology*, 40, 272-283.
19. El Hariri, D. M., Sadak, M. S., & El-Bassiouny, H. M. S. (2010) Response of flax cultivars to ascorbic acid and A-tocophorol under salinity stress conditions. *International Journal of Academic Research*, 2, 101-109.
20. Faris, J. D., Zhang, Z., Lu, H., Lu, S., Reddy, L., Cloutier, S., Fellers, J. P., Meinhard, S. W., Rasmussen, J. B., Xu, S. S., Oliver, R. P., Simons, K. J., & Friesen, T. L. (2010). A unique wheat disease resistance-like gene governs effector-triggered susceptibility to necrotrophic pathogens. *Proceedings of the National Academy of Sciences USA*, *107*, 13544-13549.
21. Foley, R. C., Kidd, B. N., Hane, J. K., Anderson, J. P., & Singh, K. B. (2016). Reactive oxygen species play a role in the infection of the necrotrophic fungi, *Rhizoctonia solani* in wheat. *PLoS One*, *11*, e0152548.

22. Gill, S. S., Singh, L. P., Gill, R., Tuteja, N. (2012). Generation and scavenging of reactive oxygen species in plants under stress. In Tuteja, N., Gill, S.S., Tiburcio, A.F., & Tuteja, R. (Eds.), *Improving Crop Resistance to Abiotic Stress* (pp. 46-69). Wiley-Blackwell, New York, USA.
23. Govrin, E. M., & Levine, A. (2000). The hypersensitive response facilitates plant infection by the necrotrophic pathogen *Botrytis cinerea*. *Current Biology*, *10*, 751-757.
24. Habibi, G. (2014). Hydrogen peroxide (H_2O_2) generation, scavenging and signaling in plants. In Ahmad, P. (Ed.), *Oxidative Damage to Plants: Antioxidant networks and signaling* (pp. 557-584). Elsevier Inc.
25. Hartman, G. L., Rupe, J. C., Sikora, E. J., Domier, L. L., Davis, J. A., & Steffey, K. L. (Eds.). (2015). *Compendium of Soybean Diseases and Pests*. American Phytopathological Society, St. Paul, MN, USA.
26. Hemmati, P., Zafari, D., Mahmoodi, S. B., Hashemi, M., Gholamhoseini, M., Dolatabadian, A., & Ataei, R. (2018). Histopathology of charcoal rot disease (*Macrophomina phaseolina*) in resistant and susceptible cultivars of soybean. *Rhizosphere*, *7*, 27-34.
27. Hira, N., Akram, N. A., & Muhammad, A. (2016). Impact of ascorbic acid on growth and some physiological attributes of cucumber (*Cucumis sativus*) plants under water-deficit conditions. *Pakistan Journal of Botany*, *48*, 877-883.
28. Hossain, M. A., Bhattacharjee, S., Armin, S. M., Qian, P., Xin, W., Li, H. Y., Burritt, D. J., Fujita, M., & Tran, L. S. P. (2015). Hydrogen peroxide priming modulates abiotic oxidative stress tolerance: insights from ROS detoxification and scavenging. *Frontiers in Plant Science*, *6*, 420.
29. Islam, M.S.; Haque, M.S.; Islam, M.M.; Emdad, E.M.; Halim, A.; Hossen, Q.M.; Hossain, M.Z.; Ahmed, B.; Rahim, S.; Rahman, M.S.; Alam, M.M.; Hou, S.; Wan, X.; Saito, J.A.; Alam M. (2012). Tools to kill: genome of one of the most destructive plant pathogenic fungi *Macrophomina phaseolina*. *BMC Genomics*, *13*, 1-16.
30. Jones, J. D., & Dangl, J. L. (2006). The plant immune system. *Nature*, *444*, 323-329.
31. Khan, A., & Ashraf, M. (2008). Exogenously applied ascorbic acid alleviates salt-induced oxidative stress in wheat. *Environmental and Experimental Botany*, *63*, 224-231.
32. Krzywinski, M., & Altman, N. (2014). Visualizing samples with box plots. *Nature Methods*, *11*, 119-120.

33. Liu, Y. H., Offler, C. E., & Ruan, Y. L. (2014). A simple, rapid, and reliable protocol to localize hydrogen peroxide in large plant organs by DAB-mediated tissue printing. *Frontiers in Plant Science*, *5*, 745.
34. Marquez, N., Giachero, M. L., Declerck, S., & Ducasse, D. A. (2021). *Macrophomina phaseolina*: General characteristics of pathogenicity and methods of control. *Frontiers in Plant Science*, *12*, 634397.
35. Masi, M.; Sautua, F.; Zatout, R.; Castaldi, S.; Arrico, L.; Isticato, R.; Pescitelli, G.; Carmona, M. A.; Evidente, A. (2021). Phaseocyclopentenones A and B, phytotoxic penta-and tetrasubstituted cyclopentenones produced by *Macrophomina phaseolina*, the causal agent of charcoal rot of soybean in Argentina. *Journal of Natural Products*, *84*, 459-465.
36. Maurino, V. G., & Flügge, U. I. (2008). Experimental systems to assess the effects of reactive oxygen species in plant tissues. *Plant Signaling & Behavior*, *3*, 923-928.
37. Miguel, G., Fontes, C., Martins, D., Neves, A., & Antunes, D. (2006). Effects of postharvest treatment and storage time on the organic acid content in Assaria and Mollar pomegranate (Punica grantum L.) fruit. *Italian Journal of Food Science*, 18, 317-322.
38. Millet, Y. A., Danna, C. H., Clay, N. K., Songnuan, W., Simon, M. D., Werck-Reichhart, D., & Ausubel, F. M. (2010). Innate immune responses activated in *Arabidopsis* roots by microbe-associated molecular patterns. *The Plant Cell*, *22*, 973-990.
39. Mittler, R., Vanderauwera, S., Gollery, M., & Van Breusegem, F. (2004). Reactive oxygen gene network of plants. *Trends in Plant Science*, *9*, 490-498.
40. Nandini, Y., & Samir, S. (2016). Reactive oxygen species, oxidative stress and ROS scavenging system in plants. *Journal of Chemical and Pharmaceutical Research*, *8*, 595-604.
41. Nath, M., Bhatt, D., Prasad, R., Gill, S. S., Anjum, N. A., & Tuteja, N. (2016). Reactive oxygen species generation-scavenging and signaling during plant-arbuscular mycorrhizal and Piriformospora indica interaction under stress condition. *Frontiers in Plant Science*, *7*, 1574.
42. Noctor, G., & Foyer, C. H. (1998). Ascorbate and glutathione: Keeping active oxygen under control. *Annual Review of Plant Biology*, *49*, 249-279.
43. Noctor, G., Mhamdi, A., & Foyer, C. H. (2014). The roles of reactive oxygen metabolism in drought: not so cut and dried. *Plant Physiology*, *164*, 1636-1648.

44. Rivero, R. M., Mittler, R., Blumwald, E., & Zandalinas, S. I. (2022). Developing climate-resilient crops: Improving plant tolerance to stress combination. *The Plant Journal*, *109*, 373-389.
45. Rogers, L. W., & Koehler, A. M. (2021). Nondestructive sampling to monitor *Macrophomina phaseolina* root colonization in overwintering *Stevia*. *Plant Health Progress*, *22*, 151-153.
46. Saleh, A. A., Ahmed, H. U., Todd, T. C., Travers, S. E., Zeller, K. A., Leslie, J. F., & Garrett, K. A. (2010). Relatedness of *Macrophomina phaseolina* isolates from tallgrass prairie, maize, soybean and sorghum. *Molecular Ecology*, *19*, 79-91.
47. Sarkar, T. S., Biswas, P., Ghosh, S. K., & Ghosh, S. (2014). Nitric oxide production by necrotrophic pathogen Macrophomina phaseolina and the host plant in charcoal rot disease of jute: complexity of the interplay between necrotroph–host plant interactions. *PLoS One*, *9*, e107348.
48. Shao, H. B., Chu, L. Y., Lu, Z. H., & Kang, C. M. (2008). Primary antioxidant free radical scavenging and redox signaling pathways in higher plant cells. *International Journal of Biological Sciences,* 4, 8.
49. Su, G., Suh, S. O., Schneider, R. W., & Russin, J. S. (2001). Host specialization in the charcoal rot fungus, *Macrophomina phaseolina*. *Phytopathology*, *91*, 120-126.
50. Tsugane, K., Kobayashi, K., Niwa, Y., Ohba, Y., Wada, K., & Kobayashi, H. (1999). A recessive Arabidopsis mutant that grows photoautotrophically under salt stress shows enhanced active oxygen detoxification. *The Plant Cell*, *11*, 1195-1206.
51. Turkan, I. (2018). ROS and RNS: Key signalling molecules in plants. *Journal of Experimental Botany*, *69*, 3313.
52. Twizeyimana, M., Hill, C. B., Pawlowski, M., Paul, C., & Hartman, G. L. (2012). A cut-stem inoculation technique to evaluate soybean for resistance to *Macrophomina phaseolina*. *Plant Disease*, *96*, 1210-1215.
53. Van Doorn, W. G., & Ketsa, S. (2014). Cross reactivity between ascorbate peroxidase and phenol (guaiacol) peroxidase. *Postharvest Biology and Technology*, *95*, 64-69.
54. Veljovic-Jovanovic, S., Noctor, G., & Foyer, C. H. (2002). Are leaf hydrogen peroxide concentrations commonly overestimated? The potential influence of artefactual interference by tissue phenolics and ascorbate. *Plant Physiology and Biochemistry*, *40*, 501-507.

55. Ye, N.; Zhu, G.; Liu, Y.; Zhang, A.; Li, Y.; Liu, R.; Shi, L.; Jia, L.; Zhang, J. (2012). Ascorbic acid and reactive oxygen species are involved in the inhibition of seed germination by abscisic acid in rice seeds. *Journal of Experimental Botany*, *63*, 1809-1822.
56. Živanov, S.T.; Dedić, B.D.; Dimitrijević, A.; Dušanić, N.; Jocić, S.; Miklič, V.; Kovačević, B.; Miladinović, D. (2019). Analysis of genetic diversity among *Macrophomina phaseolina* (Tassi) Goid. isolates from Euro-Asian countries. *Journal of Plant Diseases and Protection*, *126*, 565-573.

TABLES AND FIGURES

Table 2.1. ANOVA results for three isolates of *M. phaseolina* grown on L-ascorbic acid at 1 to 5 days post-plating (D1 to D5).

Source	DF		D1	D2	D3	D4	D5
Model	31	*F*	37.89	62.52	160.95	172.64	34.51
		P	< 0.0001	< 0.0001	< 0.0001	< 0.0001	< 0.0001
Replication	2	*F*	1.16	0.96	1.59	3.58	0.21
		P	0.3208	0.3891	0.2128	0.0341	0.8073
Isolate (I)	2	*F*	5.23	7.25	25.77	37.01	114.24
		P	0.0082	0.0015	< 0.0001	< 0.0001	< 0.0001
Concentration (C)	9	*F*	120.26	210.35	542.98	580.33	114.24
		P	< 0.0001	< 0.0001	< 0.0001	< 0.0001	< 0.0001
I x C	18	*F*	4.42	1.59	2.66	2.64	1.30
		P	< 0.0001	0.0933	0.0025	0.0027	0.2244

Table 2.2. ANOVA results for H_2O_2 concentrations (mM) in soybean stem tissue after selected treatments with L-ascorbic acid.

Source	DF[1]	SS	MS	*F*	*P*
Model	5	20299.7	4059.95	17	0.0017
Replication	2	426.16	213.08	0.89	0.458
Treatment	3	19873.6	6624.52	27.73	0.0006
Error	6	1433.28	238.88		
Total	11	21733			

[1]DF = degrees of freedom, SS = sum of squares, MS = mean squares, *F* = *F*-statistic, *P* = *P*-value

Table 2.3. Pre-treatments and treatments used in the soybean seedling stem necrosis assay.

Pre-treatment (Day –1)	**Treatment (Day +0)**
No pre-treatment	Agar plug Inoculate w/ MP[1] H_2O_2
Agar plug	L-ascorbic acid (LAA; reduced) Dehydroascorbic acid (DHAA; oxidized)
Inoculate w/ MP	LAA DHAA
LAA	Agar plug Inoculate w/ MP
DHAA	Agar plug Inoculate w/ MP
H_2O_2	Inoculate w/ MP

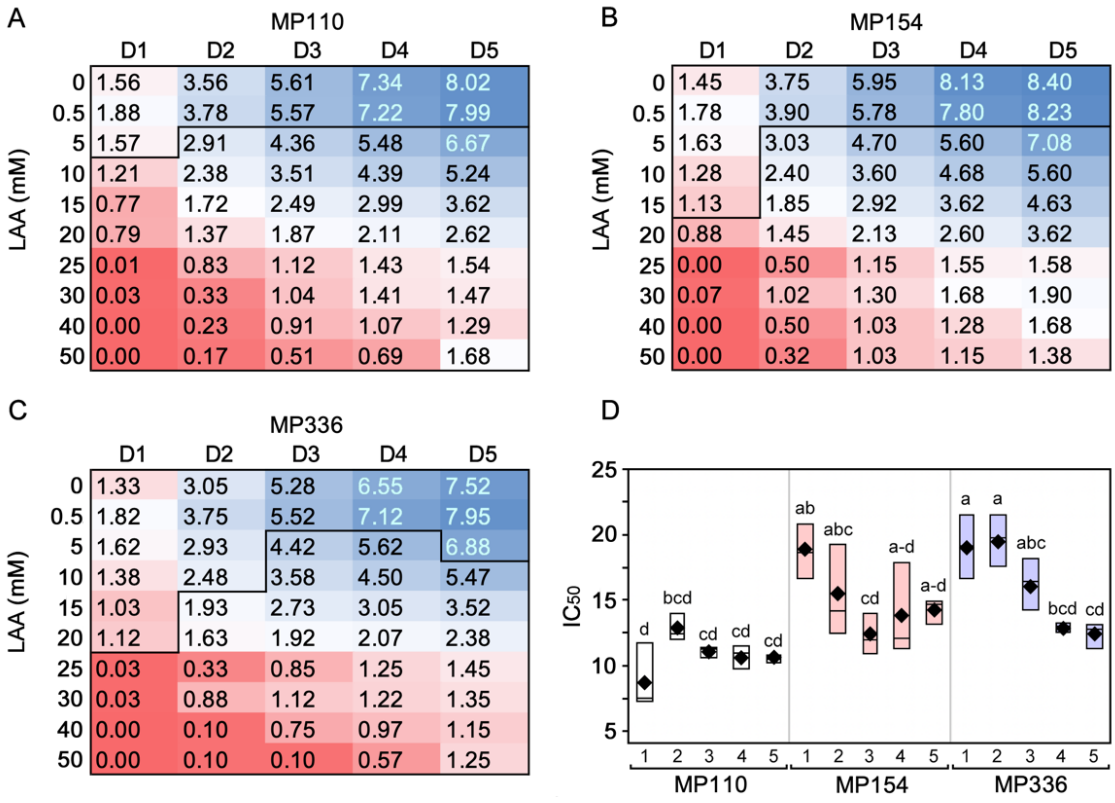

Figure 2.1. Diameters of three isolates of *Macrophomina phaseolina* (MP110, -154, and -336) grown on 0 to 50 mM L-ascorbic acid (LAA)-amended $^{1/4}$-strength PDA. Average colony growth (cm) of MP110 (A), MP154 (B), and MP336 (C). BOX plots show IC50 values (D).

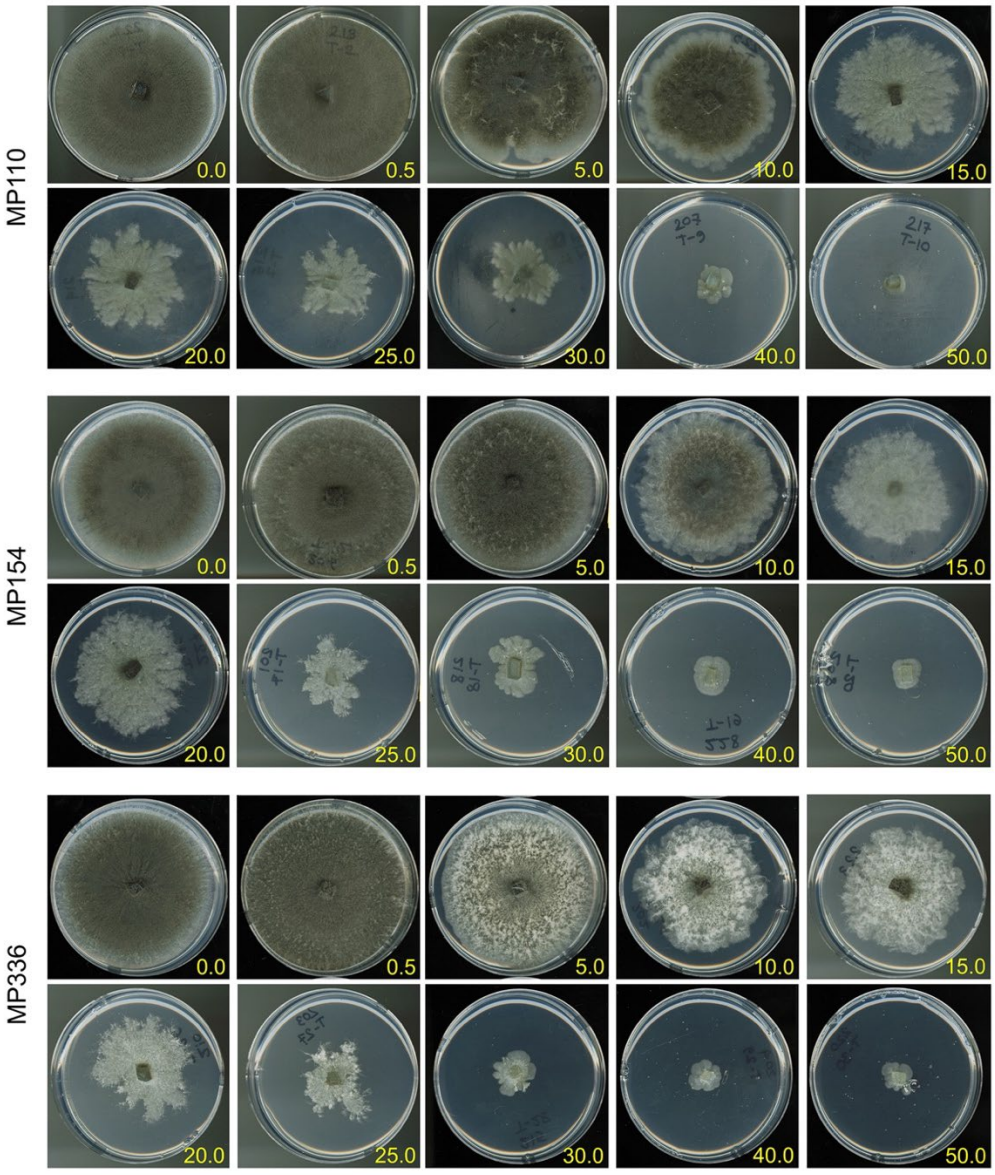

Figure 2.2. *Macrophomina phaseolina* growth morphology on varying concentrations of L-ascorbic acid. Three soybean isolates (MP110, -154, and -336) were grown on $^{1/4}$-strength PDA amended with 0 to 50 mM L-ascorbic acid.

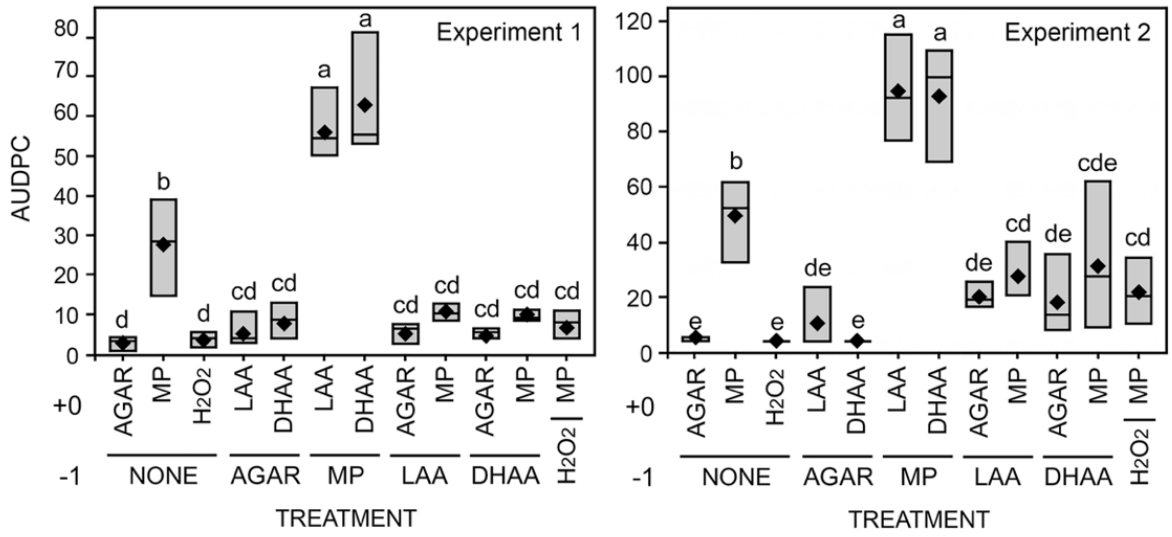

Figure 2.3. Area under the disease progress curve (AUDPC) for lesion development in the greenhouse cut-stem assay experiments. *Abbreviations*: DHAA = dehydroascorbic acid; LAA = L-ascorbic acid, MP = *M. phaseolina*. Black diamonds repreasents mean value.

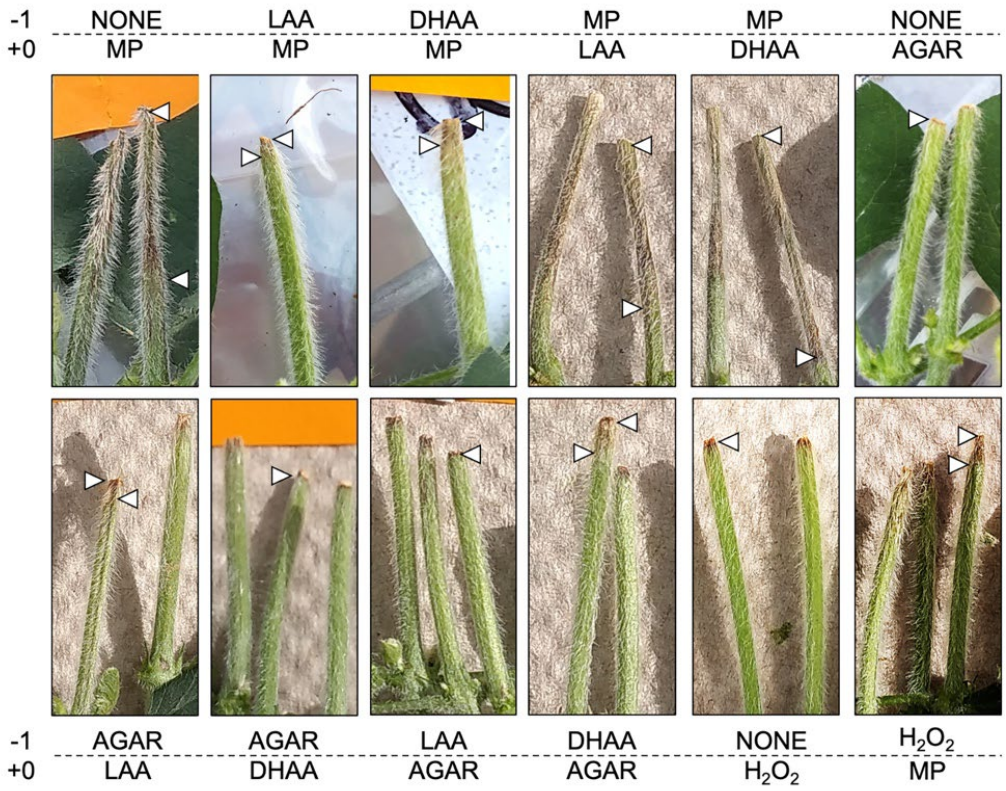

Figure 2.4. Representative soybean cut-stem pathogenicity assay lesion development after treatments were applied in the experiment. -1 indicates pre-treatment and +0 indicates post-treatment. White arrows indicate the approximate extent of necrotic lesions in stem.

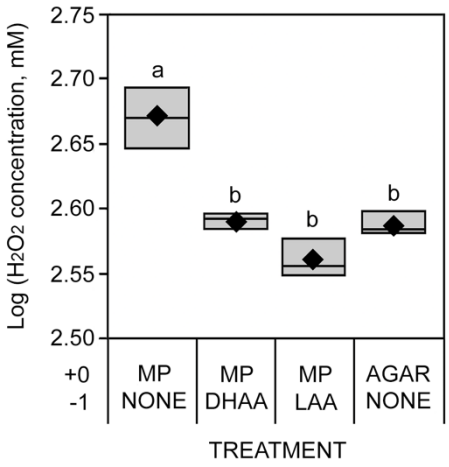

Figure 2.5. Ascorbic acid quenches pathogen-mediated H_2O_2 generation in the soybean cut-stem assay. Pre-treatments are denoted by "-1" and post-treatments are denoted by "+0". Abbreviations: DHAA = dehydroascorbic acid, LAA = L-ascorbic acid, MP = *M. phaseolina*.

Figure 2.6. Lesion development on soybean variety 'AG3039' after inoculation with agar plug ($^{1/4}$-strength PDA plug; "Control") and *M. phaseolina* ("+MP") using the cut-stem assay. White arrows indicate unifoliate nodes.

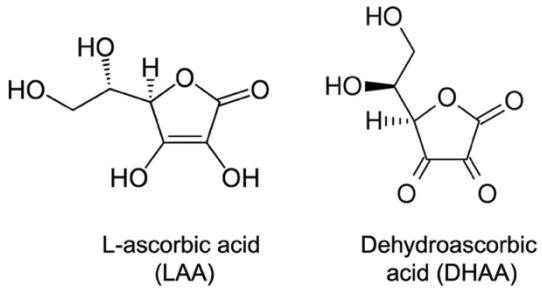

Figure 2.7. Reduced (L-ascorbic acid, LAA) and oxidized (dehydroascorbic acid, DHAA) used in this study.

Chapter 3 - RNA-seq analysis to reveal genes associated with *M. phaseolina* induced senescence in soybean stem

ABSTRACT

Charcoal rot of soybean is caused by the global crop destroyer hemibiotrophic fungus *Macrophomina phaseolina* (MP) and is an important pathogen in the midwestern USA. The quantitative nature of host resistance and the complexity of understanding soybean-*M. phaseolina* interaction in the molecular level resists the improvement in resistance breeding. In the previous chapter experiment showed L-ascorbic acid (LAA) pre-treatment following *M. phaseolina* inoculation reduced lesion length in the soybean stem. In this chapter the objective was to reveal genes associated with *M. phaseolina*-induced senescence. A *M. phaseolina* -resistant and -susceptible genotypes were used and a cut-stem method was used for inoculation, LAA and hydrogen peroxide (H_2O_2)-an oxidative stress inducer, application. RNA was extracted from the soybean stem and sequenced with three high output 75 cycles (1×75 bp) run on the NextSeq 500 Sequencing System (Illumina®). In the resistant and susceptible genotypes more genes were down-regulated than up-regulation when compared between MP-inoculated vs. mock-inoculated control. Gene Ontology (GO) term and KEGG pathways analysis detected MP induced up-regulation on receptor like kinases genes while down-regulated larger number of genes related to antioxidant, defense and hormonal pathways in both genotypes. Ascorbic acid pre-treatment induced higher number of genes related to photosynthesis and response to reactive oxygen species in both genotypes. Exogenous H_2O_2 pre-treatment following inoculation induced larger number of stress responsive genes in the up-regulated category while down-regulated hormonal signal transduction and photosynthesis related genes in both genotypes. The results of DE, GO, and pathway analysis suggest genes associated with MP-induced senescence in soybean.

INTRODUCTION

Soybean (*Glycine max* (L.) Merr.) is an economically important field crop produced in many countries of the world that contributes to global food security. Charcoal rot of soybean is caused by the aggressive polyphagous soilborne hemibiotrophic fungus *Macrophomina phaseolina* (Tassi.) Goid. This is an important and common root rot disease of soybean that negatively impacts crop quality and causes considerable economic loss especially in dry and non-irrigated cropping regions (Romero Luna et al., 2017). Soybean charcoal rot disease is prevalent in many parts of the United States since the disease was first described from the US in 1949 (Young, 1949). Considering the economic impact, this disease is among the most important soybean diseases from the past 20 years (Romero Luna et al., 2017).

M. phaseolina is ubiquitous, adapted to diverse geography, and management is critical as the primary inoculum source microsclerotia's longevity is high (nearly 2-15 years) (Short et al., 1980; Baird et al., 2003; Gupta et al., 2012, Reis et al., 2014). The fungus infects the root and stem tissue of the plant. Charcoal rot is induced by external environmental factors including drought or limited soil moisture and higher temperature. Progression of the fungus from the soybean root to the stem eventually blocks the vascular bundles of the plant and induces wilting and death; causes considerable economic loss as reported from the United States in 2006, total soybean yield loss due to charcoal rot was 497.6 thousand metric tons (Smith and Wyllie, 1999; Mengistu et al., 2007; Wrather et al., 2010). Charcoal rot disease management is critical as the fungus remains in an endophytic stage after infecting the roots without any external symptoms. Disease symptoms are visible after the fungus switches from an endophytic biotrophic phase to a necrotrophic phase (Chowdhury et al., 2017) where visible symptoms include wilting, leaf chlorosis, and plant death. Considering this phenomenon of charcoal rot disease progression, genetic resistance could be an effective and eco-friendly control measure. However, genetic mechanism of charcoal rot resistance in soybean remains unknown due to the complex molecular mechanisms underlying the host-pathogen interaction.

Since *M. phaseolina* is a generalist, resistance genes related to charcoal rot disease has not been reported. Transcriptome analysis will shed light on a better understanding of molecular and cellular responses induced in response to *M. phaseolina*.

Plants possess two layers of defense mechanisms against biotic and abiotic stressors, pattern triggered immunity (PTI) and effector triggered immunity (ETI). After the establishment of the plant innate immunity theory, PTI and ETI are known as the key regulators of plant and pathogen co-evolution (Jones and Dangle, 2006). PTI and ETI operate simultaneously in defense signaling and downstream defense of plants on the physiological level, the reactive oxygen species (ROS) burst is the first sign of defense signaling that activates the mitogen-activated protein kinase (MAPK) pathway and callose deposition (Nicaise et al., 2009). However, the accumulation of ROS intermediates including superoxide anions or H_2O_2 could cause oxidative damage to lipids, proteins, nucleic acids, and the photosynthetic machinery (Yan et al., 2021); this damage could be utilized by the necrotroph like *M. phaseolina* as studies from the necrotroph *Rhizoctonia solani*-wheat (Foley et al., 2016) and *Phytophthora infestans*-Potato (Chung et al., 2019) pathosystems showed this phenomenon. Plants also generate antioxidants such as superoxide dismutase (SOD), catalase (CAT), and peroxidase (PX) to reduce or eliminate ROS. Zhang et al. (2006) found that major ROS, including H_2O_2 could be scavenged by PX and the toxic biproduct of the reaction could eliminate the *Verticillium dahliae* proliferation. However, it is anticipated that necrotrophic invasion might take place before antioxidant accumulation. Several previous studies have established the basis of this speculation. A microarray experiment using *R. solani*-inoculated wheat lines showed significant number of expressed wheat genes associated with reactive oxygen species (ROS) and redox regulation. Similarly, two ROS/redox regulation-related genes were expressed in *R. solani* that were homologous to a *Alternaria brassicicola* ROS regulation gene, which suggested the simultaneous interaction of ROS related genes from the host and pathogen results the pathogenesis in the host (Foley et al., 2016). A study by Rossi et al. (2017) showed the role of chloroplast generated ROS in the pathogenesis of the necrotrophic fungus *Botrytis cinerea*. These authors used two transgenic tobacco (*Nicotiana tabacum*) lines that generated lower ROS in the chloroplast due to expression of a plastid-targeted cyanobacterial flavodoxin protein (the transgenic lines were named as *pfld* lines), demonstrated reduced fungal invasion, host tissue damage and fungal growth compared to the wild-type tobacco line. This research outcome showed nearly 70-80% less ROS accumulation induced by the *B. cinerea* suggested that by expressing a heterologous antioxidant protein the chloroplastic level of ROS induced by the necrotrophic pathogen could be reduced and plant health could be rescued (Rossi et al., 2017).

Host plasma membrane associated receptors contribute to fungal pathogenicity following secretion of enzymes to assist pathogen entry into the host (Zipfel and Felix, 2005; Deshmukh and Tiwari, 2021). Fungi counter host defense arsenals by secreting degradative enzymes and through other converging cascades including kinase receptors, pathogenesis-related genes, and hormone-mediated defense signal pathways that work together against the biotic stress induced by the pathogen (Deshmukh and Tiwari, 2021). The transcriptional response induced by *M. phaseolina* from a resistant and susceptible soybean genotype revealed hormone-signaling, secondary metabolites biosynthesis, and transcriptional reprogramming-related genes were commonly expressed as an infection response to the fungus (Deshmukh and Tiwari, 2021). They also proposed WRKY, LysM-RLK, and flavonoid pathway-associated genes as a potential source of resistance to *M. phaseolina* in soybean, as those defense related genes were differentially up-regulated particularly in the resistant genotype as an infection response (Deshmukh and Tiwari, 2021).

To understand the host resistance and susceptibility mechanisms for charcoal rot disease Bandara et al. (2019) studied the oxidative stress and antioxidant response induced by *M. phaseolina* from both resistant and susceptible sorghum genotypes. The transcriptome assay revealed around 96 differentially expressed genes between both genotypes that were related to oxidative stress and antioxidant machinery. Also, the functional biochemical experiments revealed significantly higher amounts of reactive oxygen species (ROS) and reactive nitrogen species from the susceptible genotype represented by higher peroxidase activity from the susceptible genotypes and catalase activity from the resistant genotype (Bandara et al., 2019).

It was previously hypothesized that *M. phaseolina* induces oxidative stress-mediated senescence in the host. To address this hypothesis, a study was conducted with pre-treatment of exogenous application of ascorbic acid to observe whether ascorbic acid functions as a reactive oxygen scavenger and can rescue the soybean plant health from the oxidative stress induced by *M. phaseolina*. Also, whether ROS like H_2O_2 induce oxidative stress and if the oxidative stress is utilized by the subsequent inoculation with *M. phaseolina* was studied using exogenous pre-treatment with H_2O_2 and pre-treatment following inoculation with *M. phaseolina*. This study resulted reduced charcoal rot lesion in the soybean stem compared to the inoculated control.

L-ascorbic acid (LAA) is a plant-derived antioxidant which is commonly known as vitamin C. LAA is water soluble and performs several physiological activities along with stress tolerance in plants (Chapman et al., 2019). As a ROS scavenger, ascorbic acid participates in the plant enzymatic reaction by donating electrons. The mechanism of L-ascorbic acid in scavenging ROS such as H_2O_2 is to convert in monodehydroascorbate either by reacting with free radicals and Fe^{3+} or by ascorbate peroxidase that catalyzes and convert H_2O_2 to water (H_2O) (Noctor and Foyer, 1998). L-ascorbic acid-altered mutants (*vtc* mutants) have been developed in *Arabidopsis*. These show a 5-fold decrease in ascorbic acid levels and although the mutations don't interfere with plant growth and development, but its capability in abiotic stress tolerance greatly compromised (Conklin et al., 1996). The biotic stress tolerance conferred by L-ascorbic acid is complex and depends on pathogen type. For biotrophic pathogen reduced level of L-ascorbic acid provided protection against oxidative damage induced by the pathogen (Pavet et al., 2005; Mukherjee et al., 2010), while in the necrotrophs higher levels of ascorbic acid enhanced resistance against pathogens (Botgana et al., 2012). It has been reported that ascorbic acid reduces disease symptoms in several pathosytems. Chung et al. (2019) investigated the role of ascorbic acid in eliminating necrotic stress induced by the necrotrophic pathogen *Phytophthora infestans* from transgenic potato plants overexpressing a D-galacturonic acid reductase gene with enhanced levels of ascorbic acid. The study revealed reduced necrotic lesions and disease symptoms in the transgenic potato plant compared to control. Also, biomarkers of oxidative stress such as hydrogen peroxide (H_2O_2) and malondialdehyde (MDA) levels were significantly lower in the transgenic plant suggesting the role of ascorbic acid in scavenging ROS and alleviating oxidative stress (Chung et al., 2019). The findings of this study suggested that ascorbic acid accumulation induced enhanced cellular antioxidant levels, plant pathogenesis-related genes, and defense related hormonal pathways assist in reduced disease symptoms (Chung et al., 2019).

Botanga et al. (2012) showed that inoculation of *Arabidopsis* with *Alternaria brassicicola* reduced the ascorbate level of the host, and the host's redox status became imbalanced, which promoted disease severity. This study also suggested a potential role of ascorbate in eliminating pathogen induced ROS to contribute on host's redox homeostasis, as we see from the reduced level of ascorbate in the inoculated plant (Botanga et al., 2012).

To reveal potential mechanisms of how ascorbic acid reduces charcoal rot symptoms in the inoculated plant, and the role of H_2O_2 in oxidative stress-mediated senescence, transcriptome analysis was necessary to screen the associated genes and pathways. Transcriptome analysis assists in understanding the actual state of a cell or tissue induced by a specific condition or any added stresses (Saliba et al., 2014). An RNA-seq experiment was conducted to analyze the global transcriptome profiles from ascorbic acid pre-treated & inoculated plants, non-pretreated & inoculated plants, control plants, H_2O_2 pre-treated & inoculated plants, and H_2O_2 treated control plants.

The soybean genome (1.1 GB) sequence accelerated genomic research that assists in dissecting the genetic basis of traits in soybean and aids in soybean breeding (Schmutz et al., 2010). Changes in genetic architecture in response to *M. phaseolina* inoculation and ascorbic acid and H_2O_2 application pre-treatment could be studied effectively from the transcriptome profile of soybean. Pairwise comparison of treatments within and between genotypes will reveal the specific genes and pathways associated with oxidative stress and resistance or susceptibility responses induced by the exogenous application and inoculation. The objective of the study was (i) to determine whether oxidative stress-related genes were expressed or affected due to inoculation with *M. phaseolina*; (ii) if plant antioxidant/ROS or oxidative scavenging-related genes were expressed or affected by pre-treatment with ascorbic acid following *M. phaseolina* inoculation; (iii) if H_2O_2 pre-treatment following inoculation with *M. phaseolina* induced enhanced expression of oxidative stress and pathogenesis-related genes; and (iv) if host susceptibility or defense-related genes differ between resistant and susceptible soybean genotypes.

MATERIALS AND METHODS

Soybean genotypes, plant growth, *Macrophomina phaseolina* isolates, experimental design, inoculation, and plant sample collection

Two soybean genotypes DT97-4290 (*M. phaseolina*-resistant line) and Pharaoh (*M. phaseolina*-susceptible line) were used for this experiment. This experiment was conducted in the Throckmorton Plant Sciences greenhouse facilities located at Kansas State University, Manhattan, Kansas, USA.

The experimental design was a RCBD with factorials and there were three replications. Two genotypes and six treatments resulted in a 2 × 6 factorial design for this experiment (Table 3.1).

For each treatment, six soybean seeds were planted in a 5 × 5 in. pot with the vermiculite (Therm-O-Rock East, Inc., USA) mix soil (silt loam soil mixed with Vermiculite in 1:1 ratio), and seedlings were thinned to four plants per pot once they were at the cotyledonary stage (VC). The remaining seedlings were grown until the 2nd trifoliate (V2) stage.

The *M. phaseolina* isolate used for this experiment (MP0336) is an aggressive soybean isolate. The isolate was grown on a 1/4-strength potato dextrose agar (PDA) media for 5 days. Younger portions of the colony edge were cut into a circular cylinder using the 200 µl micropipette. The mycelia side of the agar plug was directly placed onto the cut stem point for the inoculation

The cut-stem inoculation method of Twizeymania et al. (2012) was followed for this experiment. The apical portion of V2 soybean seedlings were cut 25 mm above the unifoliate node. Inverted two hundred µl micropipette tubes containing one of the pre-treatments and treatments listed in Table 1 were placed on the cut portion of the seedling. The inoculation or treatment with agar plug, and H_2O_2 were applied to the respective soybean plants 48 hrs after stem clipping or pre-treatment with ascorbic acid or H_2O_2.

Stem tissue was collected 48 hours after applying the final treatment (*M. phaseolina* inoculation, agar plug, or H_2O_2 application). The stem was clipped from the unifoliate node region and immediately put in liquid nitrogen to freeze tissue. Stem tissues of three biological replicates and twelve treatments (3 × 12 = 36 samples) were stored in 1.5 ml tubes. Each sample tube contained four clipped soybean stems from individual plants. Stem tissue was stored at -80˚C until grinding.

Sample preparation and RNA extraction

Soybean stem tissues from each sample tube were pooled and ground using a mortar, pestle, and liquid nitrogen. Powdered stem tissues were transferred to 1.5 ml tubes and stored in the -80˚C freezer before RNA extraction. Total RNA was extracted from the soybean tissue powder using Qiagen RNeasy mini-Plant kit (Qiagen Inc., USA) following the manufacturers protocol. RNA

quality and quantity were tested using the Nanodrop Spectrophotometer (Nanodrop one) (ThermoFisher Scientific, USA). The RNA integrity number (RIN) was checked using an Agilent 2100 Bioanalyzer (Agilent Technologies Genomics, USA).

cDNA library preparation and Illumina sequencing

One μg of high-quality total RNA was taken for RNA sequencing (RNA-seq) library construction using the TruSeq Stranded mRNA Library prep kit (Illumina Inc., USA). RNA-seq libraries were barcoded with TruSeq RNA CD dual 8 bp indexes (Illumina Inc., USA). Three pools, twelve libraries each, were created and sequenced with three high output 75 cycles (1 × 75 bp) runs on the NextSeq 500 Sequencing System according to the manufacturers protocol (Illumina Inc., USA). The library preparation and sequencing were conducted at the Kansas State University Integrated Genomics Facility (IGF) lab.

Raw sequence processing for quality check and soybean reference genome alignment

The adapter trimmed single-end sequence read were checked for phred quality score using the FastQC quality test. The FastQC resulted average phred quality score > 30. Sequence data were not needed to perform any quality trimming. Next, sequence reads were aligned with the soybean (Glycine_max_v2.1) reference genome. The soybean genome FASTA file and gene annotation file (gtf file) was downloaded from the EnsemblPlants database (*e! EnsemblPlants*). The genome FASTA file and annotation file were indexed bioinformatically using the clustered computer (Beocat, K-State) before aligning with the sequence read. STAR (Spliced Transcripts Alignment to a Reference) genome mapper software was used for sequence alignment with the reference genome (Dobin et al., 2013). The STAR genome aligner generated reads per gene count data for all 36 samples. The reads per gene count data were used for downstream analysis.

Differential gene expression analysis

Differential gene expression analysis was performed using the reads per gene count data (derived after mapping with the reference genome) and the "DESeq2" R package (Love et al., 2014). The DESeq2 tool uses a model based on the negative binomial distribution (Love et al., 2014). DEseq2

package allows the differential analysis of read count data per gene by estimating dispersion and fold changes (Love et al., 2014). The differential gene expression tool DeSeq2 executes the statistical test from the read per gene count data to find the statistically significant genes, gene expression scenario (up or down-regulation), and the magnitude of difference between each gene when pairwise comparisons are considered (McDermaid et al., 2018). All possible pairwise comparisons between samples were performed among the 36 samples to find the significantly and differentially expressed genes between two different conditions. To control the false discovery rates (FDR) at the 5% level between multiple comparisons and hypothesis testing a *q*-value (Benjamin and Hochberg, 1995) was determined. The differentially expressed genes with *q*-value < 0.05 were considered to control FDR at the 5% level. The pairwise comparison for differential expression was performed at two levels, between the soybean genotypes (resistant and susceptible) for the same treatment and between two different treatments of the same genotype (resistant or susceptible). Genes with a *q*-value < 0.05 were considered as significantly and differentially expressed (null hypothesis rejected) with 5% FDR. The statistical hypothesis tested for the DeSeq2 analysis are as follows:

H_0: Resistant genotype (trt1–trt6) = Susceptible genotype (trt1–trt6)

H_A: Resistant genotype (trt1–trt6) ≠ Susceptible genotype (trt1–trt6)

Another level of statistical hypothesis testing was between two different treatments of the same genotypes. The six different hypotheses tested across two genotypes were:

Hypothesis #1

H_0: mock-inoculated control = Inoculated

H_A: mock-inoculated control ≠ Inoculated

Hypothesis #2

H_0: Ascorbic acid-pretreated & inoculated = Inoculated

H_A: Ascorbic acid-pretreated & inoculated ≠ Inoculated

Hypothesis #3

H_0: Ascorbic acid pretreated & inoculated = Ascorbic acid-pretreated control

H_A: Ascorbic acid pretreated & inoculated ≠ Ascorbic acid-pretreated control

Hypothesis #4

H_0: Ascorbic acid-pretreated & inoculated = H_2O_2 pretreated & inoculated

H_A: Ascorbic acid-pretreated & inoculated ≠ H_2O_2 pretreated & inoculated

Hypothesis #5

H_0: Ascorbic acid-pretreated control = H_2O_2 pretreated & inoculated

H_A: Ascorbic acid-pretreated control ≠ H_2O_2 pretreated & inoculated

Hypothesis #6

H_0: Non pretreated H_2O_2 applied control = H_2O_2 pretreated inoculated

H_A: No pretreated H_2O_2 applied control ≠ H_2O_2 pretreated inoculated

Genes with the *q*-value < 0.05 with null hypothesis rejected at 5% FDR were considered significantly and differentially expressed between treatments of the same genotype.

Functional gene annotation using gene ontology GO term and KEGG pathway analysis using ShinyGO bioinformatics platform

The gene ontology (GO) term analysis was performed using the R software package "goseq" to detect significantly enriched GO terms for differentially expressed genes from the DEseq2 analysis. The gene to GO term (GO functional annotations) was obtained using the genes text file and xref.genes file from the EnsemblPlants (*e! EnsemblPlants*) and running the gene to GO term code in R software. The significantly enriched GO terms were based on a *p*-value cutoff of 0.05. Gene ontology GO terms differentiated genes into their respective biological processes (BP), molecular functions (MF), and cellular components (CC).

The genes associated with the enriched GO terms were pasted on the ShinyGO bioinformatic online platform from the South Dakota State University to discover Kyoto Encyclopedia of Genes and Genomes (KEGG)-associated pathways and gene functions (ShinyGO 0.76.1). This KEGG pathway analysis is based on the number of genes associated to the respective pathway with their log fold enrichment.

Weighted Gene Coexpression Network Analysis (WGCNA)

Weighted gene co-expression network analysis utilizes the gene correlation patterns through Pearson correlation coefficients to predict gene co-expression similarity within different samples. Through this method of gene co-expression similarity, highly interconnected genes with their correlation and phenotypes could be described. The WGCNA analysis was performed using the WGCNA package version 1.69 (Langfelder and Horvath, 2008) in R. WGCNA calculates gene co-expression in two steps. In the first step, it measures the gene network adjacency using the power function and equation $a_{ij} = | cor (x_i, x_j)|^{\beta}$, where a_{ij} is the adjacency matrix between two genes *i* and *j*, β is the soft thresholding parameter. In the second step, it clusters genes into network modules using the topological overlap module (TOM) method. The TOM method combines the adjacency of the two genes and their connection with other neighboring genes. The RPM normalized count matrix of gene expression data of all 12 samples were considered for the WGCNA analysis. Filtering was done to remove low expression genes; only gene counts > 350 genes were considered for the WGCNA analysis. The scale free gene co-expression network module was generated using the RPM normalized count matrix transformed by log2 considering the "mergeCutHeight" of 0.25 and "minModuleSize" of 100. The correlation coefficient between eigengens of modules and samples were calculated to determine biological significance of the modules.

RESULTS

Correlation analysis between biological replicates of normalized read count data/reads per kilobase per million mapped reads (RPKM) for all samples

The correlation analysis between biological replicates of the same treatment and genotypes (resistant and susceptible) for the reads per kilobase per million mapped reads (RPKM) was performed to test the gene count consistency within biological replicates of the samples. The higher R^2 value (R^2 value close to 1) indicates strong correlation between biological replicates within the same sample. This strong correlation within biological replicates also validates the RNA-seq data by exhibiting consistent and reliable gene expression. The scatter plot of the correlation analysis

between biological replicates of treatments and genotypes is given in Fig. 3.1. Out of 36 scatter plots from the 36 samples, 12 example scatter plots are presented in Fig. 3.1.

Alignment of the RNA-seq reads with the reference genome

The total input raw sequence read across all 36 sample is around 1311 million (1,311,492,419 reads) with total uniquely mapped read with the reference genome is around 1000 million (1,000,008,672 reads). The summary of the read count data across all three biological replicates and 36 samples is given in Table 3.2.

Differential gene expression analysis

Differential gene expression analysis was performed by comparing within six treatments for both resistant and susceptible genotypes. Differential gene expression analysis between pairwise treatment comparisons within genotypes and between genotypes of the same treatment shows anti-conservative type *p*-value distribution in the histogram for the normalized read counts of the informative genes. The null *p*-value distribution in the x-axis of the histogram was uniform with distribution ranges between 0 to 1. This uniform distribution of histogram allows to properly control the False Discovery Rate (FDR) conferred by type I error (reject the null hypothesis when it is true/False positive). The *p*-value histograms for the informative genes are summarized in Fig. 3.2. The DESeq2 analysis summarized the total number of informative genes, total number of significant genes, significantly and differentially up-regulated and down-regulated genes, significantly and differentially up and down regulated two-fold and four-fold genes between comparisons of two treatment groups within the same genotype and between susceptible and resistant genotypes (Table 3.3). Volcano plots given in Fig. 3.3 represents the differentially expressed genes between two treatment groups of the same genotypes or between genotypes of the same treatment. The volcano plot compares the log2 fold changes or magnitude of changes versus the negative log10 *P*-value. Significantly and differentially expressed genes are highlighted with an adjusted *P*-value cut-off of 0.05, with up-regulated genes highlighted in the right side of the volcano plot and down-regulated genes are in the left side of the plot. A mean differentiation plots in Fig. 3.4 compares the log2 fold changes versus the log2 expression values of differentially expressed genes. Significantly and differentially expressed genes are highlighted with an adjusted *P*-value cutoff of 0.05,

where up-regulated genes are highlighted on the top of the plot and down-regulated genes are highlighted below the mean differentiation line.

Gene Ontology (GO) term analysis

The gene ontology (GO) term analysis for the differential gene expression of pairwise treatment comparisons within genotypes and between genotypes screened significantly enriched up-regulated and down-regulated genes along with designated GO terms. These GO terms are classified into biological process (BP), cellular component (CC), and molecular function (MF). GO term enrichment analysis was based on a *P*-value cutoff of 0.05 and *q*-value of < 0.05 (to control positive FDR). In all pairwise comparisons within genotypes and between genotypes, the majority of the GO terms were designated as BP followed by MF and CC.

DE genes and associated GO terms in the resistant genotype induced by MP infection and exogenous application of ascorbic acid and H_2O_2

In comparison of the non-pre-treated and *M. phaseolina*-inoculated treatment with the non-pre-treated and agar plug-treated mock-inoculated control in DT97-4290, 379 genes were up-regulated, of which 117 and 83 genes were two-fold and > four-fold significantly up-regulated (Table 3.3). Up-regulated BP GO terms included nitrate import and transport, regulation of morphogenesis, phosphorylation, transport associated with ion transmembrane and oligopeptide transmembrane, and biosynthetic processes associated with diterpenoid production. The number of MF GO terms represent by different molecular activities related to DNA binding, kinase activity, ligand-gated ion channel activity, terpene synthase activity, hormone activity, ionotropic glutamate receptor activity, and protein serine/threonine kinase and protein kinase activity. The up-regulated MF GO terms (Table 3.4, Fig. 3.5) are genes associated with the pattern recognition receptors (PRRs), which are known to triggered by PAMP and MAMP (plasma membrane- and microbe-associated molecular pattern). Integral components of the membrane, membrane, plasma membrane and extracellular region, were up-regulated in the CC GO category. For the same comparison, 1191 genes were significantly and differentially down-regulated, of which 185 and 498 genes exhibiting two- and four-fold down-regulation, respectively (Table 3.3). The number of down-

regulated genes is significantly higher than up-regulated genes in this comparison. The GO terms for differentially expressed genes in the down-regulated category are higher than the up-regulated category. Down-regulated BP GO terms are xenobiotic detoxification by transmembrane in the plasma membrane, cellular oxidant detoxification, xenobiotic transmembrane transporter activity, cellular oxidant detoxification, xenobiotic transmembrane transporter activity, hydrogen peroxide catabolic process, chitin catabolic process, indole glucosinolate metabolic process, phenylpropanoid metabolic process, biosynthetic process associated to and phenylpropanoid, response to oxidative stress and chitin, and cell differentiation (Table 3.4). As in the up-regulated category, the majority of the GO terms fell in the MF category is in the down-regulated category. The MF-associated GO terms in the down-regulated class were DNA binding, ethylene and metal ion binding, activity related to chalcone synthase, ethylene receptor, peptidase inhibitor, lyase, oxidoreductase, peroxidase, monooxygenase, DNA-binding transcription factor, chitinase, and pathways associated to ethylene-activated signaling (Table 3.4). The MF category-associated GO term in this comparison between inoculated and control treatments show induced down-regulated host defense-related genes and defense related signaling genes. The CC category only showed down-regulated GO term for extracellular region (Fig. 3.5).

Comparing the ascorbic acid pre-treated followed by *M. phaseolina* inoculation with the non-pre-treated and *M. phaseolina*-inoculated control, there were a total 4029 up-regulated genes, of which 1228 genes were two-fold and 1256 genes were greater than four-fold significantly up-regulated (Table 3.3). The BP GO terms associated with these up-regulated genes (Fig. 3.6) were cellular activity related to regulation of secondary shoot formation, monopolar cell growth, cell cycle, photosynthesis, leaf formation, stomatal movement, cellulose synthase activity, abaxial cell fate specification, mitotic cell cycle phase transition, fatty acid biosynthetic process, lignin catabolic process, and response to light stimulus. The majority of the genes in the BP class are involved in the normal cell cycle, differentiation, and developmental processes. The MF category represented most of the GO among all three categories and are related to enzymatic processes (very-long-chain 3-ketoacyl-COA synthase activity, glycerol-3-phosphate 2-O-acyltransferase activity, hydrolase activity), hydroquinone: oxygen oxidoreductase activity, protein serine/threonine kinase regulator activity, DNA-binding transcription factor activity, RNA polymerase II-specific DNA-binding transcription factor activity, and binding (nucleosome, protein kinase, lipid and microtubule). The

CC category represented apoplast, chloroplast envelope, microtubule, chromosome, and extracellular region. There was a total 3465 genes differentially expressed in the down-regulated category where 1454 genes were two-fold and 540 genes were greater than four-fold significantly differentially expressed. In the BP category most down-regulated genes were associated to biological process such as protein autophosphorylation, phosphorylation, cellular oxidant detoxification; catabolic process of hydrogen peroxide, glucosinolate, L-phenylalanine; response to oxidative stress, chitin, defense response, defense response to oomycetes/bacteria, and response to biotic stimulus, and biosynthetic process related to aromatic compound, flavonoid, and cinnamic acid and metabolic process related to carboxylic acid, phenylpropanoid, glutamate, and cellular amino acid; signaling response to receptor activity, ethylene and abscisic acid-activated signaling pathway, and cell surface receptor pathway. The MF category was represented by transport activity-like transmembrane and carbohydrate; molecular activity related to regulation of protein serine/threonine phosphatase, signaling receptor, lyase, oxidoreductase, transaminase, beta-glucosidase, UDP-glycotransferase, protein kinase, monooxygenase, catalytic and DNA-binding transcription; binding of nucleotide, ATP, iron ion, abscisic acid, sequence specific DNA, ubiquitin protein ligase, polysaccharide, and pyridoxal. The MF category displays GO terms related to transcription and defense response related signaling. In the CC category most gene-associated GO terms were integral component of membrane; other significant CC were plasmodesmata and membrane (Fig. 3.6).

Comparisons of ascorbic acid pre-treated and MP inoculated with the ascorbic acid pre-treated and agar plug-inoculated revealed total 3113 up-regulated genes with 1808 two-fold and 171 greater than four-fold significantly up-regulated genes (Table 3.3). The GO terms associated with the up-regulated BP category were cellular response to light stimulus, response to reactive oxygen species, cell wall biogenesis, photosynthesis, biosynthetic process of carotenoid, chlorophyll, porphyrin-containing compound; metabolic process associated with carbohydrate and photosystem II repair (Table 3.6). Interestingly, in the BP category, response to reactive oxygen species-related genes were up-regulated in this comparison. In the MF category, transcription-related such GO terms were up-enriched as regulation of transcription initiation, chloroplast rRNA processing, iron and sulfur and chlorophyll compound binding, transporter activity related to oligopeptide transmembrane, transferase activity of xyloglucan:xyloglucosyl. Up-enriched CC GO terms involved in this comparison were chloroplast envelope, stroma, and thylakoid; plastid and plastoglobule

(Table 3.6, Fig. 3.7). There were 4315 down-regulated, differentially expressed genes in this comparison, with 1452 two-fold and 1411 greater than four-fold significantly differentially expressed (Table 3.3). BP GO terms were defense response to organism and oomycetes, dioxygenase activity, catabolic process of hydrogen peroxide, and glucosinolate, biosynthetic process of flavonoid, cinnamic and chorismite, metabolic process of phenylpropanoid, and glutathione, defense response related to programmed cell death, and calcium-mediated signaling. The MF category included transcription, DNA binding and catalytic activity-related GO terms such as metal, FMN, iron, ATP and nucleotide binding; chitinase activity, catalytic, lyase and cysteine dioxygenase activity, and glutathione transferase activity and kinase activity, immune response, defense signaling related with serine/threonine kinase. Plasma membrane was the only CC category expressed here (Fig. 3.7).

The non-pre-treated and H_2O_2 applied treatment versus the H_2O_2 pre-treated and *M. phaseolina* inoculated treatments showed 617 differentially and significantly up-regulated genes with 167 two-fold and 187 genes greater than four-fold significantly differentially expressed genes (Table 3.3). Based on the *P*-value and number of genes associated with the GO terms in the up-regulated category, the BP GO terms were cellular oxidant detoxification, response to oxidative stress and biotic stimuli; biosynthetic process of flavonoid and lignan, reduction of molecular oxygen, carbohydrate, indole glucosinolate metabolic process, and hydrogen peroxide catabolic process. MF-classified GOs included catalytic activity such as oxidoreductase activity, hydrolase activity (of glycosyl bonds), and intramolecular lyase activity; transferase activity, NAD(P)H dehydrogenase (quinone) activity, peroxidase and monooxygenase activity; and binding of iron, metal. CC-associated GO terms were apoplast and extracellular region (Fig. 3.8). In this treatment comparison, 460 genes were significantly down-regulated and lower than the number of up-regulated genes with 199 two-fold and 59 greater than four-fold significantly differentially expressed genes (Table 3.3). Down-regulated BP GO terms were regulation of salicylic acid and nitric oxide biosynthetic process, dephosphorylation, physiological process associated with fruit and anther dehiscence, carbohydrate metabolic process, and pectic catabolic process. The MF category included transmembrane transport, polygalacturonase activity, hydrolase activity, sequence specific DNA binding, DNA-binding transcription factor activity. The CC category included only extracellular region (Fig. 3.8).

DE genes and GO terms in the susceptible genotype induced by MP infection and exogenous application of ascorbic acid and H_2O_2

In the susceptible genotype Pharaoh, the pairwise comparison between non-pre-treated *M. phaseolina*-inoculated treatment with the non-pre-treated agar plug-treated mock-inoculated control showed 334 differentially and significantly up-regulated genes with 143 2-fold and 53 >4-fold significantly up-regulated genes (Table 3.3). Significant BP GO terms that were associated with higher number of genes are phosphorylation, protein phosphorylation, and defense responses. The MF category included sequence-specific DNA binding, transmembrane transport, protein kinase activity, protein serine/threonine kinase activity, regulation of transcription, and DNA-binding transcription factor activity. CC includes plasma membrane, membrane, and integral component of membrane that are represented by the majority of the genes (Table 3.5, Fig. 3.9). There were 1283 significantly down-regulated genes with 355 two-fold and 392 >4-fold significantly down-regulated genes. The down- regulated BP GO terms associated with most of the genes were cellular oxidant detoxification, defense response, hydrogen peroxide and carbohydrate catabolic process, ethylene-activated signaling pathway, and response to oxidative stress. The major MF GO categories were sequence-specific DNA binding, heme binding, transferase activity, oxidoreductase activity, catalytic activity, and DNA-binding transcription factor activity. The CC GO categories included only the plasma membrane and extracellular region (Fig. 3.9)

The comparison between the ascorbic acid pre-treated *M. phaseolina*-inoculated treatment with the non pre-treated *M. phaseolina*-inoculated control treatment for Pharoah revealed 3563 significantly up-regulated genes, which was lower than the resistant genotype DT97-4290. 951 and 837 genes were significantly two-fold and greater than four-fold significantly up-regulated (Table 3.2). BP GO terms in the up-regulated category were cell wall biogenesis, lipid oxidation; photosynthesis-related GO terms such as photosystem II assembly and repair, photoinhibition, photosynthesis and light harvesting; and response-related gene ontology such as response to reactive oxygen species, hydrogen peroxide; and lipid oxidation and metabolic processes (Table 3.7). The majority of GO terms in this comparison were in the MF category and included oxidoreductase activity, transport of transmembrane, carbohydrate and sugar transmembrane; kinases activity, lipid oxidation, DNA methylation and monooxygenase activity. In the CC category were apoplast, organelle

envelope, membrane, thylakoid, plastid, nucleus, and chloroplast (Table 3.7). There were 2016 down-regulated differentially expressed genes, which was almost two-fold higher than the number up-regulated genes, with 1041 two-fold and 237 greater than four-fold significantly differentially expressed genes (Table 3.3). The BP GO terms were hydrogen peroxide catabolic process, phosphorylation, protein phosphorylation, defense response, and ethylene-activated signaling pathway; the MF category included transferase activity, hexosyltransferase activity, incorporation or reduction of molecular oxygen, catalytic activity, ATP binding, iron ion binding, and DNA-binding transcription factor activity. The down-regulated CC category GO terms were integral component of membrane, membrane and plasma membrane (Fig. 3.10).

The comparison between the ascorbic acid pre-treated *M. phaseolina*-inoculated treatment with the ascorbic acid pre-treated agar plug-treated mock-inoculated control treatment for Pharoah revealed 1475 significantly up-regulated genes, which was lower than the resistant genotype DT97-4290, out of those 1245 and 31 genes were significantly two-fold and greater than four-fold significantly up-regulated (Table 3.3). BP GO terms in the up-regulated category were majority related to photosynthesis-related GO terms such as photosystem II assembly and repair, photoinhibition, photosynthesis and light harvesting; and response-related gene ontology such as response to reactive oxygen species, hydrogen peroxide; and lipid oxidation and metabolic processes. The majority of GO terms in this comparison were in the MF category and included oxidoreductase activity, transport of transmembrane, carbohydrate and sugar transmembrane; kinases activity, lipid oxidation, DNA methylation and monooxygenase activity. In the CC category were apoplast, organelle envelope, membrane, thylakoid, plastid, nucleus, and chloroplast. There were 3057 down-regulated differentially expressed genes, which was two-fold higher than the number of up-regulated genes, with 1414 two-fold and 749 greater than four-fold significantly differentially expressed genes (Table 3.3). The BP GO terms were metabolic processes, phosphorylation, protein phosphorylation, defense response, and ethylene-activated signaling pathway; the MF category included transferase activity, hexosyltransferase activity, incorporation or reduction of molecular oxygen, catalytic activity, ATP binding, iron ion binding, and DNA-binding transcription factor activity. The down-enriched CC category GO terms were integral component of membrane, membrane and plasma membrane (Fig. 3.11).

The comparison between the non-pre-treated H_2O_2 application with the H_2O_2-pre-treated *M. phaseolina*-inoculated treatment showed 2714 significantly up-regulated differentially expressed genes, of which 587 and 950 were two-fold and greater than four-fold significantly differentially expressed, respectively (Table 3.3). Up-regulated BP GO terms were protein autophosphorylation, metabolic process, and defense response. Up- regulated MF GO terms were oxidoreductase activity, kinase activity, protein serine/threonine kinase activity, catalytic activity, regulation of transcription, and binding related to ATP and nucleotide. CC GO terms were plasma membrane and integral component of membrane (Fig. 3.12). There were 1106 differentially expressed down-regulated genes with 455 two-fold and 137 greater than four-fold significantly differentially expressed genes (Table 3.3). BP GO terms were metabolic processes, defense responses, response to biotic stimulus. In the MF category the GO terms were transmembrane transport, oxidoreductase activity, and hydrolase activity, DNA-binding related genes and NAD(P)H oxidase H_2O_2 -forming activity. CC GO terms with significant numbers of genes were integral component of membrane, cell wall, and extracellular region (Fig. 3.12)

DE genes and GO term induced by MP infection, exogenous application of ascorbic acid and H_2O_2 between comparison of resistant and susceptible genotype

The comparison between resistant genotype (DT97-4290) and susceptible soybean genotype (Pharaoh) for the non-pre-treated *M. phaseolina*-inoculated treatment expressed significant up-regulation of 779 genes with 165 two-fold and 295 greater than four-fold significantly differentially expressed genes, respectively (Table 3.3). BP GO terms represented by higher number of genes were metabolic process, defense response, and fatty acid biosynthetic process. MF GO terms were ATP binding, negative regulation of catalytic activity, hydrolase activity, oxidoreductase activity, serine-type peptidase activity, polygalacturonase activity, and NAD+ nucleosidase activity. CC GO terms were cell wall and extracellular region. There were 724 significantly down-regulated genes, with 190 two-fold and 263 greater than four-fold significantly differentially expressed genes, respectively (Table 3.3). In the down-regulated category there were no significant GO terms with *P*-values at the FDR level of < 5%, so the *q*-value (FDR) cutoff level was adjusted to 0.1 (10% FDR). Down-regulated BP GO terms were signal transduction, defense response, and phos-

phorelay signal transduction system. MF GO terms were ATP binding, NAD+ nucleosidase activity, and protein-disulfide reductase activity. There were no down-regulated CC GO terms in this comparison (Fig. 3.13).

Pairwise comparisons between the susceptible and resistant genotype for the ascorbic acid pre-treated and *M. phaseolina*-inoculated plant revealed 2106 up-regulated genes, with 841 two-fold and 469 greater than four-fold significantly differentially expressed genes (Table 3.3). Up-regulated BP GO terms were metabolic process, carbohydrate metabolic process, and defense response. MF GO terms were ADP binding, heme binding, hydrolase activity on glycosyl bond and ester bonds, oxidoreductase activity, monooxygenase activity, and NAD+ nucleosidase activity. CC GO terms were cell wall, extracellular region, apoplast, and nucleosome. In this comparison, 2586 genes were down-regulated with 1335 two-fold and 445 greater than four-fold significantly down-regulated genes, respectively (Table 3.3). Down-regulated BP GO terms were cellular oxidant detoxification, phosphorylation, and protein phosphorylation. The MF GO terms were transferase activity, oxidoreductase activity, protein serine/threonine kinase activity, and catalytic activity. CC GO terms were plasma membrane, extracellular region, and membrane (Fig. 3.14).

The comparison between susceptible and resistant genotypes for the H_2O_2 pre-treated *M. phaseolina*-inoculated treatment showed a total up-regulation of 1418 genes, with 416 genes and 339 greater than four-fold significantly differentially expressed genes (Table 3.3). BP GO terms were phosphorylation, protein phosphorylation, metabolic process, and defense responses. MF GO terms were ATP and ADP binding, protein kinase activity, protein serine/threonine activity, and hydrolase activity. The CC GO terms included integral component of membrane, membrane, plasma membrane, and extracellular region (Fig. 3.15). There were 1484 down-regulated genes with 450 two-fold and 385 greater than four-fold significantly differentially expressed genes, respectively (Table 3.3). In the down-regulated category, BP GO terms were photosynthesis, xyloglucan metabolic process, response to defense, and light stimulus. MF GO terms were oxidoreductase activity and NAD+ nucleosidase activity, and chlorophyll binding. The CC category was apoplast, plastoglobuli, chloroplast envelope, chloroplast stroma, plastid, and chloroplast. Most GO terms associated with photosynthesis in the down-regulated category suggest the inhibition of photosynthesis-associated genes and may be due to induced oxidative stress by H_2O_2 application following *M. phaseolina* inoculation (Fig. 3.15).

KEGG pathway analysis in the genotype by treatment interactions

The DE genes that were log2-fold significant for the genotype by treatment interaction were pasted in the ShinyGO online platform to obtain the pathway annotation using the KEGG (Kyoto Encyclopedia of Genes and Genomes) database (ShinyGO 0.76.1). While comparing the non- pre-treated *M. phaseolina*-inoculated treatment with the non-pre-treated agar plug mock-inoculated control in both genotypes some common pathways were expressed such as secondary metabolite biosynthesis, isoflavonoid biosynthesis, flavonoid biosynthesis, and phenylpropanoid biosynthesis. However, in both genotypes the pathways associated to flavonoid, isoflavonoid, phenylpropanoid biosynthesis were down-regulated (Fig. 3.16 & 3.19). In the susceptible genotype only the plant-pathogen interaction and MAPK signal pathways were up-regulated (Fig. 3.19). In the susceptible genotype (Pharaoh), glucosinolate biosynthesis, amino acid biosynthesis, and ubiquinone and other terpenoid-quinone biosynthesis pathway were down-regulated (Fig. 3.19). However, in the resistant genotype (DT97-4290), stilbenoid, diarylheptanoid, and gingerol biosynthesis pathways were expressed and down-regulated (Fig. 3.16). In both genotypes, host PRR (pattern recognition receptor)-mediated defense-related signaling and mitogen activated protein kinase (MAPK) signaling pathways were expressed and down-regulated. Several metabolic pathways commonly expressed and down-regulated in both genotypes were glutathione metabolism, carbon metabolism, nitrogen metabolism, galactose metabolism, starch, and sucrose metabolism, and cyanoamino acid metabolism. In the resistant genotype, only cysteine and methionine metabolism, glutathione metabolism was significantly enriched. While in the susceptible genotype, alanine, aspartate and glutamate metabolism was down-regulated (Fig. 3.19).

Comparison of the ascorbic acid pre-treatment MP-inoculated treatment vs. ascorbic acid pre-treated agar plug treated mock-inoculated control treatment in the resistant and susceptible genotypes showed up-regulation of pathways associated to photosynthesis in both genotypes (Fig. 3.17 & 3.20), which did not show up in the inoculated vs. mock-inoculated control comparisons in either genotype. In this comparisons stress responsive metabolic pathways (Flavonoid, isoflavonoid, phenylpropanoid) were found down-regulated in both genotypes ((Fig. 3.17 & 3.20).

Treatment comparison for non pre-treated H_2O_2 applied and H_2O_2 pre-treated MP inoculated control were compared between both genotypes (susceptible and resistant) for their associated pathway analysis. In both genotypes metabolic pathways associated to flavonoid, isoflavonoid, and phenylpropanoid biosynthesis were up-regulated with 3-5 fold enrichment (Fig. 3.18 & 3.21). Glutathione metabolism pathway was up-regulated only in the resistant genotype (Fig. 3.18). For the resistant genotype in the down-regulated category phenylpropanoid biosynthesis pathway expressed with nearly five-fold enrichment (Fig., 3.18). In the susceptible more pathways showed up in the up-regulated category than down-regulated category. In the down-regulated category of susceptible genotype carotenoid biosynthesis was enriched with nearly seven folds (Fig. 3.21). Plant hormone signal transduction was also down-regulated with more than two-fold enrichment (Fig. 3.21). Several biosynthetic and metabolic pathways found up- regulated in the susceptible genotypes are stilbenoid, diarylheptanoid and gingerol biosynthesis; phenylalanine, tyrosine and tryptophan biosynthesis, and alanine, aspartate and glutamate metabolism (Fig. 3.21).

Weighted gene co-expression network analysis (WGCNA)

The gene co-expression network analysis using the Pearson correlation coefficient among the 36 samples (two genotypes × six treatment × three replicates) generated a co-expression module of 20 with different gene frequencies (Fig. 3.21 B). A cluster dendrogram represented how the genes were clustered in those modules (Fig. 3.21 A). The eigengene for each module to treatment across the 36 samples didn't show strong correlation between any module or treatment combination.

DISCUSSION

Plant physiological, molecular, and biochemical responses to biotic or abiotic stressors are induced by different pathogens or environmental factors and expresses related genes with diverse pathways associated with different mechanisms (Chaves et al., 2003). In this chapter, plants responses to biotic stress induced by *M. phaseolina*, evaluation of ROS induced by MP in two different soybean genotypes, the role of ascorbic acid as an antioxidant scavenger in ROS elimination, and the role of H_2O_2 in indued oxidative stress-mediated senescence has been evaluated by a comparative RNA-seq analysis between a resistant and susceptible genotype. The results demonstrated differential responses in treatment comparisons between and within genotypes suggesting that patho-

genicity-associated genes, stress-associated genes, antioxidant-related genes, and pathways in connection with *M. phaseolina* induced oxidative stress-mediated senescence from the contrasting genotypes with their constitutive expression differences.

Protein kinase and phosphorylation-related genes expressed as an induced oxidative stress responses by *M. phaseolina*

In the resistant genotype (DT97-4290), the comparison between non-pre-treated *M. phaseolina*-inoculated with non-pre-treated agar plug mock-inoculated control demonstrated significantly expressed genes that were associated with protein kinase activity (GO:0004672), protein serine/threonine kinase activity (GO:0004674), phosphorylation (GO:0016310), protein phosphorylation (GO:0004674), and kinase activity (GO:0016301) (Appendix A). These GO terms are related to the receptor-like protein kinase (RLKs), which are a large family of plasma membrane proteins that function in transducing extracellular signal sensed by the plant (Osakabe et al., 2013). Whereas in the susceptible genotype (Pharaoh), the number of genes associated with RLK's GO terms were significantly higher than the resistant genotype. This result suggests a possible *M. phaseolina* induced expression of higher oxidative stresses responsive genes in the susceptible genotype than resistant genotype, as these expression of RLKs gene is related to direct or indirect perception of ROS's or oxidative stress related responses (Czernic et al., 1999; Wrzaczek et al., 2013; Shapiguzov et al., 2012). RLKs are represented by three protein domains, extracellular domain that sense and perceives a ligand molecule; a transmembrane domain that integrates the protein with the cell membrane; and a cellular kinase that transmits downstream signals by phosphorylation and activation (Walker, 1994; Ouyang et al., 2010). Czernic et al. (1999) showed that the *Arabidopsis* receptor-like protein kinase gene (*At-RLK3*) is activated by the oxidative stress induced by inoculation with *Ralstonia solanacearum*, a bacterial pathogen. The possible role of *At-RLK3* in signal transduction revealed that it was activated and induced by H_2O_2 (ROS), or menadione and salicylic acid that supports our findings. Zhang et al. (2013) showed that the serine/threonine protein kinase gene GbSTK (a defense-associated gene in cotton), when overexpressed in the model plant *Arabidopsis*, enhanced pathogenicity of *Verticillium dahliae* Kleb. and increased oxidative stress following the activation of defense-signaling pathways. Their findings revealed that GbSTK responds to infection and oxidative stress induced by the pathogen (Zhang et al.,

2013). In addition to kinase activity, several genes were associated with phosphorylation, protein phosphorylation, and protein autophosphorylation. In the susceptible genotype, the number of genes associated with phosphorylation was significantly higher than that of the resistant genotype. Colcombet and Hirt (2008) stated that reversible protein phosphorylation is the key regulator of extracellular stimuli sensing and activation of downstream defense signaling cascades suggesting that defense pathways are associated with RLKs and these RLKs are activated through phosphorylation that play a key role in signaling (Zhang et al., 2013).

M. phaseolina induced down-regulation of defense and cellular oxidant detoxification genes in both genotypes

In the both resistant and susceptible genotype, high numbers of down-regulated genes were associated with the GO terms: response to oxidative stress (GO:0006979), hydrogen peroxide catabolic process (GO:0042744), cellular oxidant detoxification (GO:0098869), and peroxidase activity (PX) (GO:0004601) (Appendix B). Yan et al. (2021) showed that peroxidase activity-related genes contribute to plant defense and work as an antioxidant by contributing to pathogen-induced ROS detoxification. Also, if plants are stressed by pathogen invasion, peroxidase activity is enhanced (Yan et al., 2021; Huang et al., 2013). We observed high numbers of PX-associated genes down-regulated in both genotype, which may contribute to host compromise and promote pathogen invasion and proliferation (Appendix B-D). Cellular oxidant detoxification-related genes were also down-regulated in both genotypes. Cellular oxidant detoxification is a biological process that eliminate or scavenge cellular superoxide or ROS like H_2O_2 when it reaches to a toxic level. Thus, suggesting *M. phaseolina* might induced oxidative stress in both genotypes and the cellular oxidant scavengers related genes were not overexpressed in either genotype. *M. phaseolina* induced down-regulation of other defense related metabolic, hormonal signaling and transcriptional activity related genes in both genotypes. Specially the ethylene-activated signaling pathway (GO:0009873) were associated with higher number of genes in both genotypes. Ethylene is known to contribute on host defense along with jasmonic acid by transcriptionally regulating ethylene responsive factor 1 (ERF1) (Lorenzo et al., 2003)

Exogenous ascorbate (L-ascorbic acid) induced contrasting responses to oxidative stress, photosynthesis, and defense-related genes in the resistant and susceptible genotypes

Comparison of ascorbic acid pre-treatment following inoculation vs. ascorbic acid pre-treated mock control treatment in both genotypes showed up-regulation of several photosynthesis and photosynthetic machinery related GO terms, suggesting ascorbic acid induced over-expression of photosynthesis in both genotypes. Bilgin et al., (2010) studied the effect of different biotic stresses on photosynthesis and their study revealed that plant restrain the expression of photosynthesis genes during biotic stress while investing more energy related to defense to save resources. Chen et al., (2021) showed the role of exogenous application of ascorbic acid in rescuing salt stress induced damage and increasing photosynthesis by modulating endogenous ascorbate level. Foyer (2015) included ascorbic acid within the key antioxidant molecules required for continued photosynthesis. Chung et al. (2019) studied transgenic potato plants overexpressing the D-galacturonic acid reductase (GalUR) gene with elevated cellular L-ascorbate level showed increased m-RNA abundance of cellular antioxidants, pathogenesis-related PR genes, defense related and hormonal signaling of gibberellic acid (GA) and abscisic acid (ABA) related biosynthetic pathways when inoculated with the necrotrophic pathogen *Phytophthora infestans*. The authors also detected lower levels of hydrogen peroxide (H_2O_2) and malondialdehyde (MDA) in the transgenic plant compared to the untransformed plant (Chung et al., 2019), which supports speculation of ascorbate-mediated hydrogen peroxide scavenging in the transgenic potato plants.

Other than photosynthesis and carbohydrate metabolic process, response to reactive oxygen species related GO term was up-regulated in both genotypes. In the resistant genotype ascorbic acid pre-treatment down-regulated around 50 genes related to response to oxidative stress (GO:0006979), however in the susceptible genotype ascorbic acid pre-treatment induced up-regulation of response to hydrogen peroxide (ROS) and lipid oxidation related GO terms, both of these GO terms are related to oxidative stress. Defense, signal, and DNA binding related MF category GO terms were down-regulated in both genotypes. Specially genes that are related to ROS burst like kinases and phosphorylation were down-regulated in both genotypes due to ascorbic acid pre-treatment suggest ascorbic acid's mediated modulation of redox homeostasis in the cell.

Hydrogen peroxide induced contrasted responses of defense, oxidative stress and oxidant detoxification genes in the resistant and susceptible genotype

Comparison of H_2O_2 pre-treatment following MP inoculation vs. non pre-treated H_2O_2 applied treatment showed up-regulation of some oxidative stress responsive and ROS scavenging related genes in the resistant genotype. Response to oxidative stress related GO terms along with cellular oxidant detoxification and hydrogen peroxide catabolic process, peroxidase activity related GO terms were up-regulated. All these GO terms are related to ROS homeostasis in the cell.
However, in the susceptible genotype a different scenario has been observed, concerning genes related to NAD(P)H oxidase H_2O_2-forming activity, defense response, kinases activity was significantly overexpressed in the up-regulated category rather than resistant genotype, suggesting H_2O_2 induced enhanced oxidative stress responsive genes in the susceptible genotype than resistant genotype. In the down-regulated category along with developmental, metabolic and transcription related genes, response to oxidative stress and hydrogen peroxide related GO terms were expressed. This H_2O_2 induced contrasted phenomena suggest that resistant and susceptible plants react to oxidative stress differentially. Miller et al. (2010) stated that the hypersensitive response in the plant induces excessive H_2O_2 and NADPH- dependent H_2O_2 generation-related genes encoded by the ROS burst-associated homolog RBOH (respiratory burst oxidase homolog). It is an important source of signal-transduction-associated ROS (Mittler et al., 2004, Torres and Dangl, 2005), supporting H_2O_2 modulated pathogen-induced ROS generation.

M. phaseolina **induced contrasted biosynthetic and defense signal pathways in the resistant and susceptible genotypes**

KEGG pathway enrichment analysis reveals *M. phaseolina*-induced down-enrichment of isoflavonoid and flavonoid biosynthetic pathways in both resistant genotype and susceptible genotypes. Studies showed that pathogen-induced isoflavonoid biosynthetic genes (Moy et al., 2004, Vega-Sánchez et al., 2005) and this biosynthetic pathway are involved in the production of antimicrobial compound glyceollin, which is a phytoalexin (Sukumaran et al., 2018). On the other hand, flavonoid biosynthesis pathways are known to contribute to host adaptation (Tahara, 2007; Petroni and Tonelli, 2011), development (Lepiniec et al., 2006), reproduction (Mol et al., 1998), and oxidative damage alleviation (Albert et al., 2009; Yan et al., 2014) suggests they uniquely induced by the *M.*

phaseolina in both genotypes. *M. phaseolina* induced down-regulation of phenylpropanoid biosynthesis pathway with more than two-fold enrichment in both genotypes. Phenylpropanoid pathways are known for its great potential in ROS homeostasis, as the polyphenols works as an antioxidant to scavenge or neutralize ROS (Grace, 2005; Fracasso et al., 2016)

The host defense-associated pathway "Mitogen-activated protein kinase signaling" (MAPK) was also up-regulated with more than five folds expression in the susceptible genotype, however in the resistant genotypes MAPK pathway down-regulated with around two and half fold expression. Through epitope tagging and protoplast transient expression assay, Kovtun et al. (2000) showed that major ROS H_2O_2 regulates MAPK cascades in the leaf cells of *Arabidopsis* by activating the MAPKKK, ANP1; thus, suggesting MP induced ROS activated up-regulation of MAPK pathway in the susceptible genotype. Glutathione peroxidases are known to work as an antioxidant and showed essential role in detoxifying ROS form the sweet cherry when inoculated with the fungus *Penicillium expansum*, thus the Pathogen induced ROS-mediated damage was alleviated from the harvested sweet cherry (Xu and Tian, 2008). Glutathione metabolic pathway down-regulated in both genotypes with around three-fold expression, suggested induced by *M. phaseolina*.

Ascorbic acid pre-treatment induced contrasted pathway enrichment in the resistant and susceptible genotypes

Ascorbic acid pre-treatment following *M. phaseolina* inoculation vs. ascorbic acid pre-treated mock-inoculated control expressed a significantly higher number of genes related to photosynthetic pathways in both genotypes. The major photosynthetic pathways induced by the ascorbic acid pre-treatment are photosynthesis, carotenoid biosynthesis, porphyrin and chlorophyll metabolism in both genotypes suggesting exogenous ascorbic acid pre-treatment modulated the photosynthesis, which is in agreement with Foyer (2015), statement of "ascorbic acid as an essential antioxidant for phothosynthesis". Along with maintaining sustained photosynthesis ascorbic acid is known to detoxify chloroplastic ROS and protects the photosynthetic machinery from the ROS damage (Foyer et al., 2008; Trubitsin et al., 2014; Akram et al., 2017) A genome-wide transcriptional profiling and metabolic pathway analysis from the oxidative stress induced by environmental stressors (salinity and heat) in the tomato plants revealed the role of the ascorbate metabolic pathway in controlling the redox homeostasis (Lopez-Delacalle et al., 2021), thus also supports

the findings. However, ascorbic acid pre-treatment didn't induce up-regulation of the stress responsive metabolic pathways like flavonoid, isofavonoid and phenylpropanoid pathways in either genotype. Circadian rhythm pathway up-regulated with more than two-fold expression in the resistant genotype. Like the earlier discussion of ascorbate's role in ROS neutralization, circadian clock-associated genes have been found to involve in mounting resistance against pathogens through plant innate immune gene's related assistance (Goodspeed et al., 2012, 2013a, b), suggesting the enhanced oxidative stress might inducing the immunity responses in the resistant genotype DT97-4290.

H_2O_2 pre-treatment following *M. phaseolina* inoculation induced contrasted pathways in the resistant vs. susceptible genotypes

Hydrogen peroxide pre-treatment following *M. phaseolina* inoculation up- regulated isoflavonoid, flavonoid, and phenylpropanoid biosynthesis pathways in both genotypes. Interestingly, all those pathways are stress-responsive pathways and were found down-regulated in both genotypes when non pre-treated *M. phaseolina* inoculation vs. mock control treatment was compared. This contrasted phenomenon suggested they might be induced by the exogenous application of H_2O_2. In the resistant genotype glutathione metabolism related pathway also up-regulated with more than three-fold expression. Glutathione metabolism has significant role in ROS detoxification (Dorion et al., 2021), suggests induced by the enhanced oxidative stress imposed by exogenous application of H_2O_2 following *M. phaseolina* inoculation, thus also suggesting resistant genotype might have different arsenal of ROS neutralization. In the susceptible genotypes other than defense related metabolic pathways (Flavonoid, isoflavoid and phenylpropanoid pathways), MAPK signaling, and plant pathogen interaction related pathways enriched around two-fold, both of these pathways are related to stress responses, host defense and signal transduction.

REFERENCES

1. Akram, N. A., Shafiq, F., & Ashraf, M. (2017). Ascorbic acid-a potential oxidant scavenger and its role in plant development and abiotic stress tolerance. *Frontiers in Plant Science*, *8*, 613.

2. Albert, N. W., Lewis, D. H., Zhang, H., Irving, L. J., Jameson, P. E., & Davies, K. M. (2009). Light-induced vegetative anthocyanin pigmentation in *Petunia*. *Journal of Experimental Botany*, *60*, 2191-2202.
3. Baird, R. E., Watson, C. E., & Scruggs, M. (2003). Relative longevity of *Macrophomina phaseolina* and associated mycobiota on residual soybean roots in soil. *Plant Disease*, *87*, 563-566.
4. Bandara, A. Y., Weerasooriya, D. K., Liu, S., & Little, C. R. (2019). The necrotrophic fungus *Macrophomina phaseolina* induces oxidative stress-associated genes and related biochemical responses in charcoal rot susceptible sorghum genotypes. *bioRxiv*, 853846.
5. Benjamini, Y., & Hochberg, Y. (1995). Controlling the false discovery rate: A practical and powerful approach to multiple testing. *Journal of the Royal Statistical Society: Series B (Methodological)*, *57*, 289-300.
6. Bilgin, D. D., Zavala, J. A., Zhu, J. I. N., Clough, S. J., Ort, D. R., & DeLUCIA, E. H. (2010). Biotic stress globally downregulates photosynthesis genes. *Plant, Cell & Environment*, *33*, 1597-1613.
7. Botanga, C. J., Bethke, G., Chen, Z., Gallie, D. R., Fiehn, O., & Glazebrook, J. (2012). Metabolite profiling of *Arabidopsis* inoculated with *Alternaria brassicicola* reveals that ascorbate reduces disease severity. *Molecular Plant-Microbe Interactions*, *25*, 1628-1638.
8. Chapman, J. M., Muhlemann, J. K., Gayomba, S. R., & Muday, G. K. (2019). RBOH-dependent ROS synthesis and ROS scavenging by plant specialized metabolites to modulate plant development and stress responses. *Chemical Research in Toxicology*, *32*, 370-396.
9. Chaves, M. M., Maroco, J. P., & Pereira, J. S. (2003). Understanding plant responses to drought—from genes to the whole plant. *Functional Plant Biology*, *30*, 239-264.
10. Chen, X., Zhou, Y., Cong, Y., Zhu, P., Xing, J., Cui, J., Xu, W., Shi, Q., Diao, M., & Liu, H. Y. (2021). Ascorbic acid-induced photosynthetic adaptability of processing tomatoes to salt stress probed by fast OJIP fluorescence rise. *Frontiers in Plant Science*, *12*, 594400.
11. Chowdhury, S., Basu, A., & Kundu, S. (2017). Biotrophy-necrotrophy switch in pathogen evoke differential response in resistant and susceptible sesame involving multiple signaling pathways at different phases. *Scientific Reports*, *7*, 1-17.

12. Chung, I. M., Venkidasamy, B., Upadhyaya, C. P., Packiaraj, G., Rajakumar, G., & Thiruvengadam, M. (2019). Alleviation of *Phytophthora infestans* mediated necrotic stress in the transgenic potato (*Solanum tuberosum* L.) with enhanced ascorbic acid accumulation. *Plants*, *8*, 365.
13. Colcombet, J., & Hirt, H. (2008). *Arabidopsis* MAPKs: A complex signalling network involved in multiple biological processes. *Biochemical Journal*, *413*, 217-226.
14. Conklin, P. L., Williams, E. H., & Last, R. L. (1996). Environmental stress sensitivity of an ascorbic acid-deficient *Arabidopsis* mutant. *Proceedings of the National Academy of Sciences USA*, *93*, 9970-9974.
15. Czernic, P., Visser, B., Sun, W., Savouré, A., Deslandes, L., Marco, Y., Montagu, M. V., & Verbruggen, N. (1999). Characterization of an Arabidopsis thaliana receptor-like protein kinase gene activated by oxidative stress and pathogen attack. *The Plant Journal*, *18*, 321-327.
16. Deshmukh, R., & Tiwari, S. (2021). Molecular interaction of charcoal rot pathogenesis in soybean: a complex interaction. *Plant Cell Reports*, *40*, 1799-1812.
17. Dobin, A., Davis, C. A., Schlesinger, F., Drenkow, J., Zaleski, C., Jha, S., Batut, P., Chaisson, M., & Gingeras, T. R. (2013). STAR: Ultrafast universal RNA-seq aligner. *Bioinformatics*, *29*, 15-21.
18. Dorion, S., Ouellet, J. C., & Rivoal, J. (2021). Glutathione metabolism in plants under stress: Beyond reactive oxygen species detoxification. *Metabolites*, *11*, 641.
19. *e! EnsemblPlants* [available at https://plants.ensembl.org/Glycine_max/Info/Index] (Accessed on July 7, 2022).
20. Foley, R. C., Kidd, B. N., Hane, J. K., Anderson, J. P., & Singh, K. B. (2016). Reactive oxygen species play a role in the infection of the necrotrophic fungi, *Rhizoctonia solani* in wheat. *PLoS One*, *11*, e0152548.
21. Foyer, C. H. (2015). Redox homeostasis: Opening up ascorbate transport. *Nature Plants*, *1*, 1-2.
22. Foyer, C. H., Trebst, A., & Noctor, G. (2008). Signaling and integration of defense functions of tocopherol, ascorbate and glutathione. In Adams, B. D., Adams III, W. W., & Mattoo, A. K. (Eds.), *Photoprotection, photoinhibition, gene regulation, and environment,* (pp. 241-268). Springer, Dordrecht.

23. Foyer, C. H., & Noctor, G. (2003). Redox sensing and signalling associated with reactive oxygen in chloroplasts, peroxisomes and mitochondria. *Physiologia Plantarum*, *119*, 355-364.
24. Fracasso, A., Trindade, L. M., & Amaducci, S. (2016). Drought stress tolerance strategies revealed by RNA-Seq in two sorghum genotypes with contrasting WUE. *BMC Plant Biology*, *16*, 1-18.
25. Glycine_max_v2.1. [available at https://www.ebi.ac.uk/ena/browser/view/GCA_000004515.4?show=blobtoolkit] (Accessed on Jun 30, 2022).
26. Goodspeed, D., Chehab, E. W., Covington, M. F., & Braam, J. (2013). Circadian control of jasmonates and salicylates: The clock role in plant defense. *Plant Signaling & Behavior*, *8*, e23123.
27. Goodspeed, D., Chehab, E. W., Min-Venditti, A., Braam, J., & Covington, M. F. (2012). Arabidopsis synchronizes jasmonate-mediated defense with insect circadian behavior. *Proceedings of the National Academy of Sciences USA*, *109*, 4674-4677.
28. Goodspeed, D., Liu, J. D., Chehab, E. W., Sheng, Z., Francisco, M., Kliebenstein, D. J., & Braam, J. (2013). Postharvest circadian entrainment enhances crop pest resistance and phytochemical cycling. *Current Biology*, *23*, 1235-1241.
29. Grace, S. C. (2005). Phenolics as antioxidants. In: Smirnoff, N. (Eds.), *Antioxidants and Reactive Oxygen Species in Plants,* (pp. 141-168). Oxford: Blackwell Publishing Ltd.
30. Gupta, G. K., Sharma, S. K., & Ramteke, R. (2012). Biology, epidemiology and management of the pathogenic fungus *Macrophomina phaseolina* (Tassi) Goid with special reference to charcoal rot of soybean (*Glycine max* (L.) Merrill). *Journal of Phytopathology*, *160*, 167-180.
31. Huang, X. S., Wang, W., Zhang, Q., & Liu, J. H. (2013). A basic helix-loop-helix transcription factor, PtrbHLH, of *Poncirus trifoliata* confers cold tolerance and modulates peroxidase-mediated scavenging of hydrogen peroxide. *Plant Physiology*, *162*, 1178-1194.
32. Jones, J. D., & Dangl, J. L. (2006). The plant immune system. *Nature*, *444*, 323-329.
33. Kovtun, Y., Chiu, W. L., Tena, G., & Sheen, J. (2000). Functional analysis of oxidative stress-activated mitogen-activated protein kinase cascade in plants. *Proceedings of the National Academy of Sciences*, *97*, 2940-2945.

34. Langfelder, P., & Horvath, S. (2008). WGCNA: an R package for weighted correlation network analysis. *BMC Bioinformatics*, *9*, 1-13.
35. Lepiniec, L., Debeaujon, I., Routaboul, J. M., Baudry, A., Pourcel, L., Nesi, N., & Caboche, M. (2006). Genetics and biochemistry of seed flavonoids. *Annual Review of Plant Biology*, *57*, 405-430.
36. Lopez-Delacalle, M., Silva, C. J., Mestre, T. C., Martinez, V., Blanco-Ulate, B., & Rivero, R. M. (2021). Synchronization of proline, ascorbate and oxidative stress pathways under the combination of salinity and heat in tomato plants. *Environmental and Experimental Botany*, *183*, 104351.
37. Lorenzo, O., Piqueras, R., Sánchez-Serrano, J. J., & Solano, R. (2003). ETHYLENE RESPONSE FACTOR1 integrates signals from ethylene and jasmonate pathways in plant defense. *The Plant Cell*, *15*, 165-178.
38. Love, M. I., Huber, W., & Anders, S. (2014). Moderated estimation of fold change and dispersion for RNA-seq data with DESeq2. *Genome Biology*, *15*, 1-21.
39. McDermaid, A., Chen, X., Zhang, Y., Wang, C., Gu, S., Xie, J., & Ma, Q. (2018). A new machine learning-based framework for mapping uncertainty analysis in RNA-Seq read alignment and gene expression estimation. *Frontiers in Genetics*, *9*, 313.
40. Mengistu, A., Ray, J. D., Smith, J. R., & Paris, R. L. (2007). Charcoal rot disease assessment of soybean genotypes using a colony-forming unit index. *Crop Science*, *47*, 2453-2461.
41. Miller, G. A. D., Suzuki, N., Ciftci-Yilmaz, S. U. L. T. A. N., & Mittler, R. O. N. (2010). Reactive oxygen species homeostasis and signalling during drought and salinity stresses. *Plant, Cell & Environment*, *33*, 453-467.
42. Mittler, R., Vanderauwera, S., Gollery, M., & Van Breusegem, F. (2004). Reactive oxygen gene network of plants. *Trends in Plant Science*, *9*, 490-498.
43. Mol, J., Grotewold, E., & Koes, R. (1998). How genes paint flowers and seeds. *Trends in Plant Science*, *3*, 212-217.
44. Moy, P., Qutob, D., Chapman, B. P., Atkinson, I., & Gijzen, M. (2004). Patterns of gene expression upon infection of soybean plants by *Phytophthora sojae*. *Molecular Plant-Microbe Interactions*, *17*, 1051-1062.

45. Mukherjee, M., Larrimore, K. E., Ahmed, N. J., Bedick, T. S., Barghouthi, N. T., Traw, M. B., & Barth, C. (2010). Ascorbic acid deficiency in *Arabidopsis* induces constitutive priming that is dependent on hydrogen peroxide, salicylic acid, and the NPR1 gene. *Molecular Plant-Microbe Interactions*, *23*, 340-351.
46. Nicaise, V., Roux, M., & Zipfel, C. (2009). Recent advances in PAMP-triggered immunity against bacteria: Pattern recognition receptors watch over and raise the alarm. *Plant Physiology*, *150*, 1638-1647.
47. Noctor, G., & Foyer, C. H. (1998). Ascorbate and glutathione: Keeping active oxygen under control. *Annual Review of Plant Biology*, *49*, 249-279.
48. Osakabe, Y., Yamaguchi-Shinozaki, K., Shinozaki, K., & Tran, L. S. P. (2013). Sensing the environment: key roles of membrane-localized kinases in plant perception and response to abiotic stress. *Journal of Experimental Botany*, *64*, 445-458.
49. Ouyang, S. Q., Liu, Y. F., Liu, P., Lei, G., He, S. J., Ma, B.,Zhang, W.K., Zhang, J. S., & Chen, S. Y. (2010). Receptor-like kinase OsSIK1 improves drought and salt stress tolerance in rice (Oryza sativa) plants. *The Plant Journal*, *62*, 316-329.
50. Petroni, K., & Tonelli, C. (2011). Recent advances on the regulation of anthocyanin synthesis in reproductive organs. *Plant Science*, *181*, 219-229.
51. Pavet, V., Olmos, E., Kiddle, G., Mowla, S., Kumar, S., Antoniw, J., Alvarez, M. E., & Foyer, C. H. (2005). Ascorbic acid deficiency activates cell death and disease resistance responses in *Arabidopsis*. *Plant Physiology*, *139*, 1291-1303.
52. Reis, E. M., Boaretto, C., & Danelli, A. L. D. (2014). *Macrophomina phaseolina*: Density and longevity of microsclerotia in soybean root tissues and free on the soil, and competitive saprophytic ability. *Summa Phytopathologica*, *40*, 128-133.
53. Rezzonico, F., Rupp, O., & Fahrentrapp, J. (2017). Pathogen recognition in compatible plant-microbe interactions. *Scientific Reports*, *7*, 1-12.
54. Romero Luna, M. P., Mueller, D., Mengistu, A., Singh, A. K., Hartman, G. L., & Wise, K. A. (2017). Advancing our understanding of charcoal rot in soybeans. *Journal of Integrated Pest Management*, *8*, 1-8.
55. Rossi, F. R., Krapp, A. R., Bisaro, F., Maiale, S. J., Pieckenstain, F. L., & Carrillo, N. (2017). Reactive oxygen species generated in chloroplasts contribute to tobacco leaf infection by the necrotrophic fungus *Botrytis cinerea*. *The Plant Journal*, *92*, 761-773.

56. Saliba, A. E., Westermann, A. J., Gorski, S. A., & Vogel, J. (2014). Single-cell RNA-seq: advances and future challenges. *Nucleic Acids Research*, *42*, 8845-8860.
57. Schmutz, J., Cannon, S. B., Schlueter, J., Ma, J., Mitros, T., Nelson, W., Hyten, D. L., Song, Q., Thelen, J. J., Cheng, J., Xu, D., Hellsten, U. (2010). Genome sequence of the palaeopolyploid soybean. *Nature*, *463*, 178-183.
58. Shapiguzov, A., Vainonen, J. P., Wrzaczek, M., & Kangasjärvi, J. (2012). ROS-talk–how the apoplast, the chloroplast, and the nucleus get the message through. *Frontiers in Plant Science*, *3*, 292.
59. ShinyGO 0.76.1 [available at http://bioinformatics.sdstate.edu/go/] (Accessed on June 20, 2022)
60. Short, G. E., Wyllie, T. D., & Bristow, P. R. (1980). Survival of *Macrophomina phaseolina* in soil and in residue of soybean. *Phytopathology*, 70, 13-17.
61. Smertenko, A. (2017). Can peroxisomes inform cellular response to drought?. *Trends in Plant Science*, *22*, 1005-1007.
62. Smith, G. S. and T. D. Wyllie. 1999. Charcoal rot. In Hartman, G. L., Sinclair, J. B., & Rupe, J. C. (4 th Eds.), *Compendium of soybean diseases* (pp. 29-31). American Phyto-pathological Society, St. Paul, MN.
63. Sukumaran, A., McDowell, T., Chen, L., Renaud, J., & Dhaubhadel, S. (2018). Isoflavo-noid-specific prenyltransferase gene family in soybean: GmPT01, a pterocarpan 2-di-methylallyltransferase involved in glyceollin biosynthesis. *The Plant Journal*, *96*, 966-981.
64. Tahara, S. (2007). A journey of twenty-five years through the ecological biochemistry of flavonoids. *Bioscience, Biotechnology, and Biochemistry*, *71*, 1387-1404.
65. Torres, M. A., & Dangl, J. L. (2005). Functions of the respiratory burst oxidase in biotic interactions, abiotic stress and development. *Current Opinion in Plant Biology*, *8*, 397-403.
66. Trubitsin, B. V., Mamedov, M. D., Semenov, A. Y., & Tikhonov, A. N. (2014). Interaction of ascorbate with photosystem I. *Photosynthesis Research*, *122*, 215-231.
67. Twizeyimana, M., Hill, C. B., Pawlowski, M., Paul, C., & Hartman, G. L. (2012). A cut-stem inoculation technique to evaluate soybean for resistance to *Macrophomina phaseolina*. *Plant Disease*, *96*, 1210-1215.

68. Vega-Sánchez, M. E., Redinbaugh, M. G., Costanzo, S., & Dorrance, A. E. (2005). Spatial and temporal expression analysis of defense-related genes in soybean cultivars with different levels of partial resistance to *Phytophthora sojae*. *Physiological and Molecular Plant Pathology*, *66*, 175-182.
69. Walker, J. C. (1994). Structure and function of the receptor-like protein kinases of higher plants. *Plant Molecular Biology*, *26*, 1599-1609.
70. Wrather, A., Shannon, G., Balardin, R., Carregal, L., Escobar, R., Gupta, G. K., Ma, Z., Morel, W., Ploper D., & Tenuta, A. (2010). Effect of diseases on soybean yield in the top eight producing countries in 2006. *Plant Health Progress*, *11*, 29.
71. Wrzaczek, M., Brosché, M., & Kangasjärvi, J. (2013). ROS signaling loops—production, perception, regulation. *Current Opinion in Plant Biology*, *16*, 575-582.
72. Xu, X., & Tian, S. (2008). Salicylic acid alleviated pathogen-induced oxidative stress in harvested sweet cherry fruit. *Postharvest Biology and Technology*, *49*, 379-385.
73. Yan, J., Wang, B., Jiang, Y., Cheng, L., & Wu, T. (2014). GmFNSII-controlled soybean flavone metabolism responds to abiotic stresses and regulates plant salt tolerance. *Plant and Cell Physiology*, *55*, 74-86.
74. Yan, W., Ni, Y., Liu, X., Zhao, H., Chen, Y., Jia, M., Liu, M., Liu, H., & Tian, B. (2021). The mechanism of sesame resistance against *Macrophomina phaseolina* was revealed via a comparison of transcriptomes of resistant and susceptible sesame genotypes. *BMC Plant Biology*, *21*, 1-21.
75. Young, P. A. 1949. Charcoal rot of plants in east Texas. Bulletin Texas Agricultural Experimental Station No. 33.
76. Zhang, S. S., Hu, L., & Liu, Z. L. (2006). Relationship between the disease defense-related enzymes and the disease resistance of plants [J]. *Anhui Agricultural Science Bulletin*, *13*, 48-49.
77. Zhang, Y., Wang, X., Li, Y., Wu, L., Zhou, H., Zhang, G., & Ma, Z. (2013). Ectopic expression of a novel Ser/Thr protein kinase from cotton (*Gossypium barbadense*), enhances resistance to *Verticillium dahliae* infection and oxidative stress in *Arabidopsis*. *Plant Cell Reports*, *32*, 1703-1713.
78. Zipfel, C., & Felix, G. (2005). Plants and animals: A different taste for microbes? *Current Opinion in Plant Biology*, *8*, 353-360.

TABLES AND FIGURES

Table 3.1. Treatment scheme of soybean cut stem assay for the sample collection and RNA extraction.

Soybean cut stem assay		
Treatments	Pre-treatment	Inoculation 48 hrs after pre-treatment)
1	No	MP[a] embedded PDA[b]
2	Ascorbic acid	MP embedded PDA
3	No	PDA
4	Ascorbic acid	PDA
5	No	H_2O_2
6	H_2O_2[c]	MP embedded PDA

[a]MP = *M. phaseolina*, [b]PDA = Potato Dextrose Agar, [c]H_2O_2 = Hydrogen peroxide

Table 3.2. The average sequence read mapping summary of the RNA-seq data of the two genotypes (resistant & susceptible) and treatments across the biological replicates.

Genotype	Pre-Treatment	Inoculation	Input read	Uniquely mapped read	Uniquely mapped (%)
DT97-4290	No	MP[£]	109255596	90748314	75.39
DT97-4290	AsA[**]	MP	113881743	81263061	71.26
DT97-4290	No	AgPlug[¥]	104640629	80999777	77.42
DT97-4290	AsA	AgPlug	110712502	86115587	78
DT97-4290	No	H_2O_2	108805730	83424985	77
DT97-4290	H_2O_2	MP	111523929	84235777	75.52
Pharaoh	No	MP	115167092	86568012	75.13
Pharaoh	AsA	MP	121185775	89920289	75
Pharaoh	No	AgPlug	102266177	78699715	77
Pharaoh	AsA	AgPlug	102022305	78737938	77
Pharaoh	No	H_2O_2	106631099	82227534	77
Pharaoh	H_2O_2	MP	105399842	77067683	73

[**]AsA = Ascorbic acid, [¥]AgPlug = Agar plug, [£]MP = *M. phaseolina*

Table 3.3. Differential gene expression summary of the pairwise comparisons of treatments within genotypes and between genotypes.

Genotypes	Treatments	Informa-tive genes	Significant genes	Up-regu-lated				Down-regulated			
				1-2fc***	2-4fc	>4fc	Total	1-2fc	2-4fc	>4fc	Total
R[a]-G	Inoc* vs. Mock**	40020	1570	117	179	83	379	185	508	498	1191
R-G	AsA$_Inoc vs. Inoc	39588	7494	1228	1545	1256	4029	1454	1471	540	3465
R-G	AsA_Inoc vs. AsA_Mock	39034	7428	1808	1134	171	3113	1452	1452	1411	4315
R-G	H_2O_2 vs. H_2O_2_Inoc	39187	1077	162	268	187	617	199	202	59	460
R-G	Mock cont. vs. H_2O_2_Inoc	39833	5859	1026	1055	860	2941	873	1614	431	2918
S[b]-G	Inoc vs. Mock	40082	1617	143	138	53	334	355	536	392	1283
S-G	AsA_Inoc vs. Inoc	40037	5579	991	1735	837	3563	1041	738	237	2016
S-G	AsA_Inoc vs. AsA_Mock	39341	4532	1245	199	31	1475	1414	894	749	3057
S-G	H_2O_2 vs. H_2O_2_Inoc	39097	3820	587	1177	950	2714	455	514	137	1106
S-G	Mock cont. vs. H_2O_2_Inoc	39696	10944	2293	1736	1429	5458	1901	2140	1445	5486
R-G vs. S-G	NPT¥_Inoc	40213	1503	165	319	295	779	190	271	263	724
R-G vs. S-G	AsA_Inoc	39361	4692	841	796	469	2106	1335	806	445	2586
R-G vs. S-G	H_2O_2_Inoc	39211	2902	416	603	399	1418	450	649	385	1484
R-G vs. S-G	NPT_H_2O_2	39246	3249	709	370	301	1380	983	585	301	1869
R-G vs. S-G	NPT_Agplug£	40084	1928	314	378	262	954	321	351	302	974

[a]R-G = Resistant genotype (DT97-4290), [b]S-G = Susceptible genotype (Pharaoh), *Inoc = Inoculated, **Mock = Mock-inoculated, ***fc = Fold change,

$AsA = Ascorbic acid, £AgPlug = AgarPlug, ¥NPT = No pre-treatment

Table 3.4. Significantly and differentially expressed genes in the resistant genotype between comparison of non pre-treated inoculated vs. mock-inoculated treatment.

GO	Terms	Genes	log2FC	*p*-value	*q*-value
GO:0004364	glutathione transferase activity	GLYMA_01G106000	-1.4311	1.71E-05	0.0010
		GLYMA_02G024800	-1.7021	8.61E-10	1.42E-07
		GLYMA_03G176300	-3.5436	9.51E-13	2.66E-10
		GLYMA_08G306800	-1.1271	0.0014	0.0378
		GLYMA_11G198500	-4.2069	8.33E-51	1.11E-46
GO:0004568	chitinase activity	GLYMA_12G156600	-2.5725	8.78E-08	9.18E-06
		GLYMA_15G206800	-2.5882	7.73E-16	3.44E-13
		GLYMA_17G217000	-1.2046	0.000905	0.0277
		GLYMA_09G126200	1.5866	0.000197	0.0077
		GLYMA_11G124500	-1.3124	2.20E-10	4.07E-08
GO:0004601	peroxidase activity	GLYMA_11G101200	-7.6824	1.82E-10	3.48E-08
		GLYMA_11G162100	-2.8716	1.26E-05	0.0007
		GLYMA_14G201700	-1.9584	5.72E-13	1.68E-10
		GLYMA_09G022500	2.2481	1.57E-06	0.0001
		GLYMA_10G222400	-2.3864	3.15E-17	1.71E-14
GO:0004672	protein kinase activity	GLYMA_10G253200	0.7882	0.000705	0.022649
		GLYMA_10G253800	-3.6067	2.32E-17	1.29E-14
		GLYMA_11G055100	-2.9536	2.43E-06	0.000171
		GLYMA_10G186000	-1.4261	0.000422	0.014713
		GLYMA_10G188500	-1.0918	4.81E-06	0.0003
GO:0004673	protein histidine kinase activity	GLYMA_10G188500	-1.0918	4.81E-06	0.0003
		GLYMA_12G241700	-0.7151	0.0017	0.0438
		GLYMA_20G087000	-1.5141	6.92E-07	5.67E-05
		GLYMA_20G202200	-1.0976	1.53E-07	1.53E-05
GO:0004674	protein serine/threonine kinase activity	GLYMA_20G231000	-1.3670	0.000488	0.016511
		GLYMA_01G004800	-1.3861	0.000141	0.005838
		GLYMA_01G186900	-3.1915	0.0017	0.0441
		GLYMA_20G139500	-2.2536	5.34E-10	9.25E-08
		GLYMA_20G140100	-0.9798	0.0001	0.005996
GO:0006749	glutathione metabolic process	GLYMA_01G106000	-1.4311	1.71E-05	0.0010
		GLYMA_02G024800	-1.7021	8.61E-10	1.42E-07
		GLYMA_03G176300	-3.5436	9.51E-13	2.66E-10
		GLYMA_11G198500	-4.2069	8.33E-51	1.11E-46
GO:0006952	defense response	GLYMA_12G049300	-3.0584	1.74E-17	9.83E-15
		GLYMA_13G234400	-1.7121	0.000195	0.0077
		GLYMA_13G278000	-5.0980	1.34E-32	4.47E-29
		GLYMA_11G124500	-1.3124	2.20E-10	4.07E-08
		GLYMA_11G124700	-1.5957	6.92E-05	0.0032

GO:0006979	response to oxidative stress	GLYMA_11G162100	-2.8716	1.26E-05	0.0007
		GLYMA_14G201700	-1.9584	5.72E-13	1.68E-10
		GLYMA_15G052700	1.9487	1.08E-16	5.32E-14
GO:0007178	serine/threonine kinase pathway	GLYMA_15G059200	-2.2217	6.71E-08	7.12E-06
		GLYMA_15G074600	-1.8807	4.20E-09	5.95E-07
		GLYMA_17G224200	2.9511	0.0004	0.0128
		GLYMA_07G117700	-1.2349	0.0003	0.0118
		GLYMA_07G154100	1.6421	0.0002	0.0082
GO:0008061	chitin binding	GLYMA_11G124500	-1.3124	2.20E-10	4.07E-08
		GLYMA_15G206800	-2.5882	7.73E-16	3.44E-13
		GLYMA_17G217000	-1.2046	0.0009	0.0277
		GLYMA_02G007400	-1.3739	8.80E-07	6.94E-05
		GLYMA_02G042500	-2.3735	7.99E-08	8.39E-06
GO:0008152	metabolic process	GLYMA_02G042500	-2.3735	7.99E-08	8.39E-06
		GLYMA_02G130400	-1.9647	6.18E-09	8.41E-07
		GLYMA_03G137700	2.3546	0.0006	0.0197
		GLYMA_02G009300	1.5806	0.0008	0.0255
		GLYMA_02G015600	-0.6126	0.0008	0.0261
GO:0009698	phenylpropanoid metabolic process	GLYMA_02G309300	-1.6695	1.11E-11	2.63E-09
		GLYMA_10G209800	-0.6635	0.0013	0.0365
		GLYMA_13G145000	-0.9463	0.0008	0.0255
		GLYMA_13G372000	-0.7697	0.0010	0.0301
		GLYMA_01G232400	-1.8986	3.01E-09	4.46E-07
GO:0009717	isoflavonoid biosynthetic process	GLYMA_01G239600	-1.8826	3.31E-10	5.97E-08
		GLYMA_13G173500	-1.9986	2.05E-05	0.0011
GO:0009813	flavonoid biosynthetic process	GLYMA_13G173500	-1.9986	2.05E-05	0.0011
		GLYMA_01G239600	-1.8826	3.31E-10	5.97E-08
GO:0009873	ethylene-activated signaling path-way	GLYMA_02G006200	-2.9863	1.24E-14	4.51E-12
		GLYMA_02G006300	-5.3777	7.56E-23	8.18E-20
		GLYMA_02G066200	-1.0602	1.95E-05	0.0011
		GLYMA_20G202200	-1.0976	1.53E-07	1.53E-05
		GLYMA_20G203700	-1.4108	9.73E-06	0.0006
GO:0010200	response to chitin	GLYMA_02G094500	-1.5933	1.91E-09	2.91E-07
		GLYMA_03G173100	-2.4875	0.0012	0.0338
		GLYMA_10G045400	-3.5615	3.03E-19	2.21E-16
		GLYMA_13G337400	-2.0555	1.62E-19	1.25E-16
GO:0016301	kinase activity	GLYMA_13G352800	2.6590	1.86E-05	0.0010
		GLYMA_14G157700	0.9668	3.06E-08	3.50E-06
		GLYMA_14G158200	6.7973	8.16E-06	0.000503
		GLYMA_13G167000	1.2719	0.0018	0.0473
		GLYMA_13G275100	-1.0886	0.0010	0.0310

GO:0016310	phosphorylation	GLYMA_13G275100	-1.0886	0.0010	0.0310
		GLYMA_13G352800	2.6590	1.86E-05	0.001036
		GLYMA_14G157700	0.9668	3.06E-08	3.50E-06
		GLYMA_13G139500	-0.9000	0.0014	0.0382
		GLYMA_13G167000	1.2719	0.0018	0.0473
GO:0016491	oxidoreductase activity	GLYMA_13G173500	-1.9986	2.05E-05	0.0011
		GLYMA_13G186200	-5.0458	9.54E-26	1.59E-22
		GLYMA_13G246600	-3.1991	1.71E-23	1.96E-20
		GLYMA_13G068800	-2.5836	5.54E-12	1.40E-09
		GLYMA_13G109800	-4.0329	2.30E-21	2.14E-18
GO:0038199	ethylene receptor activity	GLYMA_20G087000	-1.5141	6.92E-07	5.67E-05
		GLYMA_20G202200	-1.0976	1.53E-07	1.53E-05
		GLYMA_10G188500	-1.0918	4.81E-06	0.0003
		GLYMA_10G188500	-1.0918	4.81E-06	0.0003
		GLYMA_12G241700	-0.7151	0.0017	0.0438
GO:0042744	hydrogen peroxide catabolic process	GLYMA_14G201700	-1.9584	5.72E-13	1.68E-10
		GLYMA_15G052700	1.9487	1.08E-16	5.32E-14
		GLYMA_15G128700	-2.0765	7.70E-05	0.0035
		GLYMA_11G101200	-7.6824	1.82E-10	3.48E-08
		GLYMA_11G162100	-2.8716	1.26E-05	0.0007
GO:0042910	xenobiotic transmembrane transporter activity	GLYMA_12G099300	-2.1655	1.25E-06	9.56E-05
		GLYMA_15G107100	-1.7265	2.13E-11	4.79E-09
		GLYMA_18G293200	-2.5075	1.87E-06	0.0001
		GLYMA_10G267300	-3.0434	0.0006	0.0191
		GLYMA_10G267700	-1.7448	6.29E-05	0.0029
GO:0098869	cellular oxidant detoxification	GLYMA_11G101200	-7.6824	1.82E-10	3.48E-08
		GLYMA_11G162100	-2.8716	1.26E-05	0.0007
		GLYMA_14G201700	-1.9584	5.72E-13	1.68E-10
		GLYMA_09G022500	2.2481	1.57E-06	0.0001
		GLYMA_10G222400	-2.3864	3.15E-17	1.71E-14
GO:0102128	chalcone synthase activity	GLYMA_11G011500	-1.7414	3.32E-09	4.84E-07
		GLYMA_01G228700	-1.6999	5.69E-07	4.83E-05
		GLYMA_02G130400	-1.9647	6.18E-09	8.41E-07
		GLYMA_08G109500	-2.1822	1.54E-08	1.91E-06
		GLYMA_09G075200	-2.4081	2.54E-05	0.0013
GO:0106310	protein serine kinase activity	GLYMA_09G075200	-2.4081	2.54E-05	0.0013
		GLYMA_11G011500	-1.7414	3.32E-09	4.84E-07
		GLYMA_01G228700	-1.6999	5.69E-07	4.83E-05
		GLYMA_08G109400	-1.5754	2.87E-07	2.65E-05
		GLYMA_08G109500	-2.1822	1.54E-08	1.91E-06

Table 3.5. Significantly and differentially expressed genes in the susceptible genotype between comparison of non pre-treated inoculated vs. mock-inoculated treatment.

GO	Terms	Genes	log2FC	*p*-value	*q*-value
GO:0004364	glutathione transferase activity	GLYMA_01G106000	-1.0459	1.81E-06	0.0001
		GLYMA_02G024600	1.3441	4.26E-05	0.0019
		GLYMA_02G187200	-1.4290	2.70E-09	3.05E-07
		GLYMA_18G190200	-1.8344	7.08E-07	5.12E-05
		GLYMA_20G101100	-1.0879	4.80E-05	0.0021
GO:0004568	chitinase activity	GLYMA_01G160100	0.9637	5.41E-05	0.0023
		GLYMA_02G042500	-2.1534	4.58E-16	1.54E-13
		GLYMA_09G126200	2.6019	2.71E-27	3.11E-24
		GLYMA_19G245400	-1.5891	1.66E-15	5.17E-13
		GLYMA_19G245500	-1.2821	1.24E-07	1.04E-05
GO:0004601	peroxidase activity	GLYMA_20G001400	-3.6206	1.44E-11	2.55E-09
		GLYMA_20G169200	-2.1200	0.0007	0.0204
		GLYMA_20G171900	-4.4386	5.88E-43	2.35E-39
		GLYMA_19G011700	-2.2600	1.40E-13	3.39E-11
		GLYMA_19G233900	-1.4631	2.20E-09	2.54E-07
GO:0004672	protein kinase activity	GLYMA_20G139000	0.6421	0.0017	0.0438
		GLYMA_20G139400	-1.2131	1.61E-05	0.0008
		GLYMA_20G139500	-1.6926	1.20E-15	3.76E-13
		GLYMA_18G294800	-1.7758	2.20E-14	5.92E-12
		GLYMA_19G167400	1.1182	0.0010	0.0285
GO:0004674	protein serine/threonine kinase activity	GLYMA_20G139000	0.6421	0.0017	0.0438
		GLYMA_20G139400	-1.2131	1.61E-05	0.0008
		GLYMA_20G139500	-1.6926	1.20E-15	3.76E-13
		GLYMA_18G225700	-0.6494	0.0014	0.0371
		GLYMA_18G237900	1.1793	5.54E-05	0.0024
GO:0004866	endopeptidase inhibitor activity	GLYMA_08G235300	-3.4608	1.97E-36	4.65E-33
		GLYMA_08G235400	-2.5109	1.25E-41	3.35E-38
		GLYMA_08G341300	-1.9387	7.18E-09	7.54E-07
		GLYMA_16G212200	-5.2104	0.0005	0.0159
		GLYMA_16G212400	-3.2442	3.35E-29	4.79E-26
GO:0004867	serine-type endopeptidase inhibitor activity	GLYMA_10G184600	-1.5682	5.00E-05	0.0022
		GLYMA_10G184700	-2.3159	1.12E-20	6.58E-18
		GLYMA_13G120600	-3.7843	0.0016	0.0412
		GLYMA_20G205700	-4.3679	1.52E-21	1.03E-18
		GLYMA_20G205800	-2.1002	0.0006	0.0176

GO:0005975	carbohydrate metabolic process	GLYMA_01G007200	-0.9884	6.41E-07	4.65E-05
		GLYMA_01G007300	-1.4802	1.55E-08	1.53E-06
		GLYMA_01G160100	0.9637	5.41E-05	0.0023
		GLYMA_19G245500	-1.2821	1.24E-07	1.04E-05
		GLYMA_20G018200	-2.3930	4.77E-09	5.11E-07
GO:0006032	chitin catabolic process	GLYMA_01G160100	0.9637	5.41E-05	0.0023
		GLYMA_02G042500	-2.1534	4.58E-16	1.54E-13
		GLYMA_11G124500	-1.3511	8.50E-11	1.32E-08
		GLYMA_19G245400	-1.5891	1.66E-15	5.17E-13
		GLYMA_19G245500	-1.2821	1.24E-07	1.04E-05
GO:0006468	protein phosphorylation	GLYMA_20G139000	0.6421	0.0017	0.0438
		GLYMA_20G139400	-1.2131	1.61E-05	0.0008
		GLYMA_20G139500	-1.6926	1.20E-15	3.76E-13
		GLYMA_18G294800	-1.7758	2.20E-14	5.92E-12
		GLYMA_19G167400	1.1182	0.0010	0.0285
GO:0006749	glutathione metabolic process	GLYMA_20G101100	-1.0879	4.80E-05	0.0021
		GLYMA_01G106000	-1.0459	1.81E-06	0.0001
		GLYMA_02G024600	1.3441	4.26E-05	0.0019
		GLYMA_15G252200	-2.6290	6.02E-15	1.71E-12
		GLYMA_18G190200	-1.8344	7.08E-07	5.12E-05
GO:0006952	defense response	GLYMA_18G205000	2.2156	4.33E-07	3.28E-05
		GLYMA_18G214700	-1.1565	0.0008	0.0222
		GLYMA_19G245400	-1.5891	1.66E-15	5.17E-13
		GLYMA_17G258500	-1.6764	4.19E-06	0.0002
		GLYMA_18G004200	-1.2331	5.22E-07	3.85E-05
GO:0006955	immune response	GLYMA_18G004200	-1.2331	5.22E-07	3.85E-05
		GLYMA_18G214700	-1.1565	0.0008	0.0222
		GLYMA_05G196800	-0.6621	0.0015	0.0385
		GLYMA_13G176600	0.7146	0.0011	0.0308
		GLYMA_15G088100	-0.8090	0.0001	0.0040
GO:0006979	response to oxidative stress	GLYMA_15G128700	-2.2275	3.65E-08	3.43E-06
		GLYMA_15G129200	-1.6922	6.51E-16	2.14E-13
		GLYMA_19G011700	-2.2600	1.40E-13	3.39E-11
		GLYMA_14G201800	-0.9868	0.0002	0.0059
		GLYMA_15G052700	1.1098	1.91E-07	1.54E-05
GO:0007178	serine/threonine kinase signaling pathway	GLYMA_15G074600	-1.6594	2.05E-10	2.88E-08
		GLYMA_17G224200	2.2141	0.0002	0.0057
		GLYMA_17G224300	1.0828	2.10E-06	0.0001
		GLYMA_09G110500	-1.4494	2.10E-10	2.94E-08
		GLYMA_12G114100	-1.1373	2.19E-07	1.75E-05

GO:0008061	chitin binding	GLYMA_14G110700	-2.5994	4.90E-07	3.65E-05
		GLYMA_16G119200	-1.5490	3.29E-06	0.0002
		GLYMA_17G217000	-1.4052	1.07E-07	9.08E-06
		GLYMA_02G042500	-2.1534	4.58E-16	1.54E-13
		GLYMA_11G124500	-1.3511	8.50E-11	1.32E-08
GO:0008152	metabolic process	GLYMA_11G095100	-1.2810	2.32E-08	2.25E-06
		GLYMA_11G129300	-3.2012	1.56E-17	6.45E-15
		GLYMA_11G129900	-1.2608	2.62E-06	0.0002
		GLYMA_10G214700	-0.5533	0.000651	0.0196
		GLYMA_11G011500	-1.6537	7.00E-11	1.12E-08
GO:0009813	flavonoid biosynthetic process	GLYMA_11G011500	-1.6537	7.00E-11	1.12E-08
		GLYMA_12G067000	1.1656	0.0009	0.0264
		GLYMA_20G241500	-1.5477	4.32E-09	4.70E-07
		GLYMA_09G075200	-2.0874	4.98E-05	0.002187
		GLYMA_10G292200	-1.3150	0.0003	0.0098
GO:0009873	ethylene-activated signaling pathway	GLYMA_11G036500	-1.0137	0.0002	0.0065
		GLYMA_13G122800	-6.4708	0.0002	0.0076
		GLYMA_13G122900	-6.1352	6.52E-05	0.0028
		GLYMA_10G188500	-0.8526	2.10E-05	0.0010
		GLYMA_10G223200	-1.0411	6.61E-06	0.0004
GO:0010200	response to chitin	GLYMA_10G257900	-1.2606	2.11E-05	0.0011
		GLYMA_10G290200	-1.9909	4.57E-16	1.54E-13
		GLYMA_13G133100	-1.4706	1.25E-09	1.55E-07
		GLYMA_02G094500	-1.5916	6.61E-12	1.25E-09
		GLYMA_10G045400	-2.9005	2.54E-30	4.08E-27
GO:0016301	kinase activity	GLYMA_10G069500	-1.2030	3.96E-09	4.33E-07
		GLYMA_10G188500	-0.8526	2.10E-05	0.0010
		GLYMA_10G023300	-1.0118	2.93E-06	0.0002
		GLYMA_10G023400	-1.1384	1.76E-09	2.08E-07
GO:0016310	phosphorylation	GLYMA_10G023300	-1.0118	2.93E-06	0.0002
		GLYMA_10G023400	-1.1384	1.76E-09	2.08E-07
		GLYMA_09G182200	1.1758	4.44E-05	0.0020
		GLYMA_09G265500	-0.5642	0.0004	0.0140
GO:0016491	oxidoreductase activity	GLYMA_09G269500	-1.3006	1.38E-09	1.68E-07
		GLYMA_10G023900	-0.5884	0.0015	0.0400
		GLYMA_09G201200	-5.1828	1.34E-05	0.0007
		GLYMA_09G205700	-1.1064	1.93E-06	0.0001

GO:0042744	hydrogen peroxide catabolic process	GLYMA_10G222400	-2.3684	1.28E-10	1.88E-08
		GLYMA_13G167100	1.0031	8.01E-06	0.0004
		GLYMA_06G302700	-5.1947	0.0004	0.0136
		GLYMA_08G179700	1.4511	1.25E-09	1.55E-07
GO:0050832	defense response to fungus	GLYMA_10G230000	0.6269	9.62E-05	0.0038
		GLYMA_12G207400	-0.9442	0.0015	0.0402
		GLYMA_03G247500	-1.1984	2.50E-12	5.04E-10
		GLYMA_05G082400	-2.7262	4.65E-23	3.80E-20
GO:0080142	salicylic acid biosynthetic process	GLYMA_05G237200	1.0450	3.47E-07	2.71E-05
		GLYMA_07G093900	1.5415	4.59E-08	4.24E-06
		GLYMA_10G148700	1.0820	0.0003	0.0098
		GLYMA_03G232400	0.7632	0.0005	0.0157
GO:0098869	cellular oxidant detoxification	GLYMA_04G220600	-1.5985	1.49E-09	1.80E-07
		GLYMA_06G114400	-0.5043	0.0007	0.0203
		GLYMA_03G038100	-3.2966	0.0011	0.0313
		GLYMA_03G038200	-5.1348	4.73E-13	1.04E-10
GO:0009626	plant-type hypersensitive response	GLYMA_05G196800	-0.6621	0.0015	0.0385
		GLYMA_11G252700	-0.9643	2.43E-05	0.0012
		GLYMA_18G004200	-1.2331	5.22E-07	3.85E-05
		GLYMA_18G214700	-1.1565	0.0008	0.0222
GO:0106310	protein serine kinase activity	GLYMA_18G225700	-0.6494	0.0014	0.0371
		GLYMA_01G131500	-0.7497	0.0005	0.0166
		GLYMA_15G187400	-0.7585	0.0016	0.0419
		GLYMA_15G258400	0.9981	0.0014	0.0381
GO:0010427	abscisic acid binding	GLYMA_17G030000	-1.7250	4.17E-08	3.87E-06
		GLYMA_17G030400	-2.1064	1.64E-14	4.45E-12
		GLYMA_09G040600	0.7979	1.16E-07	9.79E-06
		GLYMA_15G146600	-0.9576	0.0006	0.0175
GO:0009607	response to biotic stimulus	GLYMA_15G146600	-0.9576	0.0006	0.0175
		GLYMA_16G145600	-1.2279	0.0000	0.0004
		GLYMA_07G243600	-0.7095	0.0006	0.0183
		GLYMA_13G234400	-3.6524	3.98E-10	5.35E-08

Table 3.6. Significantly and differentially expressed genes in the resistant genotype between comparison of ascorbic acid pre-treated (MP-inoculated vs. mock-inoculated control) treatment.

GO	Terms	Genes	log2FC	*p*-value	*q*-value
GO:0000302	response to reactive oxygen species	GLYMA_01G106800	2.036	0.002635	0.0172
		GLYMA_02G209000	1.336	6.01E-05	0.0006
		GLYMA_02G262500	1.351	3.44E-05	0.0004
GO:0004364	glutathione transferase activity	GLYMA_01G040200	1.346	2.29E-10	6.62E-09
		GLYMA_01G106000	-2.445	9.00E-73	1.46E-69
		GLYMA_02G283900	-1.984	4.04E-10	1.12E-08
GO:0004568	chitinase activity	GLYMA_02G007400	-2.838	3.89E-16	2.02E-14
		GLYMA_02G042500	-1.915	5.89E-07	9.95E-06
		GLYMA_11G124500	-2.365	1.19E-22	1.00E-20
		GLYMA_19G245400	-2.160	2.25E-25	2.22E-23
		GLYMA_19G245500	-1.490	1.53E-05	0.0002
GO:0004601	peroxidase activity	GLYMA_01G130500	-4.196	6.04E-19	3.86E-17
		GLYMA_01G130800	-4.664	1.48E-29	1.87E-27
		GLYMA_02G008900	-5.771	2.79E-59	1.95E-56
		GLYMA_20G169200	-3.669	1.47E-37	3.08E-35
		GLYMA_20G171900	-4.003	1.02E-28	1.23E-26
GO:0004672	protein kinase activity	GLYMA_01G004800	-2.300	2.38E-22	1.96E-20
		GLYMA_01G007500	-2.004	9.24E-09	2.13E-07
		GLYMA_20G231000	-1.857	1.39E-07	2.67E-06
		GLYMA_20G246600	-2.139	0.0012	0.0090
GO:0004674	protein serine/threonine kinase activity	GLYMA_01G004800	-2.300	2.38E-22	1.96E-20
		GLYMA_01G007500	-2.004	9.24E-09	2.13E-07
		GLYMA_20G231000	-1.857	1.39E-07	2.67E-06
		GLYMA_20G246600	-2.139	0.001224	0.0090
GO:0006468	protein phosphorylation	GLYMA_20G226900	1.698	0.006089	0.0346
GO:0006749	glutathione metabolic process	GLYMA_01G040200	1.346	2.29E-10	6.62E-09
		GLYMA_01G106100	2.426	0.0022	0.0147
		GLYMA_06G193500	1.607	6.47E-06	8.82E-05
		GLYMA_14G031000	1.231	0.00257	0.0169
GO:0006979	response to oxidative stress	GLYMA_02G209000	1.336	6.01E-05	0.0006
		GLYMA_06G017900	1.083	0.000209	0.0019
		GLYMA_19G263800	1.276	0.007721	0.0421
		GLYMA_02G198400	0.990	0.000823	0.0064
		GLYMA_17G223900	0.746	4.23E-06	5.98E-05

GO:0008152	metabolic process	GLYMA_01G024800	-6.287	1.48E-32	2.26E-30
		GLYMA_01G099800	0.655	0.001894	0.0130
		GLYMA_01G196800	1.701	0.000295	0.0026
		GLYMA_01G228700	-2.730	6.38E-33	1.02E-30
		GLYMA_20G198000	-0.438	0.001321	0.0096
		GLYMA_20G240000	-1.090	9.96E-06	0.0001
GO:0009507	chloroplast	GLYMA_01G008500	0.539	0.000105	0.0011
		GLYMA_01G010200	1.038	1.10E-09	2.87E-08
		GLYMA_01G014200	-0.992	0.0003	0.0028
		GLYMA_01G014900	0.954	0.0001	0.0011
		GLYMA_01G019100	0.672	0.000733	0.0058
		GLYMA_20G221500	0.843	3.24E-05	0.0004
		GLYMA_20G249800	0.648	0.007405	0.0407
GO:0009522	photosystem I	GLYMA_01G115900	1.056	1.86E-05	0.0002
		GLYMA_02G064700	0.953	4.61E-07	7.97E-06
		GLYMA_02G305400	0.939	0.0017	0.0116
		GLYMA_20G144700	0.957	0.0002	0.0022
		GLYMA_20G212900	0.974	0.0002	0.0021
GO:0009523	photosystem II	GLYMA_01G050900	1.520	5.02E-19	3.24E-17
		GLYMA_01G115900	1.056	1.86E-05	0.0002
		GLYMA_01G180800	0.968	1.81E-05	0.0002
		GLYMA_19G161400	0.889	0.0002	0.0017
		GLYMA_20G212900	0.974	0.0002	0.0021
GO:0009535	chloroplast thylakoid membrane	GLYMA_01G115900	1.056	1.86E-05	0.0002
		GLYMA_01G214300	1.257	1.16E-05	0.0002
		GLYMA_01G223500	0.827	5.33E-06	7.40E-05
		GLYMA_20G212900	0.974	0.0002	0.0021
		GLYMA_20G224600	0.934	9.22E-05	0.0009
GO:0009536	plastid	GLYMA_01G014200	-0.992	0.0003	0.0028
		GLYMA_01G114800	0.800	0.0042	0.0256
		GLYMA_01G226700	0.809	0.0007	0.0055
		GLYMA_20G212900	0.974	0.0002	0.0021
		GLYMA_20G227900	0.801	2.74E-06	4.03E-05
GO:0009538	photosystem I reaction center	GLYMA_05G022900	1.100	5.27E-05	0.0006
GO:0009570	chloroplast stroma	GLYMA_01G014200	-0.992	0.0003	0.0028
		GLYMA_01G068000	0.459	0.0039	0.0237
		GLYMA_01G069500	2.013	3.77E-08	7.91E-07
		GLYMA_20G155600	1.189	0.0002	0.0017
		GLYMA_20G179900	-0.443	0.0015	0.0106

GO:0009579	thylakoid	GLYMA_01G050900	1.520	5.02E-19	3.24E-17
		GLYMA_01G087900	0.734	0.0018	0.0123
		GLYMA_01G115900	1.056	1.86E-05	0.0002
		GLYMA_20G150600	1.830	0.0002	0.0016
		GLYMA_20G212900	0.974	0.0002	0.0021
GO:0009654	photosystem II oxygen evolving complex	GLYMA_01G050900	1.520	5.02E-19	3.24E-17
		GLYMA_01G180800	0.968	1.81E-05	0.0002
		GLYMA_02G061100	0.973	4.40E-07	7.64E-06
		GLYMA_18G286500	0.944	0.0013	0.0094
		GLYMA_19G126700	1.151	6.79E-06	9.20E-05
GO:0009765	photosynthesis, light harvesting	GLYMA_01G115900	1.056	1.86E-05	0.0002
		GLYMA_02G064700	0.953	4.61E-07	7.97E-06
		GLYMA_02G305400	0.939	0.0017	0.0116
		GLYMA_18G028400	1.353	8.94E-06	0.0001
		GLYMA_20G212900	0.974	0.0002	0.0021
GO:0009768	light harvesting in photosystem I	GLYMA_01G115900	1.056	1.86E-05	0.0002
		GLYMA_02G064700	0.953	4.61E-07	7.97E-06
		GLYMA_02G305400	0.939	0.0017	0.0116
		GLYMA_18G028400	1.353	8.94E-06	0.0001
		GLYMA_20G212900	0.974	0.0002	0.0021
GO:0009773	electron transport in photosystem I	GLYMA_01G214300	1.257	1.16E-05	0.0002
		GLYMA_04G167400	1.562	3.65E-05	0.0004
		GLYMA_05G048000	1.239	1.15E-06	1.83E-05
		GLYMA_17G133200	1.068	5.77E-08	1.17E-06
		GLYMA_20G020600	0.681	0.0091	0.0484
GO:0009698	phenylpropanoid metabolic process	GLYMA_01G232400	-3.099	1.98E-44	6.08E-42
		GLYMA_02G309300	-2.986	2.62E-53	1.36E-50
		GLYMA_03G181600	-2.501	6.13E-10	1.66E-08
		GLYMA_19G182300	-2.280	5.94E-35	1.08E-32
		GLYMA_20G180800	-1.973	5.37E-17	2.99E-15
GO:0009813	flavonoid biosynthetic process	GLYMA_01G228700	-2.730	6.38E-33	1.02E-30
		GLYMA_01G239600	-2.718	9.67E-26	9.73E-24
		GLYMA_02G130400	-4.054	1.60E-44	4.99E-42
		GLYMA_20G241600	-2.999	2.23E-35	4.15E-33
		GLYMA_20G241700	-3.092	1.00E-27	1.14E-25
GO:0009873	ethylene-activated signaling pathway	GLYMA_01G206600	-1.097	0.0051	0.0299
		GLYMA_02G006200	-4.578	1.57E-54	9.00E-52
		GLYMA_02G006300	-4.362	9.17E-25	8.76E-23
		GLYMA_20G203500	-4.958	1.76E-18	1.09E-16
		GLYMA_20G203700	-2.197	4.17E-28	4.80E-26

GO:0010207	photosystem II assembly	GLYMA_01G147700	0.785	0.0002	0.0018
		GLYMA_01G180800	0.968	1.81E-05	0.0002
		GLYMA_02G061100	0.973	4.40E-07	7.64E-06
		GLYMA_13G302100	1.378	8.79E-10	2.34E-08
		GLYMA_16G143600	0.847	0.0002	0.0017
GO:0010287	plastoglobule	GLYMA_01G115900	1.056	1.86E-05	0.0002
		GLYMA_02G064700	0.953	4.61E-07	7.97E-06
		GLYMA_02G305400	0.939	0.0017	0.0116
		GLYMA_18G028400	1.353	8.94E-06	0.0001
		GLYMA_20G212900	0.974	0.0002	0.0021
GO:0015979	photosynthesis	GLYMA_01G050900	1.520	5.02E-19	3.24E-17
		GLYMA_01G115900	1.056	1.86E-05	0.0002
		GLYMA_01G180800	0.968	1.81E-05	0.0002
		GLYMA_20G144700	0.957	0.0002	0.0022
		GLYMA_20G212900	0.974	0.0002	0.0021
GO:0015995	chlorophyll biosynthetic process	GLYMA_01G226700	0.809	0.0007	0.0055
		GLYMA_03G119500	0.819	1.70E-06	2.61E-05
		GLYMA_03G137000	0.905	4.19E-07	7.32E-06
		GLYMA_19G123800	0.839	1.74E-06	2.67E-05
		GLYMA_19G139300	0.809	5.50E-07	9.34E-06
GO:0016168	chlorophyll binding	GLYMA_01G115900	1.056	1.86E-05	0.0002
		GLYMA_02G064700	0.953	4.61E-07	7.97E-06
		GLYMA_02G305400	0.939	0.0017	0.0116
		GLYMA_18G028400	1.353	8.94E-06	0.0001
		GLYMA_20G212900	0.974	0.0002	0.0021
GO:0016301	kinase activity	GLYMA_01G004800	-2.300	2.38E-22	1.96E-20
		GLYMA_01G007200	-1.752	2.00E-19	1.33E-17
		GLYMA_01G007300	-2.505	1.04E-28	1.25E-26
		GLYMA_01G007400	-0.697	8.91E-05	0.0009
		GLYMA_20G226900	1.698	0.0061	0.0346
		GLYMA_20G231000	-1.857	1.39E-07	2.67E-06
		GLYMA_20G246600	-2.139	0.0012	0.0090

GO:0016310	phosphorylation	GLYMA_01G004800	-2.300	2.38E-22	1.96E-20
		GLYMA_01G007200	-1.752	2.00E-19	1.33E-17
		GLYMA_01G007300	-2.505	1.04E-28	1.25E-26
		GLYMA_01G007400	-0.697	8.91E-05	0.0009
		GLYMA_20G226900	1.698	0.0061	0.0346
		GLYMA_20G231000	-1.857	1.39E-07	2.67E-06
		GLYMA_20G246600	-2.139	0.0012	0.0090
GO:0042744	hydrogen peroxide catabolic process	GLYMA_01G130500	-4.196	6.04E-19	3.86E-17
		GLYMA_01G130800	-4.664	1.48E-29	1.87E-27
		GLYMA_02G008900	-5.771	2.79E-59	1.95E-56
		GLYMA_20G169200	-3.669	1.47E-37	3.08E-35
		GLYMA_20G171900	-4.003	1.02E-28	1.23E-26
		GLYMA_20G169200	-3.669	1.47E-37	3.08E-35
		GLYMA_20G171900	-4.003	1.02E-28	1.23E-26
GO:0098869	cellular oxidant detoxification	GLYMA_01G130500	-4.196	6.04E-19	3.86E-17
		GLYMA_01G130800	-4.664	1.48E-29	1.87E-27
		GLYMA_02G008900	-5.771	2.79E-59	1.95E-56
		GLYMA_20G169200	-3.669	1.47E-37	3.08E-35
		GLYMA_20G171900	-4.003	1.02E-28	1.23E-26
GO:0106310	protein serine kinase activity	GLYMA_01G131500	-1.687	6.26E-13	2.40E-11
		GLYMA_01G206400	-4.101	2.58E-25	2.53E-23
		GLYMA_03G002900	-0.621	0.0022	0.0149
		GLYMA_20G145800	0.776	0.0047	0.0279
		GLYMA_20G246600	-2.139	0.0012	0.0090
GO:1901259	chloroplast rRNA processing	GLYMA_03G015700	0.621	0.0003	0.0026
		GLYMA_03G132000	0.589	0.0036	0.0226
		GLYMA_03G202900	0.931	7.51E-05	0.0008
		GLYMA_17G125700	1.127	3.86E-08	8.08E-07
		GLYMA_20G082800	0.816	2.95E-11	9.52E-10

GO:0015994	chlorophyll metabolic process	GLYMA_20G214000	0.789	0.0001	0.0014
		GLYMA_03G253500	0.632	0.0003	0.0030
		GLYMA_10G128400	1.015	1.65E-06	2.54E-05
		GLYMA_16G138000	0.843	0.0006	0.0046
		GLYMA_19G251000	0.940	2.41E-06	3.58E-05
GO:0009534	chloroplast thylakoid	GLYMA_01G182600	0.587	0.0016	0.0111
		GLYMA_02G138600	1.496	1.47E-06	2.29E-05
		GLYMA_02G225300	0.658	0.0023643	0.0157
		GLYMA_18G035300	1.064	1.93E-08	4.24E-07
		GLYMA_19G258300	0.977	0.0037	0.0226
GO:0009534	chloroplast thylakoid	GLYMA_01G182600	0.587	0.0016	0.0111
		GLYMA_02G138600	1.496	1.47E-06	2.29E-05
		GLYMA_03G259400	0.699	0.0002	0.0015
		GLYMA_18G035300	1.064	1.93E-08	4.24E-07
		GLYMA_19G258300	0.977	0.0037	0.0226
GO:0009767	photosynthetic electron transport chain	GLYMA_01G050900	1.520	5.02E-19	3.24E-17
		GLYMA_03G015000	1.315	9.55E-08	1.88E-06
		GLYMA_03G114600	0.821	0.0004	0.0036
		GLYMA_13G286500	1.880	0.0001	0.0012
		GLYMA_18G046700	1.697	9.34E-08	1.84E-06
GO:0009696	salicylic acid metabolic process	GLYMA_02G062900	-1.276	0.0008	0.0064
		GLYMA_02G219700	1.988	0.0031	0.0200
		GLYMA_06G141200	1.235	0.0000	0.0004
		GLYMA_16G145200	-2.208	4.37E-31	6.09E-29
		GLYMA_18G269200	-1.069	7.70E-11	2.36E-09
GO:0000302	response to reactive oxygen species	GLYMA_01G106800	2.036	0.0026	0.0172
		GLYMA_02G209000	1.336	6.01E-05	0.0006
		GLYMA_02G262500	1.351	3.44E-05	0.0004
		GLYMA_15G205900	1.105	1.81E-06	2.77E-05
		GLYMA_19G011400	2.009	0.0010	0.0077

Table 3.7. Significantly and differentially expressed genes in the susceptible genotype between comparison of ascorbic acid pre-treated (MP-inoculated vs. mock-inoculated control) treatment**.**

GO	Terms	Genes	log2FC	*p*-value	*q*-value
GO:0004601	peroxidase activity	GLYMA_01G130500	-2.0078	1.42E-06	4.03E-05
		GLYMA_01G130800	-2.5983	9.39E-07	2.77E-05
		GLYMA_01G222700	-0.7933	0.0005	0.0074
		GLYMA_20G169200	-2.8160	3.66E-35	1.26E-32
GO:0004672	protein kinase activity	GLYMA_20G162300	1.2388	1.86E-09	8.35E-08
		GLYMA_20G171900	-3.7995	6.81E-26	1.25E-23
		GLYMA_20G181100	-0.6094	0.0008	0.0106
		GLYMA_20G140100	-0.7201	4.20E-06	0.0001
		GLYMA_20G140700	0.7613	8.90E-05	0.0016
GO:0004674	protein serine/threonine kinase activity	GLYMA_01G004800	-1.6416	1.07E-14	8.09E-13
		GLYMA_01G007500	-1.1156	2.21E-06	5.96E-05
		GLYMA_01G022400	0.5413	0.0026	0.0269
		GLYMA_20G162300	1.2388	1.86E-09	8.35E-08
		GLYMA_20G231000	-1.1141	8.86E-06	0.0002
GO:0005509	calcium ion binding	GLYMA_01G050900	0.6980	9.65E-08	3.41E-06
		GLYMA_01G166100	-0.5762	0.0001	0.0019
		GLYMA_01G215100	-1.2446	4.25E-14	2.99E-12
		GLYMA_19G244500	-0.4464	0.0041	0.0383
		GLYMA_19G257800	0.6558	0.0027	0.0282
GO:0005975	carbohydrate metabolic process	GLYMA_20G018200	-1.7628	8.60E-09	3.57E-07
		GLYMA_20G026300	0.9858	5.33E-13	3.43E-11
		GLYMA_20G153600	0.4276	0.0015	0.0177
		GLYMA_19G245400	-1.5925	1.48E-18	1.57E-16
		GLYMA_19G245500	-0.9661	8.78E-08	3.12E-06
GO:0006468	protein phosphorylation	GLYMA_01G004800	-1.6416	1.07E-14	8.09E-13
		GLYMA_01G007500	-1.1156	2.21E-06	5.96E-05
		GLYMA_01G022400	-0.5334	0.0008	0.0108
		GLYMA_20G202200	-0.8166	2.35E-06	6.32E-05
		GLYMA_20G231000	-1.1141	8.86E-06	0.0002
GO:0006979	response to oxidative stress	GLYMA_01G006000	-1.3960	1.57E-10	7.89E-09
		GLYMA_01G130500	-2.0078	1.42E-06	4.03E-05
		GLYMA_01G130800	-2.5983	9.39E-07	2.77E-05
		GLYMA_20G169200	-2.8160	3.66E-35	1.26E-32
		GLYMA_20G171900	-3.7995	6.81E-26	1.25E-23
GO:0009579	thylakoid	GLYMA_01G050900	0.6980	9.65E-08	3.41E-06
		GLYMA_01G087900	0.4843	0.0018	0.0202
		GLYMA_01G115900	0.4633	0.0024	0.0251
		GLYMA_18G205800	-1.4212	1.26E-08	5.11E-07

GO:0009698	phenylpropanoid metabolic process	GLYMA_01G232400	-1.9408	1.21E-28	2.59E-26
		GLYMA_02G309300	-2.1152	2.38E-21	3.23E-19
		GLYMA_03G181600	-1.7129	3.81E-19	4.28E-17
		GLYMA_19G182300	-0.8635	2.69E-08	1.04E-06
		GLYMA_20G180800	-0.8682	0.0001	0.0020
GO:0009813	flavonoid biosynthetic process	GLYMA_01G091400	-3.0524	1.34E-14	9.99E-13
		GLYMA_01G228700	-1.6688	1.23E-19	1.44E-17
		GLYMA_01G239600	-1.8097	7.80E-20	9.44E-18
		GLYMA_20G241600	-1.7341	5.58E-35	1.88E-32
		GLYMA_20G241700	-1.9346	1.10E-14	8.28E-13
GO:0009873	ethylene-activated signaling pathway	GLYMA_01G206600	-1.1971	5.01E-12	2.97E-10
		GLYMA_02G006200	-3.9533	1.35E-36	4.96E-34
GO:0015979	photosynthesis	GLYMA_02G006300	-4.8168	3.63E-16	3.11E-14
		GLYMA_20G203500	-3.5435	2.34E-13	1.55E-11
		GLYMA_20G203700	-1.7504	5.39E-21	7.07E-19
GO:0016301	kinase activity	GLYMA_20G202200	-0.8166	2.35E-06	6.32E-05
		GLYMA_20G231000	-1.1141	8.86E-06	0.0002
		GLYMA_01G004800	-1.6416	1.07E-14	8.09E-13
		GLYMA_20G162300	1.2388	1.86E-09	8.35E-08
		GLYMA_20G189300	-0.7125	4.96E-05	0.0010
GO:0016310	phosphorylation	GLYMA_01G004800	-1.6416	1.07E-14	8.09E-13
		GLYMA_01G007200	-1.1447	2.06E-10	1.02E-08
		GLYMA_01G007300	-1.7773	7.01E-10	3.31E-08
		GLYMA_20G231000	-1.1141	8.86E-06	0.0002
		GLYMA_20G202200	-0.8166	2.35E-06	6.32E-05
GO:0016491	oxidoreductase activity	GLYMA_U027300	-3.1773	2.15E-05	0.0005
		GLYMA_U027400	-1.3400	1.70E-10	8.50E-09
		GLYMA_U038300	-0.7579	0.0004	0.0065
		GLYMA_20G196900	0.9028	0.0006	0.0082
		GLYMA_20G214400	-3.4609	0.0015	0.0177
GO:0019762	glucosinolate catabolic process	GLYMA_11G129300	-2.8207	7.82E-17	7.01E-15
		GLYMA_11G129500	-1.9497	4.37E-08	1.64E-06
		GLYMA_11G129600	-3.3600	4.03E-18	4.13E-16
		GLYMA_12G054300	-2.5357	5.10E-13	3.28E-11
		GLYMA_12G130200	-3.6889	5.25E-31	1.38E-28
GO:0034440	lipid oxidation	GLYMA_13G030300	-0.6011	0.0001	0.0021
		GLYMA_15G026300	-4.5614	5.88E-08	2.16E-06
		GLYMA_15G026500	0.7107	2.86E-05	0.0006
		GLYMA_11G197500	0.7235	0.0035	0.0340
		GLYMA_12G054700	0.5324	0.0012	0.0149

GO:0042542	response to hydrogen peroxide	GLYMA_12G058200	0.4816	0.0007	0.0091
		GLYMA_13G176300	0.5876	0.0042	0.0395
		GLYMA_13G176500	1.1488	1.87E-06	5.19E-05
		GLYMA_10G176400	0.6679	0.003978	0.037622
		GLYMA_11G134200	0.7283	1.02E-06	2.99E-05
GO:0042744	hydrogen peroxide catabolic process	GLYMA_13G138300	0.7945	2.33E-06	6.27E-05
		GLYMA_14G201700	-1.2294	3.51E-06	9.04E-05
		GLYMA_14G201800	-1.1838	3.35E-13	2.20E-11
		GLYMA_10G222400	-2.0974	1.30E-18	1.38E-16
		GLYMA_11G101200	-6.3389	3.96E-52	3.31E-49
GO:0106310	protein serine kinase activity	GLYMA_11G123500	0.5850	0.0042	0.0392
		GLYMA_11G152200	-0.8272	7.07E-05	0.001317
		GLYMA_11G235300	-0.6034	0.0027	0.0276
		GLYMA_10G228900	1.6409	0.0005	0.0070
		GLYMA_11G002600	0.4960	0.0046	0.0424
GO:0009523	photosystem II	GLYMA_13G282000	0.4073	0.0057	0.0492
		GLYMA_13G299200	0.5235	0.0053	0.0470
		GLYMA_14G003400	0.4426	0.0007	0.0099
		GLYMA_10G032200	0.4201	0.0044	0.0404
		GLYMA_10G153100	0.7215	0.0011	0.0131
GO:0006952	defense response	GLYMA_11G025600	-1.9879	9.33E-47	5.56E-44
		GLYMA_11G070500	-3.3696	4.97E-26	9.22E-24
		GLYMA_11G077700	-0.7738	0.0038	0.0363
		GLYMA_09G275800	-1.8684	0.0002	0.0035
		GLYMA_10G061800	-2.2664	0.0014	0.0165
GO:0009607	response to biotic stimulus	GLYMA_12G119300	-5.6700	1.32E-06	3.77E-05
		GLYMA_13G234400	-1.8624	9.36E-11	4.86E-09
		GLYMA_13G278400	-0.6721	0.002325	0.024753
		GLYMA_09G040400	-1.6110	4.05E-09	1.75E-07
		GLYMA_09G040500	-0.7933	4.46E-05	0.000882
GO:0010206	photosystem II repair	GLYMA_13G299200	0.5235	0.0053	0.0470
		GLYMA_17G257400	0.7394	0.0002	0.0033
		GLYMA_18G259700	1.0576	0.0005	0.0067
		GLYMA_08G086600	0.5212	0.0010	0.0125
		GLYMA_08G203200	0.6126	0.0055	0.0484
GO:0004364	glutathione transferase activity	GLYMA_10G047700	-0.8842	7.51E-06	0.0002
		GLYMA_11G198500	-0.7796	0.0044	0.0403
		GLYMA_13G129100	-2.3376	6.18E-05	0.0012
		GLYMA_08G174700	1.0206	4.13E-05	0.0008
		GLYMA_08G174900	-3.1266	2.03E-08	8.02E-07

GO:0008061	chitin binding	GLYMA_11G124500	-1.8583	7.09E-35	2.36E-32
		GLYMA_11G124600	-7.0964	1.16E-06	3.37E-05
		GLYMA_12G049100	-2.5468	1.10E-08	4.50E-07
		GLYMA_02G007400	-2.5570	2.48E-11	1.37E-09
		GLYMA_02G042500	-1.0677	2.03E-21	2.77E-19
GO:0006749	glutathione metabolic process	GLYMA_02G187200	-1.9153	1.06E-16	9.41E-15
		GLYMA_03G176300	-2.4564	3.33E-14	2.38E-12
		GLYMA_04G023200	-0.6103	4.67E-06	0.0001
		GLYMA_01G106000	-1.4493	1.18E-16	1.04E-14
		GLYMA_02G024800	-1.0861	0.0004	0.0055
GO:0009695	jasmonic acid biosynthetic process	GLYMA_03G147700	-2.9156	6.33E-18	6.36E-16
		GLYMA_02G099200	-0.7151	3.28E-06	8.51E-05
		GLYMA_19G151200	0.9261	0.0023	0.0242
		GLYMA_19G151200	-3.9374	2.80E-30	6.93E-28
GO:0009522	photosystem I	GLYMA_01G115900	0.4633	0.0024	0.0251
		GLYMA_02G064700	0.4814	0.0010	0.0122
		GLYMA_04G167900	0.4328	0.0030	0.0303
		GLYMA_16G016100	0.6312	0.0001	0.0021
		GLYMA_16G205200	0.4715	0.0018	0.0199
GO:0009738	abscisic acid-activated signaling pathway	GLYMA_01G009200	0.5793	0.0009	0.0110
		GLYMA_01G097000	0.5788	0.0007	0.0091
		GLYMA_01G166100	-0.5762	0.0001	0.0019
		GLYMA_17G030400	-0.9993	0.0023	0.0248
		GLYMA_18G096500	-0.6510	8.25E-07	2.46E-05
GO:0000302	response to reactive oxygen species	GLYMA_18G024600	0.6527	0.0056	0.0491
		GLYMA_18G205800	-1.4212	1.26E-08	5.11E-07
		GLYMA_20G015900	0.9743	0.0007	0.0093
		GLYMA_14G056800	-0.6379	1.81E-05	0.0004
		GLYMA_15G205900	0.5498	0.00078	0.0103
GO:0006629	lipid metabolic process	GLYMA_01G011600	-3.1564	4.52E-21	6.03E-19
		GLYMA_01G012100	0.9961	1.53E-05	0.0003
		GLYMA_01G014200	-0.7516	0.0002	0.0027
		GLYMA_20G092000	0.3447	0.004941	0.0445
		GLYMA_20G127800	0.6026	8.27E-05	0.0015

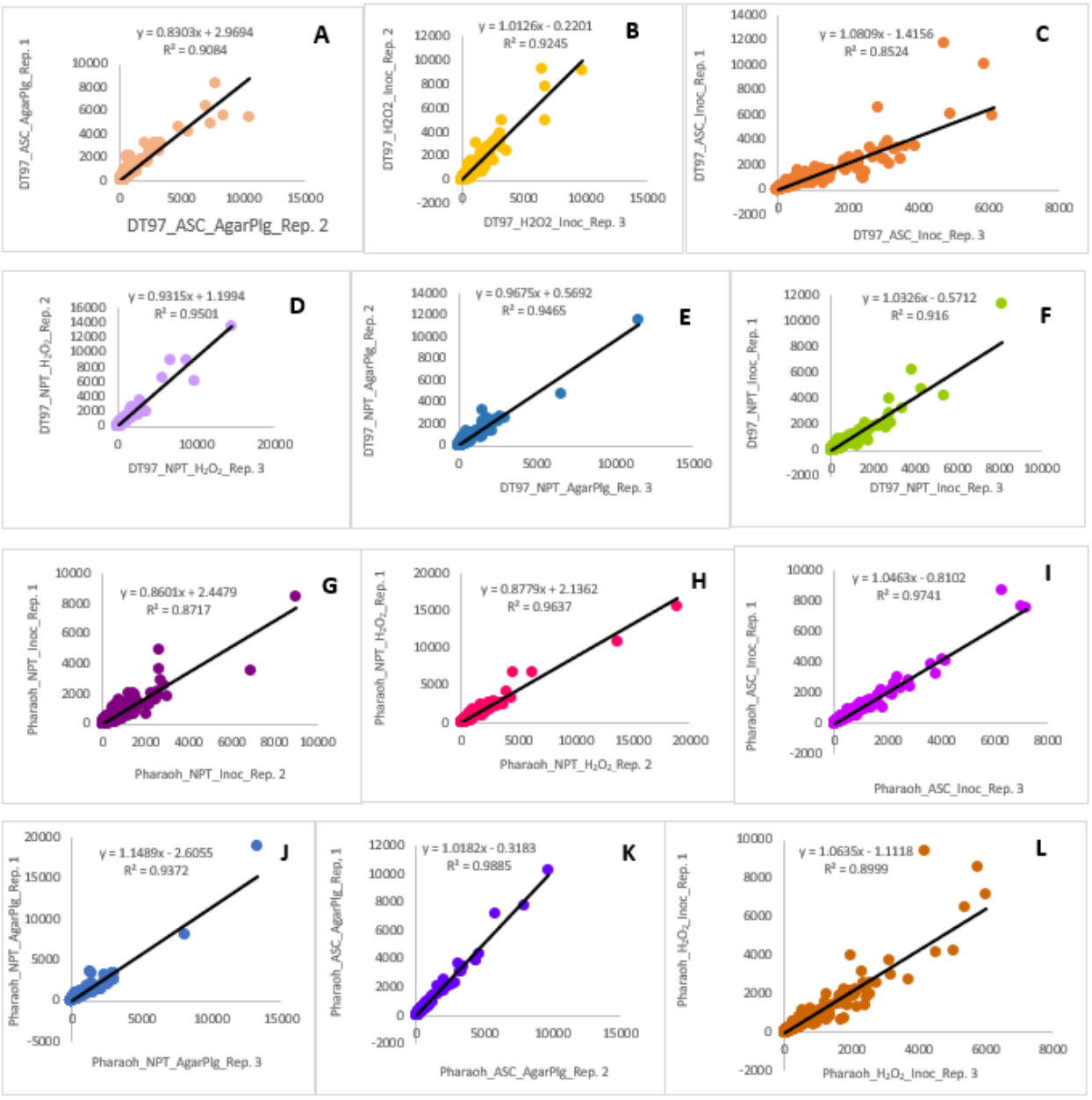
A
y = 0.8303x + 2.9694
R² = 0.9084
DT97_ASC_AgarPlg_Rep. 1
DT97_ASC_AgarPlg_Rep. 2
B
y = 1.0126x - 0.2201
R² = 0.9245
DT97_H2O2_Inoc_Rep. 2
DT97_H2O2_Inoc_Rep. 3
C
y = 1.0809x - 1.4156
R² = 0.8524
DT97_ASC_Inoc_Rep. 1
DT97_ASC_Inoc_Rep. 3
D
y = 0.9315x + 1.1994
R² = 0.9501
DT97_NPT_H2O2_Rep. 2
DT97_NPT_H2O2_Rep. 3
E
y = 0.9675x + 0.5692
R² = 0.9465
DT97_NPT_AgarPlg_Rep. 2
DT97_NPT_AgarPlg_Rep. 3
F
y = 1.0326x - 0.5712
R² = 0.916
DT97_NPT_Inoc_Rep. 1
DT97_NPT_Inoc_Rep. 3
G
y = 0.8601x + 2.4479
R² = 0.8717
Pharaoh_NPT_Inoc_Rep. 1
Pharaoh_NPT_Inoc_Rep. 2
H
y = 0.8779x + 2.1362
R² = 0.9637
Pharaoh_NPT_H2O2_Rep. 1
Pharaoh_NPT_H2O2_Rep. 2
I
y = 1.0463x - 0.8102
R² = 0.9741
Pharaoh_ASC_Inoc_Rep. 1
Pharaoh_ASC_Inoc_Rep. 3
J
y = 1.1489x - 2.6055
R² = 0.9372
Pharaoh_NPT_AgarPlg_Rep. 1
Pharaoh_NPT_AgarPlg_Rep. 3
K
y = 1.0182x - 0.3183
R² = 0.9885
Pharaoh_ASC_AgarPlg_Rep. 1
Pharaoh_ASC_AgarPlg_Rep. 2
L
y = 1.0635x - 1.1118
R² = 0.8999
Pharaoh_H2O2_Inoc_Rep. 1
Pharaoh_H2O2_Inoc_Rep. 3

Figure 3.1. Scatter plots representing the correlation analysis of RPKM values between the biological replicates of the resistant genotype DT97-4294 for the **A**) ascorbic acid pre-treated agar plug(control), **B**) H_2O_2 pre-treated following inoculation (MP inoculated), **C**) ascorbic acid pre-treated following inoculation (MP inoculation), **D**) no pre-treatment following H_2O_2 application (control), **E**) no pretreatment following agar plug insertion (control), **F**) No pre-treatment following inoculation (MP inoculation), and for the susceptible genotype Pharaoh, **G**) no pre-treatment following inoculation, **H**) no pre-treatment following H_2O_2 application (control), **I**) ascorbic acid pre-treatment following inoculation (MP inoculation), **J**) no pre-treatment following agar plug insertion (control), **K**) ascorbic acid pre-treatment following agar plug insertion (control), **L**) H_2O_2 pre-treatment following MP-inoculation.

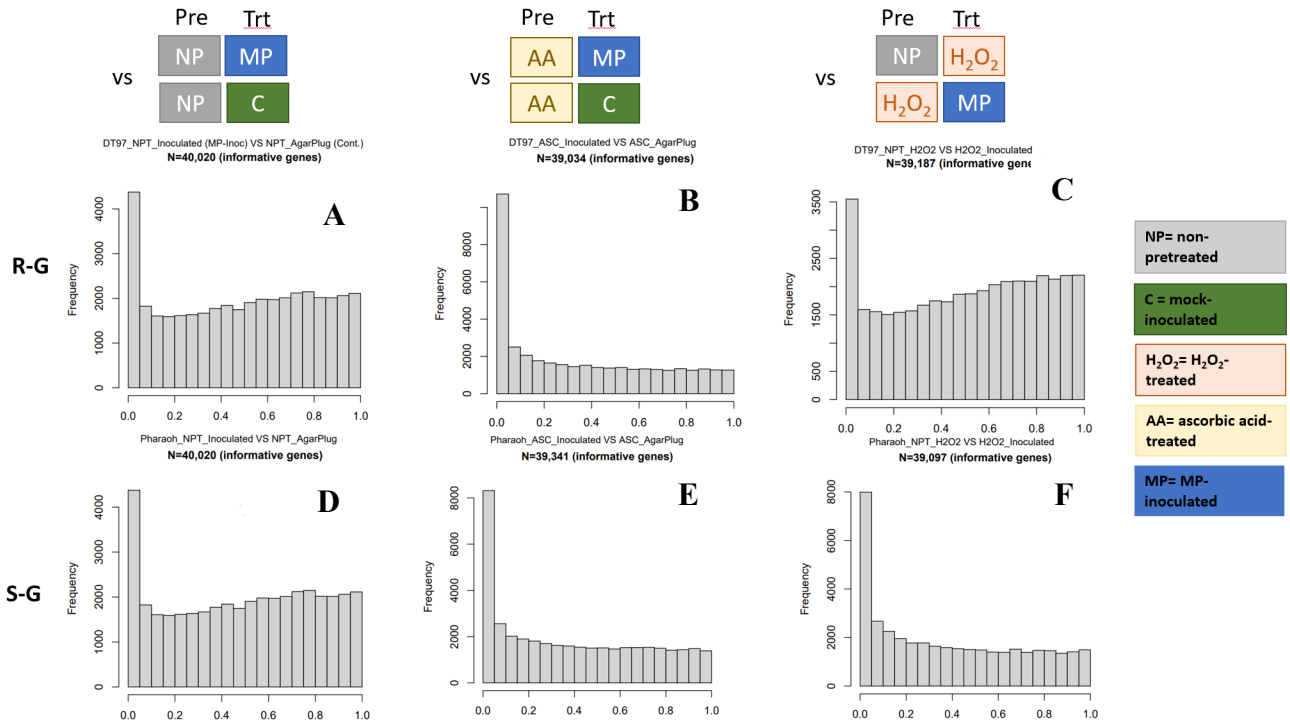

Figure 3.2. *P* value histograms of the informative genes of normalized read counts for the treatment comparisons of the resistant genotype [R-G] DT97-4290: (***Panels A-C***) for the non-pre-treated [NP] mock-inoculated [C] vs. inoculated [MP] (**A**), ascorbic acid [AA] pre-treated inoculated [MP] vs. mock-inoculated [C] (**B**), non-pre-treated H_2O_2 vs. H_2O_2 pre-treated MP-inoculated treatment (**C**). In the susceptible genotype [S-G] Pharaoh: (***Panels D-F***) for the non-pre-treated mock-inoculated [C] vs. inoculated [MP] (**D**), ascorbic acid pre-treated [AA] inoculated [MP] vs. mock-inoculated [MP] (**E**), and non-pre-treated [NP] H_2O_2 vs. H_2O_2 pre-treated inoculated [MP] treatment (**F**).

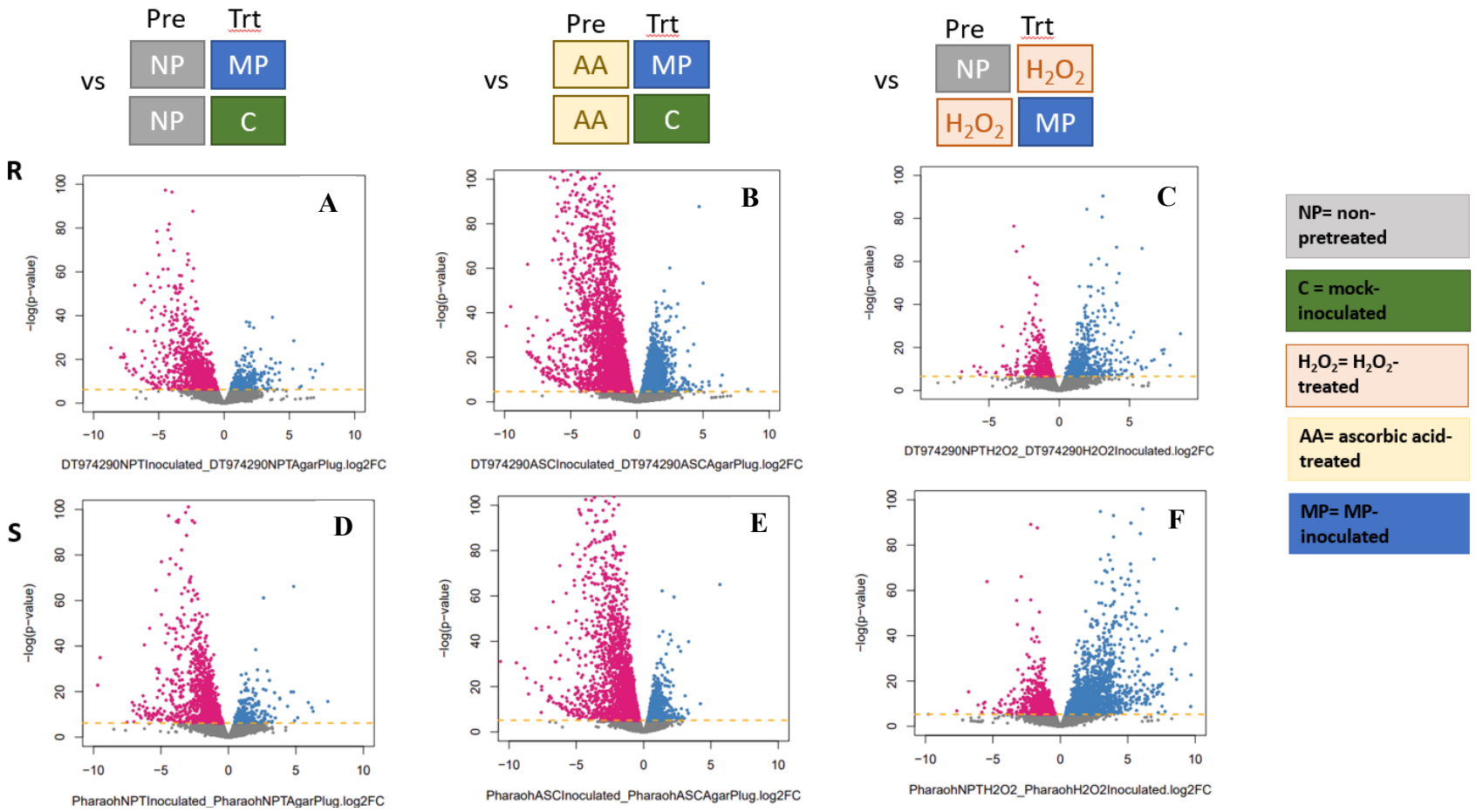

Figure 3.3. Volcano plots displaying differential gene expression of log2 fold changes versus negative log *p* values for pairwise comparisons within the resistant [R] genotype DT97-290 ***(Panels A-C)*** for MP-inoculated [MP] vs. mock-inoculated [C] (**A**); ascorbic acid pre-treated [AA] inoculated [MP] vs. mock-inoculated [C] (**B**); and non pre-treated [NP] and H_2O_2-treated vs. H_2O_2 pre-treated and inoculated [MP] (**C**); in the susceptible [S] genotype pharaoh ***(Panels D-F)*** for inoculated [MP] vs. mock inoculated [C] (**D**); ascorbic acid pre-treated and inoculated [MP] vs. mock-inoculated [C] (**E**); and non-pre-treated [NP] and H_2O_2-treated vs. H_2O_2 pre-treated and inoculated [MP] (**F**).

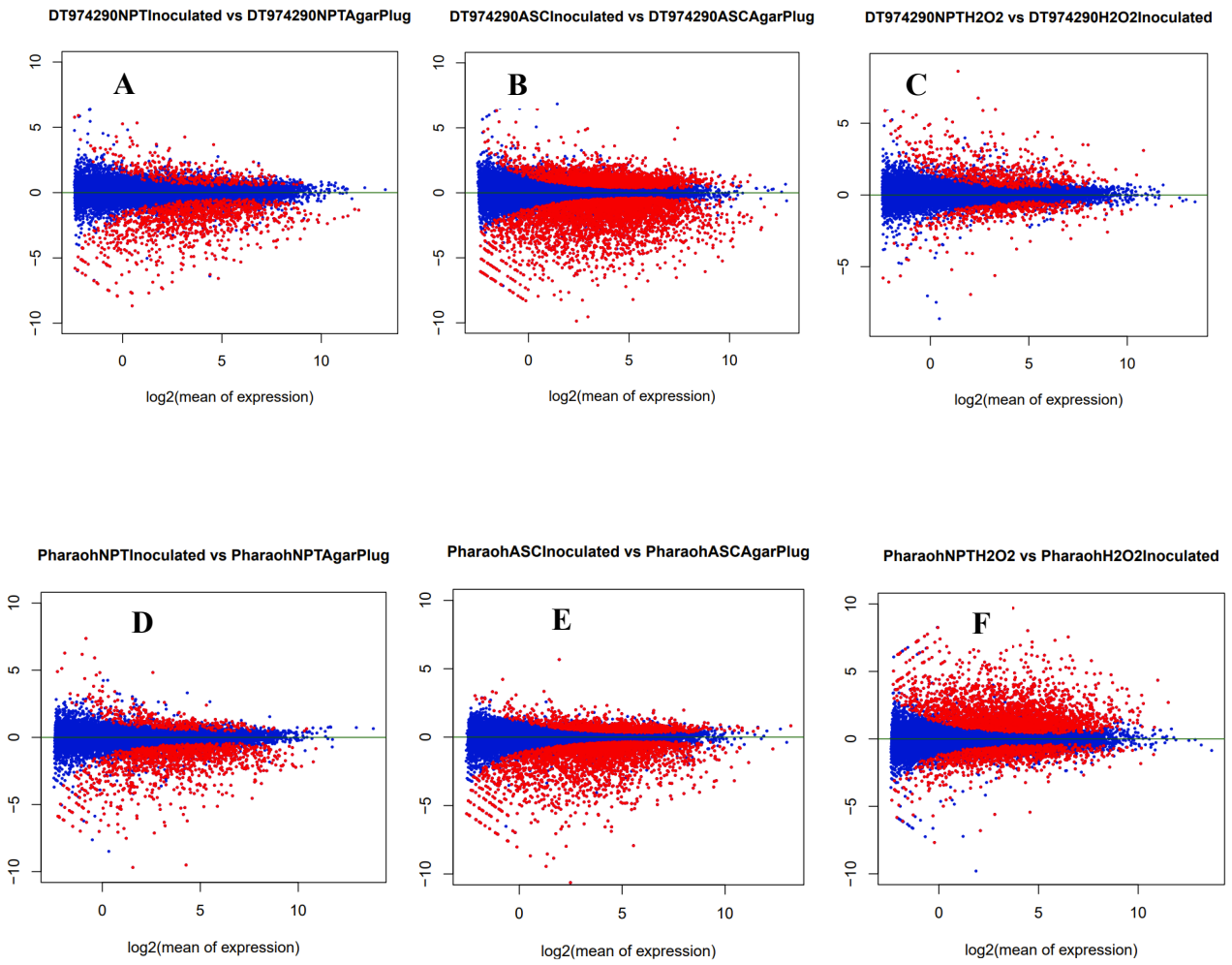

Figure 3.4. Mean differentiation plots displaying differential gene expression of log2 fold changes versus log2 mean expression values for the pairwise comparisons within the resistant genotype DT97-290 (***Panels A-C***) for inoculated vs. mock-inoculated (**A**); ascorbic acid pre-treated and MP-inoculated vs. mock-inoculated (**B**); and non-pre-treated H_2O_2 vs. H_2O_2 pre-treated MP-inoculated treatment (**C**); in the susceptible (S) genotype Pharaoh (***Panels D-F***) for MP-inoculated vs. mock-inoculated (**D**), ascorbic acid pre-treated and MP-inoculated vs. mock-inoculated (**E**); and non-pre-treated H_2O_2 vs. H_2O_2 pre-treated MP-inoculated treatment (**F**).

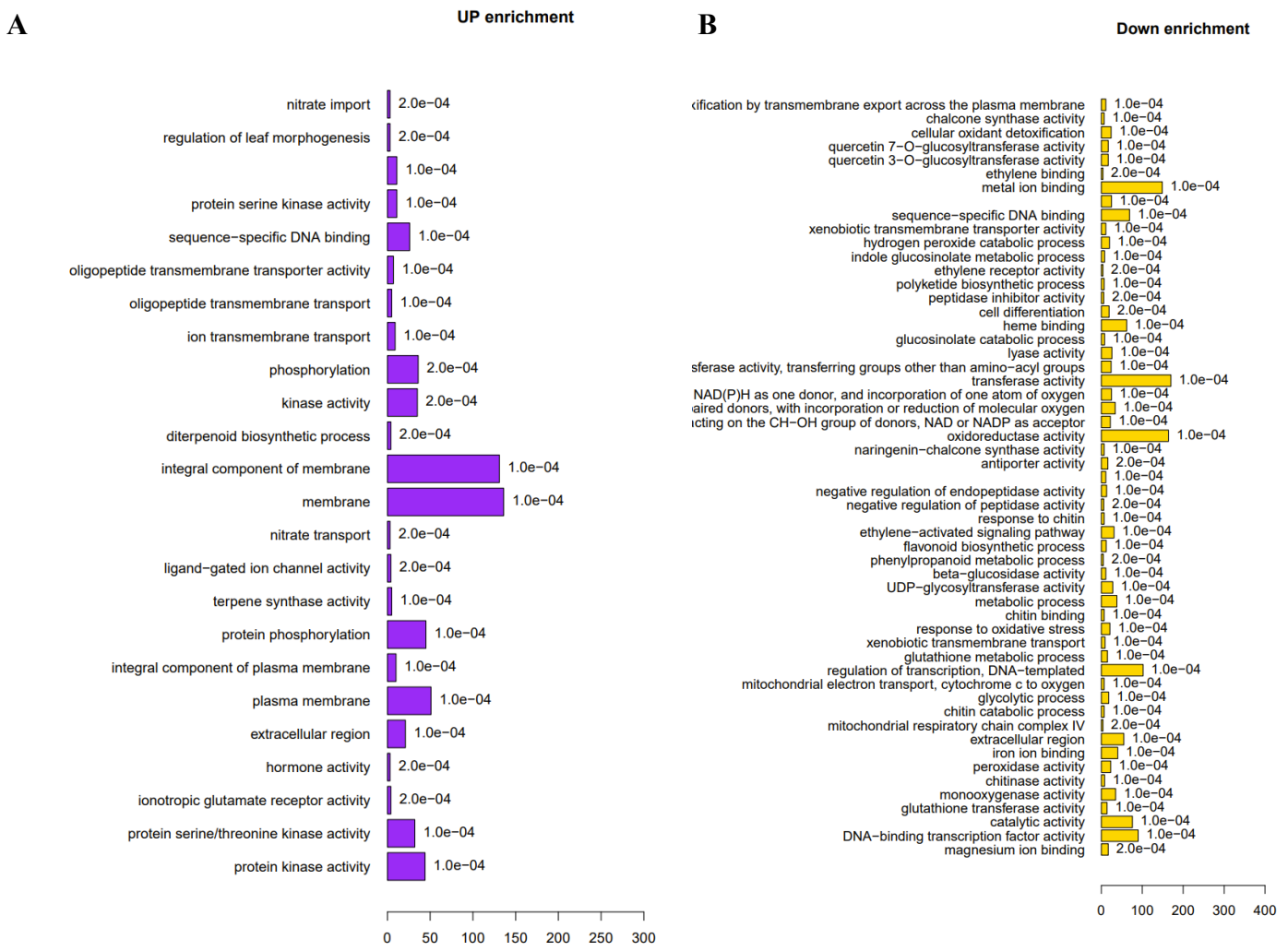

Figure 3.5. Bar plot showing Gene Ontology (GO) term analysis for the non pre-treated *M. phaseolina* inoculated treatment vs. non-pre-treated mock-inoculated treatment in the resistant genotype (DT97-4290) as up-regulated GO terms (**A**) and down-regulated GO terms (**B**).

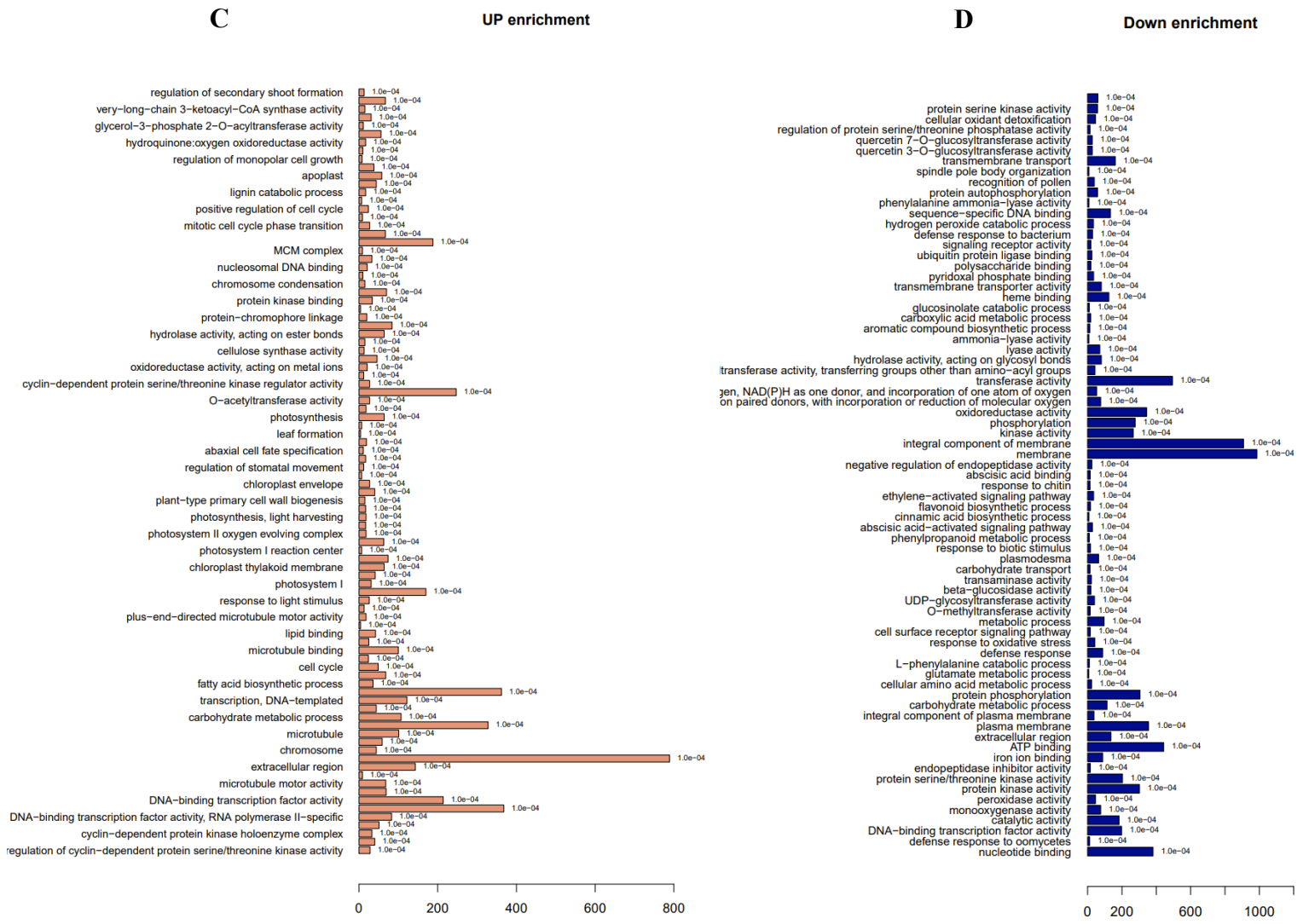

Figure 3.6. Bar plot showing Gene Ontology (GO) term analysis for the ascorbic acid pre-treated inoculated treatment vs. non-pre-treated inoculated treatment in the resistant genotype (DT97-4290) as up-regulated GO terms (**C**) and down-regulated GO terms (**D**).

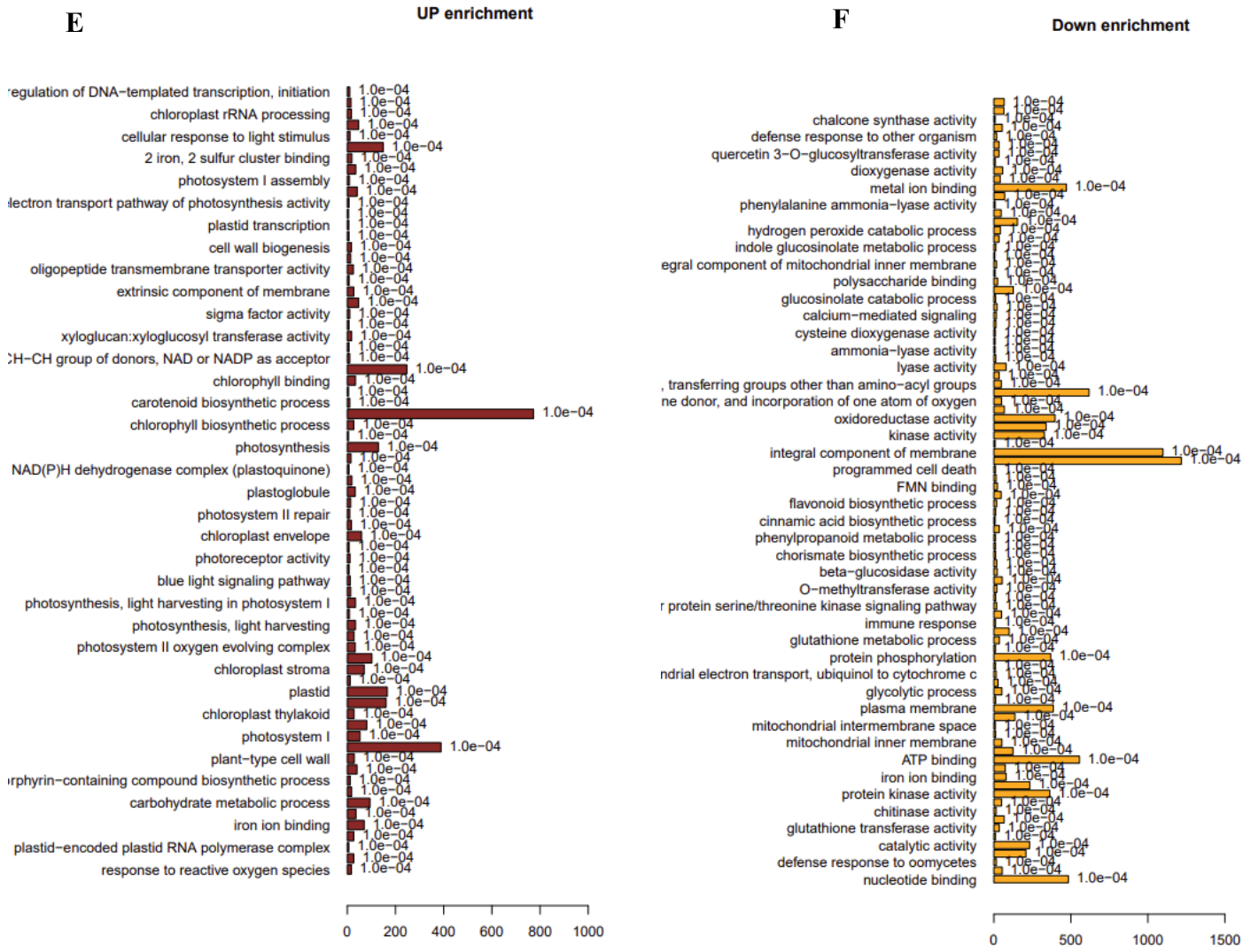

Figure 3.7. Bar plot showing Gene Ontology (GO) term analysis for the ascorbic acid pre-treated (MP-inoculated vs. mock-inoculated) treatment in the resistant genotype (DT97-4290) as up-regulated GO terms (**E**) and down-regulated GO terms (**F**).

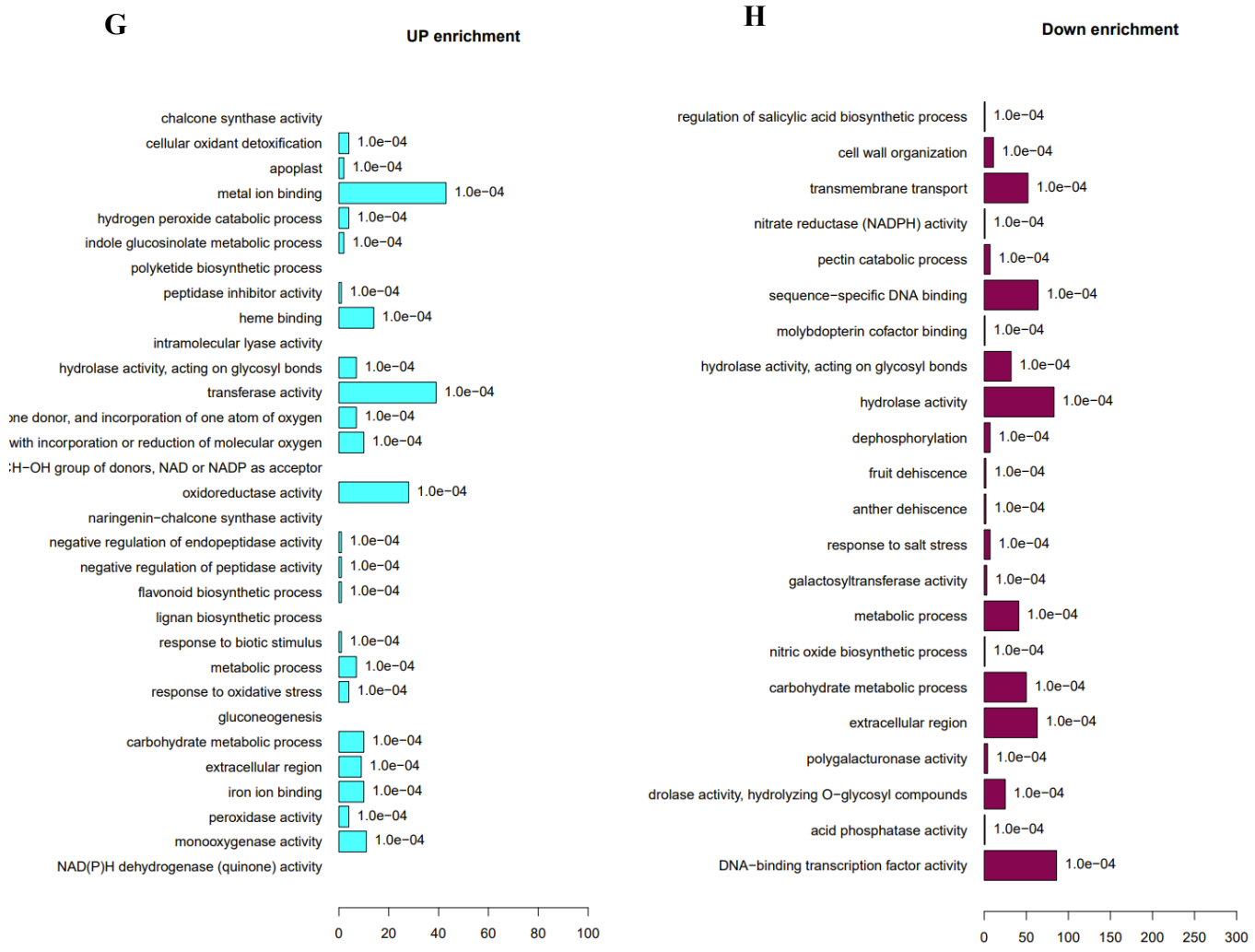

Figure 3.8. Bar plot showing Gene Ontology (GO) term analysis for the no pre-treated H_2O_2 applied treatment vs. H_2O_2 pre-treated MP inoculated control treatment in the resistant genotype (DT97-4290) as up-regulated GO terms (**G**) and down-regulated GO terms (**H**).

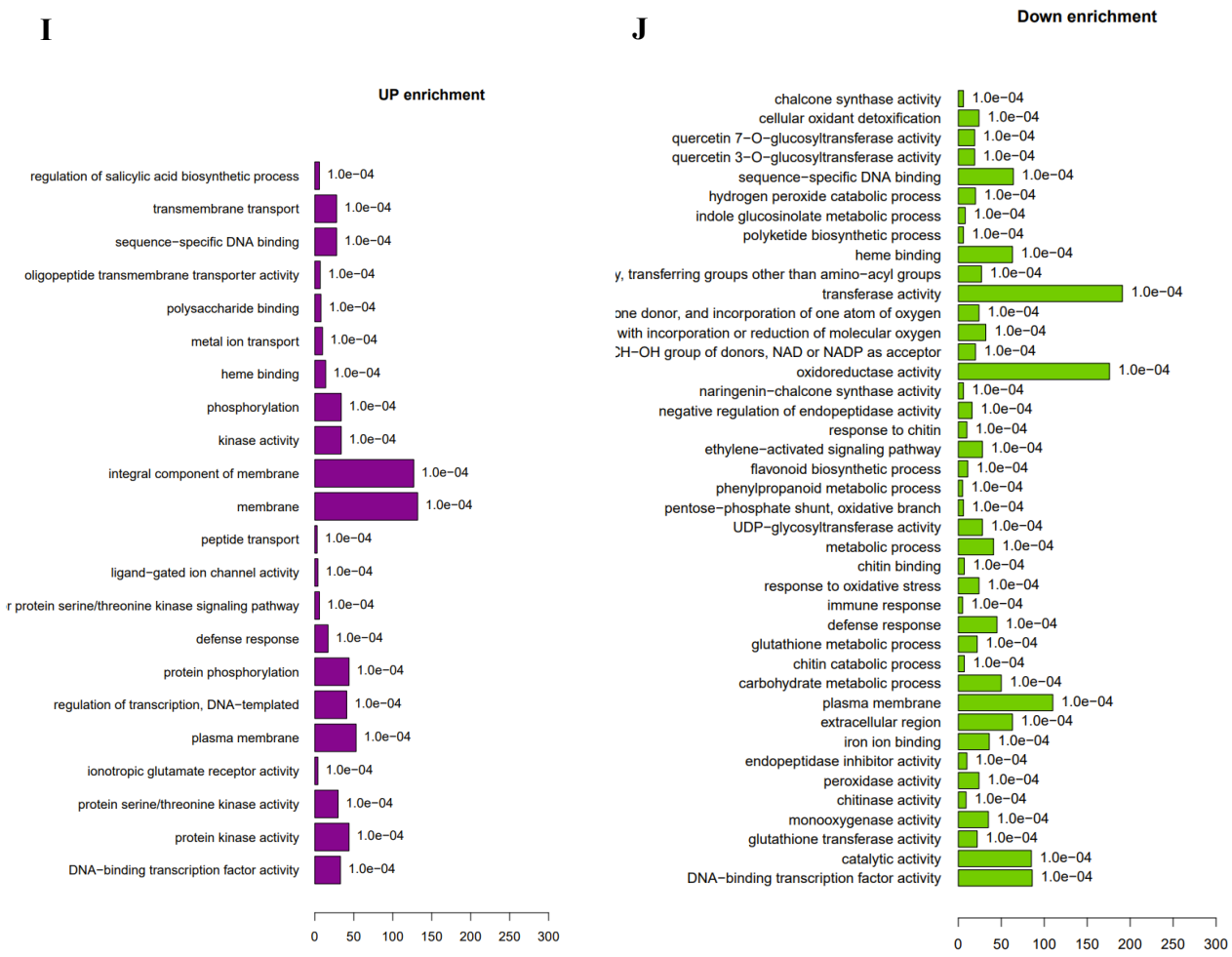

Figure 3.9. Bar plot showing Gene Ontology (GO) term analysis for the no pre-treated MP inoculated treatment vs. no pre-treated mock-inoculated treatment in the susceptible genotype (Pharaoh) as up-regulated GO terms (**I**) and down-regulated GO terms (**J**).

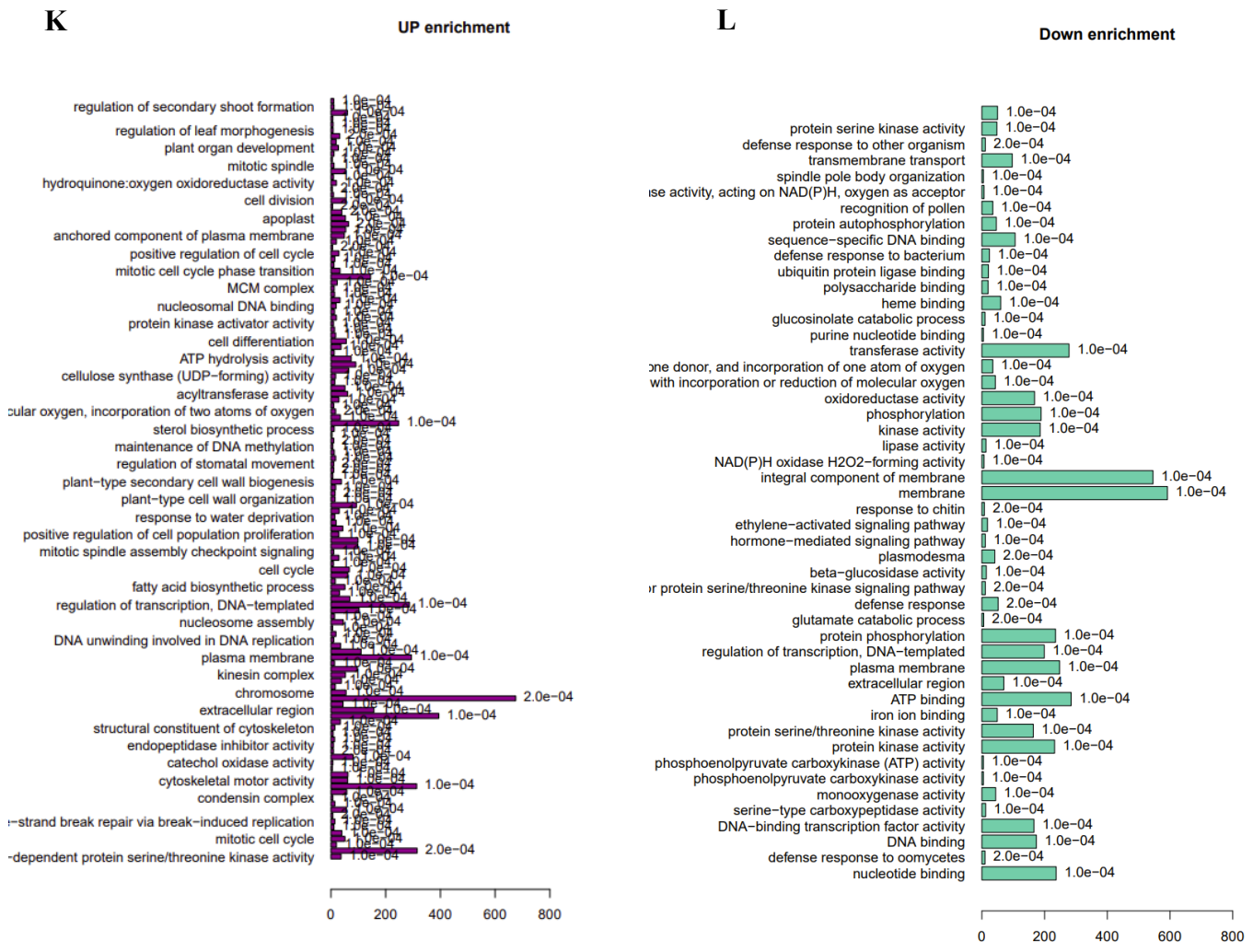

Figure 3.10. Bar plot showing Gene Ontology (GO) term analysis for the ascorbic acid pre-treated MP inoculated vs. non pre-treated MP inoculated treatment in the susceptible genotype (Pharaoh) as up-regulated GO terms (**K**) and down-regulated GO terms (**L**).

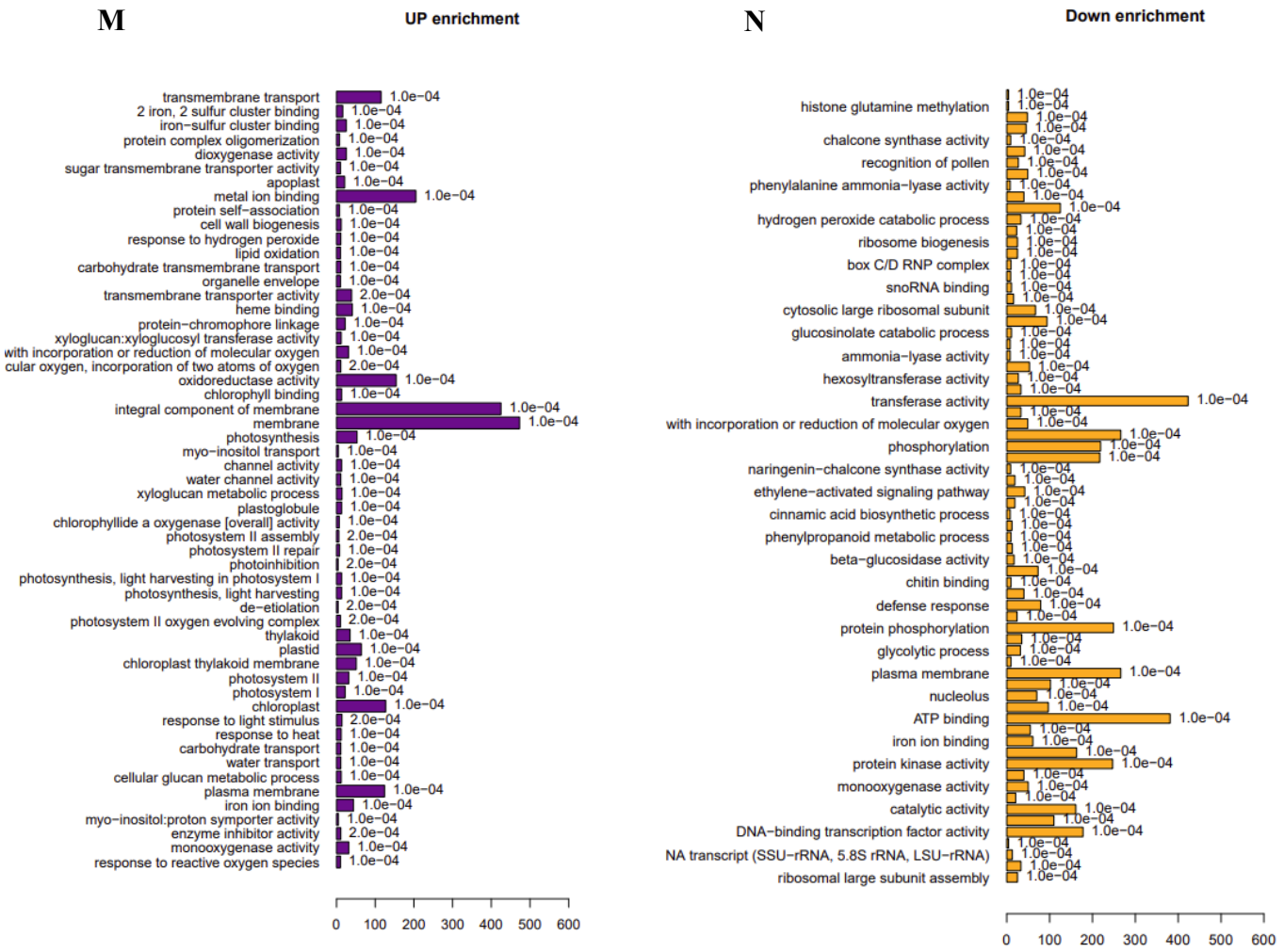

Figure 3.11. Bar plot showing Gene Ontology (GO) term analysis for the ascorbic acid pre-treated (MP inoculated vs. mock-inoculated) treatment in the susceptible genotype (Pharaoh) as up-regulated GO terms (**M**) and down-regulated GO terms **(N**).

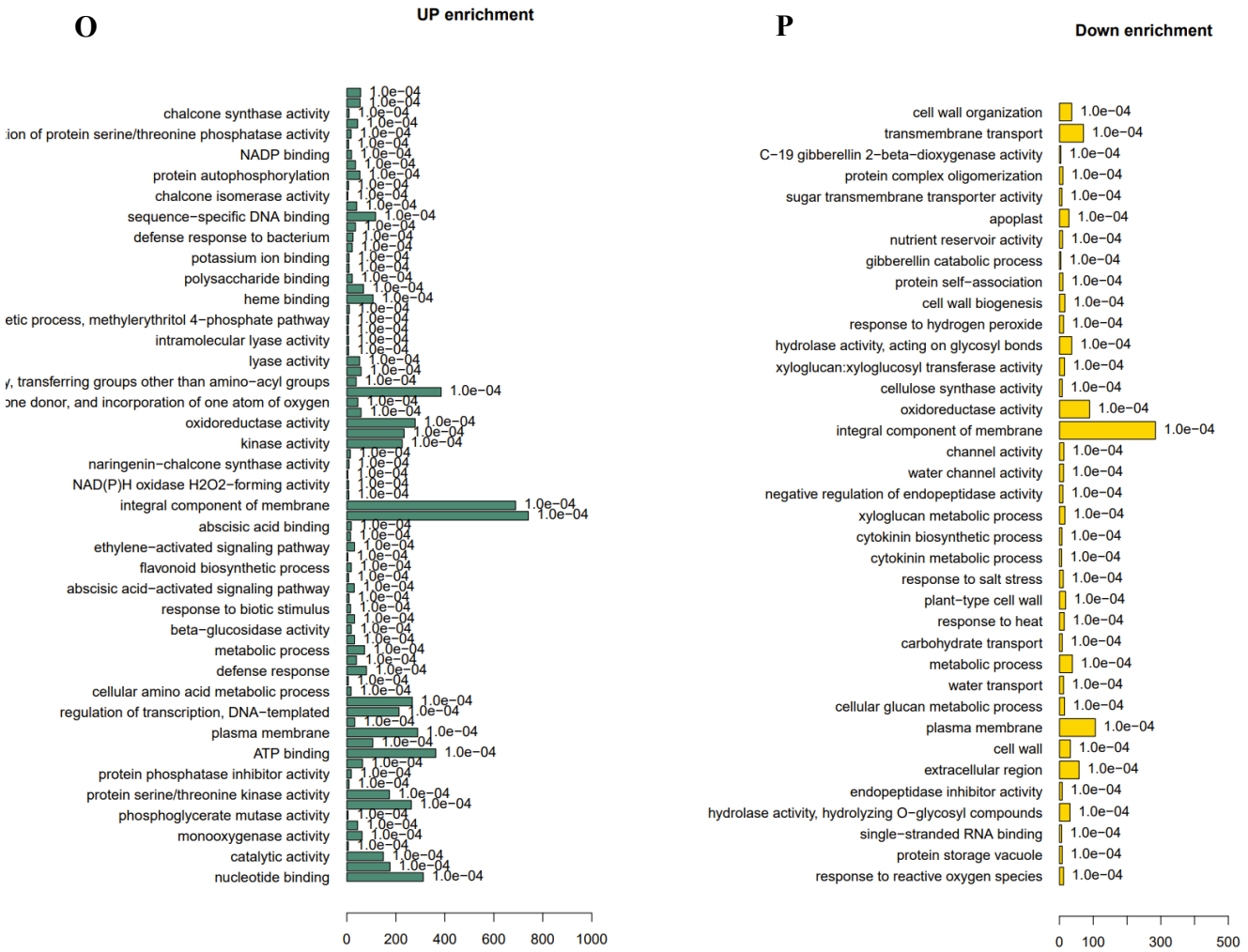

Figure 3.12. Bar plot showing Gene Ontology (GO) term analysis for no pre-treated H_2O_2 applied treatment vs. H_2O_2 pre-treated MP inoculated treatment in the susceptible genotype (Pharaoh) as up-regulated GO terms (**O**) and down-regulated GO terms (**P**).

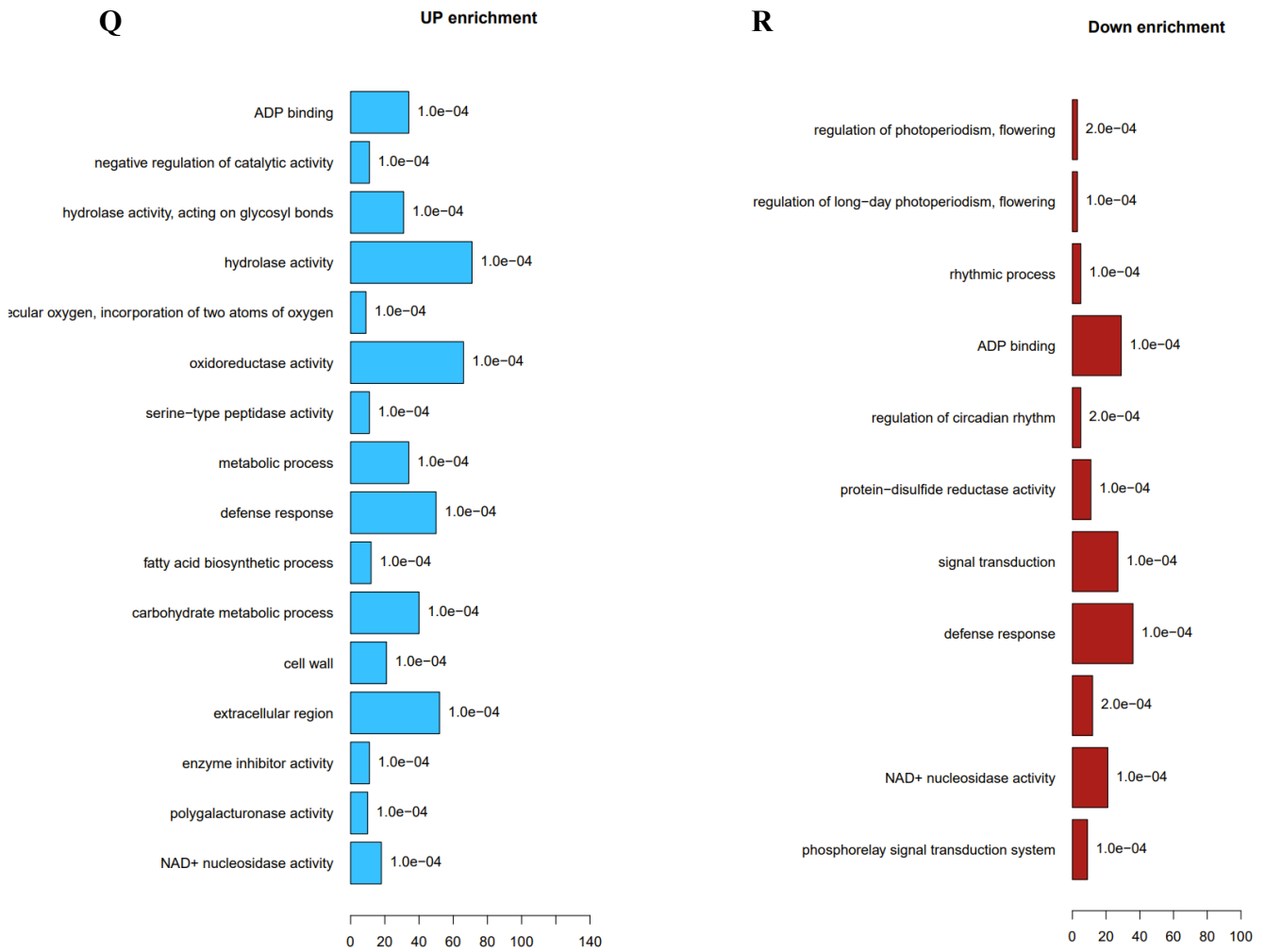

Figure 3.13. Bar plot showing Gene Ontology (GO) term analysis for non pre-treated MP inoculated treatment between comparison of resistant genotype (DT97-4290) and susceptible genotype (Pharaoh) as up-regulated GO terms (**Q**) and down-regulated GO terms (**R**).

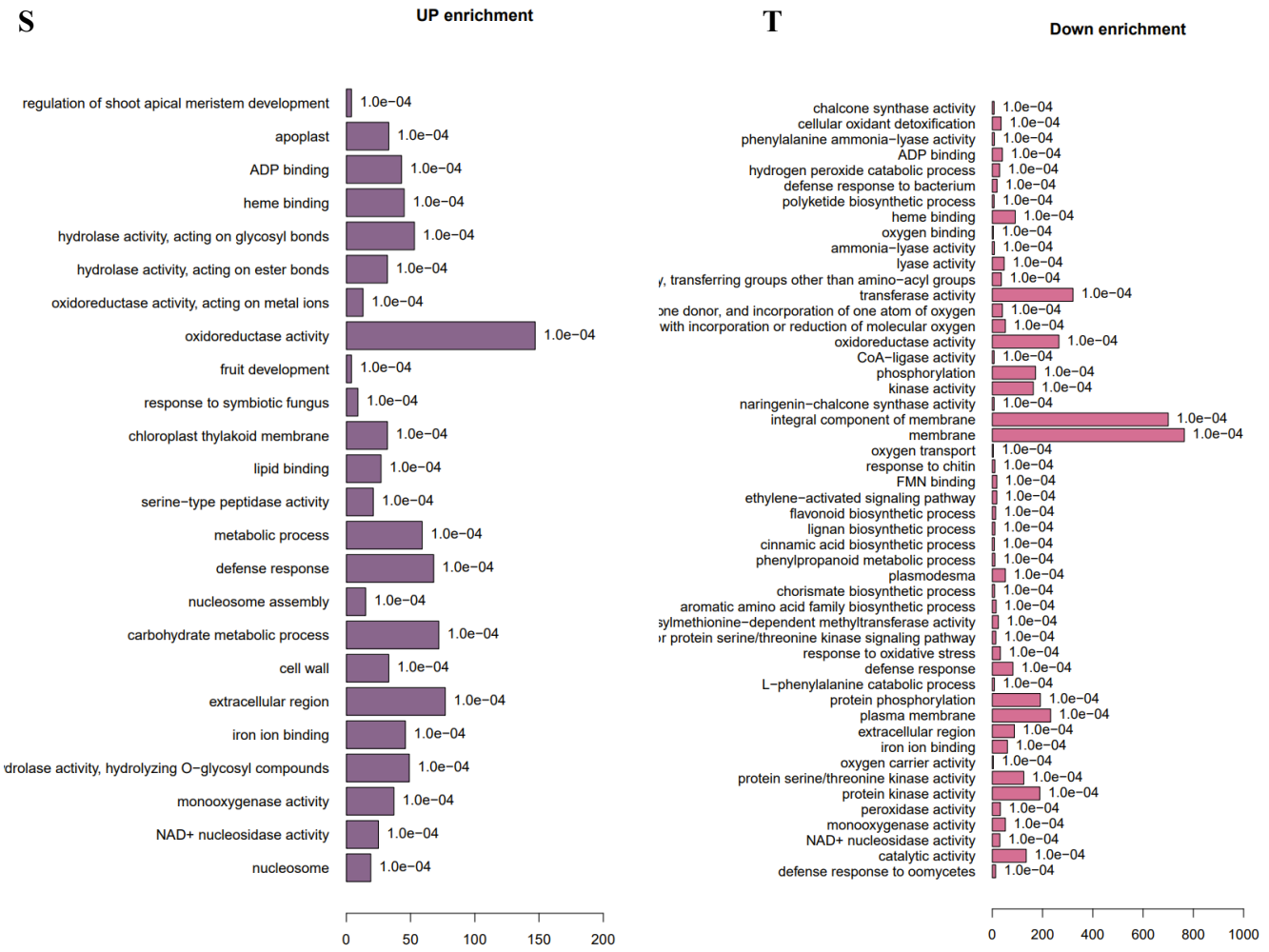

Figure 3.14. Bar plot showing Gene Ontology (GO) term analysis for the ascorbic acid pre-treated MP inoculated treatment between comparison of resistant genotype (DT97-4290) and susceptible genotype (Pharaoh) as up-regulated GO terms (**S**) and down-regulated GO terms (**T**).

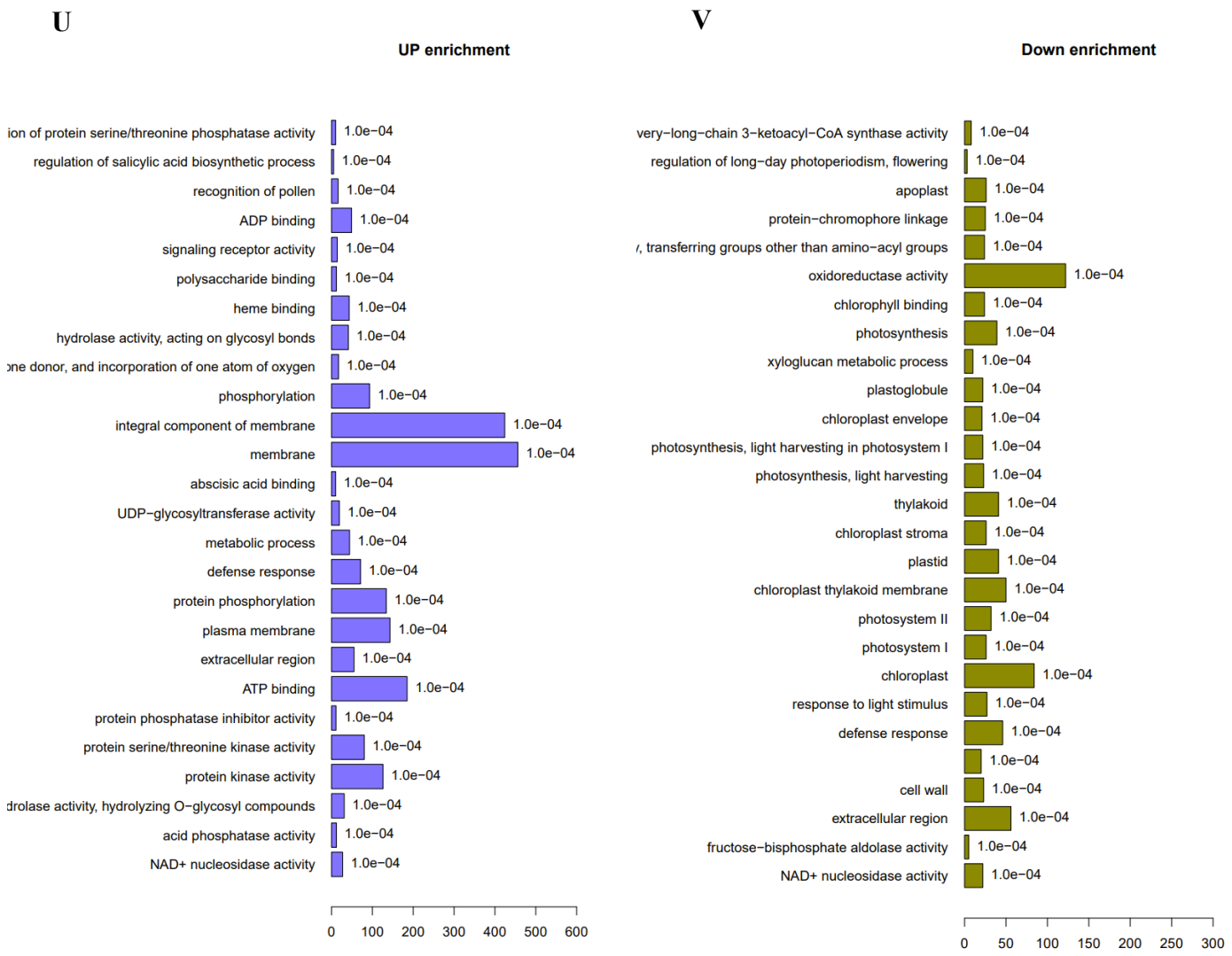

Figure 3.15. Bar plot showing Gene Ontology (GO) term analysis for the H_2O_2 pre-treated MP inoculated treatment comparison of resistant genotype (DT97-4290) and susceptible genotype (Pharaoh) as up-regulated GO terms (**U**) and down-regulated GO terms (**V**).

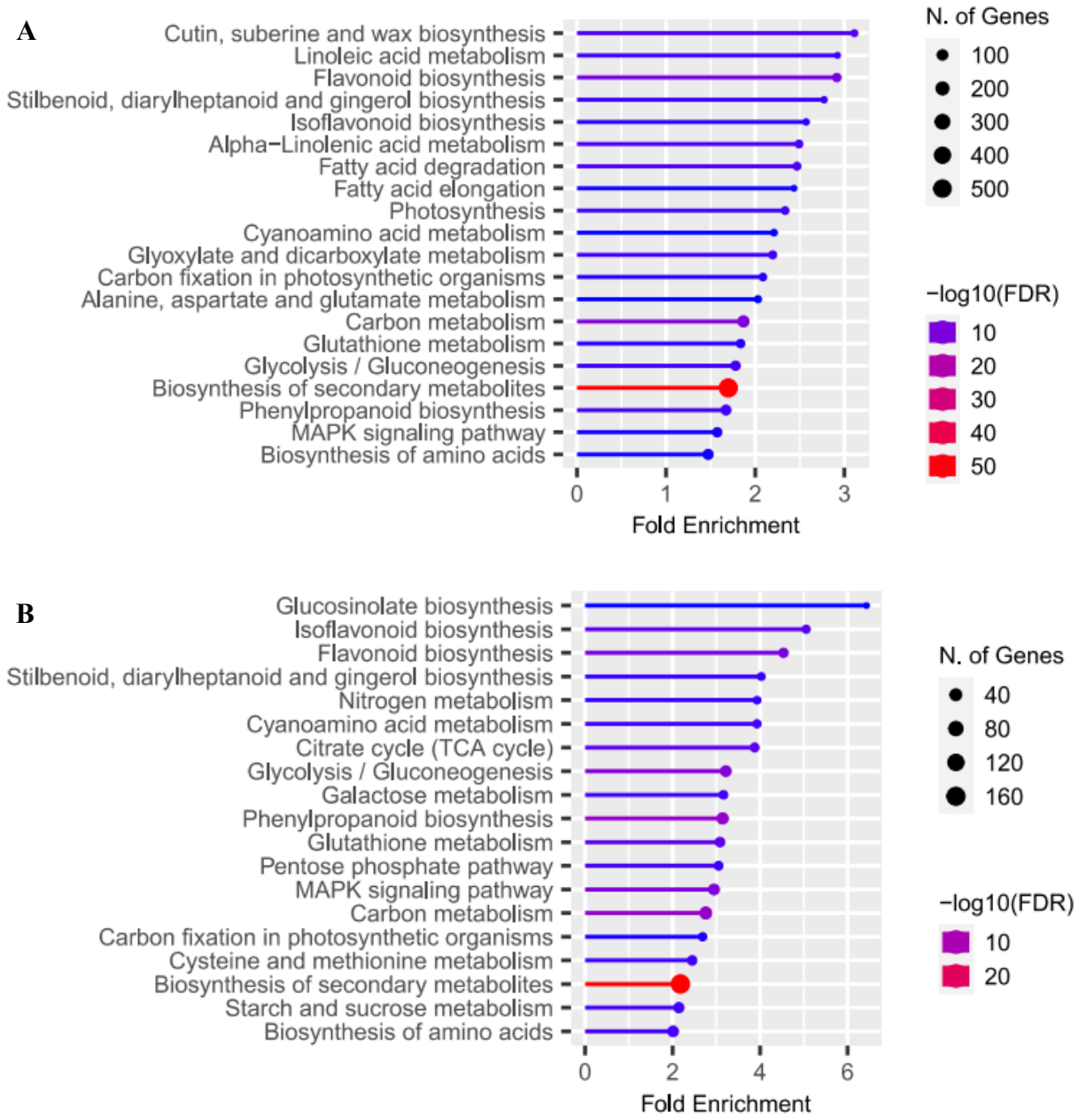

Figure 3.16. KEGG pathway induced by non pre-treated MP inoculated treatment vs non pre-treated mock-inoculated treatment in the resistant genotype (DT97-4290) in the up-down-regulated (**A**) and down-regulated (**B**) categories.

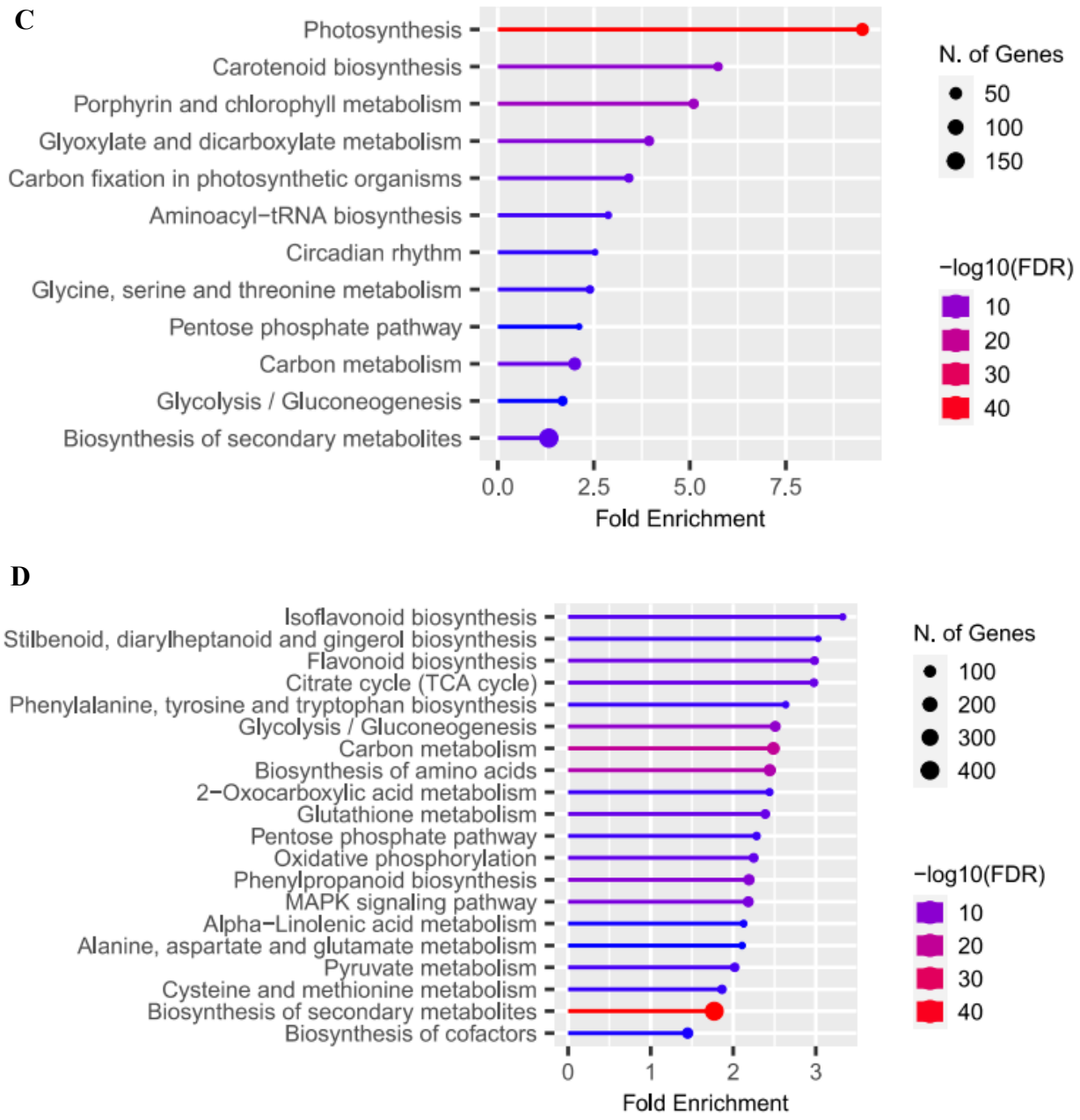

Figure 3.17. KEGG pathway induced by ascorbic acid pre-treated MP inoculated vs. ascorbic acid pre-treated mock-inoculated treatment in the resistant genotype (DT97-4290) in the up-regulated (**C**) and down-regulated (**D**) categories.

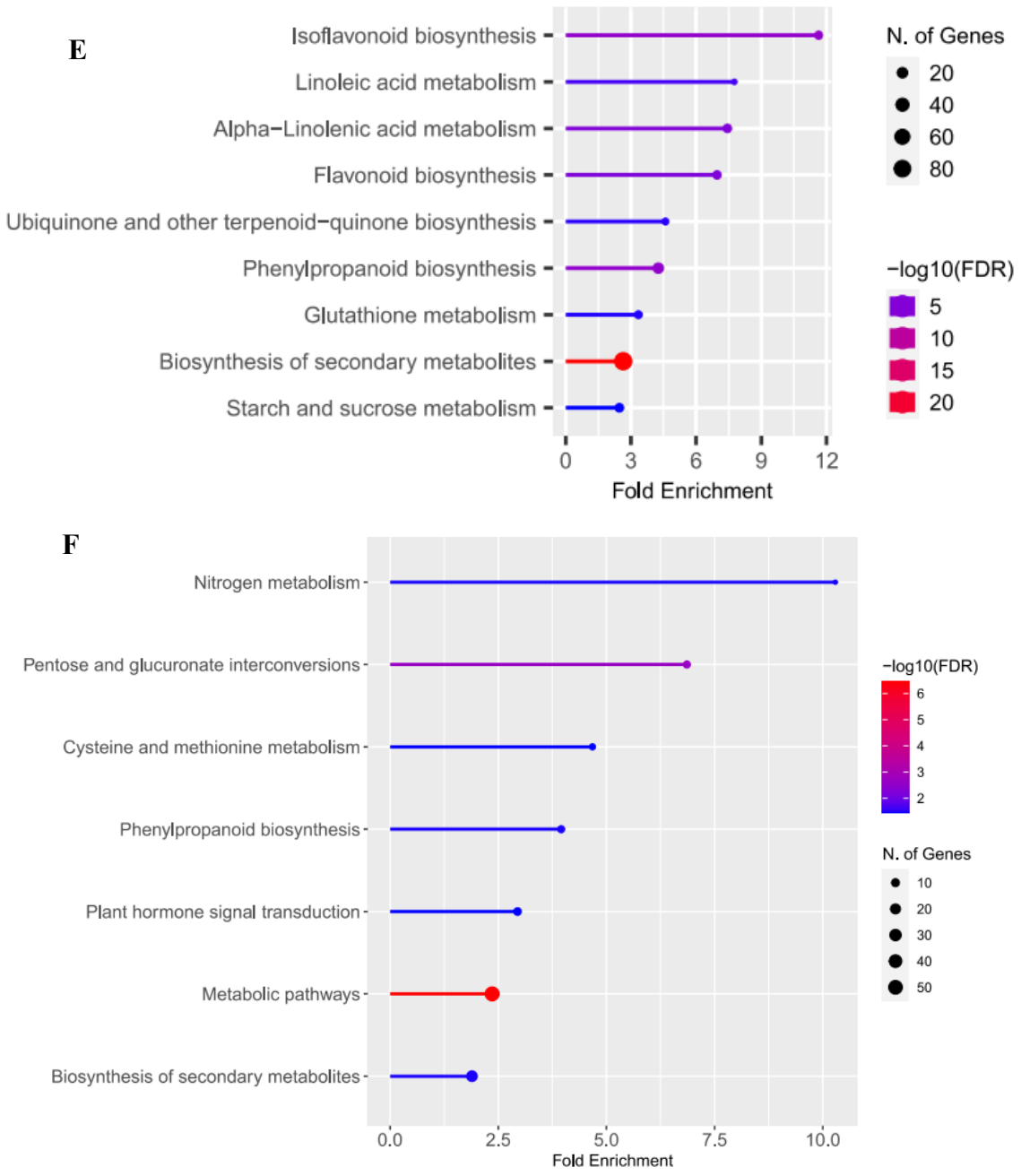

Figure 3.18. KEGG pathway induced by non pre-treated H_2O_2 applied treatment vs. H_2O_2 pre-treated MP inoculated treatment in the resistant genotype (DT97-4290) in the up-regulated (**E**) and down-regulated (**F**) categories.

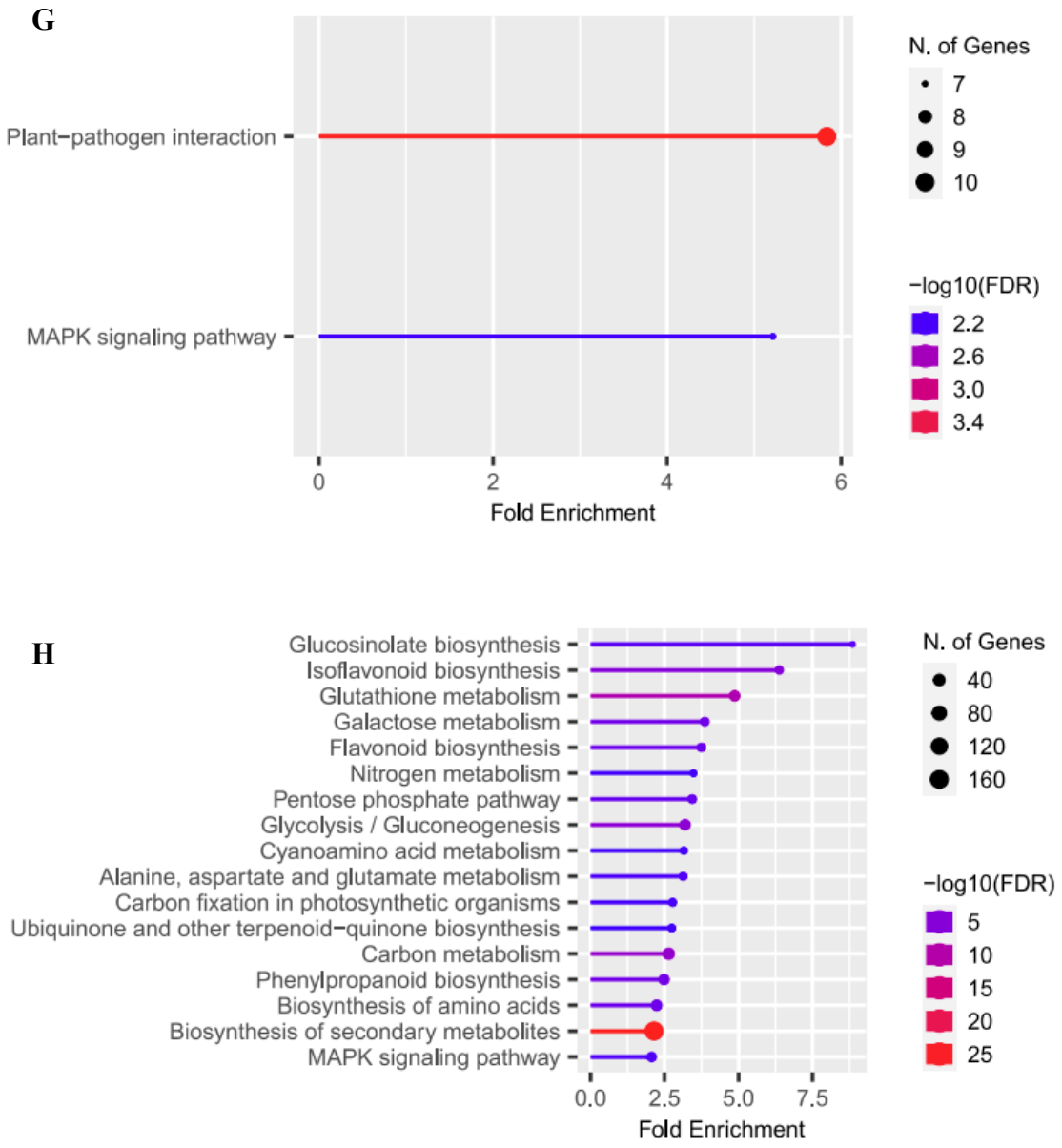

Figure 3.19. KEGG pathway induced by non pre-treated MP inoculated treatment vs. non pre-treated mock-inoculated treatment in the susceptible genotype (Pharaoh) in the up-regulated (**G**) and down-regulated (**H**) categories.

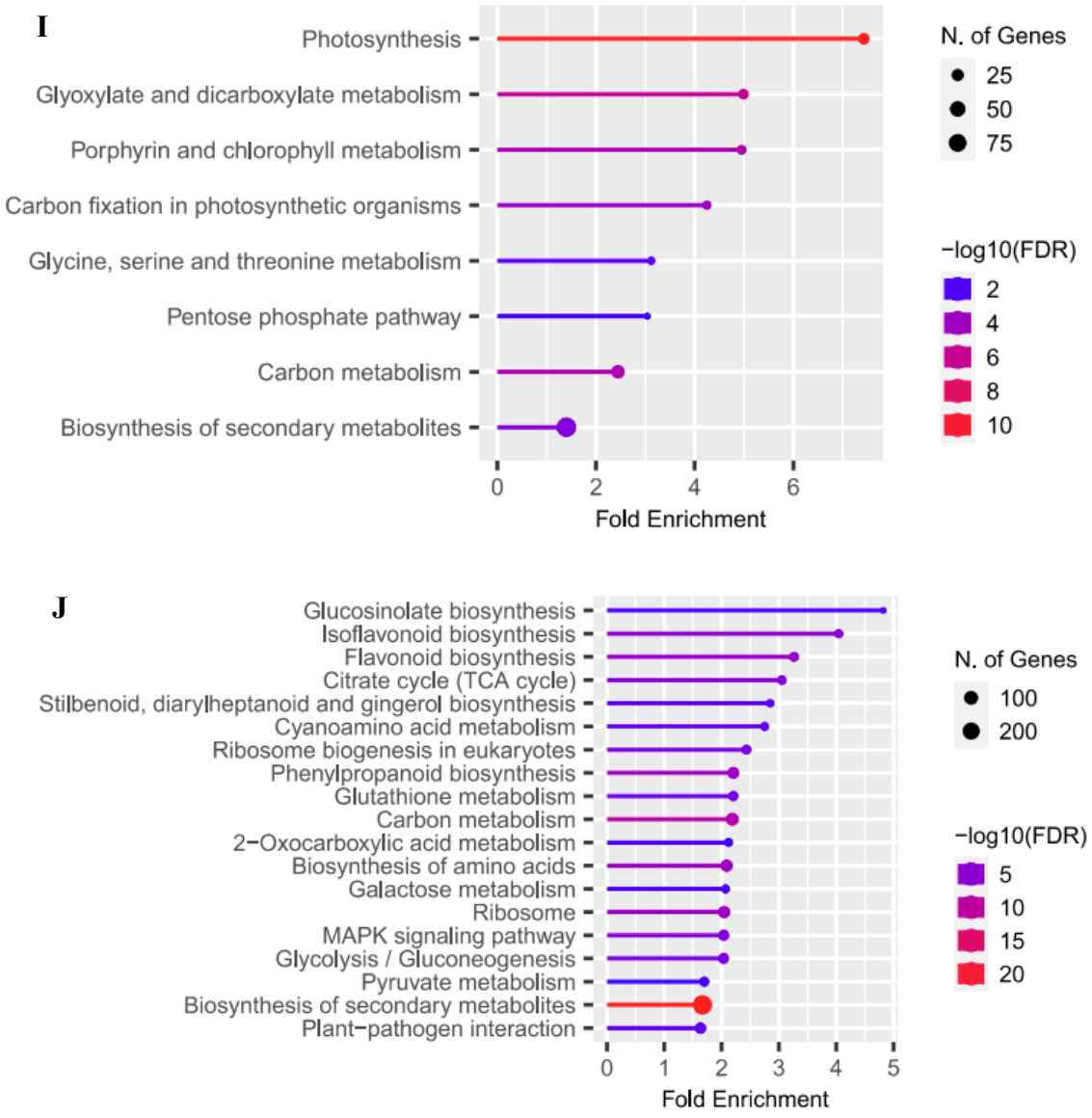

Figure 3.20. KEGG pathway induced by ascorbic acid pre-treated MP inoculated vs. ascorbic acid pre-treated mock-inoculated treatment in the susceptible genotype (Pharaoh) in the up-regulated (**I**) and down-regulated (**J**) categories.

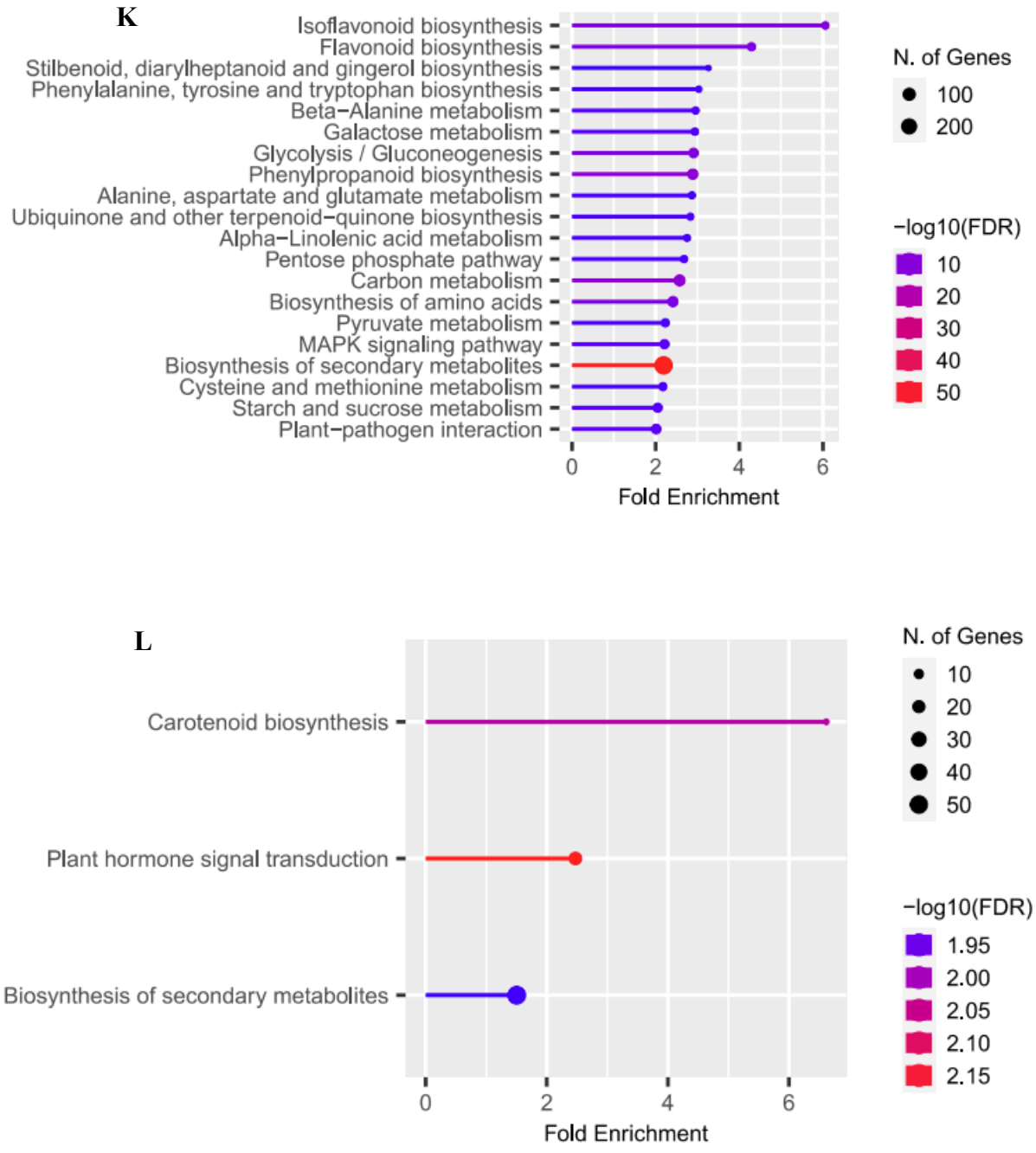

Figure 3.21. KEGG pathway induced by non pre-treated H_2O_2 applied treatment vs. H_2O_2 pre-treated MP inoculated treatment in the susceptible genotype (Pharaoh) in the up-regulated (**K**) and down-regulated (**L**) categories.

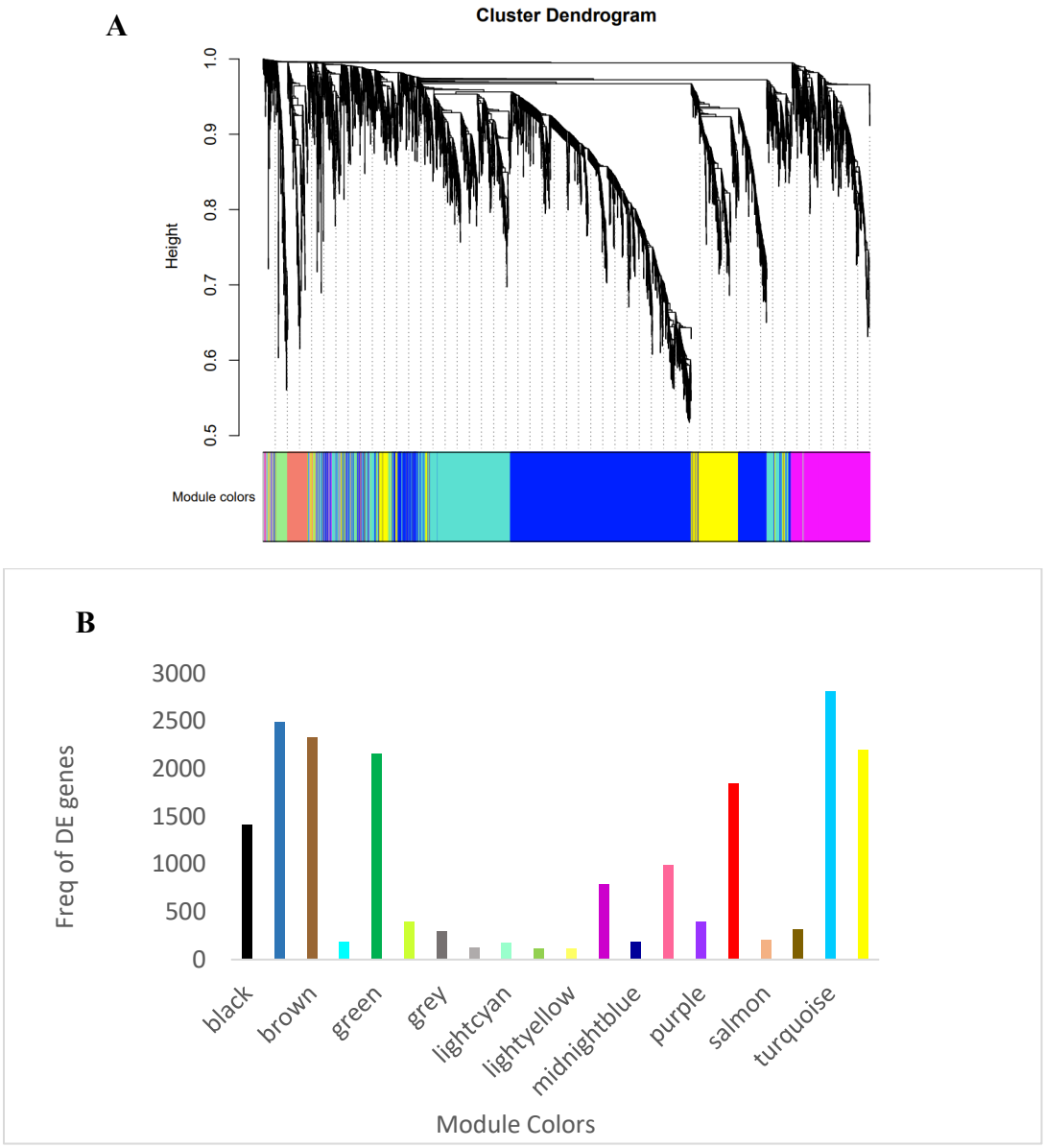

Figure 3.22. Gene co-expression module of genotypes by treatment interaction based on WGCNA. (**A**) Cluster dendrogram showing different genes in co-expression modules. (**B**) The number/frequency of genes represented by each module.

Chapter 4 - Phenotyping the sorghum nested association mapping parents for charcoal rot resistance

ABSTRACT

Charcoal rot of sorghum caused by *Macrophomina phaseolina* is an economically significant disease of sorghum in Kansas. The most effective management of this disease directs toward understanding the genetic variation behind charcoal rot resistance. The lack of accurate phenotyping and the effect of environmental variation has constrained the genetic improvement of charcoal rot resistance in many crops, including sorghum. The sorghum nested association mapping (NAM) population could be an effective background to dissect the genetic architecture of CR resistance. The sorghum NAM populations (developed by crossing ten diverse global sorghum lines with an elite breeding line, RTx430) have been used as a robust population for phenological and morphological trait dissection. The objective of this study was to phenotype the sorghum NAM parents for charcoal rot resistance using agronomic, disease, and yield trait ratings, and a quantitative real-time PCR (q-PCR) derived quantification of the fungal genomic DNA from some resistant and susceptible lines based on disease ratings. The NAM parental lines and charcoal rot-resistant and susceptible checks were phenotyped in two KS locations in 2019 and 2021. At 14 days after blooming, suspensions of MP inoculum were injected into stalks and sterilized, distilled water was used for mock inoculations. Data was collected 56 days after inoculation for morphological, disease severity, and yield traits. Results revealed significant differences among genotypes and genotypes by treatment interactions for all measured traits in both locations and years. Based on disease traits, the genotype with the highest lesion length from both locations in 2019 was Segaolane, but the results of 2021 from both locations were variable compared to 2019. The most susceptible genotype from one location in 2021 was SC1103, which showed the most resistance from both locations in 2019 based on disease ratings. Genotype Macia showed the highest charcoal rot lesion from one location in 2021 data. However, genotype SC1103 consistently showed the lowest disease traits in both locations in 2019 and from one location in 2021. A q-PCR assay was not effective in quantifying fungal DNA from the sorghum stalk. Based on the phenotyping results of three environmental data SC1103 NAM family derived recombinant inbred lines (RIL) population could be selected for phenotyping and to map for charcoal rot resistance using association study.

INTRODUCTION

Charcoal or stalk rot of sorghum (*Sorghum bicolor* (L.) Moench) is caused by the soilborne fungus *Macrophomina phaseolina* (MP), which is predominant in most tropical and temperate sorghum growing regions (Wyllie, 1998). *M. phaseolina* is a ubiquitous fungal pathogen and has nearly 500 plant hosts that include food crops, pulse crops, row crops, and oil crops (Sarker et al., 2014; Wyllie, 1998; Islam et al., 2012; Su et al., 2001; Mayek-Pérez et al., 2001; Raguchander et al., 1993; De et al., 1992). Charcoal rot is among the most important and prevalent sorghum diseases (Jardine., 2006). Usually, *M. phaseolina* infects and colonizes the host after flowering (Ilyas et al., 1976; Reed et al., 1983). During the grain-filling stage, the pathogen degrades the pith tissue (Edmund, 1964) near the base of the stalk and induces host tissue damage and senescence of stalk pith cells which blocks water and nutrient translocation through the vascular system (Hundekar and Anahosur, 1994; Tesso et al., 2012), which ultimately leads to wilting and stalk lodging and thus results in a yield penalty. Charcoal rot is also initiated by photosynthetic stress induced by drought or water deficiency during the post-flowering and grain filling stages (Dodd, 1980). Studies have shown that post-flowering water stress enhanced charcoal rot disease severity by 90% (Edmunds et al., 1964, 1965; Edmunds, 1964).

The genetics of host resistance to *M. phaseolina* is complex as multiple factors may underlie charcoal rot severity, lodging, and yield losses. Understanding genetic resistance in sorghum against *M. phaseolina* has remained evasive as the phenotypic performance of a genotype may vary between seasons or even in the same location (Dodd, 1980). In addition, genetically identical plants might not show the same magnitude of disease severity or spread due to the external factors influencing the host-pathogen interaction. Thus, selection for charcoal rot resistance has remained complex and challenging (Dodd, 1980). However, with recent advancements in genomic resources and high-throughput phenotyping (HTP) platforms, plant genetic resources are being utilized to develop more climate-resilient crops that will enhance crop productivity and assist in global food demand (Boyles et al., 2019).

Sorghum is the fifth most important cereal crop and has a wide adaptation area in the world, including Africa, the Americas, Australia, Asia, and Europe, and supplies the staple food demand of > 500 million people (Boyles et al., 2019; Xin et al., 2021). It is a C4 grass crop used for food,

animal feed, and bioenergy. Sorghum has already been genetically dissected for many traits to understand the genetic architecture of a particular trait by relating the associated phenotypic and genetic variation (Boyles et al., 2019). The sorghum nested association mapping (NAM) populations have been known for their increased power in dissecting traits (Boyles et al., 2019; Yu et al., 2008) and were developed from the concept of maize NAM populations that showed strong statistical power with combinatory mapping approaches to dissect loci with minor effects (Boyles at al., 2019). There are currently five sorghum NAM populations developed. Four were based on grain sorghum backgrounds, and one has a bioenergy sorghum background. Three of these five NAM populations were developed from crosses between two recurrent parents through the single-seed descent method, and two others were developed through the backcross method (Boyles et al., 2019).

The sorghum NAM population contained 2,121 recombinant inbred lines (RILS) and was developed and released at Kansas State University (Bouchet et al., 2017). For the development of the NAM population, eleven parental lines were selected from the sorghum association panel (Casa et al., 2008, Bouchet et al., 2017). The NAM population was derived from a cross between 10 global sorghum founder lines, with an elite US parental line, RTx430. These ten founder lines were diverse based on geographic adaption. Each founder was crossed with the common parent RTx430 to develop ten NAM families (biparental subpopulations) (Bouchet et al., 2017; Perumal et al., 2021). The ten founder lines are Ajabsido, Macia, P898012, SC1103, SC1345, SC265, SC283, SC35, SC971, and Segaolane was crossed with the common parent RTx430 (Bouchet et al., 2017). The F1 generation derived from each cross was selfed to develop F2 progeny, and from the F2's, around 250 RILS were developed through the single seed-descent method. Therefore, each NAM family consists of approximately 250 RILs, and the RIL families are named by their corresponding alternate and founder line parent (Bouchet et al., 2017).

The NAM population is used to dissect complex quantitative traits through linkage analysis or association mapping by controlling population structure and genetic diversity (Yu et al., 2008). A joint linkage mapping of flowering time and plant height with the NAM population detected known genes. Association mapping with the NAM population exhibited three-fold greater power in detecting QTL (Bouchet et al., 2017). The genotypic combinations and allelic frequencies in

the NAM population ease the screening of rare QTLs within and highly differential alleles between subpopulations (Wang et al., 2020).

Since the environment is a significant constraint in resistance breeding and selection and greatly influences charcoal rot disease, the NAM population could be a good resource for discovering charcoal rot resistance genes. Adeyanju et al. (2015) conducted a genome-wide association study (GWAS) with 300 sorghum genotypes from the sorghum diversity panel. The genome-wide screening of stalk rot diseases in sorghum using 79K SNP markers revealed 14 QTLs associated with candidate genes conferring resistance to the diseases, accounting for 19-30% variability (Adeyanju et al. 2015). The results of linkage disequilibrium and allele frequency analysis suggested that complex molecular mechanisms are working behind the host resistance for charcoal rot in sorghum (Adeyanju et al., 2015).

Plant phenotypes are qualitative and quantitative traits that are visible, measurable, and expressed by genetic and environmental interactions and variation (Herskowitz, 1977). Fiorani and Schurr (2013) described "phenotyping as a set of methodologies and protocols required to measure a plant's physiological, morphological and biochemical traits with precise accuracy from different scales of organization". Phenotyping is the characterization of desirable traits, and effective phenotyping is the key criterion for selection in breeding (Panguluri and Kumar, 2016). Therefore, phenotyping is considered of paramount importance for a successful breeding program. Therefore, sorghum NAM populations have been chosen for phenotyping to conduct a charcoal rot resistance screening assay with the ultimate goal of dissecting charcoal rot (CR) resistance gene(s). The objective of this study was to: (i) screen the sorghum NAM founder lines for charcoal rot resistance in different locations, (ii) select the NAM family based on the charcoal rot screening from the founder lines, and (iii) quantify the genomic DNA of *M. phaseolina* from a selected panel of moderately resistant and susceptible lines through quantitative real-time PCR (qPCR).

The effective resistant screening results will develop a reference for further phenotyping of the NAM RIL families for charcoal rot resistance and susceptibility. In addition, the population could be used further to phenotype for charcoal rot resistance toward Genome-Wide Association (GWAS) study to map for charcoal rot resistance.

MATERIALS AND METHODS

Experimental design, sorghum NAM parents, and checks

Ten global sorghum founder lines (Ajabsido, Macia, P898012, SC1103, SC1345, SC265, SC283, SC35, SC971, and Segaolane) and a common US pollinator line (RTx430) were selected for phenotyping. Besides these eleven NAM parental lines, three common sorghum lines (one resistant check SC599 and two susceptible lines Tx7000 & BTx623) were also included in this phenotyping experiment as checks. All these 14 parental lines (Table 4.1) were phenotyped for charcoal rot resistance in the field for two years in two different environments (locations) for four environments. The experimental design was a randomized complete block design (RCBD) with factorial arrangements. The NAM lines (genotypes) were considered as factor A (whole plot), which had 14 levels (14 genotypes). The inoculation and mock-inoculated control were included as factor B (sub-plot) and had two levels. There were four replications and five plants per treatment, which was considered an experimental unit. The field phenotyping experiment was performed in 2019 and 2021 at Ashland Bottoms Research Farm and Agronomy North Farm, Manhattan, Kansas.

Inoculum preparation and inoculation

The sorghum *M. phaseolina* isolate MP342 was used for the inoculation. MP342 was transferred to ¼-strength potato dextrose agar (PDA) plates using a sterilized scalpel and allowed to grow for 5-6 days in the 30°C incubator. After 5-6 days, the fungal isolate-containing agar plugs were cut into small squares from culture's growing edges and were transferred to Erlenmeyer flasks containing 100 ml potato dextrose broth (PDB). Five to six fungal transfers were placed in each PDB flask. Liquid cultures were allowed to grow on a shake culture at 60 rpm for 5-10 days. Afterward, mycelial suspensions were blended using a refrigerated Waring blender for 8 min at 18,000 rpm to produce mycelial fragments. The blended suspensions were filtered through four layers of sterile cheesecloth to obtain small hyphal fragments. The concentration of hyphal fragments was measured using a hemacytometer and adjusted to 5×10^4 mycelial fragments/ml by diluting with sterile 10 mM phosphate buffer solution (PBS).

Sorghum plants were tagged with colored tapes at blooming, and the blooming dates were recorded in a spreadsheet. Inoculations were performed 14 days after blooming (DAB) in each sorghum plant. Plants were inoculated above the second node after the brace node and were drilled (Milwaukee M-12 12-volt lithium-ion cordless drill, Milwaukee, WI, USA) to make a wound for syringe and needle insertion. Following pre-wounding, 1 ml of inoculum was injected into the stalk using a syringe and needle. Mock-inoculated plants received 1 ml of sterile-distilled water. The inoculation point was sealed with Vaseline petroleum jelly to prevent foreign organisms from entering through the wound and preventing desiccation of the inoculation site.

Harvesting and data collection

Harvesting was performed 56 days after inoculation. Plant height (crown to panicle) was measured using a measuring tape in the field. Sorghum panicles were bagged separately in the field, and stalks were carried to the greenhouse to strip leaves and take disease parameter data. Stripped sorghum stalks were split longitudinally, and data were recorded for total lesion length (cm) (TLL) by measuring the entire visible dark lesion in the interior of the stalk, relative lesion length (total lesion length divided by plant height; RLL), major lesion length (lesions covering an enlarged area with conspicuous tissue degradation) (MLL), and the number of nodes crossed by the lesion (NC). The images of the split stalks were acquired using a digital camera. Stalk tissues from each genotype across all replications at the Ashland Bottoms location were collected, flash-frozen in liquid nitrogen, and stored in a -80°C freezer for qPCR detection of *M. phaseolina* genomic DNA. Before collecting yield data, sorghum panicles were dried in the greenhouse for three weeks. After drying, panicles were threshed using an automated thresher. Seeds were oven dried in a dryer at 40°C for 48 hours to reduce the moisture level to approximately 60%. Total seed weight (TSW) and 100-seed weight (100-SW) were measured (g) using a balance, and total seed count (TSC) per panicle was calculated using the total seed weight and 100-seed weight (HSW).

Quantification of *M. phaseolina* DNA from the sorghum stalks using real time qPCR

Based on the disease parameters (TLL and MLL), genotypes that showed consistently higher charcoal rot lesions (i.e., Macia, Segaolane, Ajabsido, SC265, and P898012) and moderate to lower

charcoal rot lesions (SC1103 and RTx430) were selected for qPCR quantification of fungal genomic DNA from the stalk tissue of these genotypes.

Stalk tissue was collected from inoculated and mock-inoculated plants from the inoculation point and up to the last visible mark of the lesion. Tissues were collected in a 2 ml vial, immediately flash-frozen in liquid nitrogen and stored in a -80°C freezer. The stalk tissue was ground and homogenized using a mortar and pestle with the continuous addition of liquid nitrogen. The ground stalk tissue powder was stored in the -80°C freezer before DNA extraction. DNA was extracted from the sample using the DNeasy Plant mini kit following the manufacturer's protocol (Qiagen, Inc., Valencia, CA, USA). DNA concentration and quality were checked using a Nanodrop Spectrophotometer-Nanodrop One (ThermoFisher Scientific, USA). *M. phaseolina* primers (Santos et al., 2020) and sorghum primers (Reddy et al., 2016) were selected from pre-designed and validated primers. The primer pair of *M. phaseolina* was designed using the nuclear gene translation elongation factor 1-alpha (TEF1-α), and the forward primer was 5′-AAACACACTTTTCGCACTCCTGC-3′; the reverse primer sequence was 5′-TATGCTCGCAGAGAAGAACACGA -3′ (Santosh et al., 2020). The sorghum primer pair was designed using the gene *PP2A* (serine/threonine protein phosphatase). The forward primer was 5′-AACCCGCAAAACCCCAGACTA-3′; the reverse sequence was 5′-TACAGGTCGGGCTCATGGAAC-3′ (Reddy et al., 2016). Before setting up the qPCR amplification experiment, the specificity of fungal and sorghum primers was tested using PCR and gel electrophoresis. Pure fungal DNA (*M. phaseolina* isolate 342) and sorghum DNA were used for PCR amplification. PCR amplification was performed in a 25 µl reaction (12.5 µl of GoTaq® Master Mix, 6.5 µl nuclease-free water, 2 µl of each primer (forward and reverse), and 2 µl of the DNA template (20 ng/µl). The PCR products were amplified using a program for initial denaturation at 94°C for 2 min, followed by 30 cycles of denaturing at 94°C for 1 min, annealing for30 minutes at 60°C, extension at 72°C for 1 min, and final extension at 72°C for 10 min (one cycle) following final incubation at 4°C. The amplified PCR products were analyzed using 1.5% agarose gel electrophoresis with Gel Green and observed under UV light to see amplified bands. If amplification occurred for the target species and produced a single band, they were used for qPCR amplification.

Real-time qPCR amplification

Real-time qPCR was conducted using the CFX 96 Real-Time PCR System (Bio-Rad, California, USA). All DNA samples from two biological replicates were analyzed using the specific MP and sorghum primers from both inoculated and mock-inoculated samples from the same genotypes. The final volume of the qPCR master mix was 20 µl and contained 10 µl SYBR Green qPCR master mix (2×), 2 µl DNA sample, 1 µl forward and 1 µl reverse primers, and 6 µl nuclease-free water. The amplification program for the qPCR machine was set at 50°C for initial incubation for 2 min following enzyme activation at 95°C for 2 min, denaturation for 15 secs at 95°C, annealing for 15 secs at 95°C, and extension at 72°C for 45 secs following final incubation at 4°C. The specificity of qPCR assay was examined using the pure culture of MP 342 that was used for the inoculation in the field.

C_q values (threshold cycles) of relative target DNA samples were compared to determine the relative quantities of the *M. phaseolina* DNA within sorghum genotypes (Orlando et al., 1998; Li et al., 2008). The C_q value is the threshold cycle of statistically significant fluorescence detection; a lower C_q value indicates higher DNA quantities in the sample (Li et al., 2008). The relative quantities of sorghum and MP DNA were calculated from each sample by subtracting the C_q value of the MP-specific reaction and the sorghum primer *PP2A* reaction ($\Delta C_q = C_{qMP\text{-}TEF1\text{-}\alpha} - C_{qsorghum\textit{PP2A}}$) (Li et al., 2008).

For quantifying the absolute DNA quantities of MP and sorghum, standard curves were generated from DNA samples of an MP 342 pure culture and a mock-inoculated control sample of the respective sorghum genotypes. To develop the MP standard curve, 42.8 ng/µl of purified DNA from the MP 342 was 10-fold serially diluted to 1.0×10^{-6} ng/µl. A sorghum standard curve was generated separately for each genotype. Two microliters of these dilutions were mixed with the SYBR select master mix and run in the CFX 96 Real-Time PCR System**.** To develop the standard curve of *M. phaseolina* and sorghum genotype, the log10 fold changed DNA concentration, and the resulting C_q values were plotted separately for *M. phaseolina* and sorghum, respectively.

To quantify the absolute fungal and plant DNA from the inoculated and mock control samples, the C_q values of the corresponding samples were extrapolated against the regression lines generated from the corresponding standard curve of the pure *M. phaseolina* and sorghum serial dilutions.

Statistical analysis

Analysis of variance (ANOVA) for the field phenotyping experiment was performed using the PROC GLIMMIX procedure of SAS 9.4 (SAS Institute Inc.; Cary, NC, USA). Replication within a location (environment) was considered a random effect, and factors A (genotypes) and B (level of treatments) were considered fixed effect factors. Means separation tests were performed for the interaction of factors A and B using the least square mean (LSMEANS) of the SAS PROC GLIMMIX procedure. Homogeneity tests of variance for location and year were performed for all traits using F-tests at $P \leq 0.05$. Variances were heterogenous, which suggested possible genotype by environment interaction (G × E). Therefore, combined analyses were not performed. Pearson correlation coefficients were separately analyzed for all traits measured from both locations in 2019 and 2021 using the R package ggplot2 and ggcorrplot. The qPCR data for the relative DNA quantities (fungal vs. plant) and absolute fungal and plant DNA quantities were analyzed using the SAS PROC GLIMMIX procedure of ANOVA. The means separation test within the DNA quantities of the samples was performed using least square means (LSMEANS) at $P \leq 0.05$.

RESULTS

The statistical analysis revealed a significant effect of genotypes, treatments (control and inoculation), and their interaction on the measured traits. The *P*-value of the F-test from the 2019 data of the Ashland Bottoms, KS location showed that all 14 genotypes were significant for all traits. However, the treatment was not significant for physiological traits like days to flower, plant height, and yield-related traits. The genotypes by treatment interactions were significant for all traits except for major lesion length (MLL) and hundred seed weight (HSW) (Table 4.2). The North Farm location data from 2019 showed a similar response to the Ashland Bottoms location. The genotype effect was significant for all traits, but treatment effects were not significant for physiological and yield traits. Genotype-by-treatment interactions were significant except for plant height, major lesion length, and total seed count (Table 4.3).

The *P*-value of the F-test from the 2021 Ashland Bottoms location was significantly different than the 2019 Ashland Bottoms data as per the test of homogeneity. The 2021 Ashland Bottom location showed a significant genotype effect for all the traits. In addition, the treatment effect was significant for all traits except for total seed count (yield).

The genotype-by-treatment effects were also significant, except for total seed weight and total seed count (Table 4.4). The 2021 North Farm location data revealed slightly different results than the Ashland Bottoms location. The genotype effect was significant for all traits except HSW. Treatment effects were not significant for physiological traits or yield-related traits. Genotypes by treatment interactions were significant for all the traits except plant height, HSW, and total seed count (Table 4.5).

Comparison of genotype performance based on disease parameters and yield at Ashland Bottoms in 2019

Analysis of Variance (ANOVA) for total lesion length measured from the stalks of all 14 genotypes showed that genotypes and treatments were both significant at $P \leq 0.001$ (Table 4.6). The genotype-by-treatment interaction was also significant ($P = 0.002$). The ANOVA table of relative lesion length (RLL), major lesion length (MLL), and nodes crossed by the lesion (NC) (Table 4.6) also showed significant differences among genotypes and treatments at $P \leq 0.001$; the genotypes by treatments interaction were also significant ($P = 0.02$) for RLL and NC, but not for MLL. Total seed weight (TSW) and total seed count (TSC) showed significant differences between genotypes but not treatments. Genotypes by treatment interactions were also significant. Mean separations test for the total lesion length (TLL) using the least square means (LSMEANS) with $P \leq 0.05$, ranked genotypes with highest to lowest TLL. Among the 14 genotypes, Segaolane showed the highest lesion length, which was significantly different than the Segaolane mock-inoculated control treatment and all other genotypes inoculated and mock-inoculated controls (Figure 4.1). Following Segaolane, the other genotypes that showed high lesion length were P898012, Ajabsido, Macia, SC599, SC971, and SC35, but there was no significant difference with the mock control treatment for these genotypes. Three genotypes showed relatively low lesion lengths, SC1103, Tx7000, and SC1345, and were not significantly different than their mock-inoculated control

counterparts. Relative lesion length (Figure 4.2), major lesion length (Figure 4.3), and nodes crossed by the lesion (Figure 4.4) showed similar phenotypic differences among the genotypes.

Total seed weight and total seed count showed that Macia performed the highest among all genotypes. Still there were no yield differences between inoculated or the mock-inoculated control treatment suggesting tolerance to charcoal rot (Fig 4.5). The other genotypes that also showed significantly higher yield based on TSW were Ajabsido, Segaolane, BTX623, RTx430 (both inoculated and mock control), and the SC1345 mock-inoculated control treatment. Genotypes that yielded equally well irrespective of inoculation or mock-inoculation treatments and exhibited high lesion length suggests tolerance to *M. phaseolina* infection. The only genotype that showed significant yield differences between the mock-inoculated and inoculated treatments based on TSW was SC1345 (Figure 4.5). However, based on total seed count (TSC), genotypes SC1345, BTx623, and SC971 showed significant yield differences when mock-inoculated and inoculated treatments were compared for the same genotype (Figure 4.6).

Comparison of genotype performance based on disease parameters and yields of North farm location, 2019

The ANOVA table from the 2019 North Farm location for TLL showed that replications were significant. Genotypes and treatments were highly significant ($P \leq 0.001$) (Table 4.8), as were the genotype by treatment interactions ($P = 0.0004$). Replications for RLL and NC (Table 4.8) were significant, as well as genotypes, treatments, and their interactions. However, for MLL (Table 4.8), replications were not significant, but genotypes, treatments, and their interaction were significant. ANOVA for TSW showed significant reps, while reps were not significant for TSC (Table 4.8). For TSW and TSC, genotypes were significant for both traits, but treatments and genotype-by-treatment interactions were not significant for either yield-associated trait. The mean separation test at $P \leq 0.05$ revealed four genotypes (Segaolane, P898012, SC1345, and SC35) with comparatively higher lesion lengths. However, in the P898012, the mock-inoculated and inoculated treatments were not significantly different (Figure 4.7). In this location, the lowest lesion length was observed in SC971 with no significant difference compared to its mock-control counterpart. There was no statistical difference found among the inoculated controls of genotypes SC1103 and SC599 compared to SC971. However, there was no statistical difference between the mock-inoculated

and inoculated for both SC1103 and SC599 (Fig. 4.7). Relative lesion length resulted in similar genotypes with the highest relative lesion length as TLL. The inoculated and mock-control treatments were statistically different for the genotypes (SC1103, BTX623, SC971, SC283, and Macia) that showed the lowest relative lesion length, suggesting a possible correlation of lesion length with plant height. Like TLL, the SC971 inoculated treatment resulted in the lowest relative lesion length and was significantly different than its mock-inoculated control counterpart (Figure 4.8). Major lesion length (MLL) resulted in variable data. The genotypes (Segaolane, SC35) with the highest major lesion length showed statistical significance between their inoculated and mock-inoculated control partners. Macia exhibited high major lesion length but didn't show a significant difference from the mock-inoculated control treatment. The inoculated genotypes that showed relatively lower MLL didn't differ from their mock-inoculated control counterparts (Figure 4.9). The nodes crossed by the lesion (NC) data showed a significant difference between the mock-inoculated and inoculated treatments of SC35, SC265, and Macia (Figure 4.10). Still no statistical difference was observed between the mock-inoculated and inoculated treatments of genotypes P898012 and Segaolane.

Genotypes with higher TSW were Macia and Ajabsido. No statistical difference in the TSW trait was observed when compared to the mock-inoculated control with the inoculated treatments for these genotypes. However, genotype SC1103 showed the lowest disease severity in TLL, RLL, and NC but showed statistically significant yield (TSW) differences between mock-inoculated and inoculated treatments (Figure 4.11) and suggests the possible effect of charcoal rot on yield compromise.

Genotype comparison based on disease parameters and yields from the Ashland Bottoms 2021 location

TLL and RLL (Table 4.7) from the 2021 Ashland Bottoms location showed genotypes, treatments, and their interactions were highly significant ($P \leq 0.001$). Genotypes and treatments were highly significant at $P \leq 0.001$ for MLL, while their interaction effects were significant at $P = 0.0004$ (Table 4.7). The ANOVA of NC (Table 4.7) resulted in treatments as highly significant at $P \leq 0.001$, while genotypes were significant at $P = 0.015$ and genotypes by treatments were significant at $P = 0.002$. The ANOVA for TSW revealed statistically significant genotypes at $P \leq 0.001$ and

treatments at $P = 0.048$, while their interaction was non-significant (Table 4.7). Genotypes were significant, but treatments and interactions were non-significant for total seed count (TSC) (Table 4.4). However, for the hundred seed weight (HSW), genotypes ($P \leq 0.001$), treatments ($P = 0.018$), and their interactions were significant ($P = 0.007$) (Table 4.4). The mean separation test using least square means (LSMEANS) at $P \leq 0.05$ for the TLL (Figure 4.12) and MLL (Figure 4.14) showed SC1103, SC1345, SC265, and SC971 produced high lesion length, which was the opposite of 2019's Ashland Bottom's phenotyping results. Genotypes that produced lower TLL were Segaolane, SC599, RTx430, and Tx7000. For these genotypes, the mock-inoculated and inoculated were not statistically significant (Figure 4.12). The mean separation test for RLL showed similar results as TLL, except that the SC599 inoculated and mock-inoculated treatments were significantly different (Figure 4.13). NC (Figure 4.15) showed similar results as TLL, RLL, and MLL. Ajabsido, SC1103, and SC1345 exhibited the highest NC; these three genotypes were also statistically significant compared to their mock-inoculated counterparts. The genotypes that showed the lowest number of NC was Macia. However, there was no statistical difference between the mock-inoculated control and inoculated treatment.

The genotype-by-treatment interactions were not significant for TSW. The higher-yielding genotypes were Tx7000, BTx623, SC265, Macia, and P898012; these were statistically non-significant when comparing inoculated with the mock-inoculated control treatment except Tx7000. SC283 was the lowest-yielding genotype, with no statistical yield difference between the inoculated and mock-inoculated control treatments (Figure 4.16). The HSW trait showed statistically significant differences between the mock-inoculated control and inoculated treatments for genotypes with the highest HSW, including Tx7000, Ajabsido, and Segaolane. SC971 and SC283, However, the mock-inoculated and inoculated treatments for SC971 and SC283 were not significant (Figure 4.17).

Genotype comparisons based on disease parameters and yield from the 2021 North Farm location

The ANOVA table for the disease traits TLL, RLL, and MLL (Table 4.9) from the 2021 North Farm location resulted in statistically significant genotypes, treatments, and interactions at $P \leq 0.001$. NC (Table 4.9) from this location showed statistically significant genotypes and treatments

at $P \leq 0.001$, while the genotype-by-treatment interactions were significant at $P = 0.004$. TSW was significant for the genotype effect ($P \leq 0.001$), but the treatment factor was not significant. Genotypes-by-treatment interactions were significant at $P = 0.006$ (Table 4.9). However, the genotypes-by-treatment interactions for HSW and TSC were not significant (Table 4.5); therefore, those results are not discussed here. The mean separations test using least square means (LSMEANS) of TLL at $P \leq 0.05$ revealed that Macia produced the highest TLL, which was statistically significant compared to its mock-inoculated control counterpart and all other genotypes. This suggests that Macia is the most susceptible founder line to charcoal rot. Several genotypes that showed low TLL were SC1103, Segaolane, SC283, and SC35. However, there were no statistical differences between mock-inoculated and inoculated treatments for these lines (Figure 4.18). Macia and SC971 exhibited the highest RLL, they were both significantly different from each other, and their inoculated and mock-inoculated control treatments were also significantly different (Figure 4.19). SC1103, SC35, SC599, SC283, and Segaolane exhibited low RLL values; however, there were no statistical differences between the mock-inoculated control and inoculated counterpart treatments for these genotypes. Macia produced the highest MLL value, significantly different from the mock-inoculated treatment compared to other genotypes' mock-inoculated or inoculated treatment MLL values (Figure 4.20). The lowest MLL values from this year and location were in SC1103, SC35, Segaolane, and SC599. However, like TLL and RLL, there was no difference between the mock-inoculated and inoculated treatments of these genotypes, which suggests a possible resistance reaction to charcoal rot disease. Macia, Ajabsido, and SC1345 produced the highest NC values, and these genotypes were statistically significantly different for the mock-inoculated control and inoculated treatments (Table 4.21). The genotypes with low NC values were the same as those for TLL, RLL, and MLL, with no statistical difference between the mock-inoculated and inoculated treatments. Surprisingly, Segaolane and P898012 showed higher amounts of charcoal rot in the stalk, considering the TLL, RLL, MLL, and NC traits in the 2019 Ashland Bottoms and North Farm locations, yielded opposite results in 2021, which suggests strong environmental interaction for these traits.

SC1345 produced the highest TSW but was not statistically different from genotypes SC265, Macia, Ajabsido, and P898012 (Table 4.9). Among the high-yielding genotypes, mock-inoculated control and inoculated treatments were significantly different for SC1345 and SC265, which suggests inoculation affects TSW for these genotypes. Genotypes that showed relatively lower TSW

were SC1103, Segaolane, and SC283; mock-inoculated control and inoculated treatments for these genotypes were not significantly different, which suggests that charcoal rot does not affect the yield of these genotypes. The disease severity and yield traits at the 2021 North Farm location were consistent with the 2021 Ashland Bottom location data.

Pearson correlation coefficient for all traits from the Ashland Bottoms and North Farm locations of 2019 and 2021

Pearson correlation coefficient analysis among all traits from the 2019 Ashland Bottoms location showed a positive and significant correlation between TLL and NC (Figure 4.23). Relative lesion length was also significantly and positively correlated with TLL and NC. No correlations were observed between TLL, MLL, RLL, NC, and days to flowering (FD). However, moderately positive correlations were observed between plant height and TLL. No correlations were observed between disease and yield traits from this location and year. The correlation analysis from the 2021 Ashland Bottoms location showed a significantly strong and positive correlation between TLL and MLL, RLL and TLL, and MLL and NC. Total seed weight (TSW) and total seed count (TSC) were positively correlated. However, no correlation was observed between disease and yield traits. Plant height and FD showed significant and negative correlations with RLL, TLL, and MLL. Conversely, plant height (PH) and days to flower (FD) showed a significantly strong positive correlation (Figure 4.23).

Correlation analysis from the 2019 North Farm location showed a strong and positive correlation between TLL and RLL, RLL and NC, and TLL and NC. Similarly, like Ashland Bottoms, correlation analyses between TSW and TSC were positively correlated (Figure 4.24). In addition, the 2021 North Farm data resulted in similar trends as those of the 2019 North Farm and Ashland Bottoms (2019 and 2021) locations, which suggests that the correlation between traits didn't differ due to location or environmental variation.

Relative and absolute quantification of fungal and plant DNA using real-time q-PCR

Absolute DNA quantified from sorghum genotypes for plant vs. *M. phaseolina* didn't show any statistical difference between the inoculated and mock-inoculated control treatments for the genotypes selected for qPCR quantification. However, the genotypes significantly differed based on relative DNA quantities. SC1103 showed the lowest relative DNA quantities with no statistical similarities to all other genotypes and treatments (Table 4.10). No Cq value was obtained for the MP primer used from this genotype. However, sorghum DNA was quantified from this genotype (Table 4.10). Genotypes that showed lower C_q values for *M. phaseolina* primers indicate higher quantities of fungal DNA. However, the genotypes were not significantly different based on the delta C_q value. Plant DNA quantified from the mock-inoculated and inoculated treatments did not differ significantly. The absolute fungal DNA quantified from inoculated and mock-inoculated genotypes didn't differ statistically or at a detectable level. The absolute sorghum DNA quantified from the mock-inoculated and inoculated treatments showed statistical significance within genotypes but no significant difference between genotypes. The highest absolute plant DNA was quantified from the SC971 mock-inoculated control which was statistically similar to SC971 inoculated, Ajabsido mock and inoculated, P898012 mock and inoculated, and Segaolane mock and inoculated samples (Table 4.11). The lowest absolute plant DNA was quantified from the SC265 mock-inoculated and inoculated treatments, which was statistically similar to the RTx430 mock-inoculated control but significantly different than all other genotypes and treatments (Table 4.11).

DISCUSSION

Charcoal rot is one of the most important biotic constraints of sorghum worldwide (Tesso et al., 2012). Breeding for host resistance to charcoal rot is an effective means of managing the economic losses caused by the fungus *M. phaseolina*. Therefore, effective screening for charcoal rot resistance is critical for selection. Phenotyping disease symptoms are laborious, time-consuming, low scalable, and prone to subjectivity. Charcoal rot is not an exception. High throughput phenotyping platforms have been deployed for several traits in sorghum including plant height (Watanabe et al., 2017), morphological and anatomical properties of the stem (Gomez et al., 2018), stalk properties of sorghum (Batz et al., 2016) and in the soybean for charcoal rot disease detection

using hyperspectral imaging (Nagasubramanian et al., 2019; Al-Ahmadi et al., 2021). However, there is no high throughput phenotyping protocol reported to date for the charcoal rot screening in the sorghum could be due to the complexity of phenotyping as the disease developed in the internal part of the stalks. Visual charcoal rot rating using different parameters, for example, total lesion length, relative lesion length, major lesion length and nodes crossed by the lesion have been previously used for phenotyping charcoal rot in sorghum (Tesso et al., 2004; Bandara et al., 2015) and resistance or susceptibility to charcoal rot ranking was estimated based on the charcoal rot lesion in the stalk. Tesso et al. (2009) developed a method to phenotype charcoal rot resistance by relating initial inoculum density with CR rot lesion development, suggesting the resistance or susceptibility ranking depends on CR lesion length. In this phenotyping experiment, we aimed to evaluate and screen the most resistant and susceptible nested association mapping (NAM) founder lines of sorghum from four different environments using different visual rating parameters. The charcoal rot-resistant founder line will be a good reference point for phenotyping NAM family-derived recombinant inbred lines (RIL) (Bouchet et al., 2017) populations to map the charcoal rot resistance.

This study evaluated the charcoal rot reaction of fourteen sorghum genotypes. The NAM genotypes included ten globally diverse sorghum lines along with an elite US pollinator parent (Bouchet et al., 2017); three other genotypes included a resistant check SC599 (Tesso et al., 2005), a susceptible check Tx7000 (Diourte et al., 1995), and BTx623, which provided the reference genome of sorghum (Paterson et al., 2009), were phenotyped for the charcoal rot at Ashland Bottoms and Agronomy North Farm, Manhattan, Kansas in 2019 and 2021. The results demonstrated similar types of performance of genotypes in both locations within a year while the results varied from the same location between years.

In 2019, Segaolane was screened as the most susceptible line based on the disease severity traits we measured in both locations. However, it also showed a significantly higher yield. Thus, this NAM founder line, along with other high-yielding, high-disease founders, could be tolerant to charcoal rot. Caldwell et al. (1958) defined the term tolerance as the capacity of a plant to tolerate disease pressure without compromising crop yield or quality. Bandara et al. (2015) developed an $Index_{RT}$ value to evaluate genotypes for the phenotypic performance of disease and yield traits based on disease resistance and a yield loss index. Their research found no relationship between

disease pressure and yield loss and surprisingly discovered that $Index_{RT}$ and lesion length were not correlated (Bandara et al., 2015).

Correlation analysis revealed no significant association between disease and yield traits from locations and years. However, the correlation test of 2019 from both locations revealed disease trait TLL was positively correlated to NC and RLL. RLL showed a higher positive correlation with TLL and NC, which supported the idea that total lesion length and nodes crossed by the lesion length were significantly correlated to plant height. Therefore, it was suggested that stalks with greater plant height were associated with higher lesion length. and the mock-inoculated treatment exhibiting higher wound sensitivity might be due to colonization by other microbes. Das et al. (2008) assessed the relationship between stalk morphology and anatomy with charcoal rot severity, which suggested a positive relationship between stalk thickness and CR progression. Thicker stalks are more susceptible to MP-induced CR progression. The study also suggested negative relation between stalk anatomy and CR development, i.e., stalks with dense vascular bundles are more resistant to CR progression (Das et al., 2008).

However, no study of plant height's relationship with CR has been reported to date. Assessment of the relationship between plant height and CR could be an area that needs further investigation. Bandara et al. (2015) demonstrated that disease parameters-based ranking and yield based ranking are independent parameters for evaluating genotype performance. Since there was an inconsistent correlation between these two parameters, we also observed similar patterns.

The genotype SC1103 showed the highest lesion length in 2021's Ashland Bottoms location but did not demonstrate that trend from the North Farm location of 2021. On the other hand, Segaolane showed lower disease trends in 2021 from both locations, which was the opposite of 2019's results. The yield of the genotypes that showed higher disease trends were consistently higher, like 2021's Ashland bottom and 2019's both locations data, again suggesting substantial environmental and location-wise micro-environmental variation on the genotypic performance. Price et al. (2004) reasoned quantitative disease resistance is commonly influenced by the genotype by environmental (G×E) interaction. Adeyanju et al. (2015) dissected the stalk rot resistance using 300 genotypes of diverse panel grain sorghum from three environments and two years, revealing phenotyping variation between environment and years (Adeyanju et al., 2015). This reasoning agrees with our

findings due to the magnitude of changes in disease responses in the four tested environments. Mahmoud et al. (2018) stated the nature of charcoal rot resistance as "quantitative inheritance" due to high phenotypic variability for the CR resistance parameters within the sorghum accession tested for CR severity. This statement is consistent with previous studies for the nature of charcoal rot inheritance in sorghum (Pecina-quintero et al., 1999; Tesso et al., 2005; Adeyanju et al., 2015). Based on the results of three environments data, SC1103 family-derived RILs could be selected for phenotyping and mapping for charcoal rot resistance. The inconsistent performance of genotypes towards CR progression across environments signifies the complex genetic architecture underlying charcoal rot resistance in the NAM lines.

Besides visual ratings, the detection and quantification of pathogen biomass through qPCR from the plant could assist in accurately assessing pathogen progression and identifying susceptible and resistant phenotypes (Brouwer et al., 2003). However, the qPCR assays using sorghum stalk tissue further suggested the need for more precise PCR assays to execute the proper quantification of the *M. phaseolina* DNA from the sorghum stalks. The primer used for quantifying genomic DNA from the *M. phaseolina* species was designed by Santosh et al. (2020) to distinguish *M. phaseolina* species by developing species specific *M. phaseolina* primer. However, as suggested by our qPCR assay, the primer did not demonstrate accuracy in quantifying genomic DNA from the field sample. Babu et al. (2011) developed a real-time qPCR assay and primer based on the ~ 1 kb of sequence characterized amplified region (SCAR) using both SYBR green and TaqMan assay to detect *M. phaseolina* from soil and plant samples. Their real-time qPCR assay resulted in precise specificity and sensitivity in detecting genomic DNA of *M. phaseolina* from both plant and soil samples (Babu et al., 2011) suggested these primers could be evaluated to test the specificity in detecting *M. phaseolina* DNA from the field sample of sorghum stalks of NAM lines.

Another potential phenotyping could be image analysis and machine learning algorithms for detecting disease symptoms from the split sorghum stalks to screen charcoal rot progression and assessment of resistance from these genotypes to optimize disease scoring. Several studies demonstrate high throughput phenotyping over visual assessment for phenotyping disease scores (Xie et al., 2012; Marzougui et al., 2019; Dutta et al., 2022) and machine learning approaches (Shruthi et al., 2019; Mohanty et al., 2016) to optimize disease phenotyping. Since phenotyping NAM parentals lines from both locations and years suggested charcoal rot resistance as a complex quantitative

trait, precise image analysis could efficiently differentiate between the mock and inoculated treatments and rank the genotypes. Imaging analyses has been successfully deployed in soybean to detect charcoal rot (Nagasubramanian et al., 2019). Nagasubramanian et al. (2019) used a 3D deep convolutional neural network (DCNN) to analyze the hyperspectral imaging data of *M. phaseolina* inoculated and mock-inoculated soybeans and a showed disease classification accuracy of 95.73%. Besides visual rating, image analysis would boost the phenotyping accuracy of highly variable diseases due to environmental interactions.

REFERENCES

1. Adeyanju, A., Little, C., Yu, J., & Tesso, T. (2015). Genome-wide association study on resistance to stalk rot diseases in grain sorghum. *G3: Genes, Genomes, Genetics*, *5*, 1165-1175.
2. Al-Ahmadi, A., Subedi, A., Choudhary, R., Fakhoury, A., & Watson, D. (2021). Hyperspectral spectroscopy to detect different responses of two soybean (*Glycine max*) cultivars to charcoal rot (*Macrophomina phaseolina*) toxin. *Engenharia Agrícola*, *41*, 78-86.
3. Babu, B. K., Mesapogu, S., Sharma, A., Somasani, S. R., & Arora, D. K. (2011). Quantitative real-time PCR assay for rapid detection of plant and human pathogenic *Macrophomina phaseolina* from field and environmental samples. *Mycologia*, *103*, 466-473.
4. Bandara, Y. M. A. Y., Perumal, R., & Little, C. R. (2015). Integrating resistance and tolerance for improved evaluation of sorghum lines against Fusarium stalk rot and charcoal rot. *Phytoparasitica*, *43*, 485-499.
5. Batz, J., Méndez-Dorado, M. A., & Thomasson, J. A. (2016). Imaging for high-throughput phenotyping in energy sorghum. *Journal of Imaging*, *2*, 4.
6. Bouchet, S., Olatoye, M. O., Marla, S. R., Perumal, R., Tesso, T., Yu, J., Tunistra, M. & Morris, G. P. (2017). Increased power to dissect adaptive traits in global sorghum diversity using a nested association mapping population. *Genetics*, *206*, 573-585.
7. Boyles, R. E., Brenton, Z. W., & Kresovich, S. (2019). Genetic and genomic resources of sorghum to connect genotype with phenotype in contrasting environments. *The Plant Journal*, *97*, 19-39.

8. Brouwer, M., Lievens, B., Van Hemelrijck, W., Van den Ackerveken, G., Cammue, B. P., & Thomma, B. P. (2003). Quantification of disease progression of several microbial pathogens on Arabidopsis thaliana using real-time fluorescence PCR. *FEMS Microbiology Letters*, *228*, 241-248.
9. Caldwell, R. M., Schafer, J. F., Compton, L. E., & Patterson, F. L. (1958). Tolerance to cereal leaf rusts. *Science*, *128*, 714-715.
10. Casa, A. M., Pressoir, G., Brown, P. J., Mitchell, S. E., Rooney, W. L., Tuinstra, M. R., Franks, C. D. & Kresovich, S. (2008). Community resources and strategies for association mapping in sorghum. *Crop Science*, *48*, 30-40.
11. Das, I. K., & Indira, S. (2008). Role of stalk-anatomy and yield parameters in development of charcoal rot caused by *Macrophomina phaseolina* in winter sorghum. *Phytoparasitica*, *36*, 199-208.
12. De, B. K., Chattopadhya, S. B., & Arjunan, G. (1992). Effect of potash on stem rot diseases of jute caused by *Macrophomina phaseolina*. *J Mycopathol Res*, *30*, 51-55.
13. Diourte, M., Starr, J. L., Jeger, M. J., Stack, J. P., & Rosenow, D. T. (1995). Charcoal rot (*Macrophomina phaseolina*) resistance and the effects of water stress on disease development in sorghum. *Plant Pathology*, *44*, 196-202.
14. Dodd, J. L. (1980). The photosynthetic stress translocation balance concept of sorghum stalk rot. In *Proceedings of International Workshop of Sorghum Diseases* (pp. 300-305). Texas A&M University/ICRISAT Press Hyderabad, India.
15. Dutta, K., Talukdar, D., & Bora, S. S. (2022). Segmentation of unhealthy leaves in cruciferous crops for early disease detection using vegetative indices and Otsu thresholding of aerial images. *Measurement*, *189*, 110478.
16. Edmunds, L. K. (1964). Combined relation of plant maturity temperature, texture, and soil moisture to charcoal stalk rot development in grain sorghum. *Phytopathology*, *54*, 514.
17. Edmunds, L. K., Voigt, R. L., & Carasso, F. M. (1964). Use of Arizona climate to induce charcoal rot in grain sorghum. *Plant Disease Reporter*, *48*, 300-302.
18. Edmunds, L. K., Voigt, R. L., & Carasso, F. M. (1965). Charcoal rot induction and development in the field in Arizona. In *Proceedings of the Fourth Biennial Grain Sorghum Re-*

search and Utilization Conference, sponsored by the Grain Sorghum Producers' Association (GSPA) and the Sorghum Improvement Conference of North America, Lubbock, Texas. Available from GSPA, Abernathy, Texas, USA.

19. Fiorani, F., & Schurr, U. (2013). Future scenarios for plant phenotyping. *Annual Review of Plant Biology*, *64*, 267-291.
20. Gomez, F. E., Carvalho, G., Shi, F., Muliana, A. H., & Rooney, W. L. (2018). High throughput phenotyping of morpho-anatomical stem properties using X-ray computed tomography in sorghum. *Plant Methods*, *14*, 1-13.
21. Herskowitz, I. H. (1973). Principles of genetics (pp. 723-729). 2 nd Eds. Macmillan, USA.
22. Hundekar, A. R., & Anahosur, K. H. (1994). Pathogenicity of fungi associated with sorghum stalk rot. *Karnataka Journal of Agricultural Science*, *7*, 291-295.
23. Ilyas, M. B., Ellis, M. A., & Sinclair, J. B. (1976). Effect of soil fungicides on *Macrophomina phaseolina* sclerotium viability in soil and in soybean stem pieces. *Phytopathology*, *66*, 355-359.
57. Islam, M.S.; Haque, M.S.; Islam, M.M.; Emdad, E.M.; Halim, A.; Hossen, Q.M.; Hossain, M.Z.; Ahmed, B.; Rahim, S.; Rahman, M.S.; Alam, M.M.; Hou, S.; Wan, X.; Saito, J.A.; Alam M. (2012). Tools to kill: genome of one of the most destructive plant pathogenic fungi *Macrophomina phaseolina*. *BMC Genomics*, *13*, 1-16.
24. Jardine, D. (2006). Stalk Rots of Corn and Sorghum. USA: Agricultural Research Station and Cooperative Extension Service, Kansas State University.
25. Li, S., Hartman, G. L., Domier, L. L., & Boykin, D. (2008). Quantification of *Fusarium solani* f. sp. *glycines* isolates in soybean roots by colony-forming unit assays and real-time quantitative PCR. *Theoretical and Applied Genetics*, *117*, 343-352.
26. Mahmoud, A. F., Abou-Elwafa, S. F., & Shehzad, T. (2018). Identification of charcoal rot resistance QTLs in sorghum using association and in silico analyses. *Journal of Applied Genetics*, *59*, 243-251.
27. Marzougui, A., Ma, Y., Zhang, C., McGee, R. J., Coyne, C. J., Main, D., & Sankaran, S. (2019). Advanced imaging for quantitative evaluation of Aphanomyces root rot resistance in lentil. *Frontiers in Plant Science*, *10*, 383.

28. Mayek-Pérez, N., López-Castañeda, C., López-Salinas, E., Cumpián-Gutiérrez, J., & Acosta-Gallegos, J. A. (2001). *Macrophomina phaseolina* resistance in common bean under field conditions in Mexico. *Agrociencia*, *35*, 649-661.
29. Mohanty, S. P., Hughes, D. P., & Salathé, M. (2016). Using deep learning for image-based plant disease detection. *Frontiers in Plant Science*, *7*, 1419.
30. Nagasubramanian, K., Jones, S., Singh, A. K., Sarkar, S., Singh, A., & Ganapathysubramanian, B. (2019). Plant disease identification using explainable 3D deep learning on hyperspectral images. *Plant Methods*, *15*, 1-10.
31. Orlando, C., Pinzani, P., & Pazzagli, M. (1998). Developments in quantitative PCR. *Clinical Chemistry and Laboratory Medicine*, *36*, 255-269.
32. Panguluri, S. K., & Kumar, A. A. (2016). *Phenotyping for Plant Breeding*. Springer-Verlag, New York.
33. Paterson, A. H., Bowers, J. E., Bruggmann, R., Dubchak, I., Grimwood, J., Gundlach, H., Haberer, G., Hellsten, U., Mitros, T., Poliakv, A. (2009). The *Sorghum bicolor* genome and the diversification of grasses. *Nature*, *457*, 551-556.
34. Pecina-Quintero, V., Williams-Alanís, H., & Vandemark, G. J. (1999). Diallel analysis of resistance to Macrophomina phaseolina in sorghum. *Cereal Research Communications*, *27*, 99-106.
35. Perumal, R., Tesso, T. T., Morris, G. P., Jagadish, S. K., Little, C. R., Bean, S. R., Yu, J., Vara Prasad, P. V., & Tuinstra, M. R. (2021). Registration of the sorghum nested association mapping (NAM) population in RTx430 background. *Journal of Plant Registrations*, *15*, 395-402.
36. Price, J. S., Bever, J. D., & Clay, K. (2004). Genotype, environment, and genotype by environment interactions determine quantitative resistance to leaf rust (*Coleosporium asterum*) in *Euthamia graminifolia* (Asteraceae). *New Phytologist*, *162*, 729-743.
37. Raguchander, T., Samiappan, R., & Arjunan, G. J. I. P. (1993). Biocontrol of *Macrophomina* root rot of mungbean. *Indian Phytopathology*, *46*(4), 379-382.
38. Reed, J. E., Partridge, J. E., and Nordquist, P. T. (1983). Fungal colonizations of stalks and roots of grain sorghum during the growing season. *Plant Disease*, *67*, 417-420.

39. Santos, K. M., Lima, G. S., Barros, A. P., Machado, A. R., Souza-Motta, C. M., Correia, K. C., & Michereff, S. J. (2020). Novel specific primers for rapid identification of *Macrophomina* species. *European Journal of Plant Pathology*, *156*, 1213-1218.
40. Sarkar, T. S., Biswas, P., Ghosh, S. K., & Ghosh, S. (2014). Nitric oxide production by necrotrophic pathogen *Macrophomina phaseolina* and the host plant in charcoal rot disease of jute: Complexity of the interplay between necrotroph-host plant interactions. *PLoS One*, *9*, e107348.
41. Shruthi, U., Nagaveni, V., & Raghavendra, B. K. (2019). A review on machine learning classification techniques for plant disease detection. In *2019 5th International conference on advanced computing & communication systems (ICACCS)* (pp. 281-284). IEEE.
42. Su, G., Suh, S. O., Schneider, R. W., Russin, J. S. (2001) Host specialization in the charcoal rot fungus, *Macrophomina phaseolina*. *Phytopathology*, *91*: 120–126.
43. Sudhakar Reddy, P., Srinivas Reddy, D., Sivasakthi, K., Bhatnagar-Mathur, P., Vadez, V., & Sharma, K. K. (2016). Evaluation of sorghum [*Sorghum bicolor* (L.)] reference genes in various tissues and under abiotic stress conditions for quantitative real-time PCR data normalization. *Frontiers in Plant Science*, *7*, 529.
44. Tesso, T. T., Claflin, L. E., & Tuinstra, M. R. (2005). Analysis of stalk rot resistance and genetic diversity among drought tolerant sorghum genotypes. *Crop Science*, *45*, 645-652.
45. Tesso, T. T., Perumal, R., Little, C. R., Adeyanju, A., Radwan, G. L., Prom, L. K., & Magill, C. W. (2012). Sorghum pathology and biotechnology-a fungal disease perspective: Part II. Anthracnose, stalk rot, and downy mildew. *European Journal of Plant Science and Biotechnology*, *6*, 31-44.
46. Tesso, T., Claflin, L. E., & Tuinstra, M. R. (2004). Estimation of combining ability for resistance to Fusarium stalk rot in grain sorghum. *Crop Science*, *44*, 1195-1199.
47. Tesso, T., Ochanda, N., Claflin, L., & Tuinstra, M. (2009). An improved method for screening Fusarium stalk rot resistance in grain sorghum (*Sorghum bicolor* [L.] Moench.). *African Journal of Plant Science*, *3*, 254-262.
48. Wang, Q., Tang, J., Han, B., & Huang, X. (2020). Advances in genome-wide association studies of complex traits in rice. *Theoretical and Applied Genetics*, *133*, 1415-1425.
49. Watanabe, K., Guo, W., Arai, K., Takanashi, H., Kajiya-Kanegae, H., Kobayashi, M., Yano, K., Tokunaga, T., Fujiwara, T., Tsutsumi, N., & Iwata, H. (2017). High-throughput

phenotyping of sorghum plant height using an unmanned aerial vehicle and its application to genomic prediction modeling. *Frontiers in Plant Science*, *8*, 421.

50. Wyllie, T. D. (1998). Charcoal rot. In Sinclair, J. B., & Backman, P. A. (Eds.), *Compendium of soybean diseases* (pp. 114-118), 3rd eds. APS Press, St. Paul, MN.
51. Wyllie, T. D. (1998). Soybean Diseases of the North Central Region. In Wyllie, T. D., & Scott, D. H. (Eds.), *Charcoal rot of soybean-current status*, (pp. 106-113). APS, St. Paul, MN.
52. Xie, W., Yu, K., Pauls, K. P., & Navabi, A. (2012). Application of image analysis in studies of quantitative disease resistance, exemplified using common bacterial blight–common bean pathosystem. *Phytopathology*, *102*, 434-442.
53. Xin, Z., Wang, M., Cuevas, H. E., Chen, J., Harrison, M., Pugh, N., & Morris, G. (2021). Sorghum genetic, genomic, and breeding resources. *Planta*, *254*, 1-24.
54. Yu, J., Holland, J. B., McMullen, M. D., & Buckler, E. S. (2008). Genetic design and statistical power of nested association mapping in maize. *Genetics*, *178*, 539-551.

TABLES AND FIGURES

Table 4.1. Description of the NAM parental lines and other checks used for the charcoal rot phenotyping.

Sorghum lines	Origin	Type
RTx430	Texas A&M	Pollinator parent
SC283	Tanzania	Converted landrace
SC1103	Nigeria	Converted landrace
Segaolane	Botswana	Selected landrace
Macia	ICRISAT	Global variety
SC35	Ethiopia	Converted landrace
Ajabsido	Sudan	Selected landrace
SC971	Puerto Rico	Converted landrace
SC265	Burkina Faso	Converted landrace
SC1345	Mali	Converted landrace
P898012	Purdue	Public line
BTx623	Texas	Reference genome
Tx7000	USA	R-line
SC599	USA	Resistant check

Table 4.2. The *P* values (statistical significance) of F-tests from the ANOVA table of 14 genotypes with different trait parameters after inoculation and mock-inoculated control from the Ashland Bottoms 2019 data.

Source	df	FD	PH	TLL	RLL	MLL	NC	TSW	HSW	TSC
Genotypes	13	<0.0001	<0.0001	<0.0001	<0.0001	0.0002	<0.0001	<0.0001	0.2026	<0.0001
Treatment	1	0.671	0.3411	<0.0001	<0.0001	0.0005	<0.0001	0.2829	0.2511	0.2123
Genotypes×Treatment	13	<0.0001	0.0009	0.002	0.0288	0.2612	0.0074	0.0203	0.4085	0.0046

[¥]FD = days to flower; PH = plant height (cm); TLL = total lesion length (cm), RLL = relative lesion length; MLL = major lesion length (cm); NC = nodes crossed by the lesion; TSW = total seed weight per panicle (g); HSW = hundred seed weight (g); TSC = total seed count per panicle.

Table 4.3. The *P* values (statistical significance) of F-tests from the ANOVA table of 14 genotypes with different trait parameters after inoculation and mock-inoculated control from the North Farms 2019 data.

Source	df	FD	PH	TLL	RLL	MLL	NC	TSW	HSW	TSC
Genotypes	13	<0.0001	<0.0001	<0.0001	<0.0001	0.0010	<0.0001	<0.0001	<0.0001	<0.0001
Treatment	1	0.2533	0.6065	<0.0001	<0.0001	<0.0001	<0.0001	0.9967	0.0054	0.4015
Genotypes×Treatment	13	<0.0001	0.1550	0.0089	0.0004	0.3292	<0.0001	0.0593	<0.0001	0.1100

[¥]FD = days to flower; PH = plant height (cm); TLL = total lesion length (cm), RLL = relative lesion length; MLL = major lesion length (cm); NC = nodes crossed by the lesion; TSW = total seed weight per panicle (g); HSW = hundred seed weight (g); TSC = total seed count per panicle.

Table 4.4. The *P* values (statistical significance) of F-tests from the ANOVA table of 14 genotypes with different trait parameters after inoculation and mock-inoculated control from the Ashland Bottoms 2021 data.

Source	df	FD	PH	TLL	RLL	MLL	NC	TSW	HSW	TSC
Genotypes	13	<0.0001	<0.0001	<0.0001	<0.0001	<0.0001	0.0158	<0.0001	<.0001	<.0001
Treatment	1	0.0397	0.0801	<0.0001	<0.0001	<0.0001	<0.0001	0.0483	0.0188	0.3401
Genotyps×Treatment	13	<0.0001	<0.0001	<0.0001	<0.0001	0.0004	0.0018	0.0955	0.0076	0.3758

[¥]FD = days to flower; PH = plant height (cm); TLL = total lesion length (cm), RLL = relative lesion length; MLL = major lesion length (cm); NC = nodes crossed by the lesion; TSW = total seed weight per panicle (g); HSW = hundred seed weight (g); TSC = total seed count per panicle.

Table 4.5. The *P* values (statistical significance) of F-tests from the ANOVA table of 14 genotypes with different trait parameters after inoculation and mock-inoculated control from the North Farm location in 2021.

Source	df	FD	PH	TLL	RLL	MLL	NC	TSW	HSW	TSC
Genotypes	13	<0.0001	<0.0001	<0.0001	<0.0001	<0.0001	<0.0001	<0.0001	0.3635	<0.0001
Treatment	1	0.0537	0.8758	<0.0001	<0.0001	<0.0001	<0.0001	0.1117	0.268	0.7417
Genotyps×Treatment	13	0.0001	0.2041	<0.0001	<0.0001	<0.0001	0.0045	0.0069	0.3624	0.0639

[¥]FD = days to flower; PH = plant height (cm); TLL = total lesion length (cm), RLL = relative lesion length; MLL = major lesion length (cm); NC = nodes crossed by the lesion; TSW = total seed weight per panicle (g); HSW = hundred seed weight (g); TSC = total seed count per panicle.

Table 4.6. Mixed model analysis of variance (ANOVA) for the traits measured from the Ashland Bottoms location in 2019.

Trait[a]	Source	df	Mean square	F value	Pr>F	
TLL	Rep	3	401.128	0.94	0.79	
	Genotypes (A)	13	6862.544	16.12	<0.0001	***
	Treatments (B)	1	8783.417	20.63	<0.0001	***
	Genotypes × Treatments	13	1092.470	2.57	0.002	**
	Error	452	425.748	-	-	
RLL	Rep	3	0.014	0.69	0.5609	
	Genotypes (A)	13	0.181	8.84	<0.0001	***
	Treatments (B)	1	0.486	23.68	<0.0001	***
	Genotypes × Treatments	13	0.039	1.89	0.0288	*
	Error	452	0.021	-	-	
MLL	Rep	3	211.800	4	0.0079	**
	Genotypes (A)	13	166.361	3.14	0.0002	**
	Treatments (B)	1	652.980	12.33	0.0005	**
	Genotypes × Treatments	13	64.626	1.22	0.2612	
	Error	452	52.960	-	-	
NC	Rep	3	9.866	1.41	0.2386	
	Genotypes (A)	13	57.116	8.17	<0.0001	***
	Treatments (B)	1	156.146	22.35	<0.0001	***
	Genotypes × Treatments	13	15.697	2.25	0.0074	**
	Error	451	6.988	-	-	
TSW	Rep	3	65.593	0.23	0.8725	
	Genotypes (A)	13	3083.654	11.01	<0.0001	***
	Treatments (B)	1	323.496	1.16	0.2829	
	Genotypes × Treatments	13	555.333	1.98	0.0203	*
	Error	522	280.012	-	-	

[a]TLL, total lesion length; RLL, relative lesion length; MLL, major lesion length; NC, nodes crossed by the lesion; TSW, total seed weight (g). *, **, *** Indicate significance at the $P < 0.05$, $P < 0.01$, and $P < 0.001$ levels, respectively.

Table 4.7. Mixed model analysis of variance (ANOVA) for the traits measured from the Ashland Bottoms location in 2021.

Trait[a]	Source	df	Mean square	F value	Pr>F	
TLL	Rep	3	502.427	2.63	0.0492	*
	Genotypes (A)	13	1935.185	10.14	<0.0001	***
	Treatments (B)	1	10626	55.7	<0.0001	***
	Genotypes × Treatments	13	683.121	3.58	<0.0001	***
	Error	524	190.766	-	-	
RLL	Rep	3	0.071	3.94	0.0084	**
	Genotypes (A)	13	0.147	8.24	<0.0001	***
	Treatments (B)	1	1.029	57.52	<0.0001	***
	Genotypes × Treatments	13	0.006	3.59	<0.0001	***
	Error	524	0.018	-	-	
MLL	Rep	3	184.570	2.17	0.0905	
	Genotypes (A)	13	605.198	7.12	<0.0001	***
	Treatments (B)	1	2014.912	23.7	<0.0001	***
	Genotypes × Treatments	13	248.884	2.93	0.0004	**
	Error	524	85.024	-	-	
NC	Rep	3	4.308	0.53	0.6623	
	Genotypes (A)	13	16.660	2.05	0.0158	*
	Treatments (B)	1	216.697	26.63	<0.0001	***
	Genotypes × Treatments	13	21.010	2.58	0.0018	**
	Error	524	8.138	-	-	
TSW	Rep	3	2129.930	8.54	<0.0001	***
	Genotypes (A)	13	4984.643	19.97	<0.0001	***
	Treatments (B)	1	977.827	3.92	0.0483	*
	Genotypes × Treatments	13	386.971	1.55	0.0955	
	Error	524	249.544	-	-	

[a] TLL, total lesion length; RLL, relative lesion length; MLL, major lesion length; NC, nodes crossed by the lesion; TSW, total seed weight (g). *, **, *** Indicate significance at the $P < 0.05$, $P < 0.01$, and $P < 0.0001$ levels, respectively.

Table 4.8. Mixed model analysis of variance (ANOVA) for the traits measured from the North Farm location in 2019.

Trait[a]	Source	df	Mean square	F value	Pr>F	
TLL	Rep	3	9427.698	16.63	<0.0001	***
	Genotypes (A)	13	21051	37.13	<0.0001	***
	Treatments (B)	1	62717	110.62	<0.0001	***
	Genotypes × Treatments	13	1246.497	2.2	0.0089	**
	Error	452	566.984	-	-	
RLL	Rep	3	0.467	16.66	<0.0001	***
	Genotypes (A)	13	0.735	26.22	<0.0001	***
	Treatments (B)	1	3.364	120.06	<0.0001	***
	Genotypes × Treatments	13	0.083	2.96	0.0004	**
	Error	452	0.028	-	-	
MLL	Rep	3	3.725	0.09	0.9631	
	Genotypes (A)	13	107.334	2.72	<0.0001	***
	Treatments (B)	1	1140.438	28.93	<0.0001	***
	Genotypes × Treatments	13	44.628	1.13	0.3292	
	Error	453	39.423	-	-	
NC	Rep	3	135.556	22.61	<0.0001	***
	Genotypes (A)	13	125.826	20.99	<0.0001	***
	Treatments (B)	1	785.917	131.1	<0.0001	***
	Genotypes × Treatments	13	25.016	4.17	<0.0001	***
	Error	517	5.995	-	-	
TSW	Rep	3	1017.182	5.07	0.0018	**
	Genotypes (A)	13	12502.128	62.36	<0.0001	***
	Treatments (B)	1	0.004	0	0.9967	
	Genotypes × Treatments	13	338.974	1.69	0.0593	
	Error	547	200.496	-	-	

[a] TLL, total lesion length; RLL, relative lesion length; MLL, major lesion length; NC, nodes crossed by the lesion; TSW, total seed weight (g). *, **, *** Indicate significance at the $P < 0.05$, $P < 0.01$, and $P < 0.0001$ levels, respectively.

Table 4.9. Mixed model analysis of variance (ANOVA) for the traits measured from the North Farm location in 2021

Trait[a]	Source	df	Mean square	F value	Pr>F	
TLL	Rep	3	30.669	0.27	0.8482	
	Genotypes (A)	13	1235.420	10.81	<0.0001	***
	Treatments (B)	1	12413	108.62	<0.0001	***
	Genotypes × Treatments	13	865.021	7.57	<0.0001	***
	Error	528	114.286	-	-	
RLL	Rep	3	0.010	0.41	0.7455	
	Genotypes (A)	13	0.254	10.94	<0.0001	***
	Treatments (B)	1	2.529	109.16	<0.0001	***
	Genotypes × Treatments	13	0.175	7.55	<0.0001	***
	Error	528	0.023	-	-	
MLL	Rep	3	42.480	0.69	0.56	
	Genotypes (A)	13	754.497	12.21	<0.0001	***
	Treatments (B)	1	5019.203	81.23	<0.0001	***
	Genotypes × Treatments	13	470.717	7.62	<0.0001	***
	Error	528	61.793	-	-	
NC	Rep	3	22.139	1.52	0.2088	
	Genotypes (A)	13	62.342	4.27	<0.0001	***
	Treatments (B)	1	704.651	48.32	<0.0001	***
	Genotypes × Treatments	13	34.420	2.36	0.0045	**
	Error	528	14.584	-	-	
TSW	Rep	3	3923.968	10.91	<0.0001	***
	Genotypes (A)	13	4246.017	11.8	<0.0001	***
	Treatments (B)	1	913.363	2.54	0.1117	
	Genotypes × Treatments	13	811.351	2.25	0.0069	**
	Error	528	359.818	-	-	

[a]TLL, total lesion length; RLL, relative lesion length; MLL, major lesion length; NC, nodes crossed by the lesion; TSW, total seed weight (g). *, **, *** Indicate significance at the $P < 0.05$, $P < 0.01$, and $P < 0.0001$ levels, respectively.

Table 4.10. Relative DNA quantities of *M. phasolina* and sorghum plants from the inoculated and mock-inoculated stalk tissue of sorghum obtained by real-time q-PCR assay.

Treatments	$C_{qTef1\text{-}\alpha}$[a]	C_{qPP2A}[b]	ΔC_q[c]
Macia Inoculated	33.79	24.37	8.69 ab[x]
Macia Mock Control	34.33	22.91	10.83 ab
Ajabsido Inoculated	34.52	23.12	8.86 ab
Ajabsido Mock Control	35.82	22.52	12.93 a
SC971 Inoculated	35.93	22.84	13.11 a
SC971 Mock Control	35.69	22.42	14.24 a
SC265 Inoculated	31.21	23.85	11.22 ab
SC265 Mock Control	36.79	23.57	12.79 a
P898012 Inoculated	31.54	21.89	9.14 ab
P898012 Mock Control	38.87	22.39	-3.25 b
RTx430 Inoculated	35.54	22.21	12.49 a
RTx430 Mock Control	38.51	22.74	15.64 a
SC1103 Inoculated	-	22.51	-21.69 c
SC1103 Mock Control	-	22.74	-22.74 c
Segaolane Inoculated	31.01	22.69	6.7 ab
Segaolane Mock Control	38.31	22.41	15.9 a

[a]The threshold cycle ($C_{qTef1\text{-}\alpha}$) of the stalk tissue DNA using the *M. phaseolina* specific primer *TEF1-α* from the real-time q-PCR amplification. The Cq value is the mean of two biological replicates and two technical replicates; [b] The threshold cycle (C_{qPP2A}) of the stalk tissue DNA using the sorghum specific primer *PP2A* from the real-time q-PCR amplification. The Cq value is the mean of two biological replicates and two technical replicates; [c]Delta C_q value (ΔC_q = $CqTef_{1\text{-}\alpha}$ - C_{qPP2A}) represents the relative quantities of fungal and plant DNA in a sample; [x]Treatments means followed by the same letter are not statistically significant based on the Fisher's protected LSD ($P \leq 0.05$).

Table 4.11. Absolute DNA quantities of *M. phasolina* and sorghum plants from the inoculated and mock-inoculated treatments obtained from the real-time q-PCR assays using the stalk tissue of sorghum and standard curve of MP and sorghum.

Genotyeps	Treatments	[a]Absolute DNA Conc.^{MP}	[b]Absolute DNA Conc.^{Plant}
Macia	Inoculated	-1.23 ab	1.76 cd
Macia	Mock control	-1.75 ab	1.96 bcd
Ajabsido	Inoculated	-1.41 ab	2.18 abc
Ajabsido	Mock control	-2.66 ab	2.39 ab
SC971	Inoculated	-2.47 ab	2.2 abc
SC971	Mock control	-2.59 ab	2.5 a
SC265	Inoculated	-2.5 ab	0.88 f
SC265	Mock control	-3.11 ab	0.81 f
P898012	Inoculated	-1.67 ab	2.43 ab
P898012	Mock control	-3.17 ab	2.2 abc
RTx430	Inoculated	-1.96 ab	1.47 de
RTx430	Mock control	-3.18 b	1.2 ef
SC1103	Inoculated	-	1.95 bcd
SC1103	Mock control	-	1.87 cd
Segaolane	Inoculated	-0.42 a	2.12 abc
Segaolane	Mock control	-3.07 ab	2.23 abc

[a]Absolute DNA quantifies from the inoculated and mock control stalk tissue of sorghum using the MP specific primer *TEF1-α*;

[b]Absolute DNA quantifies from the inoculated and mock control stalk tissue of sorghum using the sorghum specific primer *PP2A*.

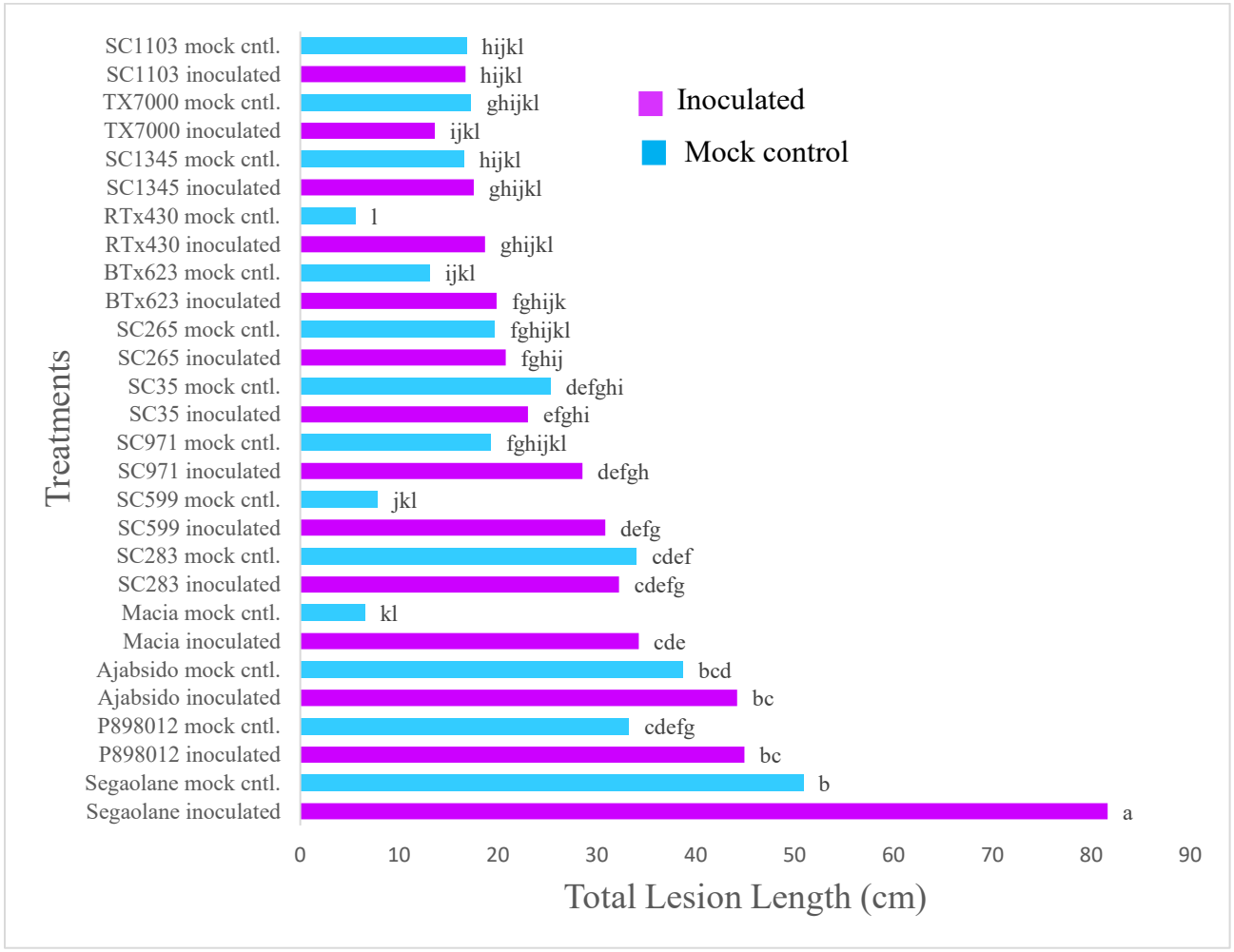

Figure 4.1. Bar plot showing the total lesion length (TLL) measured for all genotypes for both the inoculated and mock-inoculated treatments from the Ashland Bottoms 2019 data.

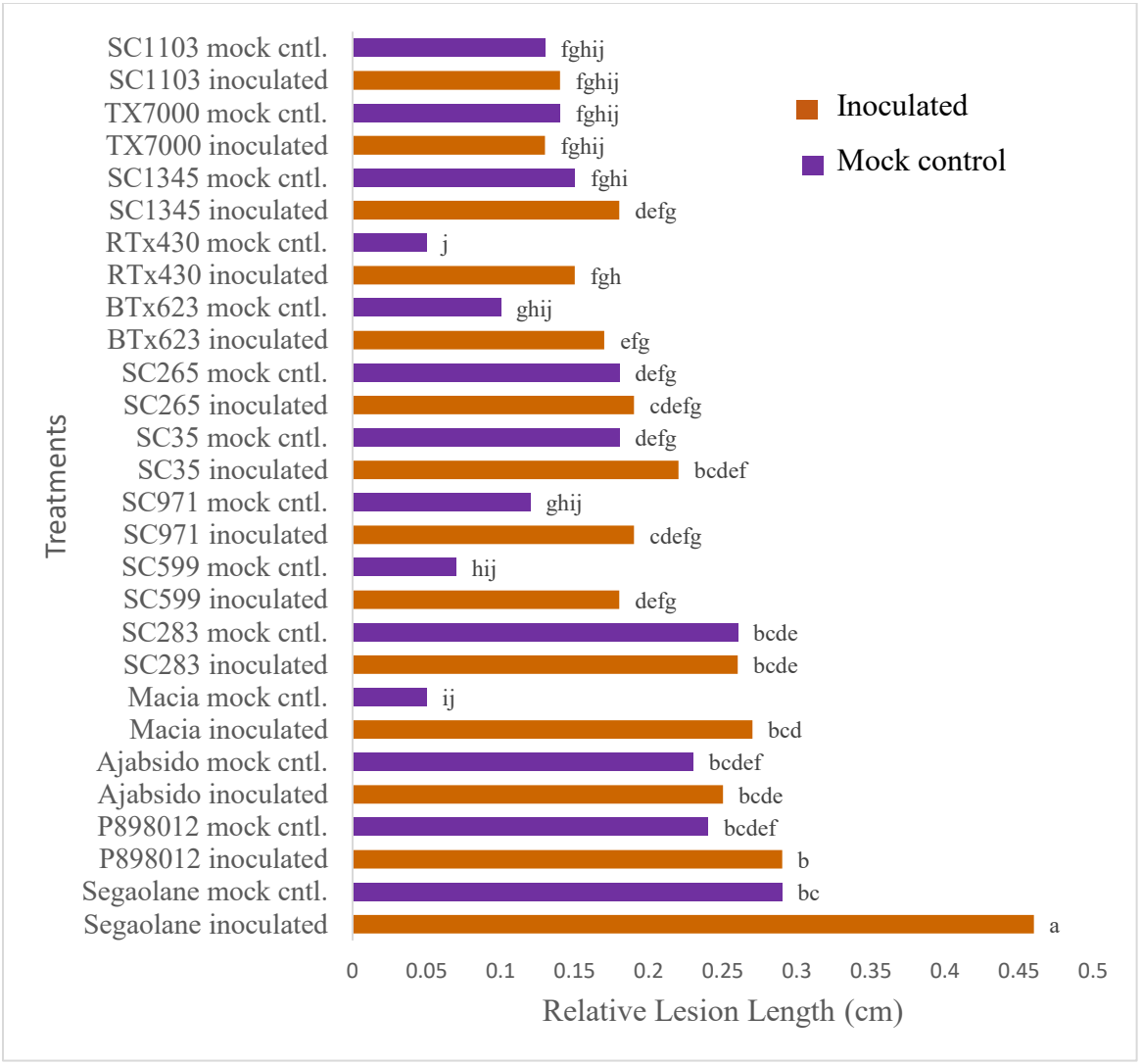

Figure 4.2. Bar plot showing the relative lesion length (RLL) measured for all genotypes for both the inoculated and mock-inoculated treatments from the Ashland Bottoms 2019 data.

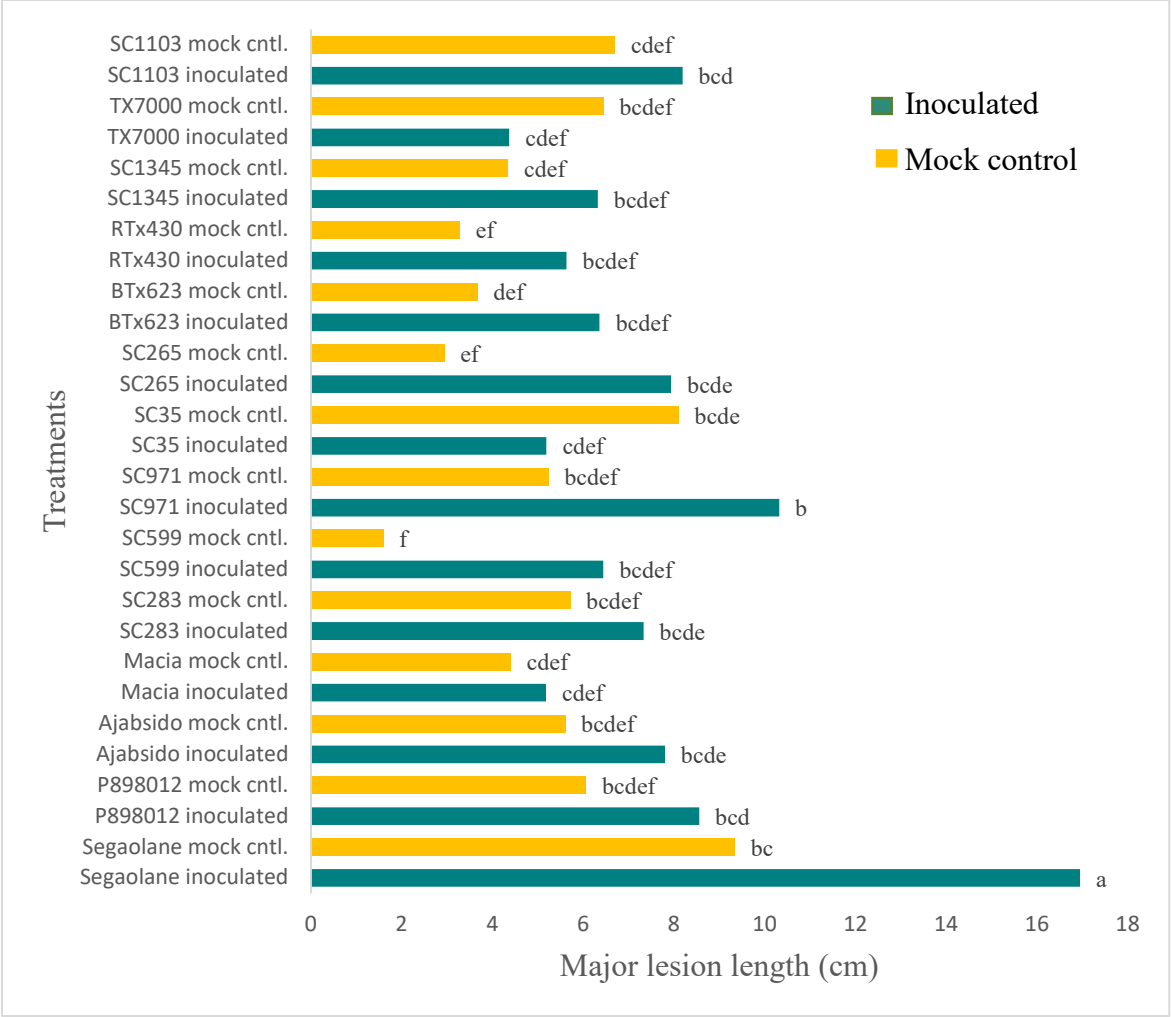

Figure 4.3. Bar plot showing the major lesion length (MLL) measured for all genotypes for both the inoculated and mock-inoculated treatments from the Ashland Bottoms 2019 data.

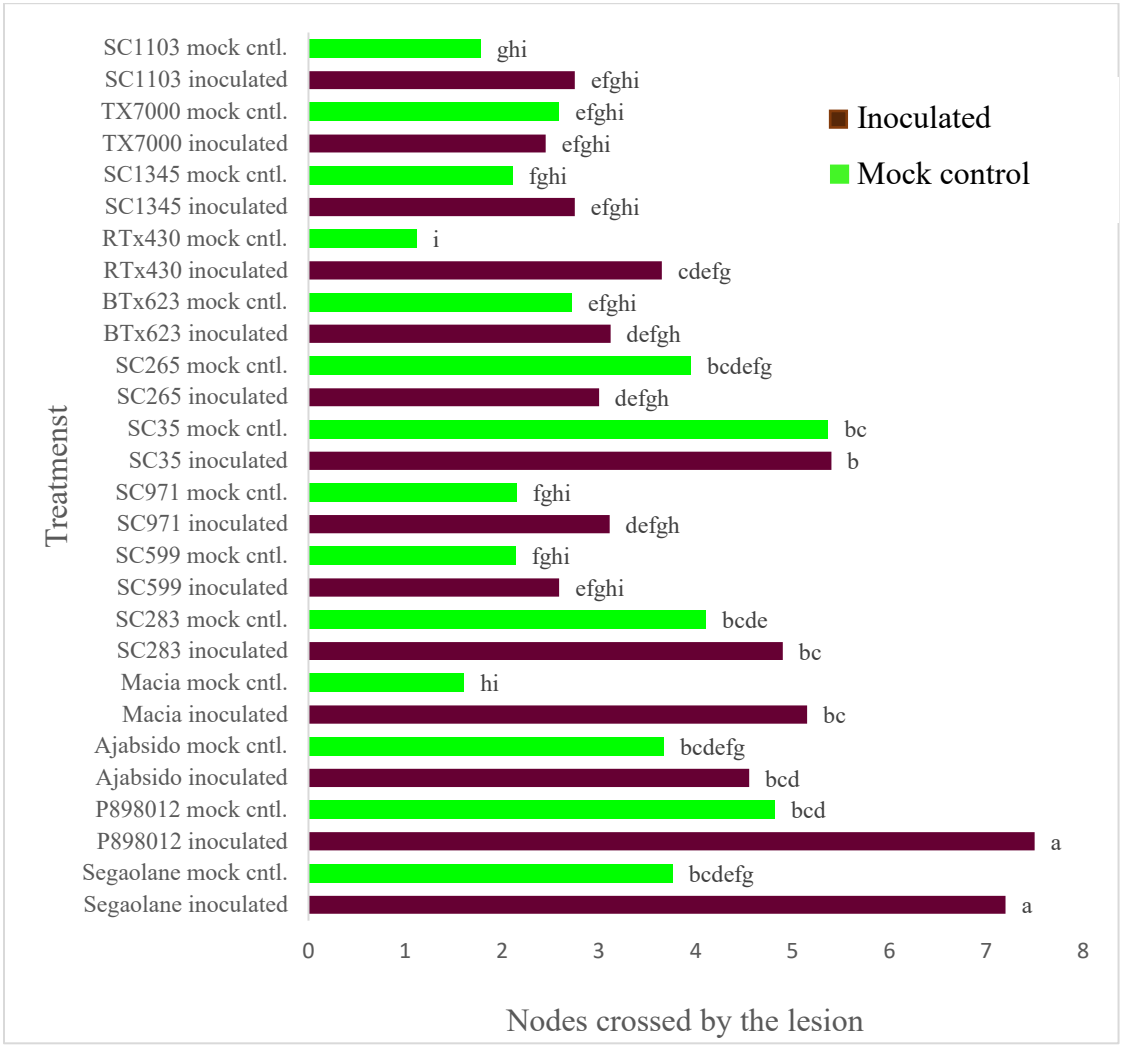

Figure 4.4. Bar plot showing the nodes crossed by the lesion (NC) measured for all genotypes for both the inoculated and mock-inoculated treatments from the Ashland Bottoms 2019 data.

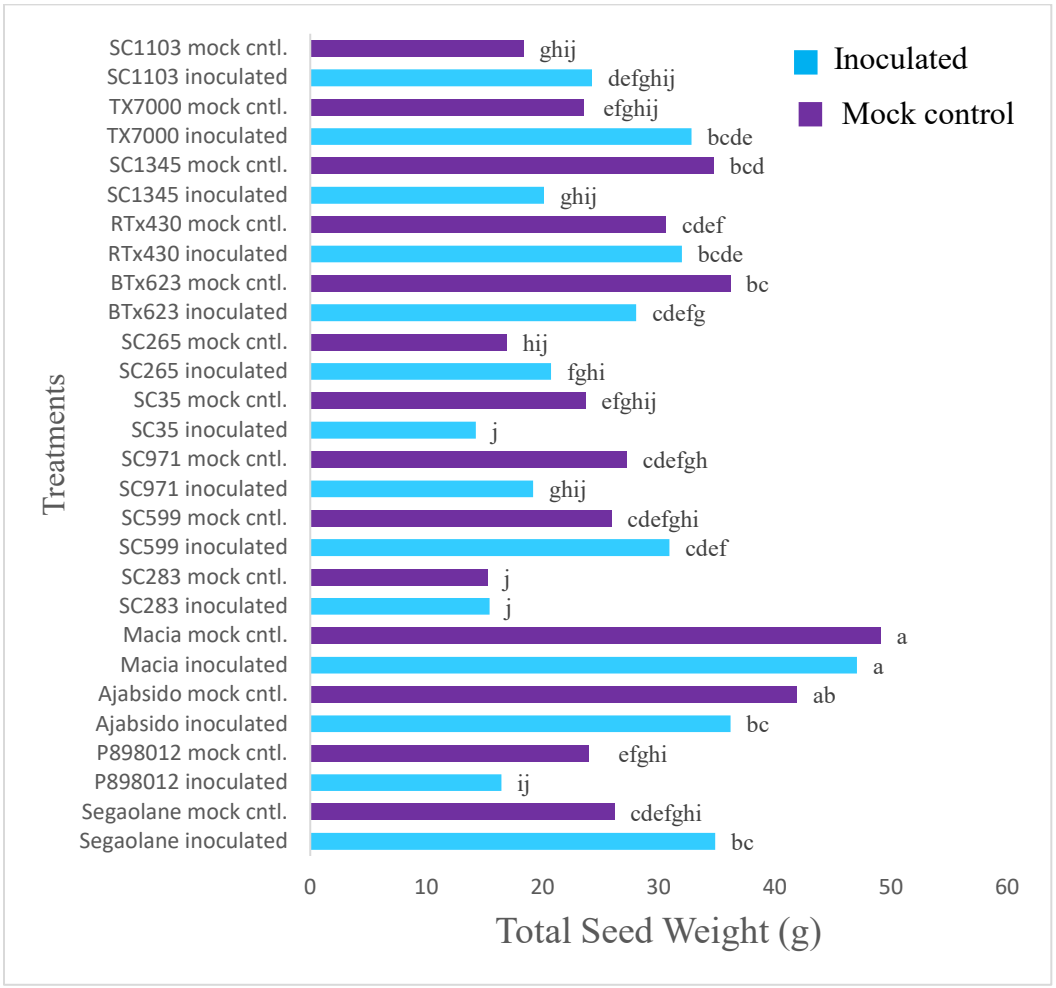

Figure 4.5. Bar plot showing the total seed weight (TSW) measured for all genotypes for both the inoculated and mock-inoculated treatments from the Ashland Bottoms 2019 data.

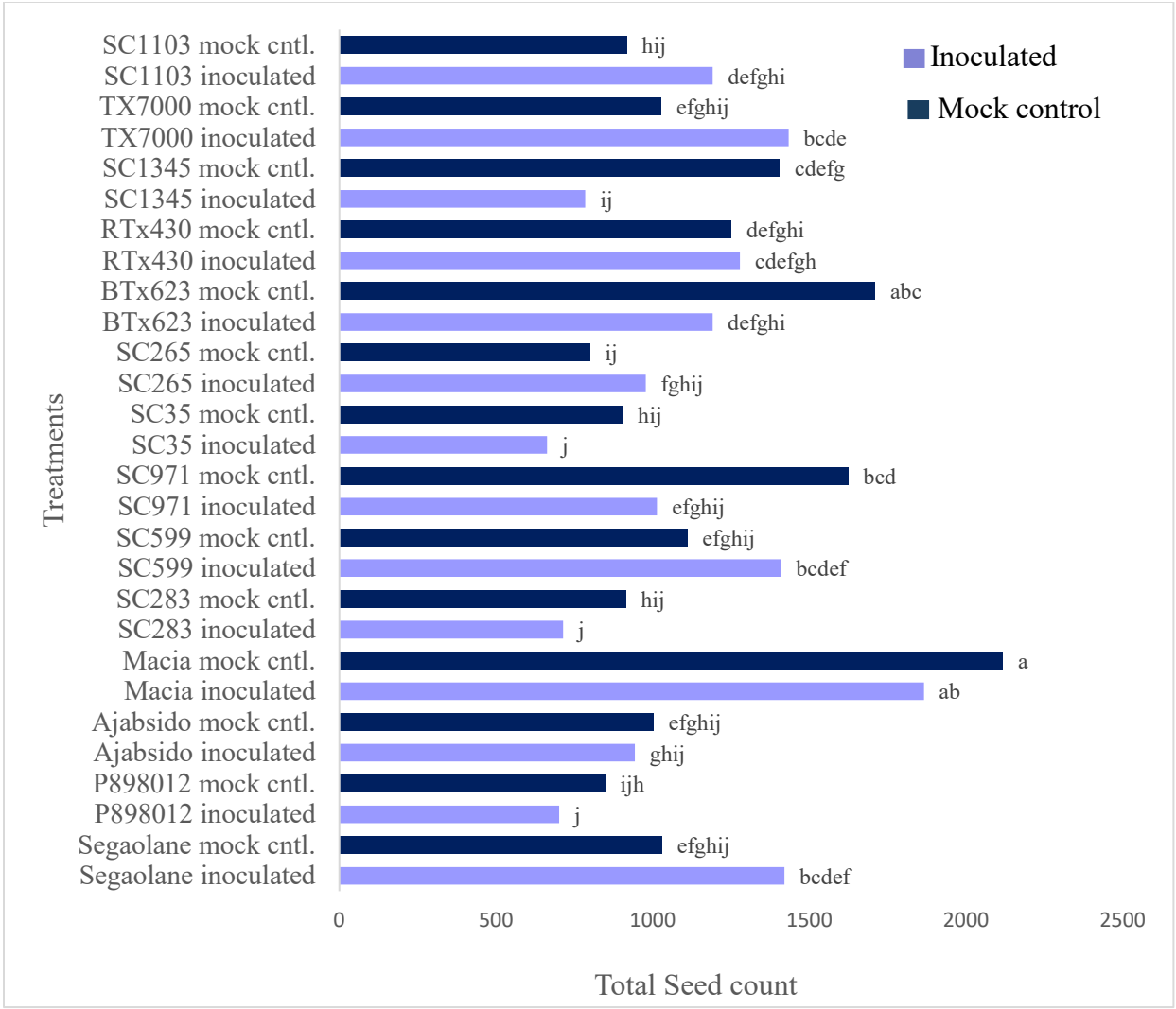

Figure 4.6. Bar plot showing the total seed count (TSC) measured for all genotypes for both the inoculated and mock-inoculated treatments from the Ashland Bottoms 2019 data.

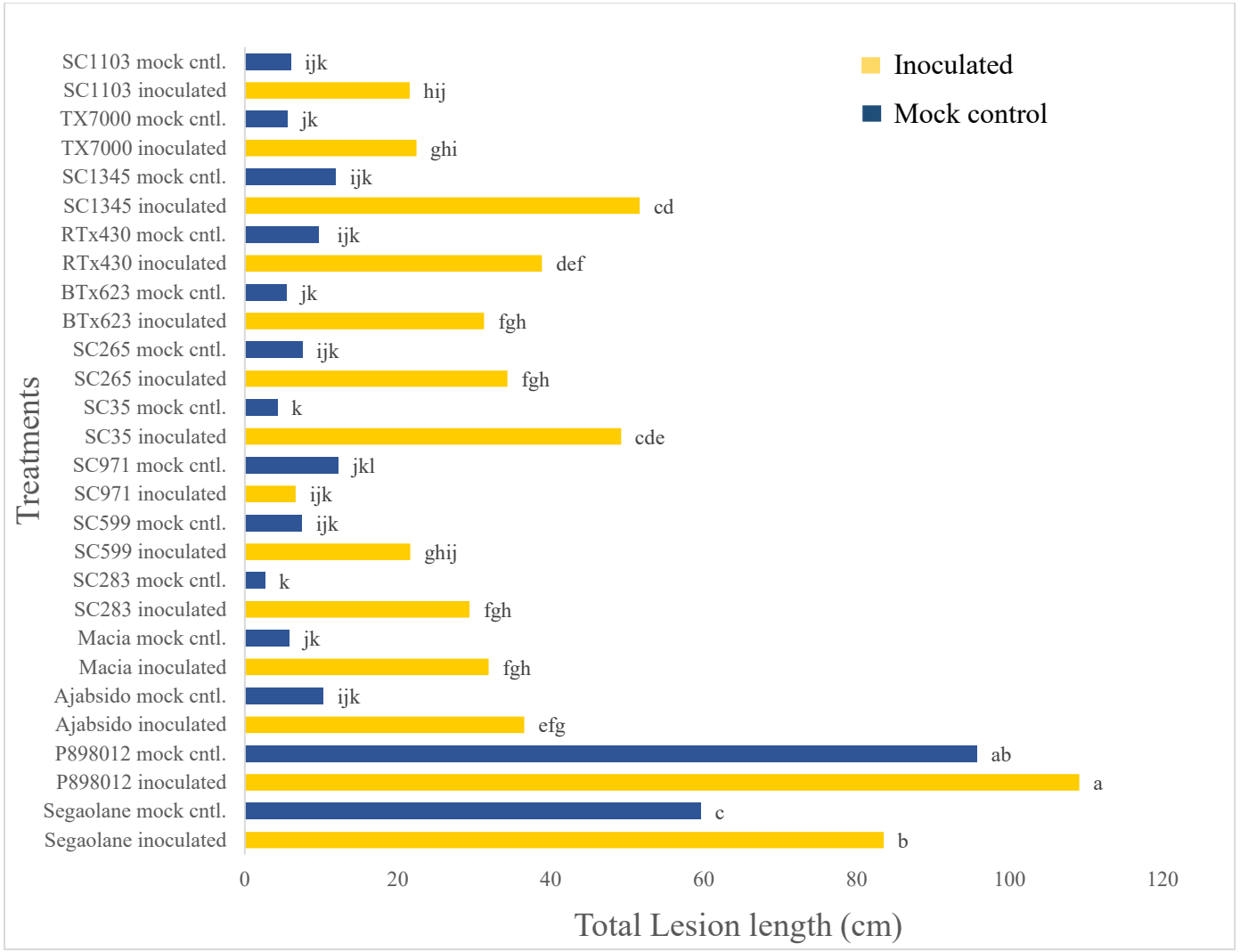

Figure 4.7. Bar plot showing the total lesion length (TLL) measured for all genotypes for both the inoculated and mock-inoculated treatments from the North Farm 2019 data.

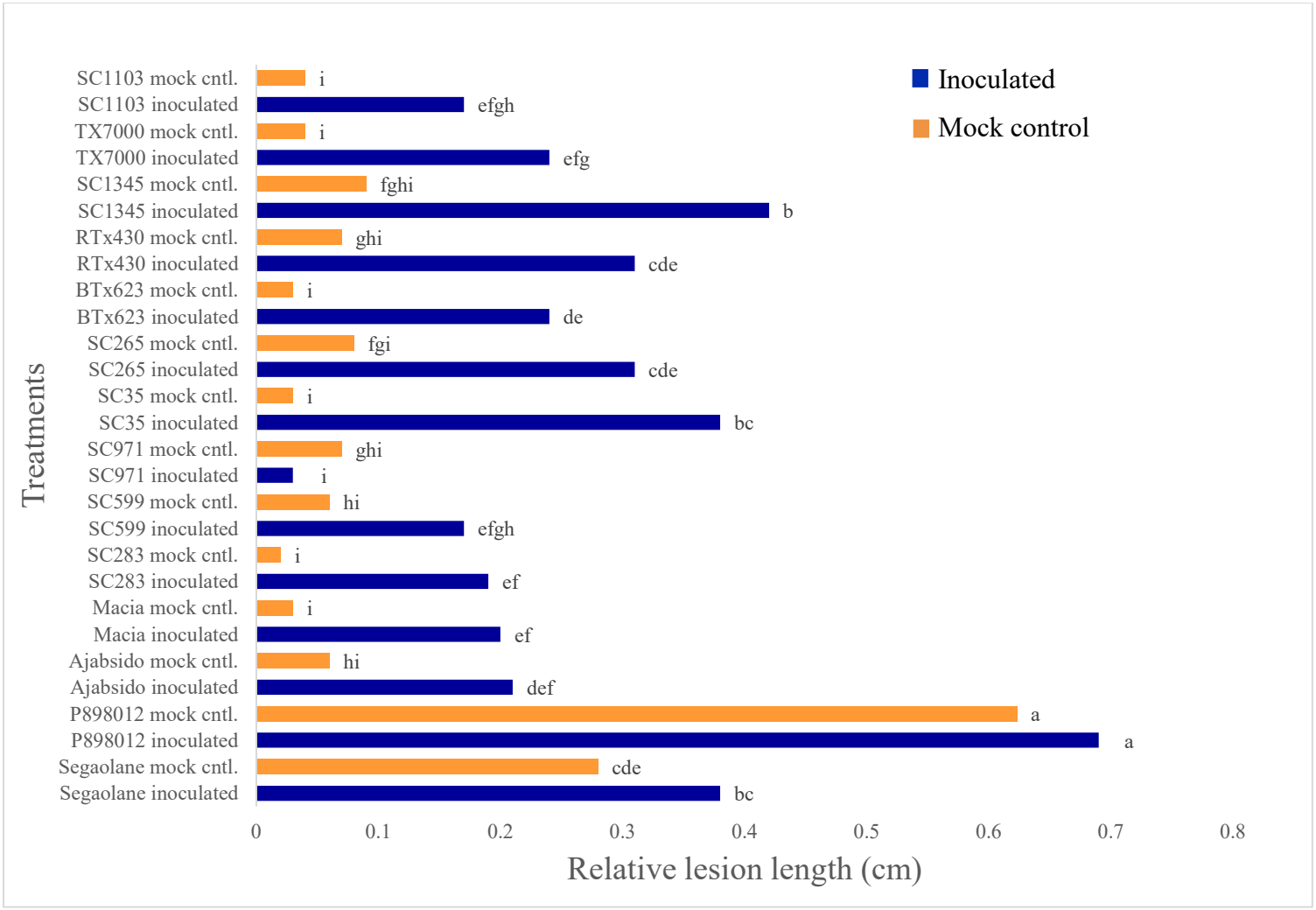

Figure 4.8. Bar plot showing the relative lesion length (RLL) measured for all genotypes for both the inoculated and mock-inoculated treatments from the North Farm 2019 data.

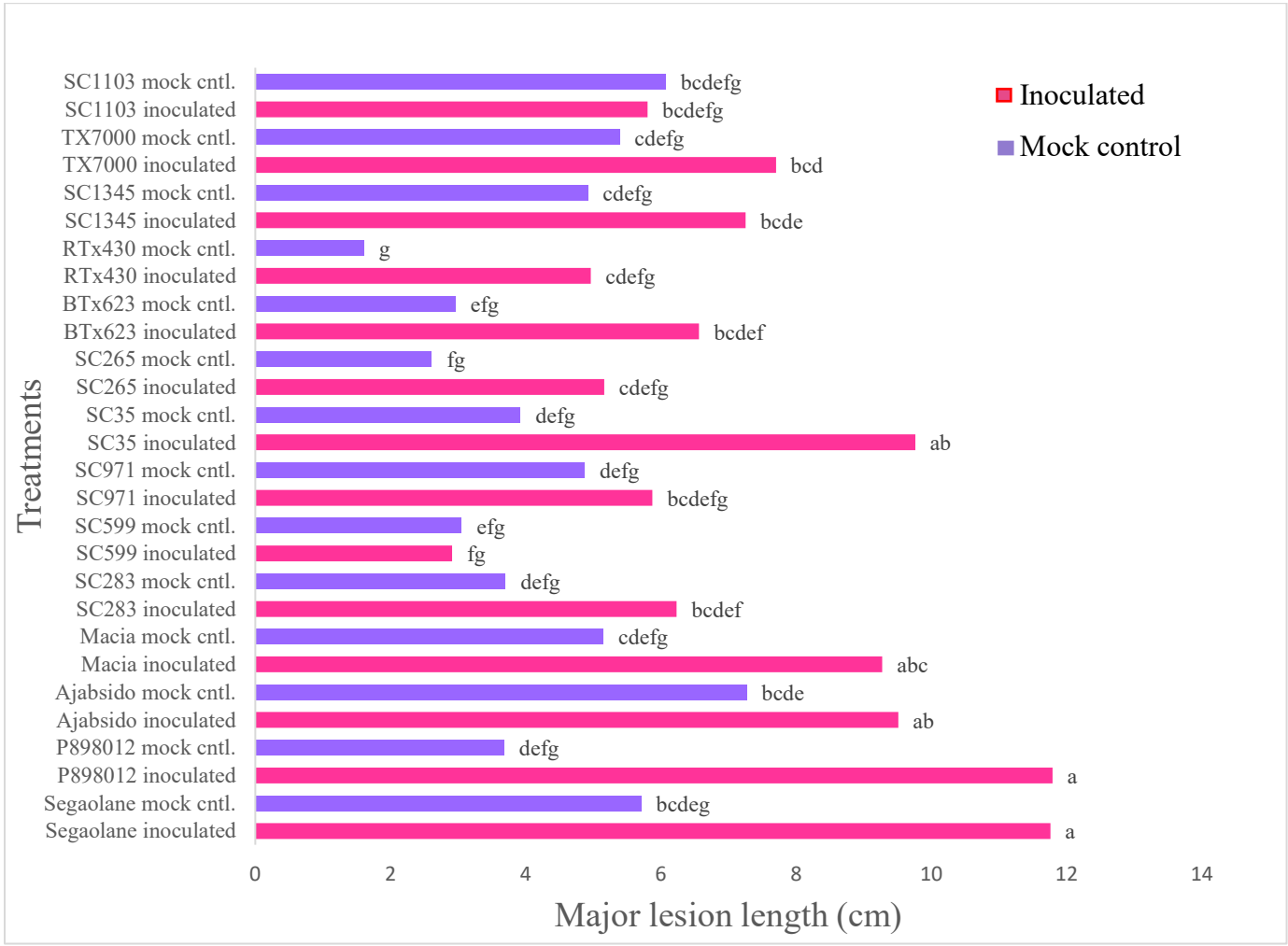

Figure 4.9. Bar plot showing the major lesion length (MLL) measured for all genotypes for both the inoculated and mock-inoculated treatments from the North Farm 2019 data.

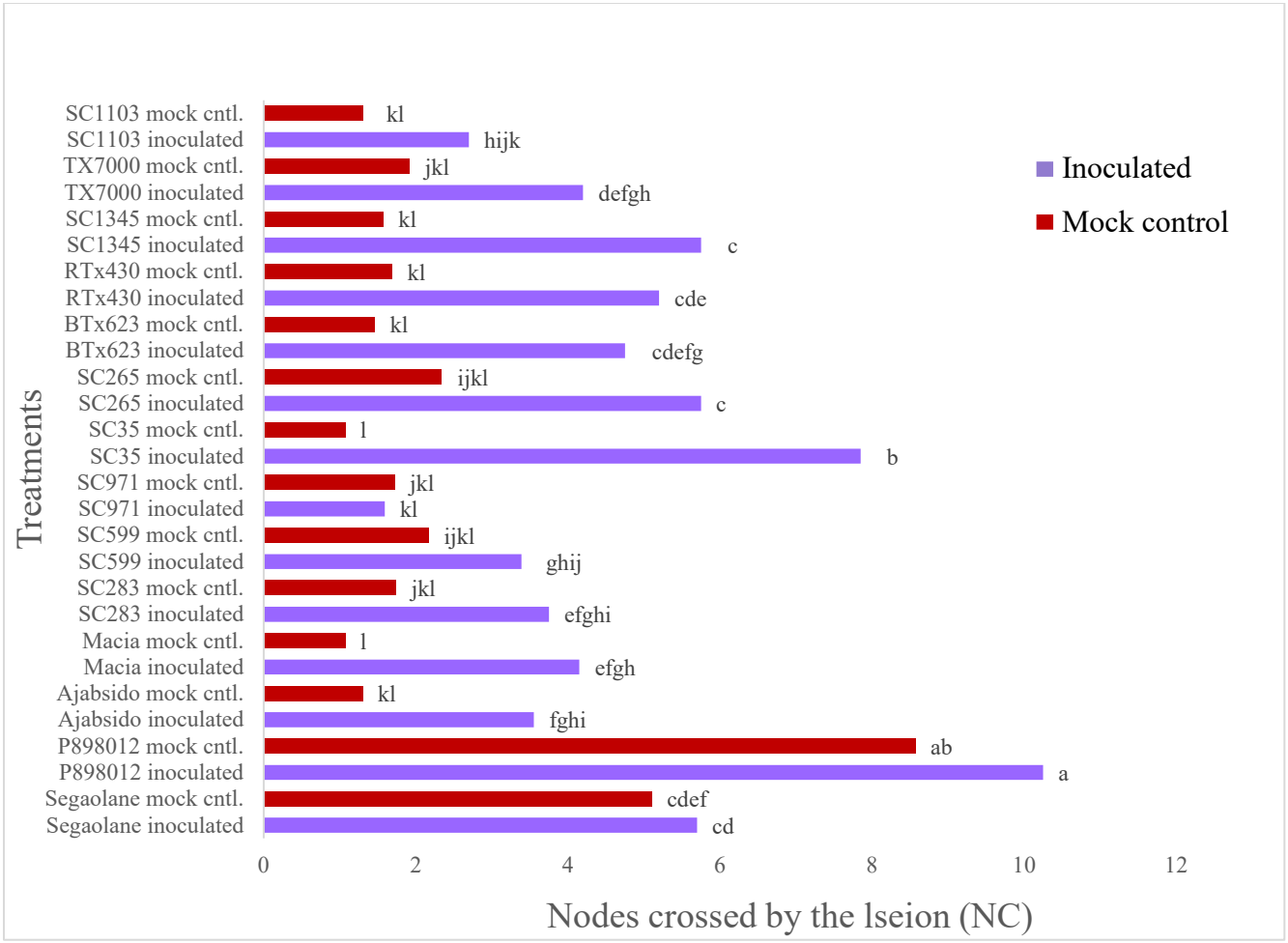

Figure 4.10. Bar plot showing the nodes crossed by the lesion (NC) measured for all genotypes for both the inoculated and mock-inoculated treatments from the North Farm 2019 data.

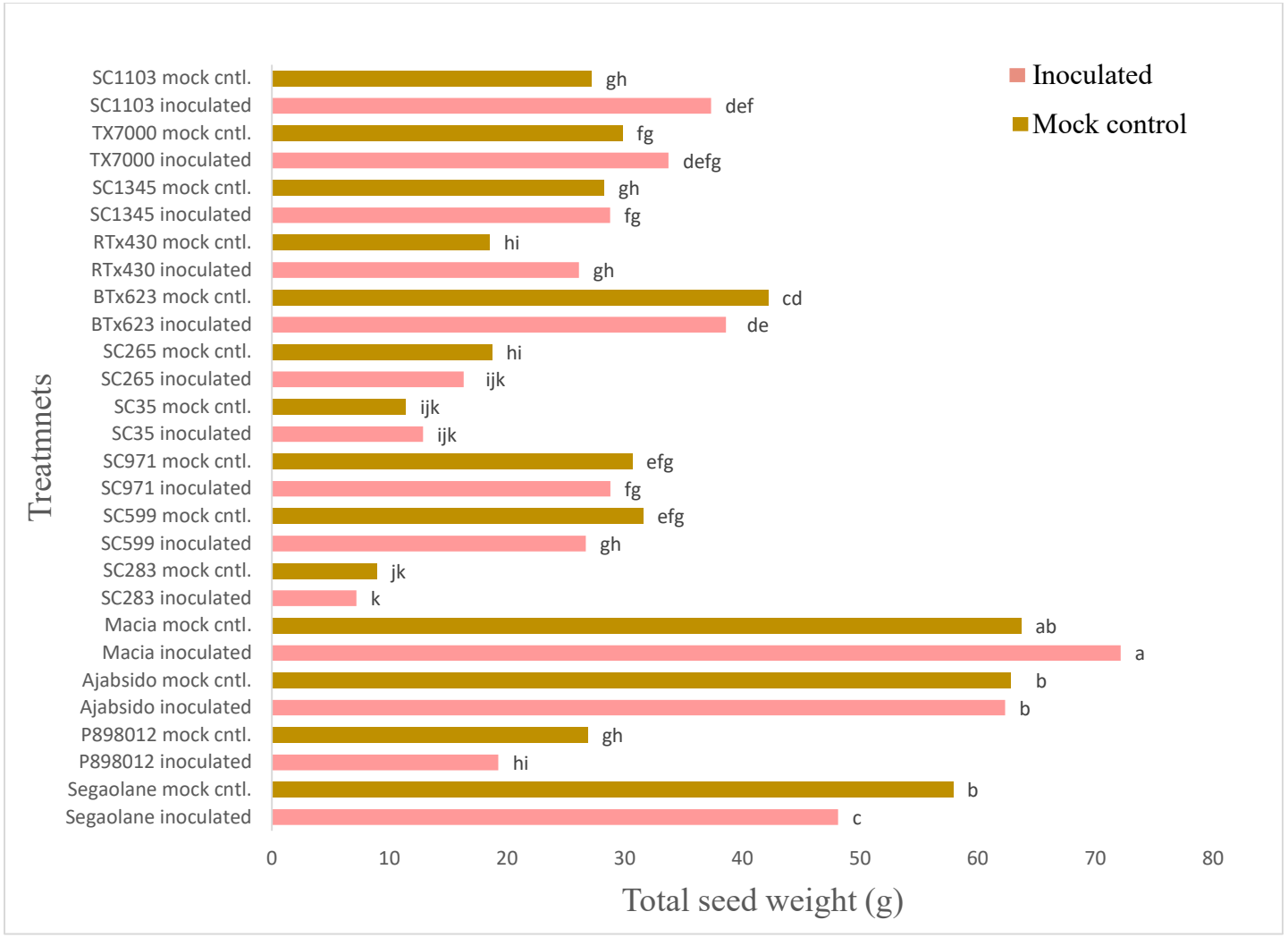

Figure 4.11. Bar plot showing the total seed weight (TSW) measured for all genotypes for both the inoculated and mock-inoculated treatments from the North Farm 2019 data.

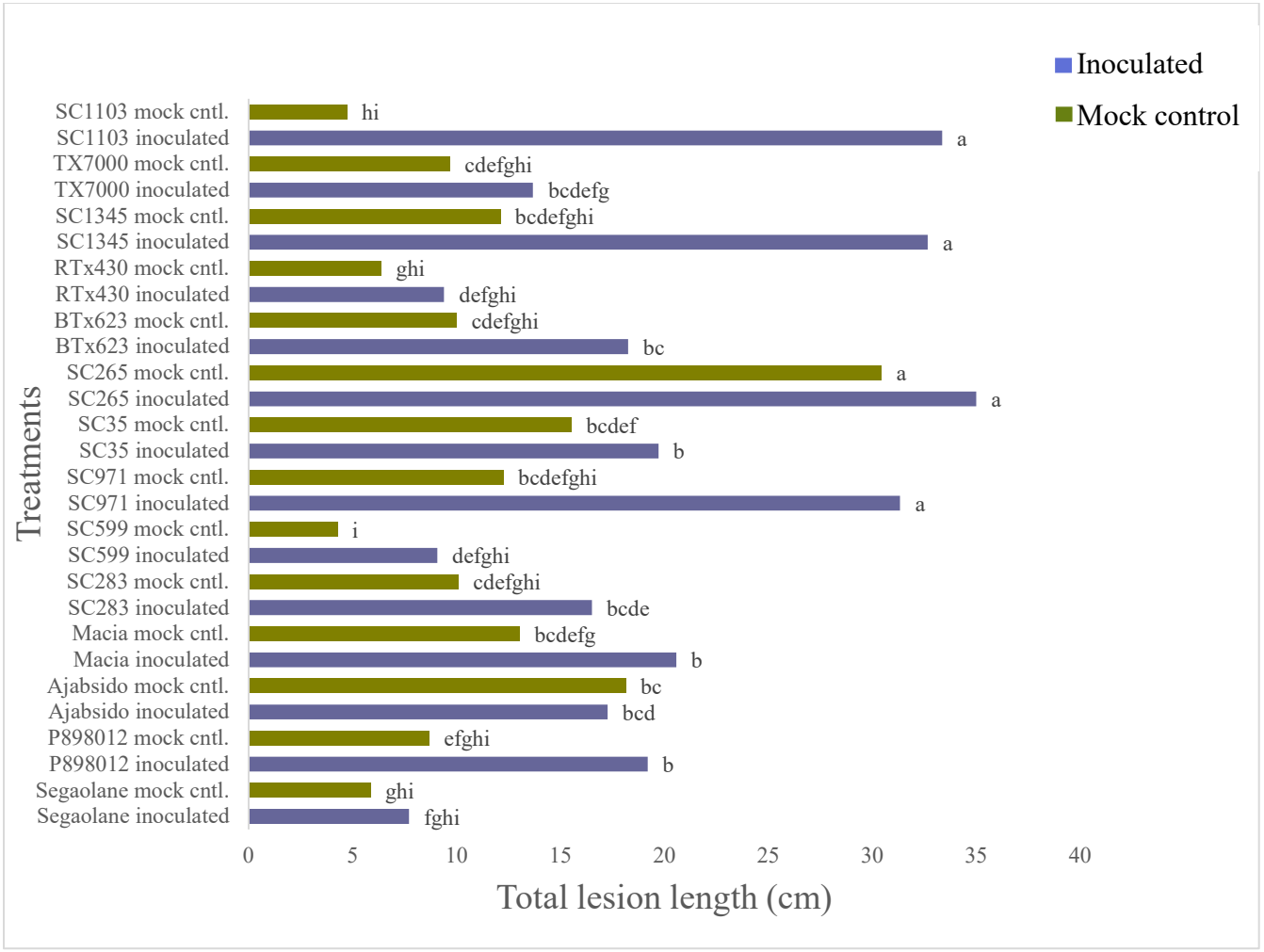

Figure 4.12. Bar plot showing the total lesion length (TLL) measured for all genotypes for both the inoculated and mock-inoculated treatments from the Ashland Bottoms 2021 data.

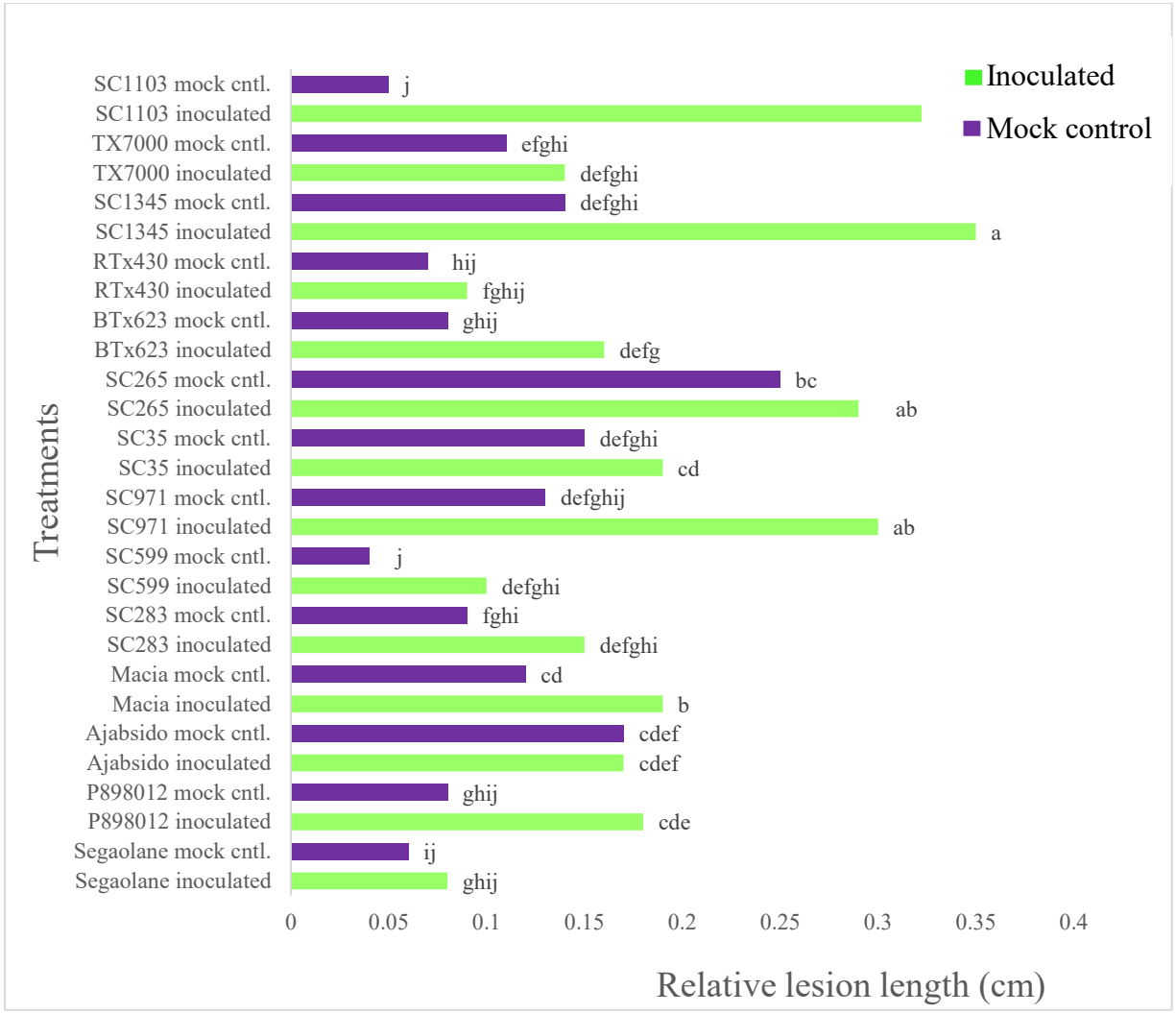

Figure 4.13. Bar plot showing the relative lesion length (RLL) measured for all genotypes for both the inoculated and mock-inoculated treatments from the Ashland Bottoms 2021 data.

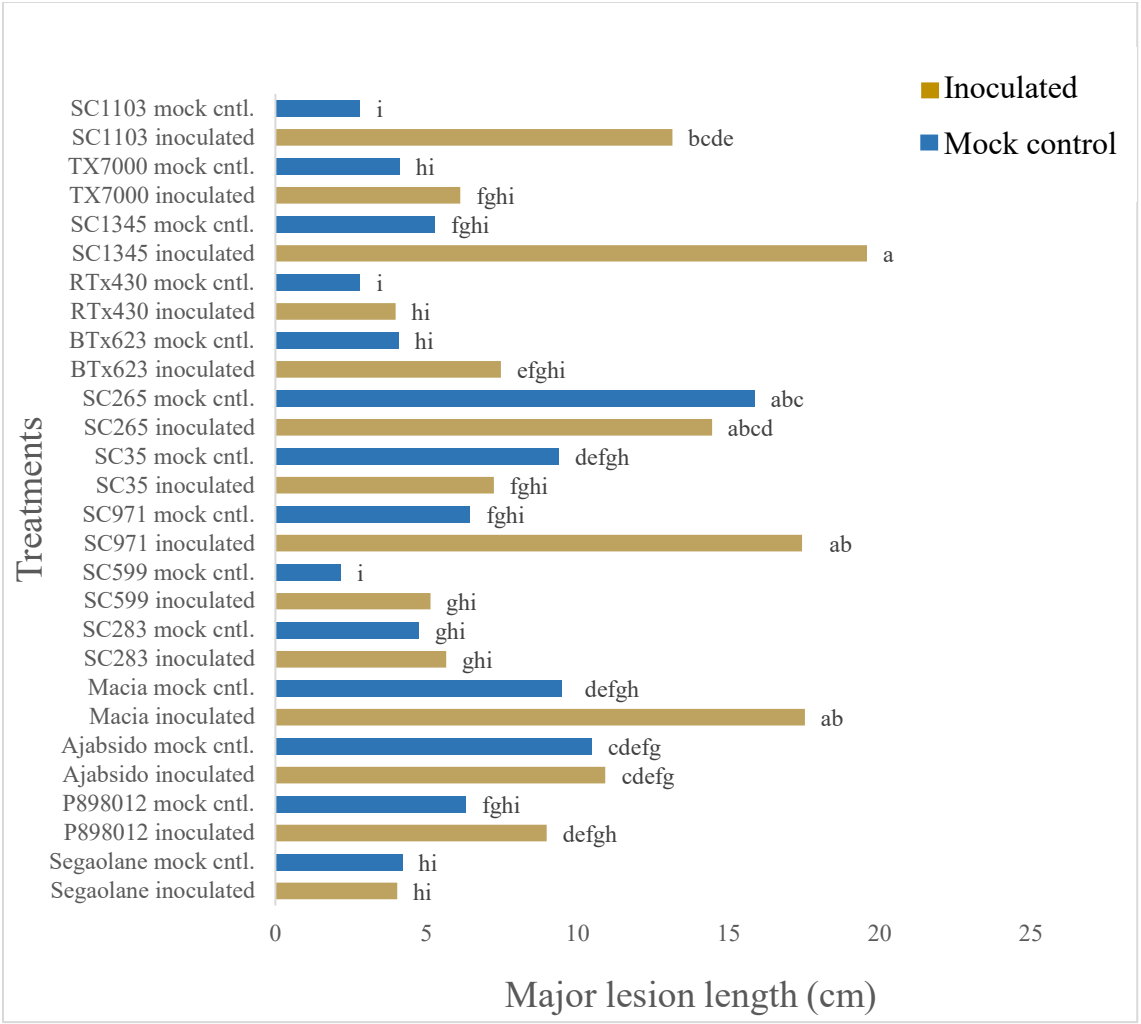

Figure 4.14. Bar plot showing for the major lesion length (MLL) measured for all genotypes for both the inoculated and mock-inoculated treatments from the Ashland Bottoms 2021 data.

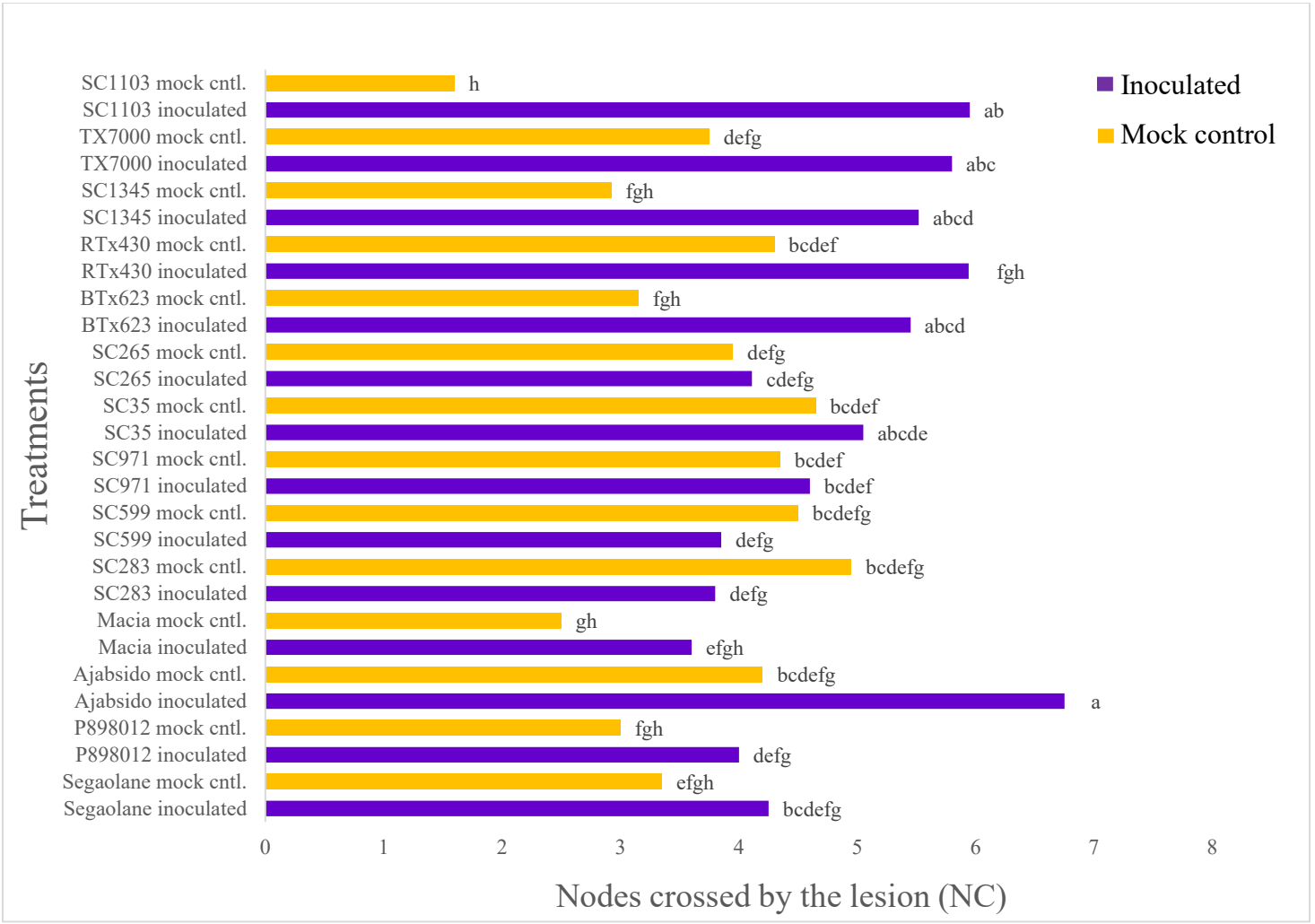

Figure 4.15. Bar plot showing the nodes crossed by the lesion (NC) measured for all genotypes for both the inoculated and mock-inoculated treatments from the Ashland Bottoms 2021 data.

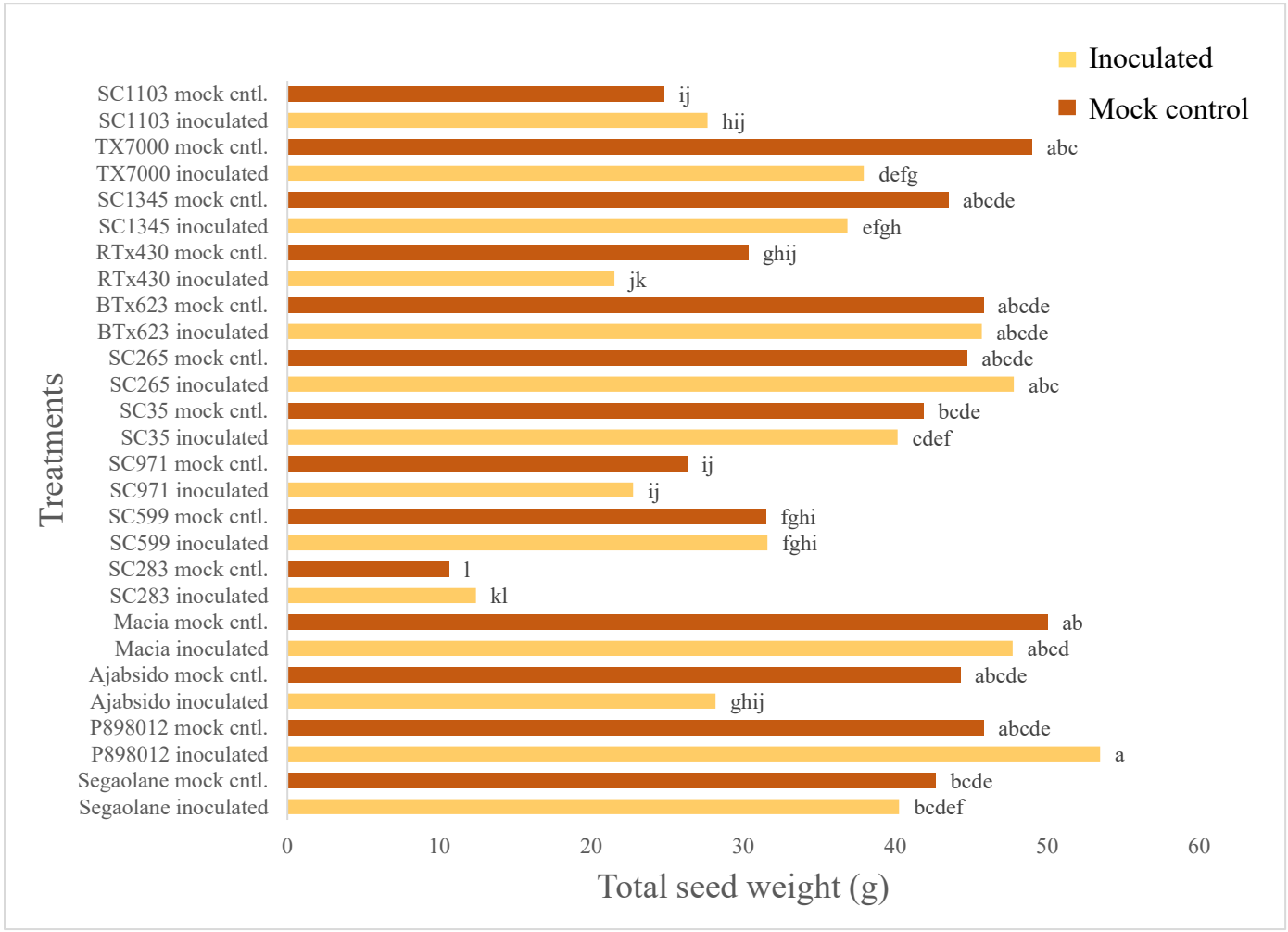

Figure 4.16. Bar plot showing the total seed weight (TSW) measured for all genotypes for both the inoculated and mock-inoculated treatments from the Ashland Bottoms 2021 data.

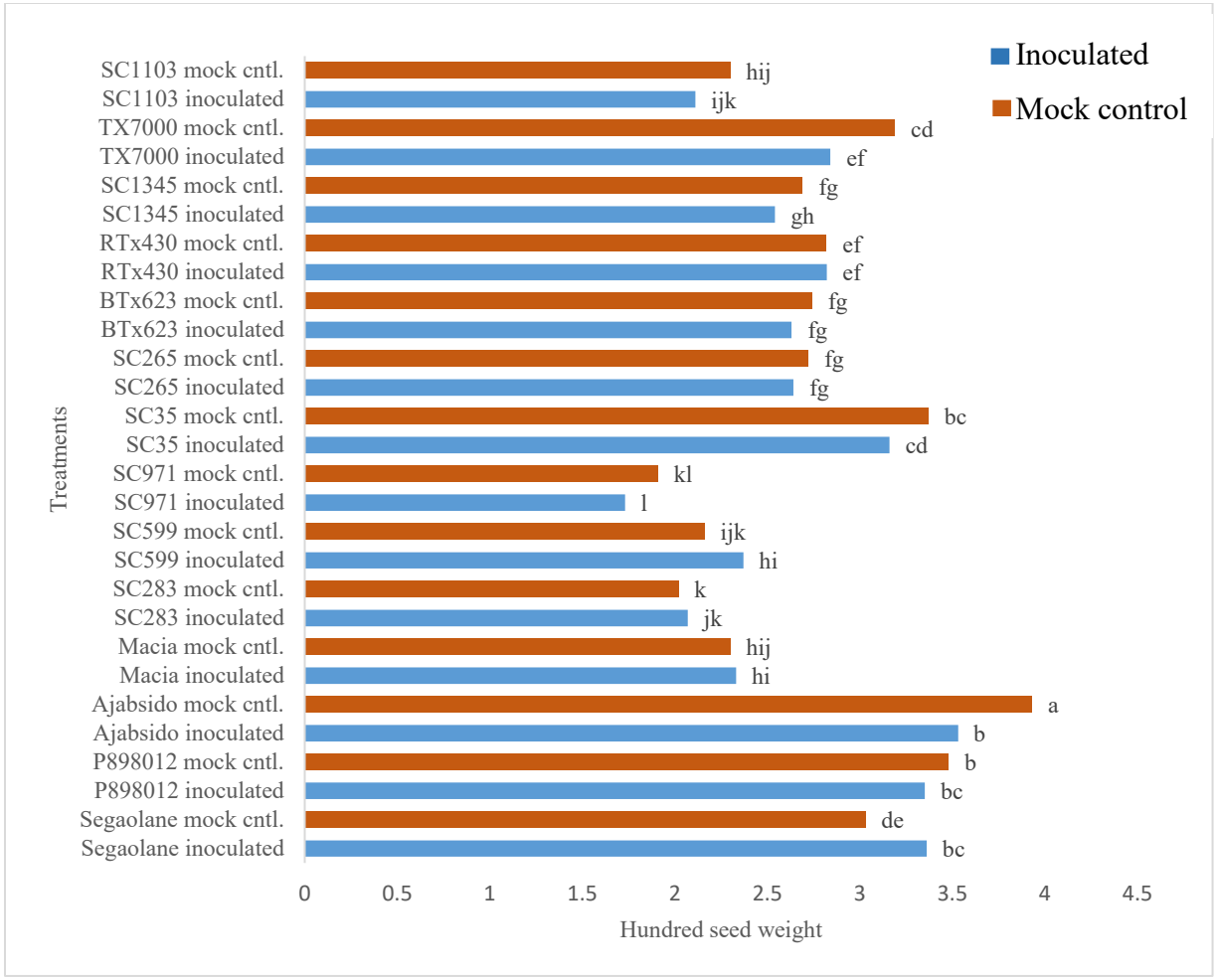

Figure 4.17. Bar plot showing the hundred seed weight (HSW) measured for all genotypes for both the inoculated and mock-inoculated treatments from the Ashland Bottoms 2021 data.

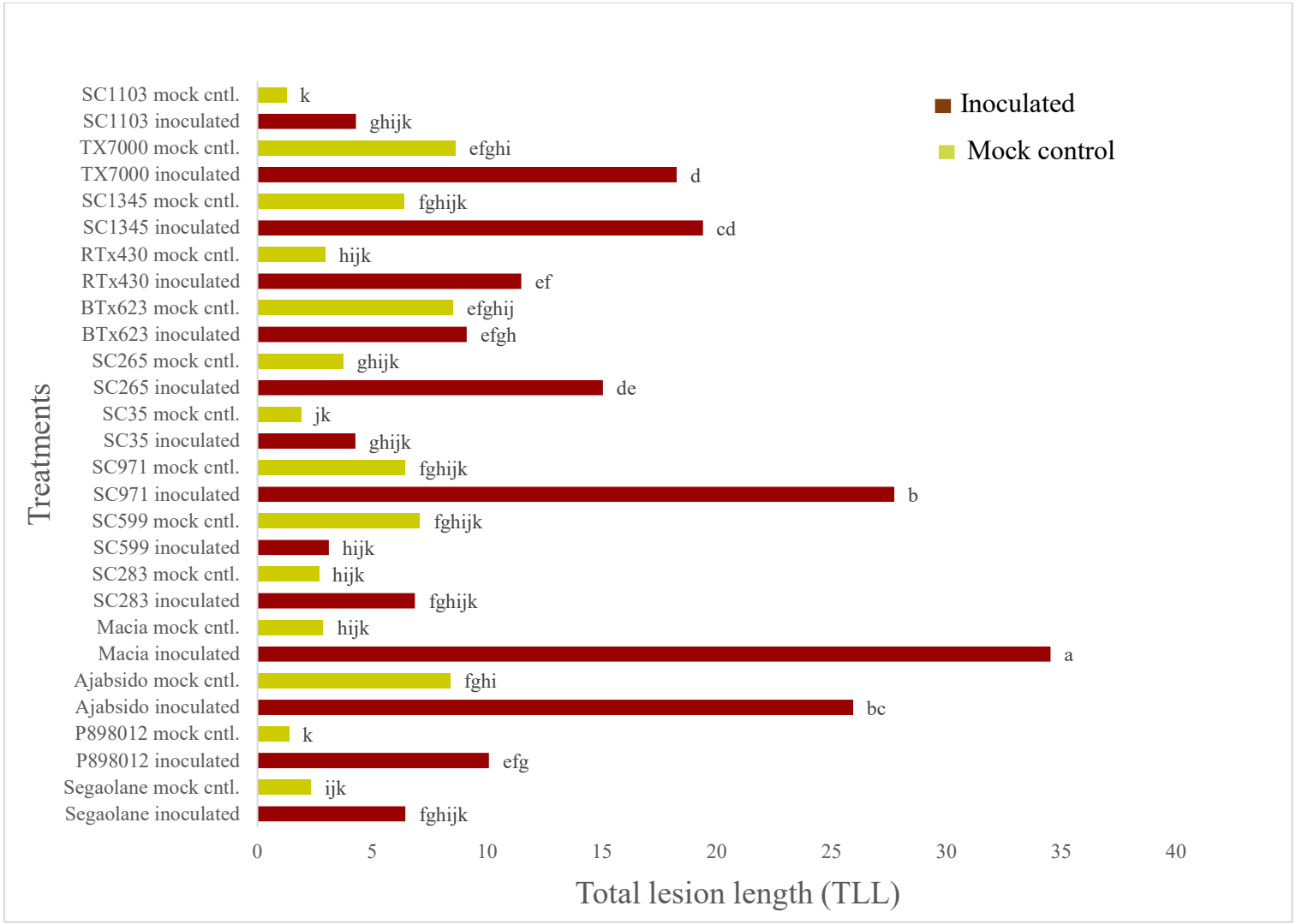

Figure 4.18. Bar plot showing the total lesion length (TLL) measured for all genotypes for both the inoculated and mock-inoculated treatments from the North Farm 2021 data.

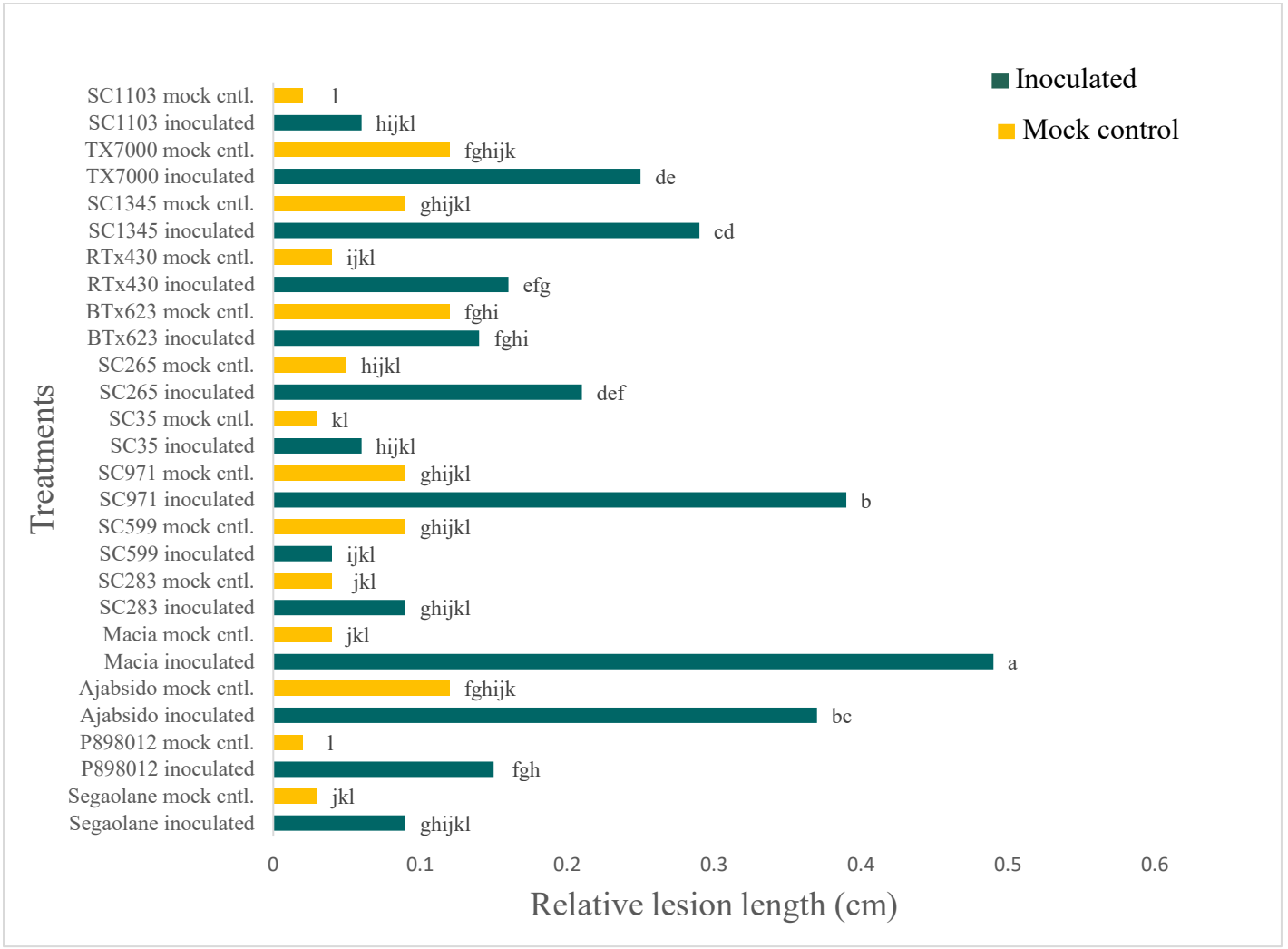

Figure 4.19. Bar plot showing the relative lesion length (RLL) measured for all genotypes for both the inoculated and mock-inoculated treatments from the North Farm 2021 data.

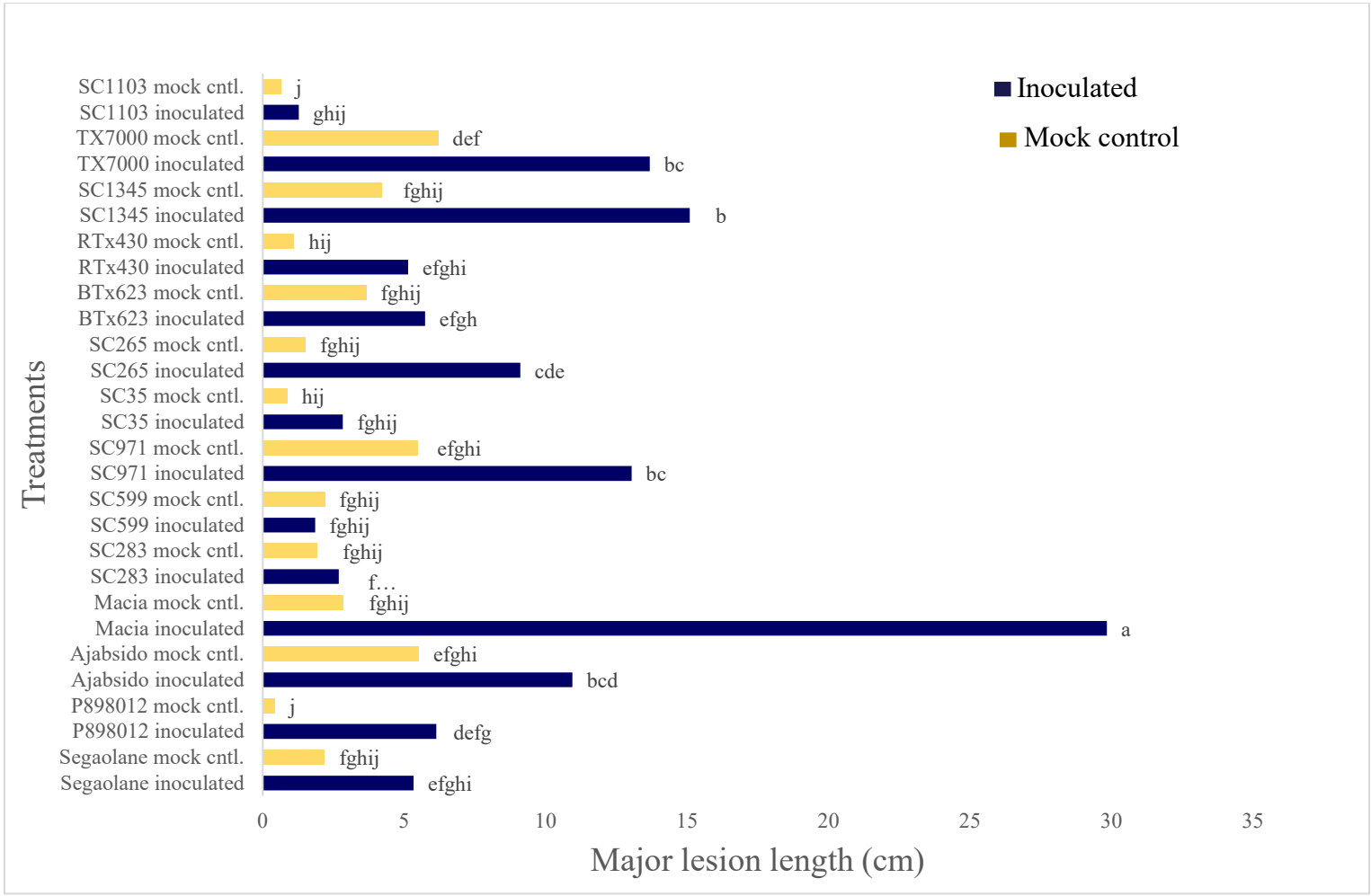

Figure 4.20. Bar plot showing the major lesion length (MLL) measured for all genotypes for both the inoculated and mock-inoculated treatments from the North Farm 2021 data.

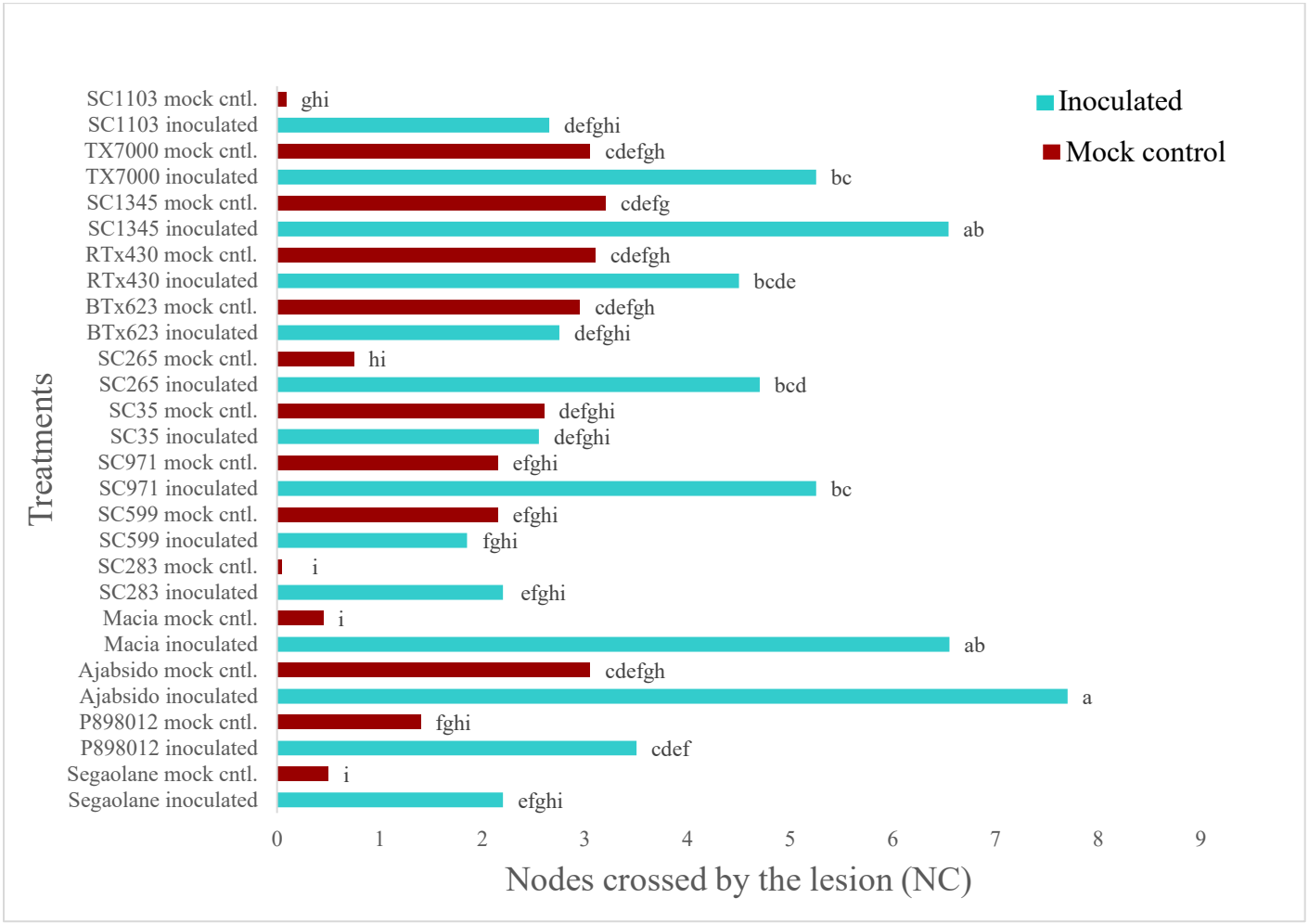

Figure 4.21. Bar plot showing the nodes crossed by the lesion (NC) measured for all genotypes for both the inoculated and mock-inoculated treatments from the North Farm 2021 data.

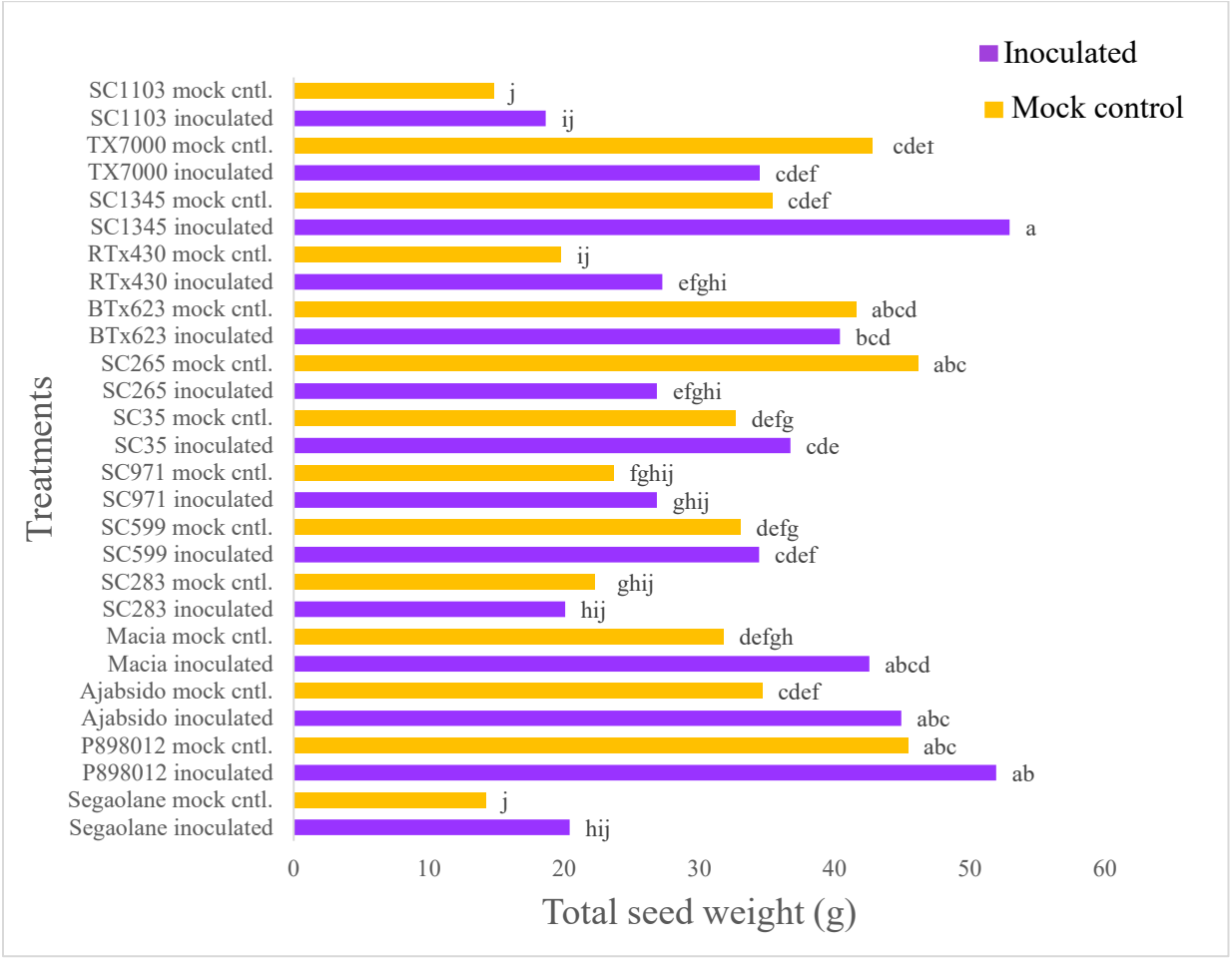

Figure 4.22. Bar plot showing the total seed weight (TSW) measured for all genotypes for both the inoculated and mock-inoculated treatments from the North Farm 2021 data.

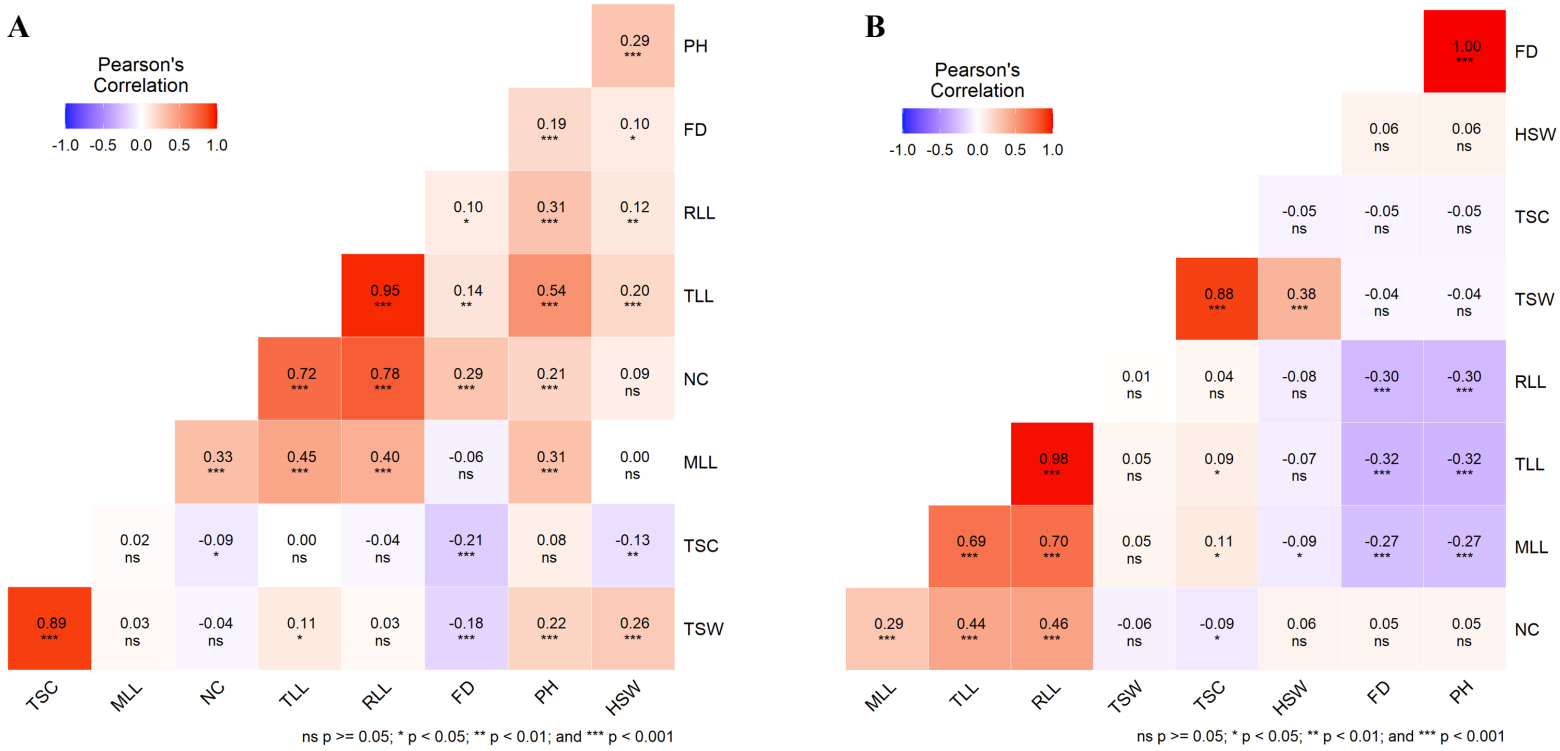

Figure 4.23. Pearson correlation coefficient results among all traits of Ashland Bottoms in 2019 (A) and 2021 (B).

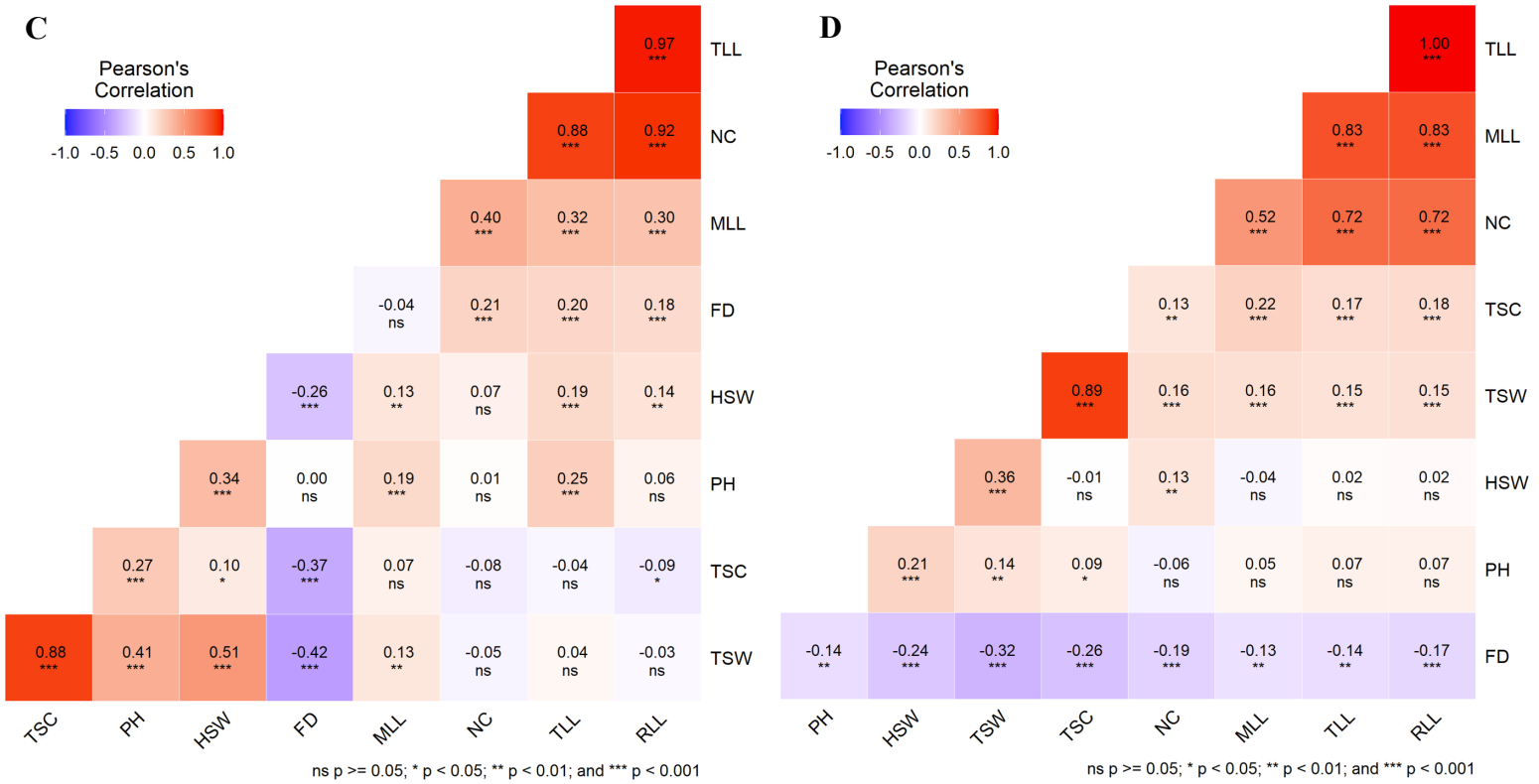

Figure 4.24. Pearson correlation coefficient results among all traits from North Farm in 2019 (C) and 2021 (D).

Chapter 5 - Conclusions

The research was framed to reveal the complex mechanism of the host's physiological, molecular, and genetic mechanisms of resistance to charcoal rot disease caused by *M. phaseolina* (MP). The specific objectives were to investigate the *M. phaseolina*-induced oxidative stress mediated senescence in the soybean. We also phenotyped the sorghum nested association mapping (NAM) lines to screen the charcoal rot resistant and susceptible lines to determine the appropriate NAM population to map the charcoal rot resistance.

In the first chapter, we evaluated the role of ascorbic acid in reducing *M. phaseolina*-induced senescence from the soybean host. Follow-up research was carried out to validate ROS-mediated senescence by quantifying the major reactive oxygen species (ROS), hydrogen peroxide (H_2O_2). In this chapter, an in-vitro *M. phaseolina* isolates sensitivity test was conducted using three different soybean isolates with an ascorbic acid amended PDA media. The in-vitro growth test showed that all three isolates were sensitive to concentrations of ascorbic acid at ≥ 15 mM. Ascorbic acid (reduced and oxidized forms) was used as a potential ROS scavenger. It was exogenously applied in the soybean cut-stem assay as a pre-treatment before inoculation with the *M. phaseolina*. The exogenous application of ascorbic acid significantly reduced *M. phaseolina*-induced senescence. A ROS (H_2O_2) quantification assay was conducted to validate ROS induced by MP from the inoculated, ascorbic acid pre-treated MP-inoculated plant and mock-inoculated soybean plant, which showed that MP induced significantly higher amounts of H_2O_2 in inoculated plants than in the ascorbic acid pre-treated inoculated or mock-inoculated plants.

In the second chapter, we studied gene expression during MP-induced host senescence. Ascorbic acid mediated senescence rescue and impact of exogenous ROS (H_2O_2) on MP-induced senescence from the comparative transcriptome analysis of resistant and susceptible soybean genotypes. The differential gene expression revealed that MP induced significantly higher numbers of genes in the downregulated category. The associated gene ontology terms were related to antioxidant, defense response, and stress responsive metabolic and hormonal pathways in both genotypes. Ascorbic acid pre-treatment following MP inoculation vs. ascorbic acid pre-treated and mock-inoculated

treatment comparisons revealed higher number of upregulated photosynthesis genes for both genotypes. Ascorbic acid pre-treatment also upregulated responses to ROS-related genes in both genotypes. The H_2O_2 pre-treatment following MP inoculation significantly induced larger number of genes in the upregulated category for the susceptible genotype than the resistant genotype. Pathway enrichment analysis revealed exogenous H_2O_2 application induced upregulation of large numbers of oxidative stress responsive metabolic pathways in both genotypes, while it downregulated hormonal signal transduction and photosynthetic pathways.

The third chapter aimed to phenotype the sorghum nested association mapping (NAM) parental lines charcoal rot resistance. The sorghum NAM lines, and three other checks, were phenotyped for charcoal rot in two Kansas locations in 2019 and 2021. Segaolane was the most susceptible line, while SC1103 exhibited resistance to CR in 2019. Combined analyses across four environments was not possible due to significant genotype by environment (G × E) interactions, but SC1103 was determined to be the most charcoal rot resistant line from the analysis of three environments' data. However, the relative inconsistency of the lines for disease reaction across environments suggested the complex genetic architecture of charcoal rot resistance in sorghum and deserves further investigation.

Appendix A - Differentially expressed and significantly up-enriched gene ontology (GO) terms and associated gene numbers represented between the comparison of the non-pre-treated MP-inoculated treatment vs non-pre-treated agar plug-inoculated mock control in the resistant genotype (DT97-4290).

GO	*p*-value	*q*-value	Term	Gene No.
GO:0000166	0.039496	1	nucleotide binding	42
GO:0000287	0.043896	1	magnesium ion binding	5
GO:0002229	0.011099	0.93401	defense response to oomycetes	3
GO:0003700	0.0008	0.14115	DNA-binding transcription factor activity	28
GO:0003727	0.017698	1	single-stranded RNA binding	2
GO:0004497	0.016398	1	monooxygenase activity	8
GO:0004650	0.016298	1	polygalacturonase activity	3
GO:0004672	1.00E-04	0.03646	protein kinase activity	44
GO:0004674	1.00E-04	0.03646	protein serine/threonine kinase activity	32
GO:0004740	0.043696	1	pyruvate dehydrogenase (acetyl-transferring) kinase activity	1
GO:0004970	0.0002	0.04558	ionotropic glutamate receptor activity	4
GO:0005179	0.0002	0.04558	hormone activity	3
GO:0005351	0.023098	1	carbohydrate:proton symporter activity	3
GO:0005355	0.020798	1	glucose transmembrane transporter activity	3
GO:0005509	0.015698	1	calcium ion binding	9
GO:0005524	0.013699	1	ATP binding	50
GO:0005576	1.00E-04	0.03646	extracellular region	21
GO:0005886	1.00E-04	0.03646	plasma membrane	51
GO:0005887	1.00E-04	0.03646	integral component of plasma membrane	10
GO:0005901	0.018398	1	caveola	1
GO:0005985	0.029097	1	sucrose metabolic process	2
GO:0006355	0.045995	1	regulation of transcription, DNA-templated	32
GO:0006468	1.00E-04	0.03646	protein phosphorylation	45
GO:0006820	0.0048	0.49535	anion transport	3
GO:0006865	0.032797	1	amino acid transport	4
GO:0006986	0.031497	1	response to unfolded protein	2
GO:0006996	0.040996	1	organelle organization	2
GO:0007166	0.0038	0.42416	cell surface receptor signaling pathway	4
GO:0007178	0.0023	0.2859	protein serine/threonine kinase signaling pathway	4
GO:0008152	0.048195	1	metabolic process	10
GO:0008160	0.016698	1	protein tyrosine phosphatase activator activity	1
GO:0008236	0.012499	1	serine-type peptidase activity	5
GO:0008381	0.0036	0.41021	mechanosensitive ion channel activity	2

GO:0008506	0.005199	0.51711	sucrose:proton symporter activity	2
GO:0008515	0.003	0.34911	sucrose transmembrane transporter activity	2
GO:0008645	0.020798	1	hexose transmembrane transport	3
GO:0009505	0.038096	1	plant-type cell wall	4
GO:0009506	0.014799	1	plasmodesma	10
GO:0009650	0.014699	1	UV protection	1
GO:0009671	0.030097	1	nitrate:proton symporter activity	1
GO:0009686	0.0017	0.24469	gibberellin biosynthetic process	3
GO:0009690	0.0014	0.20695	cytokinin metabolic process	3
GO:0009691	0.049495	1	cytokinin biosynthetic process	2
GO:0009694	0.022098	1	jasmonic acid metabolic process	2
GO:0009705	0.030097	1	plant-type vacuole membrane	3
GO:0009755	0.008699	0.80651	hormone-mediated signaling pathway	3
GO:0009901	0.0004	0.07544	anther dehiscence	2
GO:0009909	0.015498	1	regulation of flower development	2
GO:0009911	0.018998	1	positive regulation of flower development	1
GO:0010039	0.009999	0.89663	response to iron ion	2
GO:0010047	0.0004	0.07544	fruit dehiscence	2
GO:0010168	0.023298	1	ER body	1
GO:0010223	0.0004	0.07544	secondary shoot formation	2
GO:0010333	1.00E-04	0.03646	terpene synthase activity	5
GO:0010906	0.043696	1	regulation of glucose metabolic process	1
GO:0015112	0.010399	0.91442	nitrate transmembrane transporter activity	2
GO:0015276	0.0002	0.04558	ligand-gated ion channel activity	4
GO:0015293	0.011299	0.93644	symporter activity	5
GO:0015706	0.0002	0.04558	nitrate transport	3
GO:0015770	0.005199	0.51711	sucrose transport	2
GO:0015833	0.0047	0.49435	peptide transport	2
GO:0016020	1.00E-04	0.03646	membrane	136
GO:0016021	1.00E-04	0.03646	integral component of membrane	131
GO:0016102	0.0002	0.04558	diterpenoid biosynthetic process	4
GO:0016301	0.0002	0.04558	kinase activity	35
GO:0016310	0.0002	0.04558	phosphorylation	36
GO:0016491	0.021298	1	oxidoreductase activity	28
GO:0016602	0.0018	0.24613	CCAAT-binding factor complex	3
GO:0016705	0.033197	1	oxidoreductase activity, acting on paired donors	7
GO:0016787	0.005699	0.55654	hydrolase activity	34
GO:0016798	0.017698	1	hydrolase activity, acting on glycosyl bonds	10
GO:0016829	0.038996	1	lyase activity	7
GO:0016985	0.030397	1	mannan endo-1,4-beta-mannosidase activity	2
GO:0019139	0.005799	0.55654	cytokinin dehydrogenase activity	2
GO:0020037	0.024998	1	heme binding	10
GO:0022857	0.039496	1	transmembrane transporter activity	10
GO:0030001	0.0018	0.24613	metal ion transport	7

GO:0030093	0.032897	1	chloroplast photosystem I	1
GO:0030247	0.034197	1	polysaccharide binding	3
GO:0031625	0.0012	0.19304	ubiquitin protein ligase binding	6
GO:0033214	0.0014	0.20695	siderophore-dependent iron import into cell	2
GO:0034220	1.00E-04	0.03646	ion transmembrane transport	9
GO:0035672	1.00E-04	0.03646	oligopeptide transmembrane transport	5
GO:0035673	1.00E-04	0.03646	oligopeptide transmembrane transporter activity	7
GO:0038023	0.0044	0.48131	signaling receptor activity	4
GO:0042343	0.028097	1	indole glucosinolate metabolic process	2
GO:0043565	1.00E-04	0.03646	sequence-specific DNA binding	26
GO:0044853	0.018398	1	plasma membrane raft	1
GO:0045487	0.0019	0.24743	gibberellin catabolic process	2
GO:0046355	0.008299	0.7827	mannan catabolic process	2
GO:0046777	0.0046	0.49332	protein autophosphorylation	9
GO:0046872	0.010599	0.91442	metal ion binding	45
GO:0048316	0.0025	0.30386	seed development	2
GO:0048364	0.010699	0.91442	root development	3
GO:0048544	0.0007	0.12762	recognition of pollen	6
GO:0051213	0.0028	0.33292	dioxygenase activity	8
GO:0051787	0.009699	0.88423	misfolded protein binding	3
GO:0051980	0.0014	0.20695	iron-nicotianamine transmembrane transporter activity	2
GO:0052634	0.0019	0.24743	C-19 gibberellin 2-beta-dioxygenase activity	2
GO:0055085	0.0011	0.18801	transmembrane transport	26
GO:0071249	0.0004	0.07544	cellular response to nitrate	2
GO:0071446	0.033697	1	cellular response to salicylic acid stimulus	1
GO:0071493	0.023098	1	cellular response to UV-B	1
GO:0072659	0.044196	1	protein localization to plasma membrane	1
GO:0080142	0.012199	0.99593	regulation of salicylic acid biosynthetic process	2
GO:0080153	0.046295	1	negative regulation of reductive pentose-phosphate cycle	1
GO:0097573	0.033197	1	glutathione oxidoreductase activity	3
GO:0098542	0.0021	0.26711	defense response to other organism	4
GO:0106310	1.00E-04	0.03646	protein serine kinase activity	11
GO:1901371	0.0002	0.04558	regulation of leaf morphogenesis	3
GO:1901601	0.0012	0.19304	strigolactone biosynthetic process	2
GO:1902025	0.0002	0.04558	nitrate import	3
GO:2000280	0.0003	0.06563	regulation of root development	3

Appendix B - Differentially expressed and significantly down-enriched gene ontology (GO) term and associated gene numbers represented between comparison of non-pre-treated MP-inoculated treatment vs non-pre-treated agar plug-inoculated mock control in the resistant genotype (DT97-4290).

GO	*p*-value	*q*-value	Term	Gene No.
GO:0000155	0.046395	0.929219	phosphorelay sensor kinase activity	4
GO:0000287	0.0002	0.019889	magnesium ion binding	17
GO:0000822	0.049195	0.950873	inositol hexakisphosphate binding	2
GO:0000976	0.007099	0.29419	transcription cis-regulatory region binding	15
GO:0001678	0.0041	0.202025	cellular glucose homeostasis	3
GO:0003700	1.00E-04	0.01189	DNA-binding transcription factor activity	90
GO:0003824	1.00E-04	0.01189	catalytic activity	76
GO:0003849	0.016898	0.496956	3-deoxy-7-phosphoheptulonate synthase activity	2
GO:0003854	0.045995	0.928394	3-beta-hydroxy-delta5-steroid dehydrogenase activity	2
GO:0003864	0.022998	0.606565	3-methyl-2-oxobutanoate hydroxymethyltransferase activity	1
GO:0003866	0.0018	0.109389	3-phosphoshikimate 1-carboxyvinyltransferase activity	2
GO:0003878	0.0006	0.045579	ATP citrate synthase activity	4
GO:0003885	0.026797	0.64859	D-arabinono-1,4-lactone oxidase activity	2
GO:0003935	0.015598	0.4714	GTP cyclohydrolase II activity	2
GO:0003954	0.006199	0.267013	NADH dehydrogenase activity	4
GO:0003979	0.028397	0.654984	UDP-glucose 6-dehydrogenase activity	2
GO:0004012	0.010099	0.358711	NA	4
GO:0004024	0.018098	0.512938	alcohol dehydrogenase activity, zinc-dependent	3
GO:0004032	0.047995	0.937621	alditol:NADP+ 1-oxidoreductase activity	3
GO:0004033	0.0012	0.079076	aldo-keto reductase (NADP) activity	4
GO:0004067	0.014099	0.448368	asparaginase activity	2
GO:0004097	0.023898	0.613709	catechol oxidase activity	3
GO:0004129	0.0003	0.027347	cytochrome-c oxidase activity	4
GO:0004322	0.047395	0.929219	ferroxidase activity	2
GO:0004340	0.0041	0.202025	glucokinase activity	3
GO:0004347	0.020798	0.565993	glucose-6-phosphate isomerase activity	2
GO:0004352	0.017398	0.506215	glutamate dehydrogenase (NAD+) activity	2
GO:0004364	1.00E-04	0.01189	glutathione transferase activity	14
GO:0004365	0.009899	0.358593	glyceraldehyde-3-phosphate dehydrogenase (NAD+) (phosphorylating) activity	4
GO:0004396	0.0041	0.202025	hexokinase activity	3
GO:0004450	0.025797	0.64099	isocitrate dehydrogenase (NADP+) activity	2
GO:0004497	1.00E-04	0.01189	monooxygenase activity	35
GO:0004540	0.048195	0.938177	ribonuclease activity	3
GO:0004553	0.0006	0.045579	hydrolase activity, hydrolyzing O-glycosyl compounds	25
GO:0004568	1.00E-04	0.01189	chitinase activity	8
GO:0004586	0.028797	0.654984	ornithine decarboxylase activity	1

GO:0004592	0.026497	0.64418	pantoate-beta-alanine ligase activity	1
GO:0004601	1.00E-04	0.01189	peroxidase activity	23
GO:0004611	0.015398	0.470556	phosphoenolpyruvate carboxykinase activity	2
GO:0004612	0.015398	0.470556	phosphoenolpyruvate carboxykinase (ATP) activity	2
GO:0004616	0.0013	0.082678	phosphogluconate dehydrogenase (decarboxylating) activity	3
GO:0004619	0.039596	0.826681	phosphoglycerate mutase activity	2
GO:0004620	0.010599	0.36577	phospholipase activity	4
GO:0004657	0.009199	0.342306	proline dehydrogenase activity	2
GO:0004673	0.0035	0.193365	protein histidine kinase activity	4
GO:0004742	0.017698	0.512219	dihydrolipoyllysine-residue acetyltransferase activity	2
GO:0004805	0.008799	0.338952	trehalose-phosphatase activity	3
GO:0004806	0.007399	0.303859	triglyceride lipase activity	3
GO:0004857	0.012999	0.425766	enzyme inhibitor activity	7
GO:0004864	0.024698	0.627974	protein phosphatase inhibitor activity	5
GO:0004866	0.0005	0.041435	endopeptidase inhibitor activity	7
GO:0004867	0.0006	0.045579	serine-type endopeptidase inhibitor activity	4
GO:0005506	1.00E-04	0.01189	iron ion binding	40
GO:0005536	0.0041	0.202025	glucose binding	3
GO:0005576	1.00E-04	0.01189	extracellular region	55
GO:0005740	0.005299	0.237607	mitochondrial envelope	2
GO:0005746	0.008899	0.340407	mitochondrial respirasome	2
GO:0005751	0.0002	0.019889	mitochondrial respiratory chain complex IV	4
GO:0005758	0.012399	0.416081	mitochondrial intermembrane space	3
GO:0005886	0.0013	0.082678	plasma membrane	96
GO:0005975	0.0003	0.027347	carbohydrate metabolic process	44
GO:0006006	0.009099	0.342306	glucose metabolic process	6
GO:0006024	0.028397	0.654984	glycosaminoglycan biosynthetic process	2
GO:0006032	1.00E-04	0.01189	chitin catabolic process	7
GO:0006065	0.028397	0.654984	UDP-glucuronate biosynthetic process	2
GO:0006085	0.0008	0.055387	acetyl-CoA biosynthetic process	4
GO:0006090	0.010399	0.362308	pyruvate metabolic process	4
GO:0006094	0.014899	0.466603	gluconeogenesis	5
GO:0006096	1.00E-04	0.01189	glycolytic process	18
GO:0006098	0.017898	0.512582	pentose-phosphate shunt	5
GO:0006101	0.035296	0.751252	citrate metabolic process	2
GO:0006116	0.0031	0.178477	NADH oxidation	4
GO:0006122	0.047295	0.929219	mitochondrial electron transport, ubiquinol to cytochrome c	3
GO:0006123	1.00E-04	0.01189	mitochondrial electron transport, cytochrome c to oxygen	7
GO:0006351	0.0003	0.027347	transcription, DNA-templated	40
GO:0006355	1.00E-04	0.01189	regulation of transcription, DNA-templated	102
GO:0006520	0.0041	0.202025	cellular amino acid metabolic process	8
GO:0006538	0.017298	0.505998	glutamate catabolic process	3
GO:0006559	0.033097	0.715569	L-phenylalanine catabolic process	3
GO:0006560	0.009199	0.342306	proline metabolic process	2

GO:0006562	0.009199	0.342306	proline catabolic process	2
GO:0006564	0.048495	0.940668	L-serine biosynthetic process	2
GO:0006739	0.025797	0.64099	NADP metabolic process	2
GO:0006749	1.00E-04	0.01189	glutathione metabolic process	15
GO:0006855	1.00E-04	0.01189	xenobiotic transmembrane transport	9
GO:0006952	0.0006	0.045579	defense response	33
GO:0006970	0.022298	0.597886	response to osmotic stress	2
GO:0006979	1.00E-04	0.01189	response to oxidative stress	21
GO:0008061	1.00E-04	0.01189	chitin binding	7
GO:0008152	1.00E-04	0.01189	metabolic process	38
GO:0008194	1.00E-04	0.01189	UDP-glycosyltransferase activity	28
GO:0008272	0.028697	0.654984	sulfate transport	4
GO:0008299	0.042996	0.886994	isoprenoid biosynthetic process	5
GO:0008381	0.034997	0.747777	mechanosensitive ion channel activity	2
GO:0008422	1.00E-04	0.01189	beta-glucosidase activity	11
GO:0008483	0.0008	0.055387	transaminase activity	9
GO:0008643	0.031497	0.703215	carbohydrate transport	5
GO:0008652	0.018998	0.527511	cellular amino acid biosynthetic process	12
GO:0008661	0.005	0.227894	1-deoxy-D-xylulose-5-phosphate synthase activity	3
GO:0008686	0.015598	0.4714	3,4-dihydroxy-2-butanone-4-phosphate synthase activity	2
GO:0008798	0.014099	0.448368	beta-aspartyl-peptidase activity	2
GO:0008824	0.047395	0.929219	cyanate hydratase activity	1
GO:0008865	0.007699	0.307407	fructokinase activity	4
GO:0009001	0.032097	0.710807	serine O-acetyltransferase activity	2
GO:0009051	0.004	0.202025	pentose-phosphate shunt, oxidative branch	4
GO:0009058	0.0036	0.1969	biosynthetic process	12
GO:0009073	0.013099	0.426487	aromatic amino acid family biosynthetic process	5
GO:0009228	0.032997	0.715569	thiamine biosynthetic process	3
GO:0009346	0.009699	0.353691	ATP-independent citrate lyase complex	2
GO:0009423	0.005599	0.247008	chorismate biosynthetic process	4
GO:0009439	0.047395	0.929219	cyanate metabolic process	1
GO:0009505	0.024398	0.62362	plant-type cell wall	9
GO:0009607	0.023298	0.606565	response to biotic stimulus	5
GO:0009611	0.014899	0.466603	response to wounding	5
GO:0009620	0.008499	0.332074	response to fungus	3
GO:0009651	0.0005	0.041435	response to salt stress	11
GO:0009693	0.009699	0.353691	ethylene biosynthetic process	3
GO:0009695	0.0015	0.092182	jasmonic acid biosynthetic process	4
GO:0009698	0.0002	0.019889	phenylpropanoid metabolic process	5
GO:0009717	0.016398	0.490159	isoflavonoid biosynthetic process	2
GO:0009723	0.023098	0.606565	response to ethylene	4
GO:0009727	0.0049	0.227121	detection of ethylene stimulus	3
GO:0009735	0.0008	0.055387	response to cytokinin	6
GO:0009800	0.006499	0.275593	cinnamic acid biosynthetic process	3

GO:0009807	0.009999	0.358711	lignan biosynthetic process	4
GO:0009808	0.0032	0.180436	lignin metabolic process	2
GO:0009813	1.00E-04	0.01189	flavonoid biosynthetic process	12
GO:0009815	0.0049	0.227121	1-aminocyclopropane-1-carboxylate oxidase activity	3
GO:0009873	1.00E-04	0.01189	ethylene-activated signaling pathway	31
GO:0010026	0.047295	0.929219	trichome differentiation	2
GO:0010030	0.006699	0.281887	positive regulation of seed germination	3
GO:0010033	0.018498	0.516249	response to organic substance	4
GO:0010105	0.0035	0.193365	negative regulation of ethylene-activated signaling pathway	4
GO:0010133	0.0008	0.055387	proline catabolic process to glutamate	3
GO:0010155	0.015998	0.480831	regulation of proton transport	2
GO:0010181	0.0012	0.079076	FMN binding	9
GO:0010200	1.00E-04	0.01189	response to chitin	7
GO:0010227	0.013799	0.446618	floral organ abscission	2
GO:0010427	0.012799	0.424297	abscisic acid binding	5
GO:0010466	0.0002	0.019889	negative regulation of peptidase activity	6
GO:0010951	1.00E-04	0.01189	negative regulation of endopeptidase activity	13
GO:0015112	0.012599	0.420214	nitrate transmembrane transporter activity	3
GO:0015114	0.043296	0.886994	phosphate ion transmembrane transporter activity	2
GO:0015116	0.028697	0.654984	sulfate transmembrane transporter activity	4
GO:0015238	1.00E-04	0.01189	NA	11
GO:0015297	0.0002	0.019889	antiporter activity	16
GO:0015940	0.0009	0.061531	pantothenate biosynthetic process	2
GO:0016114	0.0024	0.141147	terpenoid biosynthetic process	4
GO:0016125	0.007499	0.303859	sterol metabolic process	6
GO:0016207	0.0007	0.052447	4-coumarate-CoA ligase activity	3
GO:0016210	1.00E-04	0.01189	naringenin-chalcone synthase activity	7
GO:0016298	0.0039	0.202025	lipase activity	7
GO:0016301	0.022498	0.600306	kinase activity	64
GO:0016310	0.028597	0.654984	phosphorylation	65
GO:0016405	0.033097	0.715569	CoA-ligase activity	3
GO:0016412	0.032097	0.710807	serine O-acyltransferase activity	2
GO:0016491	1.00E-04	0.01189	oxidoreductase activity	164
GO:0016540	0.032597	0.713217	protein autoprocessing	2
GO:0016616	1.00E-04	0.01189	oxidoreductase activity, acting on the CH-OH group of donors	22
GO:0016639	0.0015	0.092182	oxidoreductase activity, acting on the CH-NH2 group of donors	4
GO:0016705	1.00E-04	0.01189	oxidoreductase activity, acting on paired donors	34
GO:0016709	1.00E-04	0.01189	oxidoreductase activity, acting on paired donors	25
GO:0016710	0.0032	0.180436	trans-cinnamate 4-monooxygenase activity	2
GO:0016740	1.00E-04	0.01189	transferase activity	170
GO:0016744	0.005	0.227894	transketolase or transaldolase activity	3
GO:0016746	0.0011	0.074277	acyltransferase activity	20

GO:0016747	1.00E-04	0.01189	acyltransferase activity, transferring groups other than amino-acyl groups	24
GO:0016757	0.002	0.120208	glycosyltransferase activity	39
GO:0016758	0.0005	0.041435	hexosyltransferase activity	13
GO:0016773	0.028897	0.654984	phosphotransferase activity, alcohol group as acceptor	5
GO:0016776	0.032497	0.713217	phosphotransferase activity, phosphate group as acceptor	2
GO:0016798	0.0006	0.045579	hydrolase activity, acting on glycosyl bonds	29
GO:0016829	1.00E-04	0.01189	lyase activity	26
GO:0016830	0.038696	0.810988	carbon-carbon lyase activity	3
GO:0016836	0.0006	0.045579	hydro-lyase activity	5
GO:0016841	0.006499	0.275593	ammonia-lyase activity	3
GO:0016846	0.008499	0.332074	carbon-sulfur lyase activity	3
GO:0016866	0.007699	0.307407	intramolecular transferase activity	4
GO:0016872	0.010299	0.361124	intramolecular lyase activity	3
GO:0016881	0.025497	0.64099	acid-amino acid ligase activity	4
GO:0016998	0.019598	0.536006	cell wall macromolecule catabolic process	3
GO:0017076	0.025897	0.64099	purine nucleotide binding	2
GO:0018106	0.0027	0.157101	peptidyl-histidine phosphorylation	4
GO:0018580	0.040996	0.852652	nitronate monooxygenase activity	1
GO:0019158	0.0041	0.202025	mannokinase activity	3
GO:0019318	0.0015	0.092182	hexose metabolic process	4
GO:0019478	0.028297	0.654984	D-amino acid catabolic process	1
GO:0019521	0.0013	0.082678	D-gluconate metabolic process	3
GO:0019762	1.00E-04	0.01189	glucosinolate catabolic process	8
GO:0019853	0.008599	0.333598	L-ascorbic acid biosynthetic process	3
GO:0020037	1.00E-04	0.01189	heme binding	62
GO:0022857	0.021398	0.579437	transmembrane transporter activity	26
GO:0030154	0.0002	0.019889	cell differentiation	19
GO:0030170	0.023198	0.606565	pyridoxal phosphate binding	11
GO:0030414	0.0002	0.019889	peptidase inhibitor activity	6
GO:0030523	0.0021	0.124846	dihydrolipoamide S-acyltransferase activity	2
GO:0030599	0.023798	0.613709	pectinesterase activity	5
GO:0030639	1.00E-04	0.01189	polyketide biosynthetic process	7
GO:0031405	0.007499	0.303859	lipoic acid binding	2
GO:0031956	0.023398	0.606565	medium-chain fatty acid-CoA ligase activity	2
GO:0032451	0.043296	0.886994	demethylase activity	2
GO:0033345	0.014099	0.448368	asparagine catabolic process via L-aspartate	2
GO:0033356	0.044096	0.893344	UDP-L-arabinose metabolic process	2
GO:0033387	0.028797	0.654984	putrescine biosynthetic process from ornithine	1
GO:0034219	0.010299	0.361124	carbohydrate transmembrane transport	5
GO:0035435	0.005199	0.235051	phosphate ion transmembrane transport	4
GO:0038199	0.0002	0.019889	ethylene receptor activity	4
GO:0042343	1.00E-04	0.01189	indole glucosinolate metabolic process	8
GO:0042545	0.015098	0.466603	cell wall modification	5
GO:0042742	0.0049	0.227121	defense response to bacterium	9

GO:0042744	1.00E-04	0.01189	hydrogen peroxide catabolic process	20
GO:0042910	1.00E-04	0.01189	xenobiotic transmembrane transporter activity	11
GO:0042973	0.008499	0.332074	glucan endo-1,3-beta-D-glucosidase activity	7
GO:0043086	0.019098	0.527609	negative regulation of catalytic activity	7
GO:0043231	0.027397	0.654984	intracellular membrane-bounded organelle	34
GO:0043565	1.00E-04	0.01189	sequence-specific DNA binding	69
GO:0044271	0.026497	0.64418	cellular nitrogen compound biosynthetic process	1
GO:0045254	0.0003	0.027347	pyruvate dehydrogenase complex	3
GO:0045330	0.015098	0.466603	aspartyl esterase activity	5
GO:0045332	0.017798	0.512401	phospholipid translocation	4
GO:0045430	0.012899	0.425036	chalcone isomerase activity	2
GO:0045490	0.021698	0.584666	pectin catabolic process	6
GO:0045548	0.010899	0.368006	phenylalanine ammonia-lyase activity	3
GO:0045551	0.033897	0.729978	cinnamyl-alcohol dehydrogenase activity	2
GO:0046148	0.014999	0.466603	pigment biosynthetic process	3
GO:0046177	0.0039	0.202025	D-gluconate catabolic process	3
GO:0046294	0.024798	0.627974	formaldehyde catabolic process	3
GO:0046423	0.030397	0.68144	allene-oxide cyclase activity	2
GO:0046658	0.010699	0.36577	anchored component of plasma membrane	13
GO:0046835	0.018398	0.516249	carbohydrate phosphorylation	5
GO:0046872	1.00E-04	0.01189	metal ion binding	149
GO:0046910	0.038496	0.8099	pectinesterase inhibitor activity	4
GO:0046912	0.016798	0.496956	acyltransferase, acyl groups converted into alkyl on transfer	3
GO:0047372	0.0038	0.202025	acylglycerol lipase activity	3
GO:0047834	0.0008	0.055387	D-threo-aldose 1-dehydrogenase activity	7
GO:0048029	0.038496	0.8099	monosaccharide binding	2
GO:0048531	0.0047	0.227121	beta-1,3-galactosyltransferase activity	2
GO:0048544	0.029097	0.654984	recognition of pollen	7
GO:0050105	0.016898	0.496956	L-gulonolactone oxidase activity	2
GO:0050486	0.032597	0.713217	intramolecular transferase activity, transferring hydroxy groups	1
GO:0050660	0.027597	0.654984	flavin adenine dinucleotide binding	12
GO:0050661	0.0004	0.035287	NADP binding	12
GO:0050793	0.004	0.202025	regulation of developmental process	2
GO:0050832	0.006799	0.283911	defense response to fungus	7
GO:0050982	0.010699	0.36577	detection of mechanical stimulus	2
GO:0051091	0.022698	0.602702	positive regulation of DNA-binding transcription factor activity	2
GO:0051119	0.0049	0.227121	sugar transmembrane transporter activity	5
GO:0051156	0.0003	0.027347	glucose 6-phosphate metabolic process	5
GO:0051176	0.028397	0.654984	positive regulation of sulfur metabolic process	1
GO:0051213	0.034697	0.744275	dioxygenase activity	14
GO:0051287	0.0008	0.055387	NAD binding	14
GO:0051604	0.036496	0.773779	protein maturation	2
GO:0051740	0.0002	0.019889	ethylene binding	4

GO:0051903	0.018098	0.512938	S-(hydroxymethyl)glutathione dehydrogenase activity	3
GO:0052691	0.044096	0.893344	UDP-arabinopyranose mutase activity	2
GO:0052865	0.0043	0.209988	1-deoxy-D-xylulose 5-phosphate biosynthetic process	3
GO:0055085	0.005799	0.251768	transmembrane transport	57
GO:0055114	0.005699	0.249407	NA	9
GO:0061158	0.026097	0.64303	3'-UTR-mediated mRNA destabilization	2
GO:0061408	0.009499	0.35108	positive regulation of transcription from RNA polymerase II	5
GO:0070988	0.043296	0.886994	demethylation	2
GO:0071281	0.043996	0.893344	cellular response to iron ion	3
GO:0071398	0.0049	0.227121	cellular response to fatty acid	3
GO:0071669	0.029097	0.654984	plant-type cell wall organization or biogenesis	2
GO:0071732	0.005599	0.247008	cellular response to nitric oxide	3
GO:0071949	0.010799	0.366895	FAD binding	9
GO:0080030	0.019298	0.530454	methyl indole-3-acetate esterase activity	3
GO:0080043	1.00E-04	0.01189	quercetin 3-O-glucosyltransferase activity	17
GO:0080044	1.00E-04	0.01189	quercetin 7-O-glucosyltransferase activity	17
GO:0080163	0.047295	0.929219	regulation of protein serine/threonine phosphatase activity	4
GO:0097054	0.025597	0.64099	L-glutamate biosynthetic process	2
GO:0097249	0.028197	0.654984	NA	1
GO:0098542	0.0004	0.035287	defense response to other organism	8
GO:0098869	1.00E-04	0.01189	cellular oxidant detoxification	24
GO:0102128	1.00E-04	0.01189	chalcone synthase activity	7
GO:0140326	0.010099	0.358711	ATPase-coupled intramembrane lipid transporter activity	4
GO:1900150	0.046995	0.929219	regulation of defense response to fungus	2
GO:1901564	0.0005	0.041435	organonitrogen compound metabolic process	4
GO:1901700	0.018498	0.516249	response to oxygen-containing compound	4
GO:1902358	0.028697	0.654984	sulfate transmembrane transport	4
GO:1990961	1.00E-04	0.01189	xenobiotic detoxification by transmembrane export	11

Appendix C - Differentially expressed and significantly up-enriched gene ontology (GO) term associated gene numbers represented between comparison of non-pre-treated MP-inoculated treatment vs non-pre-treated agar plug-inoculated mock control in the susceptible genotype (Pharaoh).

GO	*p*-value	*q*-value	Term	Gene No
GO:0000166	0.019598	1	nucleotide binding	40
GO:0000325	0.015398	1	plant-type vacuole	3
GO:0000421	0.043296	1	autophagosome membrane	1
GO:0002229	0.0017	0.251253	defense response to oomycetes	4
GO:0003677	0.0019	0.273423	DNA binding	35
GO:0003700	1.00E-04	0.024857	DNA-binding transcription factor activity	33
GO:0003855	0.036096	1	3-dehydroquinate dehydratase activity	1
GO:0004497	0.0003	0.060761	monooxygenase activity	11
GO:0004523	0.020798	1	RNA-DNA hybrid ribonuclease activity	2
GO:0004525	0.017898	1	ribonuclease III activity	2
GO:0004556	0.042296	1	alpha-amylase activity	1
GO:0004568	0.033097	1	chitinase activity	2
GO:0004659	0.034397	1	prenyltransferase activity	2
GO:0004672	1.00E-04	0.024857	protein kinase activity	44
GO:0004674	1.00E-04	0.024857	protein serine/threonine kinase activity	30
GO:0004675	0.010199	0.845125	transmembrane receptor protein serine/threonine kinase activity	7
GO:0004764	0.036096	1	shikimate 3-dehydrogenase (NADP+) activity	1
GO:0004784	0.007799	0.743368	superoxide dismutase activity	2
GO:0004970	1.00E-04	0.024857	ionotropic glutamate receptor activity	4
GO:0005102	0.0041	0.533825	signaling receptor binding	2
GO:0005274	0.026297	1	allantoin:proton symporter activity	1
GO:0005385	0.023098	1	zinc ion transmembrane transporter activity	2
GO:0005506	0.005	0.619758	iron ion binding	10
GO:0005509	0.0003	0.060761	calcium ion binding	12
GO:0005516	0.001	0.165711	calmodulin binding	8
GO:0005524	0.0009	0.158762	ATP binding	52
GO:0005886	1.00E-04	0.024857	plasma membrane	53
GO:0005887	0.0027	0.369121	integral component of plasma membrane	7
GO:0005901	0.008299	0.743368	caveola	1
GO:0006355	1.00E-04	0.024857	regulation of transcription, DNA-templated	41

GO:0006468	1.00E-04	0.024857	protein phosphorylation	44
GO:0006801	0.007799	0.743368	superoxide metabolic process	2
GO:0006874	0.025097	1	cellular calcium ion homeostasis	2
GO:0006952	1.00E-04	0.024857	defense response	17
GO:0007166	0.0017	0.251253	cell surface receptor signaling pathway	4
GO:0007178	1.00E-04	0.024857	protein serine/threonine kinase signaling pathway	6
GO:0008171	0.009899	0.832887	O-methyltransferase activity	3
GO:0009505	0.007099	0.743368	plant-type cell wall	5
GO:0009506	0.023298	1	plasmodesma	9
GO:0009705	0.027997	1	plant-type vacuole membrane	3
GO:0009755	0.008299	0.743368	hormone-mediated signaling pathway	3
GO:0010333	0.0007	0.131997	terpene synthase activity	3
GO:0015112	0.012599	0.984322	nitrate transmembrane transporter activity	2
GO:0015276	1.00E-04	0.024857	ligand-gated ion channel activity	4
GO:0015333	0.016398	1	peptide:proton symporter activity	3
GO:0015369	0.007899	0.743368	calcium:proton antiporter activity	2
GO:0015505	0.026297	1	uracil:cation symporter activity	1
GO:0015720	0.026297	1	allantoin transport	1
GO:0015833	1.00E-04	0.024857	peptide transport	3
GO:0016020	1.00E-04	0.024857	membrane	132
GO:0016021	1.00E-04	0.024857	integral component of membrane	127
GO:0016102	0.0006	0.117181	diterpenoid biosynthetic process	3
GO:0016301	1.00E-04	0.024857	kinase activity	34
GO:0016310	1.00E-04	0.024857	phosphorylation	34
GO:0016442	0.007799	0.743368	RISC complex	2
GO:0016491	0.005799	0.67483	oxidoreductase activity	28
GO:0016602	0.025597	1	CCAAT-binding factor complex	2
GO:0016705	0.001	0.165711	oxidoreductase activity, incorporation or reduction of molecular oxygen	10
GO:0016709	0.0012	0.18749	oxidoreductase activity	7
GO:0019430	0.014099	1	removal of superoxide radicals	2
GO:0019438	0.005099	0.619758	aromatic compound biosynthetic process	3
GO:0020037	1.00E-04	0.024857	heme binding	14
GO:0022857	0.012399	0.982737	transmembrane transporter activity	11
GO:0030001	1.00E-04	0.024857	metal ion transport	10
GO:0030246	0.0012	0.18749	carbohydrate binding	7
GO:0030247	1.00E-04	0.024857	polysaccharide binding	8

GO:0030422	0.0025	0.350542	production of siRNA involved in RNA interference	3
GO:0030433	0.031697	1	ubiquitin-dependent ERAD pathway	3
GO:0031072	0.024198	1	heat shock protein binding	3
GO:0033214	0.047095	1	siderophore-dependent iron import into cell	1
GO:0033511	0.008599	0.743368	luteolin biosynthetic process	1
GO:0033759	0.016898	1	flavone synthase activity	1
GO:0034220	0.008699	0.743368	ion transmembrane transport	6
GO:0034620	0.0042	0.534128	cellular response to unfolded protein	3
GO:0035529	0.007899	0.743368	NADH pyrophosphatase activity	2
GO:0035672	0.0003	0.060761	oligopeptide transmembrane transport	4
GO:0035673	1.00E-04	0.024857	oligopeptide transmembrane transporter activity	7
GO:0038023	0.0003	0.060761	signaling receptor activity	5
GO:0042026	0.022698	1	protein refolding	3
GO:0042343	0.025397	1	indole glucosinolate metabolic process	2
GO:0042644	0.008399	0.743368	chloroplast nucleoid	2
GO:0042742	0.015998	1	defense response to bacterium	4
GO:0042744	0.032197	1	hydrogen peroxide catabolic process	4
GO:0043565	1.00E-04	0.024857	sequence-specific DNA binding	28
GO:0044183	0.012299	0.982737	protein folding chaperone	3
GO:0044853	0.008299	0.743368	plasma membrane raft	1
GO:0046777	0.0002	0.047552	protein autophosphorylation	11
GO:0046872	0.003	0.400131	metal ion binding	43
GO:0046873	0.007999	0.743368	metal ion transmembrane transporter activity	3
GO:0047631	0.006499	0.725407	ADP-ribose diphosphatase activity	2
GO:0051082	0.033897	1	unfolded protein binding	6
GO:0051085	0.045295	1	chaperone cofactor-dependent protein refolding	3
GO:0051213	0.024598	1	dioxygenase activity	6
GO:0051553	0.008599	0.743368	flavone biosynthetic process	1
GO:0051787	0.0008	0.145825	misfolded protein binding	4
GO:0051980	0.047095	1	iron-nicotianamine transmembrane transporter activity	1
GO:0052689	0.029697	1	carboxylic ester hydrolase activity	2
GO:0055085	1.00E-04	0.024857	transmembrane transport	28
GO:0071249	0.024498	1	cellular response to nitrate	1
GO:0071577	0.023098	1	zinc ion transmembrane transport	2
GO:0071705	0.042196	1	nitrogen compound transport	1
GO:0072659	0.031797	1	protein localization to plasma membrane	1
GO:0080142	1.00E-04	0.024857	regulation of salicylic acid biosynthetic process	6

GO:0090502	0.011199	0.914129	RNA phosphodiester bond hydrolysis, endonucleolytic	4
GO:0098542	0.018398	1	defense response to other organism	3
GO:0102767	0.007199	0.743368	flavanone 4'-O-methyltransferase activity	1
GO:0103025	0.042296	1	alpha-amylase activity (releasing maltohexaose)	1
GO:0106310	0.005699	0.67483	protein serine kinase activity	7
GO:1903791	0.026297	1	uracil transmembrane transport	1
GO:1904680	0.016398	1	peptide transmembrane transporter activity	3

Appendix D - Differentially expressed and significantly down-enriched gene ontology (GO) term associated gene numbers represented between comparison of non-pre-treated MP-inoculated treatment vs non-pre-treated agar plug-inoculated mock control in the susceptible genotype (Pharaoh).

GO	*p*-value	*q*-value	Term	Gene No.
GO:0000103	0.034897	0.815594	sulfate assimilation	3
GO:0000287	0.0008	0.059118	magnesium ion binding	17
GO:0000325	0.027897	0.679927	plant-type vacuole	6
GO:0000976	0.005799	0.245868	transcription cis-regulatory region binding	16
GO:0001561	0.0017	0.11337	fatty acid alpha-oxidation	2
GO:0001678	0.005	0.217002	cellular glucose homeostasis	3
GO:0003700	1.00E-04	0.013338	DNA-binding transcription factor activity	86
GO:0003824	1.00E-04	0.013338	catalytic activity	85
GO:0003841	0.037696	0.862597	1-acylglycerol-3-phosphate O-acyltransferase activity	2
GO:0003864	0.028297	0.68175	3-methyl-2-oxobutanoate hydroxymethyltransferase activity	1
GO:0003878	0.012199	0.401898	ATP citrate synthase activity	3
GO:0003935	0.014399	0.444891	GTP cyclohydrolase II activity	2
GO:0003950	0.006599	0.269342	NAD+ ADP-ribosyltransferase activity	3
GO:0003954	0.009299	0.336799	NADH dehydrogenase activity	4
GO:0003955	0.027197	0.67304	NAD(P)H dehydrogenase (quinone) activity	3
GO:0004020	0.033697	0.797779	adenylylsulfate kinase activity	2
GO:0004022	0.028097	0.679927	alcohol dehydrogenase (NAD+) activity	1
GO:0004032	0.010399	0.355449	alditol:NADP+ 1-oxidoreductase activity	4
GO:0004033	0.0018	0.118593	aldo-keto reductase (NADP) activity	4
GO:0004067	0.0006	0.046872	asparaginase activity	3
GO:0004084	0.035896	0.828344	branched-chain-amino-acid transaminase activity	2
GO:0004089	0.023598	0.605894	carbonate dehydratase activity	3
GO:0004097	0.006799	0.275362	catechol oxidase activity	4
GO:0004324	0.031897	0.758451	ferredoxin-NADP+ reductase activity	2
GO:0004340	0.005	0.217002	glucokinase activity	3
GO:0004345	0.0039	0.193882	glucose-6-phosphate dehydrogenase activity	3
GO:0004352	0.023498	0.605894	glutamate dehydrogenase (NAD+) activity	2
GO:0004364	1.00E-04	0.013338	glutathione transferase activity	22
GO:0004396	0.005	0.217002	hexokinase activity	3

GO:0004450	0.026297	0.656214	isocitrate dehydrogenase (NADP+) activity	2
GO:0004497	1.00E-04	0.013338	monooxygenase activity	35
GO:0004553	0.0019	0.119426	hydrolase activity, hydrolyzing O-glycosyl compounds	25
GO:0004564	0.011699	0.390127	beta-fructofuranosidase activity	3
GO:0004568	1.00E-04	0.013338	chitinase activity	9
GO:0004575	0.011699	0.390127	sucrose alpha-glucosidase activity	3
GO:0004601	1.00E-04	0.013338	peroxidase activity	24
GO:0004611	0.015798	0.464525	phosphoenolpyruvate carboxykinase activity	2
GO:0004612	0.015798	0.464525	phosphoenolpyruvate carboxykinase (ATP) activity	2
GO:0004616	0.0019	0.119426	phosphogluconate dehydrogenase (decarboxylating) activity	3
GO:0004619	0.0037	0.189096	phosphoglycerate mutase activity	3
GO:0004620	0.014099	0.443726	phospholipase activity	4
GO:0004657	0.009099	0.331753	proline dehydrogenase activity	2
GO:0004672	0.0047	0.214181	protein kinase activity	82
GO:0004674	0.0031	0.169522	protein serine/threonine kinase activity	56
GO:0004781	0.008399	0.312483	sulfate adenylyltransferase (ATP) activity	2
GO:0004864	0.009899	0.349275	protein phosphatase inhibitor activity	6
GO:0004866	1.00E-04	0.013338	endopeptidase inhibitor activity	10
GO:0004867	0.0003	0.028781	serine-type endopeptidase inhibitor activity	5
GO:0005506	1.00E-04	0.013338	iron ion binding	36
GO:0005536	0.005	0.217002	glucose binding	3
GO:0005576	1.00E-04	0.013338	extracellular region	63
GO:0005758	0.015898	0.464965	mitochondrial intermembrane space	3
GO:0005775	0.017898	0.499415	vacuolar lumen	2
GO:0005868	0.009599	0.343119	cytoplasmic dynein complex	3
GO:0005886	1.00E-04	0.013338	plasma membrane	110
GO:0005975	1.00E-04	0.013338	carbohydrate metabolic process	50
GO:0006006	0.0034	0.180512	glucose metabolic process	7
GO:0006032	1.00E-04	0.013338	chitin catabolic process	7
GO:0006085	0.012099	0.40102	acetyl-CoA biosynthetic process	3
GO:0006096	0.0003	0.028781	glycolytic process	17
GO:0006098	0.0006	0.046872	pentose-phosphate shunt	8
GO:0006116	0.0027	0.157073	NADH oxidation	4
GO:0006123	0.009899	0.349275	mitochondrial electron transport, cytochrome c to oxygen	3
GO:0006351	0.0006	0.046872	transcription, DNA-templated	38
GO:0006355	0.0038	0.190643	regulation of transcription, DNA-templated	102
GO:0006468	0.013299	0.430358	protein phosphorylation	82

GO:0006520	0.0021	0.129031	cellular amino acid metabolic process	9
GO:0006535	0.017198	0.487344	cysteine biosynthetic process from serine	4
GO:0006538	0.003	0.167402	glutamate catabolic process	4
GO:0006541	0.043296	0.954774	glutamine metabolic process	5
GO:0006559	0.035496	0.826085	L-phenylalanine catabolic process	3
GO:0006560	0.009099	0.331753	proline metabolic process	2
GO:0006562	0.009099	0.331753	proline catabolic process	2
GO:0006598	0.015598	0.464525	polyamine catabolic process	3
GO:0006631	0.034097	0.803768	fatty acid metabolic process	11
GO:0006654	0.023998	0.613284	phosphatidic acid biosynthetic process	2
GO:0006739	0.026297	0.656214	NADP metabolic process	2
GO:0006749	1.00E-04	0.013338	glutathione metabolic process	22
GO:0006855	0.008299	0.310878	xenobiotic transmembrane transport	6
GO:0006952	1.00E-04	0.013338	defense response	45
GO:0006955	1.00E-04	0.013338	immune response	5
GO:0006979	1.00E-04	0.013338	response to oxidative stress	24
GO:0008061	1.00E-04	0.013338	chitin binding	7
GO:0008152	1.00E-04	0.013338	metabolic process	41
GO:0008194	1.00E-04	0.013338	UDP-glycosyltransferase activity	28
GO:0008299	0.022298	0.586281	isoprenoid biosynthetic process	6
GO:0008422	0.0006	0.046872	beta-glucosidase activity	9
GO:0008483	0.0004	0.03472	transaminase activity	11
GO:0008652	0.009999	0.350542	cellular amino acid biosynthetic process	14
GO:0008661	0.006999	0.275362	1-deoxy-D-xylulose-5-phosphate synthase activity	3
GO:0008686	0.014399	0.444891	3,4-dihydroxy-2-butanone-4-phosphate synthase activity	2
GO:0008734	0.023298	0.605894	L-aspartate oxidase activity	1
GO:0008798	0.0006	0.046872	beta-aspartyl-peptidase activity	3
GO:0009001	0.038996	0.877653	serine O-acetyltransferase activity	2
GO:0009051	1.00E-04	0.013338	pentose-phosphate shunt, oxidative branch	6
GO:0009058	0.004	0.197061	biosynthetic process	13
GO:0009081	0.014199	0.443726	branched-chain amino acid metabolic process	2
GO:0009228	0.038496	0.877231	thiamine biosynthetic process	3
GO:0009346	0.021398	0.573651	ATP-independent citrate lyase complex	2
GO:0009505	0.048295	1	plant-type cell wall	9
GO:0009607	0.006199	0.258812	response to biotic stimulus	6
GO:0009611	0.025397	0.640086	response to wounding	5
GO:0009626	0.0003	0.028781	plant-type hypersensitive response	5

GO:0009651	0.047995	1	response to salt stress	7
GO:0009694	0.039196	0.878538	jasmonic acid metabolic process	3
GO:0009695	0.0034	0.180512	jasmonic acid biosynthetic process	4
GO:0009696	0.015498	0.464525	salicylic acid metabolic process	3
GO:0009698	1.00E-04	0.013338	phenylpropanoid metabolic process	5
GO:0009717	0.013999	0.443726	isoflavonoid biosynthetic process	2
GO:0009735	0.028597	0.685955	response to cytokinin	4
GO:0009800	0.007099	0.275362	cinnamic acid biosynthetic process	3
GO:0009807	0.010199	0.355275	lignan biosynthetic process	4
GO:0009808	0.0046	0.213177	lignin metabolic process	2
GO:0009809	0.005099	0.219599	lignin biosynthetic process	4
GO:0009813	1.00E-04	0.013338	flavonoid biosynthetic process	11
GO:0009873	1.00E-04	0.013338	ethylene-activated signaling pathway	28
GO:0009901	0.006899	0.275362	anther dehiscence	2
GO:0010026	0.048095	1	trichome differentiation	2
GO:0010047	0.006899	0.275362	fruit dehiscence	2
GO:0010133	0.024898	0.630391	proline catabolic process to glutamate	2
GO:0010155	0.020598	0.571453	regulation of proton transport	2
GO:0010181	0.0002	0.022785	FMN binding	11
GO:0010200	1.00E-04	0.013338	response to chitin	10
GO:0010227	0.007299	0.281125	floral organ abscission	2
GO:0010279	0.021698	0.578856	indole-3-acetic acid amido synthetase activity	2
GO:0010325	0.016398	0.477035	raffinose family oligosaccharide biosynthetic process	3
GO:0010427	0.0043	0.208092	abscisic acid binding	6
GO:0010466	0.0002	0.022785	negative regulation of peptidase activity	6
GO:0010951	1.00E-04	0.013338	negative regulation of endopeptidase activity	16
GO:0012501	0.0003	0.028781	programmed cell death	5
GO:0015114	0.048395	1	phosphate ion transmembrane transporter activity	2
GO:0015247	0.017298	0.487651	aminophospholipid flippase activity	2
GO:0015914	0.006599	0.269342	phospholipid transport	6
GO:0016114	0.0003	0.028781	terpenoid biosynthetic process	5
GO:0016125	0.036596	0.840947	sterol metabolic process	5
GO:0016207	0.0008	0.059118	4-coumarate-CoA ligase activity	3
GO:0016210	1.00E-04	0.013338	naringenin-chalcone synthase activity	6
GO:0016298	0.045595	0.98953	lipase activity	5
GO:0016301	0.0037	0.189096	kinase activity	74
GO:0016310	0.0019	0.119426	phosphorylation	78

GO:0016405	0.041996	0.929858	CoA-ligase activity	3
GO:0016412	0.038996	0.877653	serine O-acyltransferase activity	2
GO:0016491	1.00E-04	0.013338	oxidoreductase activity	176
GO:0016540	0.0035	0.182282	protein autoprocessing	3
GO:0016616	1.00E-04	0.013338	oxidoreductase activity, acting on the CH-OH group of donors	20
GO:0016639	0.0016	0.109369	oxidoreductase activity, acting on the CH-NH2 group of donors	4
GO:0016705	1.00E-04	0.013338	oxidoreductase activity, acting on paired donors	32
GO:0016709	1.00E-04	0.013338	oxidoreductase activity, acting on paired donors	24
GO:0016710	0.0046	0.213177	trans-cinnamate 4-monooxygenase activity	2
GO:0016740	1.00E-04	0.013338	transferase activity	191
GO:0016744	0.006999	0.275362	transketolase or transaldolase activity	3
GO:0016746	0.031297	0.747435	acyltransferase activity	17
GO:0016747	1.00E-04	0.013338	acyltransferase activity	27
GO:0016757	0.0009	0.064758	glycosyltransferase activity	44
GO:0016758	0.0041	0.200184	hexosyltransferase activity	11
GO:0016760	0.048695	1	cellulose synthase (UDP-forming) activity	5
GO:0016798	0.0002	0.022785	hydrolase activity, acting on glycosyl bonds	32
GO:0016829	0.0002	0.022785	lyase activity	26
GO:0016830	0.0016	0.109369	carbon-carbon lyase activity	5
GO:0016836	0.0016	0.109369	hydro-lyase activity	5
GO:0016841	0.007099	0.275362	ammonia-lyase activity	3
GO:0016846	0.010799	0.366828	carbon-sulfur lyase activity	3
GO:0016872	0.015298	0.464525	intramolecular lyase activity	3
GO:0016881	0.0007	0.053914	acid-amino acid ligase activity	6
GO:0016998	0.023598	0.605894	cell wall macromolecule catabolic process	3
GO:0017076	0.028097	0.679927	purine nucleotide binding	2
GO:0019158	0.005	0.217002	mannokinase activity	3
GO:0019318	0.0026	0.152881	hexose metabolic process	4
GO:0019344	0.035896	0.828344	cysteine biosynthetic process	4
GO:0019478	0.040196	0.897273	D-amino acid catabolic process	1
GO:0019499	0.0047	0.214181	cyanide metabolic process	2
GO:0019521	0.0019	0.119426	D-gluconate metabolic process	3
GO:0019762	0.0003	0.028781	glucosinolate catabolic process	5
GO:0020037	1.00E-04	0.013338	heme binding	63
GO:0030154	0.046195	0.998587	cell differentiation	13
GO:0030170	0.0046	0.213177	pyridoxal phosphate binding	14
GO:0030198	0.016998	0.484186	extracellular matrix organization	3

GO:0030247	0.0024	0.142655	polysaccharide binding	8
GO:0030286	0.020898	0.571453	dynein complex	3
GO:0030414	0.0002	0.022785	peptidase inhibitor activity	6
GO:0030574	0.016998	0.484186	collagen catabolic process	3
GO:0030599	0.034897	0.815594	pectinesterase activity	5
GO:0030639	1.00E-04	0.013338	polyketide biosynthetic process	6
GO:0031012	0.016998	0.484186	extracellular matrix	3
GO:0031225	0.016898	0.484186	anchored component of membrane	6
GO:0031956	0.0029	0.165193	medium-chain fatty acid-CoA ligase activity	3
GO:0033345	0.0006	0.046872	asparagine catabolic process via L-aspartate	3
GO:0035435	0.007899	0.297936	phosphate ion transmembrane transport	4
GO:0036149	0.006599	0.269342	phosphatidylinositol acyl-chain remodeling	2
GO:0038023	0.038796	0.877653	signaling receptor activity	6
GO:0042343	1.00E-04	0.013338	indole glucosinolate metabolic process	8
GO:0042545	0.021998	0.581188	cell wall modification	5
GO:0042626	0.0002	0.022785	ATPase-coupled transmembrane transporter activity	16
GO:0042742	0.0006	0.046872	defense response to bacterium	11
GO:0042744	1.00E-04	0.013338	hydrogen peroxide catabolic process	20
GO:0042910	0.0029	0.165193	xenobiotic transmembrane transporter activity	8
GO:0042973	0.014499	0.445464	glucan endo-1,3-beta-D-glucosidase activity	7
GO:0043565	1.00E-04	0.013338	sequence-specific DNA binding	64
GO:0044318	0.023298	0.605894	L-aspartate:fumarate oxidoreductase activity	1
GO:0045330	0.021998	0.581188	aspartyl esterase activity	5
GO:0045332	0.0002	0.022785	phospholipid translocation	8
GO:0045430	0.021098	0.573651	chalcone isomerase activity	2
GO:0045490	0.011099	0.37469	pectin catabolic process	7
GO:0045505	0.020898	0.571453	dynein intermediate chain binding	3
GO:0045548	0.012899	0.419899	phenylalanine ammonia-lyase activity	3
GO:0045551	0.044196	0.966823	cinnamyl-alcohol dehydrogenase activity	2
GO:0045927	0.043996	0.966313	positive regulation of growth	3
GO:0046148	0.0038	0.190643	pigment biosynthetic process	4
GO:0046177	0.0044	0.209228	D-gluconate catabolic process	3
GO:0046274	0.007899	0.297936	lignin catabolic process	5
GO:0046423	0.040896	0.909186	allene-oxide cyclase activity	2
GO:0046592	0.021298	0.573651	polyamine oxidase activity	3
GO:0046658	0.010299	0.355449	anchored component of plasma membrane	14
GO:0046777	0.012499	0.409315	protein autophosphorylation	19

GO:0046872	0.0004	0.03472	metal ion binding	151
GO:0047372	0.045595	0.98953	acylglycerol lipase activity	2
GO:0047834	0.0004	0.03472	D-threo-aldose 1-dehydrogenase activity	8
GO:0048046	0.015698	0.464525	apoplast	14
GO:0048194	0.017698	0.496367	Golgi vesicle budding	3
GO:0048531	0.0049	0.217002	beta-1,3-galactosyltransferase activity	2
GO:0048544	0.0012	0.085223	recognition of pollen	10
GO:0050017	0.0022	0.133673	L-3-cyanoalanine synthase activity	2
GO:0050660	0.0034	0.180512	flavin adenine dinucleotide binding	15
GO:0050661	0.0009	0.064758	NADP binding	12
GO:0050793	0.0044	0.209228	regulation of developmental process	2
GO:0050832	0.0003	0.028781	defense response to fungus	10
GO:0051091	0.027997	0.679927	positive regulation of DNA-binding transcription	2
GO:0051156	0.0031	0.169522	glucose 6-phosphate metabolic process	4
GO:0051176	0.027897	0.679927	positive regulation of sulfur metabolic process	1
GO:0051604	0.003	0.167402	protein maturation	3
GO:0051959	0.020898	0.571453	dynein light intermediate chain binding	3
GO:0052654	0.014199	0.443726	L-leucine transaminase activity	2
GO:0052655	0.014199	0.443726	L-valine transaminase activity	2
GO:0052656	0.014199	0.443726	L-isoleucine transaminase activity	2
GO:0052716	0.007899	0.297936	hydroquinone:oxygen oxidoreductase activity	5
GO:0052865	0.005999	0.25239	1-deoxy-D-xylulose 5-phosphate biosynthetic process	3
GO:0061408	0.010399	0.355449	positive regulation of transcription from RNA polymerase II	5
GO:0071949	0.005199	0.222156	FAD binding	10
GO:0080030	0.0023	0.138214	methyl indole-3-acetate esterase activity	4
GO:0080031	0.015498	0.464525	methyl salicylate esterase activity	3
GO:0080032	0.015498	0.464525	methyl jasmonate esterase activity	3
GO:0080043	1.00E-04	0.013338	quercetin 3-O-glucosyltransferase activity	19
GO:0080044	1.00E-04	0.013338	quercetin 7-O-glucosyltransferase activity	19
GO:0097054	0.026397	0.656214	L-glutamate biosynthetic process	2
GO:0098542	0.0035	0.182282	defense response to other organism	7
GO:0098869	1.00E-04	0.013338	cellular oxidant detoxification	24
GO:0102128	1.00E-04	0.013338	chalcone synthase activity	6
GO:0106310	0.021198	0.573651	protein serine kinase activity	15
GO:0140326	0.0004	0.03472	ATPase-coupled intramembrane lipid transporter activity	6
GO:0140359	0.0003	0.028781	ABC-type transporter activity	16
GO:1990961	0.0008	0.059118	xenobiotic detoxification by transmembrane	8

GO:2000031	0.0017	0.11337	regulation of salicylic acid mediated signaling pathway	5

Appendix E - Differentially expressed and significantly up-enriched gene ontology (GO) term associated gene numbers represented between ascorbic acid pre-treated MP-inoculated treatment with the non-pre-treated MP-inoculated treatment in the resistant genotype (DT97-4290).

GO	*p*-value	*q*-value	Term	Gene No.
GO:0000079	1.00E-04	0.005948	protein serine/threonine kinase activity	28
GO:0000082	0.027897	0.464077	G1/S transition of mitotic cell cycle	4
GO:0000166	0.012599	0.266284	nucleotide binding	333
GO:0000170	0.020698	0.377599	sphingosine hydroxylase activity	3
GO:0000226	0.0022	0.074317	microtubule cytoskeleton organization	17
GO:0000247	0.034697	0.551977	C-8 sterol isomerase activity	2
GO:0000254	0.0006	0.025854	C-4 methylsterol oxidase activity	5
GO:0000278	1.00E-04	0.005948	mitotic cell cycle	40
GO:0000307	1.00E-04	0.005948	cyclin-dependent protein kinase holoenzyme complex	33
GO:0000326	0.006299	0.164959	protein storage vacuole	11
GO:0000333	0.019198	0.35497	telomerase catalytic core complex	2
GO:0000347	0.0002	0.010626	THO complex	8
GO:0000405	0.038796	0.593104	bubble DNA binding	2
GO:0000725	0.017398	0.335284	recombinational repair	5
GO:0000727	0.0006	0.025854	double-strand break repair via break-induced replication	8
GO:0000779	0.010199	0.230657	condensed chromosome, centromeric region	3
GO:0000786	1.00E-04	0.005948	nucleosome	51
GO:0000796	0.042196	0.625213	condensin complex	4
GO:0000819	0.018298	0.346526	sister chromatid segregation	4
GO:0000976	0.011199	0.247143	transcription cis-regulatory region binding	40
GO:0000978	0.049795	0.682688	DNA binding	43
GO:0000981	1.00E-04	0.005948	DNA-binding transcription factor activity	83
GO:0001676	0.0002	0.010626	long-chain fatty acid metabolic process	9
GO:0003677	1.00E-04	0.005948	DNA binding	368
GO:0003700	1.00E-04	0.005948	DNA-binding transcription factor activity	214
GO:0003721	0.019198	0.35497	telomerase RNA reverse transcriptase activity	2
GO:0003774	1.00E-04	0.005948	cytoskeletal motor activity	69
GO:0003777	1.00E-04	0.005948	microtubule motor activity	68
GO:0003824	0.022898	0.397839	catalytic activity	128
GO:0004013	0.023298	0.402234	adenosylhomocysteinase activity	2
GO:0004021	0.012799	0.267356	L-alanine:2-oxoglutarate aminotransferase activity	2

GO:0004024	0.038196	0.588867	alcohol dehydrogenase activity, zinc-dependent	4
GO:0004028	0.007199	0.18412	3-chloroallyl aldehyde dehydrogenase activity	4
GO:0004144	0.018098	0.345127	diacylglycerol O-acyltransferase activity	6
GO:0004252	0.026297	0.442848	serine-type endopeptidase activity	27
GO:0004324	0.019998	0.368515	ferredoxin-NADP+ reductase activity	2
GO:0004332	0.0014	0.052837	fructose-bisphosphate aldolase activity	5
GO:0004467	1.00E-04	0.005948	long-chain fatty acid-CoA ligase activity	9
GO:0004506	0.024498	0.420298	squalene monooxygenase activity	3
GO:0004512	0.011499	0.249735	inositol-3-phosphate synthase activity	2
GO:0004553	0.0002	0.010626	hydrolase activity, hydrolyzing O-glycosyl compounds	64
GO:0004568	0.043396	0.633345	chitinase activity	6
GO:0004760	0.0023	0.076748	serine-pyruvate transaminase activity	2
GO:0004769	0.034697	0.551977	steroid delta-isomerase activity	2
GO:0005200	0.0006	0.025854	structural constituent of cytoskeleton	11
GO:0005244	0.018998	0.354869	voltage-gated ion channel activity	2
GO:0005464	0.021298	0.382175	UDP-xylose transmembrane transporter activity	4
GO:0005506	0.035796	0.559718	iron ion binding	54
GO:0005507	0.0034	0.101674	copper ion binding	24
GO:0005524	0.0009	0.03569	ATP binding	410
GO:0005576	1.00E-04	0.005948	extracellular region	143
GO:0005618	0.0005	0.023188	cell wall	39
GO:0005634	1.00E-04	0.005948	nucleus	789
GO:0005694	1.00E-04	0.005948	chromosome	44
GO:0005764	0.041896	0.625213	lysosome	9
GO:0005773	0.012399	0.265072	vacuole	30
GO:0005819	0.0011	0.042392	spindle	14
GO:0005856	0.0003	0.014925	cytoskeleton	33
GO:0005871	1.00E-04	0.005948	kinesin complex	59
GO:0005874	1.00E-04	0.005948	microtubule	101
GO:0005875	0.025297	0.431318	microtubule associated complex	3
GO:0005880	0.0005	0.023188	nuclear microtubule	10
GO:0005884	0.048895	0.678198	actin filament	3
GO:0005886	1.00E-04	0.005948	plasma membrane	328
GO:0005938	0.009599	0.223037	cell cortex	7
GO:0005975	1.00E-04	0.005948	carbohydrate metabolic process	107
GO:0005986	0.0021	0.071826	sucrose biosynthetic process	6
GO:0006000	0.009299	0.223037	fructose metabolic process	7

GO:0006073	0.0026	0.082245	cellular glucan metabolic process	12
GO:0006081	0.007199	0.18412	cellular aldehyde metabolic process	4
GO:0006116	0.039796	0.606695	NADH oxidation	6
GO:0006268	0.0031	0.093727	DNA unwinding involved in DNA replication	9
GO:0006270	0.010799	0.242223	DNA replication initiation	9
GO:0006284	0.035896	0.559718	base-excision repair	11
GO:0006334	1.00E-04	0.005948	nucleosome assembly	44
GO:0006351	1.00E-04	0.005948	transcription, DNA-templated	122
GO:0006355	1.00E-04	0.005948	regulation of transcription, DNA-templated	362
GO:0006357	0.001	0.03937	regulation of transcription by RNA polymerase II	86
GO:0006468	0.007899	0.20015	protein phosphorylation	242
GO:0006544	0.0026	0.082245	glycine metabolic process	4
GO:0006629	0.033497	0.542388	lipid metabolic process	54
GO:0006631	0.010399	0.234212	fatty acid metabolic process	21
GO:0006633	1.00E-04	0.005948	fatty acid biosynthetic process	36
GO:0006855	0.035896	0.559718	xenobiotic transmembrane transport	12
GO:0006857	0.0003	0.014925	oligopeptide transport	9
GO:0006880	0.049695	0.682688	intracellular sequestering of iron ion	5
GO:0006996	0.049895	0.682688	organelle organization	6
GO:0007015	0.016398	0.324001	actin filament organization	14
GO:0007017	0.0029	0.090686	microtubule-based process	14
GO:0007018	1.00E-04	0.005948	microtubule-based movement	68
GO:0007019	0.0009	0.03569	microtubule depolymerization	5
GO:0007049	1.00E-04	0.005948	cell cycle	49
GO:0007052	0.0017	0.062859	mitotic spindle organization	7
GO:0007076	0.0005	0.023188	mitotic chromosome condensation	7
GO:0007088	1.00E-04	0.005948	regulation of mitotic nuclear division	24
GO:0007142	0.007999	0.201749	male meiosis II	6
GO:0007163	0.0025	0.081923	establishment or maintenance of cell polarity	9
GO:0007264	0.016598	0.326772	small GTPase mediated signal transduction	8
GO:0007266	0.014099	0.285784	Rho protein signal transduction	8
GO:0007275	0.0025	0.081923	multicellular organism development	18
GO:0008017	1.00E-04	0.005948	microtubule binding	100
GO:0008152	0.002	0.071071	metabolic process	78
GO:0008233	0.021298	0.382175	peptidase activity	61
GO:0008236	0.0026	0.082245	serine-type peptidase activity	25
GO:0008242	0.007199	0.18412	omega peptidase activity	2

GO:0008271	0.017698	0.33868	secondary active sulfate transmembrane transporter activity	6
GO:0008272	0.012699	0.266284	sulfate transport	7
GO:0008283	0.0031	0.093727	cell population proliferation	7
GO:0008284	1.00E-04	0.005948	positive regulation of cell population proliferation	25
GO:0008289	1.00E-04	0.005948	lipid binding	42
GO:0008352	0.011099	0.247143	katanin complex	3
GO:0008374	0.024998	0.427535	O-acyltransferase activity	8
GO:0008453	1.00E-04	0.005948	alanine-glyoxylate transaminase activity	4
GO:0008483	0.021798	0.386082	transaminase activity	12
GO:0008526	0.012999	0.269477	phosphatidylinositol transfer activity	4
GO:0008574	1.00E-04	0.005948	plus-end-directed microtubule motor activity	18
GO:0008725	0.0028	0.088062	DNA-3-methyladenine glycosylase activity	7
GO:0008909	0.018498	0.347905	isochorismate synthase activity	2
GO:0008911	0.012299	0.263965	lactaldehyde dehydrogenase activity	2
GO:0008942	0.048195	0.678198	nitrite reductase [NAD(P)H] activity	1
GO:0008974	0.0026	0.082245	phosphoribulokinase activity	2
GO:0009058	0.017298	0.335284	biosynthetic process	21
GO:0009157	0.043696	0.636027	deoxyribonucleoside monophosphate biosynthetic process	3
GO:0009360	0.006299	0.164959	DNA polymerase III complex	4
GO:0009409	0.011299	0.247355	response to cold	8
GO:0009414	1.00E-04	0.005948	response to water deprivation	13
GO:0009416	1.00E-04	0.005948	response to light stimulus	26
GO:0009505	0.020198	0.369711	plant-type cell wall	21
GO:0009506	0.0003	0.014925	plasmodesma	76
GO:0009507	1.00E-04	0.005948	chloroplast	170
GO:0009522	1.00E-04	0.005948	photosystem I	31
GO:0009523	1.00E-04	0.005948	photosystem II	41
GO:0009535	1.00E-04	0.005948	chloroplast thylakoid membrane	64
GO:0009536	1.00E-04	0.005948	plastid	74
GO:0009538	1.00E-04	0.005948	photosystem I reaction center	7
GO:0009570	0.0005	0.023188	chloroplast stroma	38
GO:0009574	0.021898	0.386602	preprophase band	2
GO:0009579	1.00E-04	0.005948	thylakoid	63
GO:0009610	0.0007	0.029242	response to symbiotic fungus	12
GO:0009654	1.00E-04	0.005948	photosystem II oxygen evolving complex	18
GO:0009668	0.003	0.092753	plastid membrane organization	3
GO:0009686	0.041996	0.625213	gibberellin biosynthetic process	7

GO:0009688	0.040696	0.615273	abscisic acid biosynthetic process	2
GO:0009691	0.049195	0.678198	cytokinin biosynthetic process	10
GO:0009707	0.008199	0.205845	chloroplast outer membrane	11
GO:0009725	1.00E-04	0.005948	response to hormone	17
GO:0009734	0.042396	0.625213	auxin-activated signaling pathway	57
GO:0009753	0.041896	0.625213	response to jasmonic acid	3
GO:0009765	1.00E-04	0.005948	photosynthesis, light harvesting	18
GO:0009767	0.037496	0.581351	photosynthetic electron transport chain	5
GO:0009768	1.00E-04	0.005948	photosynthesis, light harvesting in photosystem I	17
GO:0009773	0.0039	0.114131	photosynthetic electron transport in photosystem I	7
GO:0009813	0.030197	0.494815	flavonoid biosynthetic process	6
GO:0009833	1.00E-04	0.005948	plant-type primary cell wall biogenesis	15
GO:0009834	1.00E-04	0.005948	plant-type secondary cell wall biogenesis	40
GO:0009853	0.009899	0.224802	photorespiration	5
GO:0009909	0.0038	0.112407	regulation of flower development	7
GO:0009927	0.005699	0.152907	histidine phosphotransfer kinase activity	6
GO:0009941	1.00E-04	0.005948	chloroplast envelope	27
GO:0009944	0.006099	0.161266	polarity specification of adaxial/abaxial axis	4
GO:0009956	0.045095	0.649494	radial pattern formation	3
GO:0009965	1.00E-04	0.005948	leaf morphogenesis	7
GO:0010023	0.0038	0.112407	proanthocyanidin biosynthetic process	3
GO:0010025	0.0002	0.010626	wax biosynthetic process	7
GO:0010032	0.012999	0.269477	meiotic chromosome condensation	3
GO:0010033	0.026897	0.45018	response to organic substance	8
GO:0010037	0.025997	0.439147	response to carbon dioxide	3
GO:0010039	0.024198	0.416457	response to iron ion	4
GO:0010048	0.008899	0.218407	vernalization response	5
GO:0010052	0.0021	0.071826	guard cell differentiation	9
GO:0010115	0.0046	0.128435	regulation of abscisic acid biosynthetic process	2
GO:0010119	1.00E-04	0.005948	regulation of stomatal movement	12
GO:0010143	1.00E-04	0.005948	cutin biosynthetic process	17
GO:0010154	0.0007	0.029242	fruit development	4
GO:0010158	1.00E-04	0.005948	abaxial cell fate specification	11
GO:0010168	0.042396	0.625213	ER body	2
GO:0010197	0.005299	0.143584	polar nucleus fusion	3
GO:0010207	0.002	0.071071	photosystem II assembly	6
GO:0010242	0.006099	0.161266	oxygen evolving activity	3

GO:0010277	0.016698	0.327563	chlorophyllide a oxygenase [overall] activity	3
GO:0010287	1.00E-04	0.005948	plastoglobule	19
GO:0010305	0.013699	0.278709	leaf vascular tissue pattern formation	4
GO:0010338	1.00E-04	0.005948	leaf formation	4
GO:0010345	0.009599	0.223037	suberin biosynthetic process	4
GO:0010374	0.0021	0.071826	stomatal complex development	9
GO:0010389	0.027897	0.464077	regulation of G2/M transition of mitotic cell cycle	4
GO:0010411	0.0007	0.029242	xyloglucan metabolic process	16
GO:0010417	0.042996	0.630873	glucuronoxylan biosynthetic process	5
GO:0010424	0.041896	0.625213	DNA methylation on cytosine within a CG sequence	2
GO:0010478	0.013599	0.277707	chlororespiration	2
GO:0010598	1.00E-04	0.005948	NAD(P)H dehydrogenase complex (plastoquinone)	7
GO:0010997	0.021698	0.385559	anaphase-promoting complex binding	5
GO:0015116	0.012699	0.266284	sulfate transmembrane transporter activity	7
GO:0015137	0.048895	0.678198	citrate transmembrane transporter activity	2
GO:0015301	0.017698	0.33868	anion:anion antiporter activity	6
GO:0015333	0.0004	0.019372	peptide:proton symporter activity	18
GO:0015746	0.048895	0.678198	citrate transport	2
GO:0015790	0.021298	0.382175	UDP-xylose transmembrane transport	4
GO:0015976	0.043296	0.633345	carbon utilization	3
GO:0015979	1.00E-04	0.005948	photosynthesis	64
GO:0015995	0.012199	0.26285	chlorophyll biosynthetic process	8
GO:0016094	0.035196	0.553535	polyprenol biosynthetic process	3
GO:0016117	0.025497	0.433377	carotenoid biosynthetic process	5
GO:0016123	0.013599	0.277707	xanthophyll biosynthetic process	3
GO:0016126	0.0031	0.093727	sterol biosynthetic process	11
GO:0016168	1.00E-04	0.005948	chlorophyll binding	18
GO:0016298	0.040596	0.615273	lipase activity	12
GO:0016308	0.031097	0.50804	1-phosphatidylinositol-4-phosphate 5-kinase activity	5
GO:0016413	1.00E-04	0.005948	O-acetyltransferase activity	27
GO:0016442	0.041696	0.625213	RISC complex	3
GO:0016477	0.011299	0.247355	cell migration	7
GO:0016491	1.00E-04	0.005948	oxidoreductase activity	247
GO:0016538	1.00E-04	0.005948	protein serine/threonine kinase regulator activity	27
GO:0016584	0.0003	0.014925	nucleosome positioning	9
GO:0016597	0.008299	0.206461	amino acid binding	5
GO:0016614	1.00E-04	0.005948	oxidoreductase activity, acting on CH-OH group of donors	12

GO:0016620	0.0017	0.062859	oxidoreductase activity, acting on the aldehyde or oxo group	15
GO:0016655	0.0002	0.010626	oxidoreductase activity, acting on NAD(P)H	6
GO:0016702	0.044496	0.644244	oxidoreductase activity, acting on single donors	12
GO:0016722	1.00E-04	0.005948	oxidoreductase activity, acting on metal ions	21
GO:0016746	0.0021	0.071826	acyltransferase activity	48
GO:0016747	1.00E-04	0.005948	acyltransferase activity	46
GO:0016759	1.00E-04	0.005948	cellulose synthase activity	13
GO:0016760	1.00E-04	0.005948	cellulose synthase (UDP-forming) activity	15
GO:0016762	0.0026	0.082245	xyloglucan:xyloglucosyl transferase activity	12
GO:0016788	1.00E-04	0.005948	hydrolase activity, acting on ester bonds	64
GO:0016798	0.0002	0.010626	hydrolase activity, acting on glycosyl bonds	76
GO:0016799	0.0033	0.099226	hydrolase activity, hydrolyzing N-glycosyl compounds	8
GO:0016851	0.021098	0.382175	magnesium chelatase activity	3
GO:0016887	1.00E-04	0.005948	ATP hydrolysis activity	84
GO:0016985	0.049195	0.678198	mannan endo-1,4-beta-mannosidase activity	7
GO:0017116	0.0002	0.010626	single-stranded DNA helicase activity	8
GO:0018298	1.00E-04	0.005948	protein-chromophore linkage	20
GO:0018812	0.034997	0.551977	3-hydroxyacyl-CoA dehydratase activity	2
GO:0019253	1.00E-04	0.005948	reductive pentose-phosphate cycle	4
GO:0019265	0.0023	0.076748	glycine biosynthetic process	2
GO:0019464	0.047795	0.675926	glycine decarboxylation via glycine cleavage system	3
GO:0019898	0.0006	0.025854	extrinsic component of membrane	14
GO:0019901	1.00E-04	0.005948	protein kinase binding	34
GO:0030001	0.0021	0.071826	metal ion transport	29
GO:0030093	0.0017	0.062859	chloroplast photosystem I	2
GO:0030145	0.0044	0.124117	manganese ion binding	13
GO:0030154	1.00E-04	0.005948	cell differentiation	70
GO:0030198	0.004	0.114606	extracellular matrix organization	7
GO:0030244	0.0002	0.010626	cellulose biosynthetic process	15
GO:0030261	1.00E-04	0.005948	chromosome condensation	15
GO:0030295	0.0012	0.045923	protein kinase activator activity	8
GO:0030332	0.040396	0.614131	cyclin binding	4
GO:0030388	1.00E-04	0.005948	fructose 1,6-bisphosphate metabolic process	10
GO:0030497	0.009899	0.224802	fatty acid elongation	3
GO:0030574	0.004	0.114606	collagen catabolic process	7
GO:0030705	0.011899	0.2574	cytoskeleton-dependent intracellular transport	5
GO:0030838	0.017398	0.335284	positive regulation of actin filament polymerization	5

GO:0030865	0.0042	0.11909	cortical cytoskeleton organization	7
GO:0031012	0.004	0.114606	extracellular matrix	7
GO:0031047	0.009899	0.224802	gene silencing by RNA	11
GO:0031225	0.0003	0.014925	anchored component of membrane	19
GO:0031408	0.0019	0.068859	oxylipin biosynthetic process	10
GO:0031492	1.00E-04	0.005948	nucleosomal DNA binding	21
GO:0031532	0.017398	0.335284	actin cytoskeleton reorganization	5
GO:0031967	0.014299	0.288768	organelle envelope	4
GO:0032432	0.029897	0.49137	actin filament bundle	3
GO:0032502	1.00E-04	0.005948	developmental process	33
GO:0032508	0.034797	0.551977	DNA duplex unwinding	12
GO:0032797	0.047395	0.672006	SMN complex	3
GO:0032956	0.0045	0.126287	regulation of actin cytoskeleton organization	7
GO:0033612	0.0006	0.025854	receptor serine/threonine kinase binding	8
GO:0034090	0.0006	0.025854	maintenance of meiotic sister chromatid cohesion	4
GO:0034440	0.0019	0.068859	lipid oxidation	10
GO:0034722	0.007199	0.18412	gamma-glutamyl-peptidase activity	2
GO:0035097	0.019098	0.35497	histone methyltransferase complex	5
GO:0035336	0.009599	0.223037	long-chain fatty-acyl-CoA metabolic process	4
GO:0035442	0.009699	0.223037	dipeptide transmembrane transport	5
GO:0035673	0.0006	0.025854	oligopeptide transmembrane transporter activity	20
GO:0042132	0.0007	0.029242	fructose 1,6-bisphosphate 1-phosphatase activity	5
GO:0042546	0.0026	0.082245	cell wall biogenesis	13
GO:0042549	0.0011	0.042392	photosystem II stabilization	4
GO:0042555	1.00E-04	0.005948	MCM complex	9
GO:0042578	0.021598	0.385033	phosphoric ester hydrolase activity	6
GO:0042626	0.021998	0.387119	ATPase-coupled transmembrane transporter activity	24
GO:0042800	0.025897	0.438813	histone methyltransferase activity (H3-K4 specific)	2
GO:0042937	0.0009	0.03569	tripeptide transmembrane transporter activity	7
GO:0042938	0.009699	0.223037	dipeptide transport	5
GO:0042939	0.0009	0.03569	tripeptide transport	7
GO:0042973	0.013299	0.274655	glucan endo-1,3-beta-D-glucosidase activity	15
GO:0042995	0.003	0.092753	cell projection	7
GO:0043424	0.014899	0.29868	protein histidine kinase binding	5
GO:0043565	1.00E-04	0.005948	sequence-specific DNA binding	188
GO:0044772	1.00E-04	0.005948	mitotic cell cycle phase transition	27
GO:0044774	0.0041	0.11686	mitotic DNA integrity checkpoint signaling	2

GO:0045017	0.0025	0.081923	glycerolipid biosynthetic process	5
GO:0045038	0.0047	0.130561	protein import into chloroplast thylakoid membrane	3
GO:0045132	0.022998	0.398311	meiotic chromosome segregation	4
GO:0045144	0.0006	0.025854	meiotic sister chromatid segregation	4
GO:0045165	1.00E-04	0.005948	cell fate commitment	9
GO:0045486	0.017398	0.335284	naringenin 3-dioxygenase activity	2
GO:0045491	0.015998	0.317244	xylan metabolic process	6
GO:0045492	0.0003	0.014925	xylan biosynthetic process	12
GO:0045547	0.014899	0.29868	dehydrodolichyl diphosphate synthase activity	3
GO:0045735	0.005999	0.160169	nutrient reservoir activity	13
GO:0045787	1.00E-04	0.005948	positive regulation of cell cycle	24
GO:0045893	0.0008	0.032917	positive regulation of transcription, DNA-templated	42
GO:0045910	0.0005	0.023188	negative regulation of DNA recombination	10
GO:0045930	0.018898	0.35421	negative regulation of mitotic cell cycle	3
GO:0045962	1.00E-04	0.005948	positive regulation of development, heterochronic	7
GO:0046274	1.00E-04	0.005948	lignin catabolic process	17
GO:0046373	0.0039	0.114131	L-arabinose metabolic process	3
GO:0046406	0.011399	0.24855	magnesium protoporphyrin IX methyltransferase activity	2
GO:0046467	0.011199	0.247143	membrane lipid biosynthetic process	3
GO:0046556	0.020798	0.378163	alpha-L-arabinofuranosidase activity	5
GO:0046577	0.046895	0.666644	long-chain-alcohol oxidase activity	3
GO:0046658	0.004	0.114606	anchored component of plasma membrane	37
GO:0046863	0.029497	0.489204	ribulose-1,5-bisphosphate carboxylase/oxygenase activity	2
GO:0046900	0.007199	0.18412	tetrahydrofolylpolyglutamate metabolic process	2
GO:0046982	1.00E-04	0.005948	protein heterodimerization activity	44
GO:0046983	0.0011	0.042392	protein dimerization activity	67
GO:0047196	0.0013	0.049404	long-chain-alcohol O-fatty-acyltransferase activity	5
GO:0047750	0.034697	0.551977	cholestenol delta-isomerase activity	2
GO:0047938	0.009599	0.223037	glucose-6-phosphate 1-epimerase activity	5
GO:0047958	0.0022	0.074317	glycine:2-oxoglutarate aminotransferase activity	2
GO:0048038	0.012499	0.26617	quinone binding	7
GO:0048046	1.00E-04	0.005948	apoplast	58
GO:0048366	0.0009	0.03569	leaf development	10
GO:0048448	0.022798	0.397363	stamen morphogenesis	2
GO:0048564	0.046895	0.666644	photosystem I assembly	4
GO:0048653	0.022798	0.397363	anther development	2
GO:0048731	0.018198	0.345829	system development	6

GO:0048831	0.0021	0.071826	regulation of shoot system development	5
GO:0050794	0.031297	0.508272	regulation of cellular process	10
GO:0051014	0.018398	0.347218	actin filament severing	3
GO:0051015	0.042496	0.625213	actin filament binding	18
GO:0051017	0.0002	0.010626	actin filament bundle assembly	13
GO:0051213	0.005299	0.143584	dioxygenase activity	38
GO:0051225	0.042496	0.625213	spindle assembly	10
GO:0051301	1.00E-04	0.005948	cell division	38
GO:0051307	0.045995	0.660716	meiotic chromosome separation	2
GO:0051513	1.00E-04	0.005948	regulation of monopolar cell growth	8
GO:0051537	0.008299	0.206461	2 iron, 2 sulfur cluster binding	11
GO:0051607	1.00E-04	0.005948	defense response to virus	10
GO:0051639	0.029897	0.49137	actin filament network formation	3
GO:0051753	0.002	0.071071	mannan synthase activity	10
GO:0051783	0.048495	0.678198	regulation of nuclear division	2
GO:0051903	0.038196	0.588867	S-(hydroxymethyl)glutathione dehydrogenase activity	4
GO:0052324	0.044096	0.640146	plant-type cell wall cellulose biosynthetic process	4
GO:0052716	1.00E-04	0.005948	hydroquinone:oxygen oxidoreductase activity	17
GO:0052793	0.008699	0.214461	pectin acetylesterase activity	7
GO:0055072	0.0031	0.093727	iron ion homeostasis	10
GO:0055085	0.031297	0.508272	transmembrane transport	161
GO:0060236	0.0003	0.014925	regulation of mitotic spindle organization	8
GO:0061673	0.046395	0.662981	mitotic spindle astral microtubule	2
GO:0061820	0.038796	0.593104	telomeric D-loop disassembly	2
GO:0061821	0.038796	0.593104	telomeric D-loop binding	2
GO:0070409	0.036696	0.570565	carbamoyl phosphate biosynthetic process	3
GO:0071554	0.015998	0.317244	cell wall organization or biogenesis	6
GO:0071555	1.00E-04	0.005948	cell wall organization	56
GO:0071916	0.009699	0.223037	dipeptide transmembrane transporter activity	5
GO:0072686	0.0008	0.032917	mitotic spindle	9
GO:0080019	0.009599	0.223037	fatty-acyl-CoA reductase (alcohol-forming) activity	4
GO:0080043	0.049195	0.678198	quercetin 3-O-glucosyltransferase activity	18
GO:0080044	0.049195	0.678198	quercetin 7-O-glucosyltransferase activity	18
GO:0090307	0.005199	0.142284	mitotic spindle assembly	8
GO:0090447	1.00E-04	0.005948	glycerol-3-phosphate 2-O-acyltransferase activity	11
GO:0097027	0.009699	0.223037	ubiquitin-protein transferase activator activity	5
GO:0097502	0.029897	0.49137	mannosylation	11

GO:0098796	0.021498	0.384502	membrane protein complex	2
GO:0099402	1.00E-04	0.005948	plant organ development	31
GO:0102158	0.034997	0.551977	very-long-chain 3-hydroxyacyl-CoA dehydratase activity	2
GO:0102343	0.034997	0.551977	3-hydroxy-arachidoyl-CoA dehydratase activity	2
GO:0102344	0.034997	0.551977	3-hydroxy-behenoyl-CoA dehydratase activity	2
GO:0102345	0.034997	0.551977	3-hydroxy-lignoceroyl-CoA dehydratase activity	2
GO:0102756	1.00E-04	0.005948	very-long-chain 3-ketoacyl-CoA synthase activity	15
GO:0102965	0.009599	0.223037	alcohol-forming fatty acyl-CoA reductase activity	4
GO:0140359	0.005199	0.142284	ABC-type transporter activity	27
GO:0140575	0.009599	0.223037	transmembrane monodehydroascorbate reductase activity	4
GO:1901031	0.011199	0.247143	regulation of response to reactive oxygen species	3
GO:1901673	0.015698	0.313568	regulation of mitotic spindle assembly	2
GO:1901700	0.026897	0.45018	response to oxygen-containing compound	8
GO:1901811	0.044996	0.649494	beta-carotene catabolic process	1
GO:1902183	0.0002	0.010626	regulation of shoot apical meristem development	4
GO:1902358	0.012699	0.266284	sulfate transmembrane transport	7
GO:1902975	0.020098	0.369115	mitotic DNA replication initiation	4
GO:1904482	0.005399	0.145573	cellular response to tetrahydrofolate	3
GO:1904667	0.048495	0.678198	negative regulation of ubiquitin protein ligase activity	2
GO:1904668	0.009699	0.223037	positive regulation of ubiquitin protein ligase activity	5
GO:1904680	0.0004	0.019372	peptide transmembrane transporter activity	18
GO:1905775	0.005	0.138193	negative regulation of DNA helicase activity	2
GO:1990023	0.046395	0.662981	mitotic spindle midzone	2
GO:2000024	0.0004	0.019372	regulation of leaf development	4
GO:2000032	1.00E-04	0.005948	regulation of secondary shoot formation	13

Appendix F - Differentially expressed and significantly down-enriched gene ontology (GO) term associated gene numbers represented between ascorbic acid pre-treated MP-inoculated treatment with the non-pre-treated MP-inoculated treatment in the resistant genotype (DT97-4290).

GO	*p*-value	*q*-value	Term	Gene No.
GO:0000048	0.039096	0.644497	peptidyltransferase activity	2
GO:0000166	1.00E-04	0.007497	nucleotide binding	381
GO:0000272	0.0025	0.090007	polysaccharide catabolic process	14
GO:0000287	0.0003	0.016925	magnesium ion binding	35
GO:0000326	0.005699	0.176232	protein storage vacuole	8
GO:0000976	0.0046	0.146356	transcription cis-regulatory region binding	34
GO:0001561	0.016498	0.373122	fatty acid alpha-oxidation	2
GO:0002229	1.00E-04	0.007497	defense response to oomycetes	12
GO:0003333	0.042496	0.672194	amino acid transmembrane transport	16
GO:0003700	1.00E-04	0.007497	DNA-binding transcription factor activity	198
GO:0003824	1.00E-04	0.007497	catalytic activity	183
GO:0003854	0.024198	0.496005	3-beta-hydroxy-delta5-steroid dehydrogenase activity	4
GO:0003866	0.029597	0.5605	3-phosphoshikimate 1-carboxyvinyltransferase activity	2
GO:0003878	0.038496	0.642346	ATP citrate synthase activity	4
GO:0003885	0.049995	0.737527	D-arabinono-1,4-lactone oxidase activity	3
GO:0003987	0.028897	0.554926	acetate-CoA ligase activity	2
GO:0003993	0.044796	0.692559	acid phosphatase activity	11
GO:0003994	0.010299	0.25738	aconitate hydratase activity	4
GO:0004017	0.012899	0.308274	adenylate kinase activity	5
GO:0004024	0.022798	0.470837	alcohol dehydrogenase activity, zinc-dependent	5
GO:0004044	0.036696	0.633562	amidophosphoribosyltransferase activity	2
GO:0004067	0.009799	0.250608	asparaginase activity	3
GO:0004069	0.018798	0.403459	L-aspartate:2-oxoglutarate aminotransferase activity	4
GO:0004097	0.048595	0.730156	catechol oxidase activity	5
GO:0004107	0.029497	0.5605	chorismate synthase activity	2
GO:0004108	0.0032	0.109449	citrate (Si)-synthase activity	4
GO:0004149	0.029197	0.556779	dihydrolipoyllysine-residue succinyltransferase activity	2
GO:0004190	0.018498	0.40016	aspartic-type endopeptidase activity	22
GO:0004332	0.007199	0.208474	fructose-bisphosphate aldolase activity	6
GO:0004334	0.032797	0.589476	fumarylacetoacetase activity	2

GO:0004335	0.037896	0.640963	galactokinase activity	2
GO:0004351	0.0011	0.046664	glutamate decarboxylase activity	5
GO:0004352	0.039596	0.644968	glutamate dehydrogenase (NAD+) activity	3
GO:0004364	0.0008	0.036483	glutathione transferase activity	21
GO:0004371	0.024798	0.502655	glycerone kinase activity	2
GO:0004452	0.037496	0.640963	isopentenyl-diphosphate delta-isomerase activity	2
GO:0004497	1.00E-04	0.007497	monooxygenase activity	76
GO:0004506	0.039096	0.644497	squalene monooxygenase activity	3
GO:0004553	0.0003	0.016925	hydrolase activity, hydrolyzing O-glycosyl compounds	57
GO:0004564	0.0031	0.106696	beta-fructofuranosidase activity	6
GO:0004568	0.0003	0.016925	chitinase activity	11
GO:0004575	0.0026	0.092996	sucrose alpha-glucosidase activity	6
GO:0004601	1.00E-04	0.007497	peroxidase activity	46
GO:0004611	0.032797	0.589476	phosphoenolpyruvate carboxykinase activity	3
GO:0004612	0.032797	0.589476	phosphoenolpyruvate carboxykinase (ATP) activity	3
GO:0004616	0.047295	0.723036	phosphogluconate dehydrogenase (decarboxylating) activity	3
GO:0004620	0.009799	0.250608	phospholipase activity	7
GO:0004650	0.0003	0.016925	polygalacturonase activity	13
GO:0004657	0.0009	0.040042	proline dehydrogenase activity	4
GO:0004672	1.00E-04	0.007497	protein kinase activity	302
GO:0004674	1.00E-04	0.007497	protein serine/threonine kinase activity	203
GO:0004675	0.037196	0.640174	receptor protein serine/threonine kinase activity	30
GO:0004683	0.043496	0.683275	calmodulin-dependent protein kinase activity	11
GO:0004737	0.0008	0.036483	pyruvate decarboxylase activity	4
GO:0004753	0.016498	0.373122	saccharopine dehydrogenase activity	2
GO:0004842	0.005999	0.184465	ubiquitin-protein transferase activity	44
GO:0004851	0.009699	0.250608	uroporphyrin-III C-methyltransferase activity	2
GO:0004857	0.0008	0.036483	enzyme inhibitor activity	17
GO:0004864	0.0002	0.012727	protein phosphatase inhibitor activity	15
GO:0004866	1.00E-04	0.007497	endopeptidase inhibitor activity	16
GO:0004867	0.0024	0.088147	serine-type endopeptidase inhibitor activity	6
GO:0004869	0.047795	0.728644	cysteine-type endopeptidase inhibitor activity	4
GO:0005344	0.006599	0.196295	oxygen carrier activity	3
GO:0005351	0.0003	0.016925	carbohydrate:proton symporter activity	16
GO:0005355	0.0003	0.016925	glucose transmembrane transporter activity	16
GO:0005471	0.010299	0.25738	ATP:ADP antiporter activity	6
GO:0005504	0.031997	0.587646	fatty acid binding	6

GO:0005506	1.00E-04	0.007497	iron ion binding	88
GO:0005509	0.007699	0.216092	calcium ion binding	53
GO:0005516	0.025297	0.510897	calmodulin binding	29
GO:0005524	1.00E-04	0.007497	ATP binding	443
GO:0005543	0.0011	0.046664	phospholipid binding	12
GO:0005576	1.00E-04	0.007497	extracellular region	136
GO:0005618	0.0002	0.012727	cell wall	36
GO:0005746	0.019598	0.415737	mitochondrial respirasome	3
GO:0005777	0.017898	0.394988	peroxisome	24
GO:0005868	0.031897	0.587646	cytoplasmic dynein complex	4
GO:0005886	1.00E-04	0.007497	plasma membrane	355
GO:0005887	1.00E-04	0.007497	integral component of plasma membrane	37
GO:0005975	1.00E-04	0.007497	carbohydrate metabolic process	113
GO:0005987	0.007899	0.216162	sucrose catabolic process	4
GO:0005992	0.009699	0.250608	trehalose biosynthetic process	8
GO:0006032	0.0015	0.060805	chitin catabolic process	8
GO:0006085	0.038096	0.640963	acetyl-CoA biosynthetic process	4
GO:0006096	0.0003	0.016925	glycolytic process	31
GO:0006097	0.0002	0.012727	glyoxylate cycle	6
GO:0006099	0.0002	0.012727	tricarboxylic acid cycle	24
GO:0006101	0.0002	0.012727	citrate metabolic process	6
GO:0006102	0.048595	0.730156	isocitrate metabolic process	4
GO:0006351	0.007599	0.215496	transcription, DNA-templated	77
GO:0006355	0.012599	0.302425	regulation of transcription, DNA-templated	239
GO:0006468	1.00E-04	0.007497	protein phosphorylation	305
GO:0006520	1.00E-04	0.007497	cellular amino acid metabolic process	23
GO:0006536	1.00E-04	0.007497	glutamate metabolic process	7
GO:0006538	0.0003	0.016925	glutamate catabolic process	8
GO:0006559	1.00E-04	0.007497	L-phenylalanine catabolic process	10
GO:0006560	0.0009	0.040042	proline metabolic process	4
GO:0006562	0.0009	0.040042	proline catabolic process	4
GO:0006631	0.039796	0.645717	fatty acid metabolic process	22
GO:0006666	0.006699	0.197126	3-keto-sphinganine metabolic process	2
GO:0006749	0.001	0.043432	glutathione metabolic process	23
GO:0006796	0.007899	0.216162	phosphate-containing compound metabolic process	6
GO:0006839	0.015198	0.355476	mitochondrial transport	3
GO:0006844	0.042796	0.674988	acyl carnitine transport	2

GO:0006862	0.040396	0.650256	nucleotide transport	4
GO:0006865	0.0044	0.14164	amino acid transport	21
GO:0006885	0.046695	0.719897	regulation of pH	4
GO:0006952	1.00E-04	0.007497	defense response	88
GO:0006955	0.0004	0.021461	immune response	8
GO:0006979	1.00E-04	0.007497	response to oxidative stress	42
GO:0007166	1.00E-04	0.007497	cell surface receptor signaling pathway	16
GO:0007178	0.0016	0.062542	protein serine/threonine kinase signaling pathway	12
GO:0008061	0.0025	0.090007	chitin binding	8
GO:0008152	1.00E-04	0.007497	metabolic process	96
GO:0008171	1.00E-04	0.007497	O-methyltransferase activity	15
GO:0008194	1.00E-04	0.007497	UDP-glycosyltransferase activity	40
GO:0008299	0.007499	0.214887	isoprenoid biosynthetic process	13
GO:0008422	1.00E-04	0.007497	beta-glucosidase activity	19
GO:0008483	1.00E-04	0.007497	transaminase activity	22
GO:0008643	1.00E-04	0.007497	carbohydrate transport	14
GO:0008645	0.0003	0.016925	hexose transmembrane transport	16
GO:0008798	0.009799	0.250608	beta-aspartyl-peptidase activity	3
GO:0008865	0.027597	0.537508	fructokinase activity	6
GO:0008970	0.0048	0.151837	phospholipase A1 activity	4
GO:0009058	0.0002	0.012727	biosynthetic process	31
GO:0009073	0.0013	0.05349	aromatic amino acid family biosynthetic process	12
GO:0009083	0.0019	0.072206	branched-chain amino acid catabolic process	4
GO:0009240	0.037496	0.640963	isopentenyl diphosphate biosynthetic process	2
GO:0009337	0.033197	0.589476	sulfite reductase complex (NADPH)	2
GO:0009423	0.0008	0.036483	chorismate biosynthetic process	8
GO:0009506	1.00E-04	0.007497	plasmodesma	64
GO:0009514	0.0029	0.101084	glyoxysome	5
GO:0009607	1.00E-04	0.007497	response to biotic stimulus	17
GO:0009620	0.044796	0.692559	response to fungus	4
GO:0009626	0.0007	0.033311	plant-type hypersensitive response	8
GO:0009651	0.0004	0.021461	response to salt stress	20
GO:0009695	0.008799	0.23959	jasmonic acid biosynthetic process	6
GO:0009696	0.033497	0.589476	salicylic acid metabolic process	4
GO:0009698	1.00E-04	0.007497	phenylpropanoid metabolic process	10
GO:0009727	0.027197	0.53161	detection of ethylene stimulus	4
GO:0009733	0.015298	0.356292	response to auxin	16

GO:0009735	0.0035	0.116082	response to cytokinin	9
GO:0009738	1.00E-04	0.007497	abscisic acid-activated signaling pathway	28
GO:0009753	0.039396	0.644968	response to jasmonic acid	3
GO:0009755	0.0049	0.154109	hormone-mediated signaling pathway	10
GO:0009800	1.00E-04	0.007497	cinnamic acid biosynthetic process	8
GO:0009807	0.0036	0.117969	lignan biosynthetic process	8
GO:0009813	1.00E-04	0.007497	flavonoid biosynthetic process	17
GO:0009815	0.027197	0.53161	1-aminocyclopropane-1-carboxylate oxidase activity	4
GO:0009852	0.038196	0.640963	auxin catabolic process	2
GO:0009873	1.00E-04	0.007497	ethylene-activated signaling pathway	35
GO:0009931	0.013599	0.322188	calcium-dependent protein serine/threonine kinase activity	11
GO:0009975	0.026697	0.5294	cyclase activity	2
GO:0010026	0.006499	0.196295	trichome differentiation	4
GO:0010030	0.033297	0.589476	positive regulation of seed germination	4
GO:0010090	0.018298	0.40016	trichome morphogenesis	4
GO:0010133	0.0005	0.025103	proline catabolic process to glutamate	5
GO:0010167	0.041696	0.661453	response to nitrate	4
GO:0010179	0.048995	0.730156	IAA-Ala conjugate hydrolase activity	3
GO:0010181	0.0023	0.08621	FMN binding	17
GO:0010200	1.00E-04	0.007497	response to chitin	14
GO:0010227	0.009799	0.250608	floral organ abscission	3
GO:0010427	1.00E-04	0.007497	abscisic acid binding	15
GO:0010466	0.0006	0.029581	negative regulation of peptidase activity	10
GO:0010493	0.011399	0.279758	Lewis a epitope biosynthetic process	2
GO:0010951	1.00E-04	0.007497	negative regulation of endopeptidase activity	25
GO:0012501	0.0004	0.021461	programmed cell death	8
GO:0015145	0.0016	0.062542	monosaccharide transmembrane transporter activity	6
GO:0015171	0.040896	0.655737	amino acid transmembrane transporter activity	16
GO:0015217	0.022498	0.469963	ADP transmembrane transporter activity	2
GO:0015248	0.049795	0.736563	sterol transporter activity	5
GO:0015292	0.016198	0.372495	uniporter activity	3
GO:0015293	0.0012	0.04975	symporter activity	24
GO:0015662	0.027097	0.53161	P-type ion transporter activity	7
GO:0015671	0.006599	0.196295	oxygen transport	3
GO:0015749	0.0016	0.062542	monosaccharide transmembrane transport	6
GO:0015866	0.0005	0.025103	ADP transport	5
GO:0015867	0.015998	0.369448	ATP transport	5

GO:0015914	0.007699	0.216092	phospholipid transport	11
GO:0015940	0.007599	0.215496	pantothenate biosynthetic process	2
GO:0016002	0.033197	0.589476	sulfite reductase activity	2
GO:0016020	1.00E-04	0.007497	membrane	986
GO:0016021	1.00E-04	0.007497	integral component of membrane	908
GO:0016042	0.0027	0.094716	lipid catabolic process	16
GO:0016114	0.0004	0.021461	terpenoid biosynthetic process	8
GO:0016125	0.041096	0.655737	sterol metabolic process	9
GO:0016161	0.0012	0.04975	beta-amylase activity	7
GO:0016174	0.0027	0.094716	NAD(P)H oxidase H2O2-forming activity	7
GO:0016207	0.027897	0.541424	4-coumarate-CoA ligase activity	3
GO:0016208	0.033997	0.5962	AMP binding	5
GO:0016210	0.0002	0.012727	naringenin-chalcone synthase activity	8
GO:0016298	0.0003	0.016925	lipase activity	16
GO:0016301	1.00E-04	0.007497	kinase activity	266
GO:0016310	1.00E-04	0.007497	phosphorylation	277
GO:0016491	1.00E-04	0.007497	oxidoreductase activity	344
GO:0016540	0.041096	0.655737	protein autoprocessing	3
GO:0016616	0.0004	0.021461	oxidoreductase activity, acting on the CH-OH group	38
GO:0016624	0.020498	0.431482	oxidoreductase activityon the aldehyde or oxo group	5
GO:0016639	0.023998	0.493755	oxidoreductase activity, acting on the CH-NH2 group	5
GO:0016702	0.005699	0.176232	oxidoreductase activity, acting on single donors	15
GO:0016705	1.00E-04	0.007497	oxidoreductase activity, acting on paired donors	76
GO:0016709	1.00E-04	0.007497	oxidoreductase activity, acting on paired donors	53
GO:0016740	1.00E-04	0.007497	transferase activity	494
GO:0016747	1.00E-04	0.007497	acyltransferase activity	43
GO:0016757	0.018098	0.397797	glycosyltransferase activity	88
GO:0016758	0.048095	0.730156	hexosyltransferase activity	18
GO:0016773	0.011999	0.290573	phosphotransferase activity, alcohol group as acceptor	11
GO:0016776	0.006899	0.201925	phosphotransferase activity	4
GO:0016798	1.00E-04	0.007497	hydrolase activity, acting on glycosyl bonds	80
GO:0016829	1.00E-04	0.007497	lyase activity	71
GO:0016830	0.0008	0.036483	carbon-carbon lyase activity	8
GO:0016831	0.003	0.103907	carboxy-lyase activity	15
GO:0016836	0.0007	0.033311	hydro-lyase activity	9
GO:0016841	1.00E-04	0.007497	ammonia-lyase activity	8
GO:0016846	0.030997	0.577027	carbon-sulfur lyase activity	4

GO:0016866	0.044096	0.687565	intramolecular transferase activity	6
GO:0016872	0.0005	0.025103	intramolecular lyase activity	7
GO:0016881	0.030097	0.566051	acid-amino acid ligase activity	7
GO:0016998	0.0037	0.120524	cell wall macromolecule catabolic process	6
GO:0017077	0.009899	0.250821	oxidative phosphorylation uncoupler activity	3
GO:0017172	0.0002	0.012727	cysteine dioxygenase activity	7
GO:0019205	0.011199	0.277337	nucleobase-containing compound kinase activity	5
GO:0019344	0.013499	0.321209	cysteine biosynthetic process	8
GO:0019354	0.009699	0.250608	siroheme biosynthetic process	2
GO:0019427	0.028897	0.554926	acetyl-CoA biosynthetic process from acetate	2
GO:0019438	1.00E-04	0.007497	aromatic compound biosynthetic process	13
GO:0019499	0.038296	0.640963	cyanide metabolic process	2
GO:0019521	0.047295	0.723036	D-gluconate metabolic process	3
GO:0019722	0.005699	0.176232	calcium-mediated signaling	10
GO:0019752	1.00E-04	0.007497	carboxylic acid metabolic process	18
GO:0019762	1.00E-04	0.007497	glucosinolate catabolic process	10
GO:0019825	0.006599	0.196295	oxygen binding	3
GO:0019853	0.015698	0.364057	L-ascorbic acid biosynthetic process	5
GO:0020037	1.00E-04	0.007497	heme binding	124
GO:0022821	0.039996	0.645717	potassium ion antiporter activity	3
GO:0022857	1.00E-04	0.007497	transmembrane transporter activity	80
GO:0030125	0.026097	0.523191	clathrin vesicle coat	6
GO:0030136	0.0021	0.079256	clathrin-coated vesicle	10
GO:0030145	0.029997	0.566051	manganese ion binding	10
GO:0030148	0.018398	0.40016	sphingolipid biosynthetic process	6
GO:0030170	1.00E-04	0.007497	pyridoxal phosphate binding	35
GO:0030198	0.0033	0.110792	extracellular matrix organization	6
GO:0030234	0.006999	0.203762	enzyme regulator activity	9
GO:0030247	1.00E-04	0.007497	polysaccharide binding	19
GO:0030388	0.007799	0.216162	fructose 1,6-bisphosphate metabolic process	8
GO:0030414	0.0006	0.029581	peptidase inhibitor activity	10
GO:0030523	0.024798	0.502655	dihydrolipoamide S-acyltransferase activity	2
GO:0030574	0.0033	0.110792	collagen catabolic process	6
GO:0030599	0.031897	0.587646	pectinesterase activity	9
GO:0030639	0.0002	0.012727	polyketide biosynthetic process	8
GO:0030976	0.0036	0.117969	thiamine pyrophosphate binding	7
GO:0031012	0.0033	0.110792	extracellular matrix	6

GO:0031225	0.0005	0.025103	anchored component of membrane	14
GO:0031305	0.0011	0.046664	integral component of mitochondrial inner membrane	11
GO:0031405	0.009399	0.250608	lipoic acid binding	3
GO:0031468	0.047295	0.723036	nuclear membrane reassembly	2
GO:0031625	1.00E-04	0.007497	ubiquitin protein ligase binding	25
GO:0031956	0.006199	0.189549	medium-chain fatty acid-CoA ligase activity	4
GO:0032580	0.043696	0.683275	Golgi cisterna membrane	3
GO:0032587	0.039496	0.644968	ruffle membrane	2
GO:0032869	0.020198	0.426809	cellular response to insulin stimulus	6
GO:0033345	0.009799	0.250608	asparagine catabolic process via L-aspartate	3
GO:0033512	0.0005	0.025103	L-lysine catabolic process to acetyl-CoA via saccharopine	4
GO:0033897	0.018598	0.400739	ribonuclease T2 activity	3
GO:0033926	0.007899	0.216162	glycopeptide alpha-N-acetylgalactosaminidase activity	4
GO:0034220	0.034097	0.5962	ion transmembrane transport	25
GO:0034605	0.0024	0.088147	cellular response to heat	19
GO:0035435	0.021398	0.448699	phosphate ion transmembrane transport	6
GO:0035436	0.038196	0.640963	triose phosphate transmembrane transport	3
GO:0036374	0.039096	0.644497	glutathione hydrolase activity	2
GO:0036444	0.049095	0.730156	calcium import into the mitochondrion	3
GO:0038023	1.00E-04	0.007497	signaling receptor activity	19
GO:0042343	0.0003	0.016925	indole glucosinolate metabolic process	10
GO:0042545	0.019598	0.415737	cell wall modification	9
GO:0042626	0.024698	0.502655	ATPase-coupled transmembrane transporter activity	24
GO:0042742	1.00E-04	0.007497	defense response to bacterium	29
GO:0042744	1.00E-04	0.007497	hydrogen peroxide catabolic process	34
GO:0043086	0.0002	0.012727	negative regulation of catalytic activity	20
GO:0043169	0.035796	0.61998	cation binding	14
GO:0043436	0.0035	0.116082	oxoacid metabolic process	6
GO:0043565	1.00E-04	0.007497	sequence-specific DNA binding	133
GO:0044281	0.007899	0.216162	small molecule metabolic process	10
GO:0045252	0.018498	0.40016	oxoglutarate dehydrogenase complex	4
GO:0045254	0.008899	0.241113	pyruvate dehydrogenase complex	3
GO:0045330	0.019598	0.415737	aspartyl esterase activity	9
GO:0045332	0.0007	0.033311	phospholipid translocation	11
GO:0045430	0.027997	0.541444	chalcone isomerase activity	3
GO:0045490	0.022698	0.470837	pectin catabolic process	12
GO:0045548	1.00E-04	0.007497	phenylalanine ammonia-lyase activity	8

GO:0045735	0.0005	0.025103	nutrient reservoir activity	14
GO:0046148	0.030997	0.577027	pigment biosynthetic process	5
GO:0046177	0.0018	0.068884	D-gluconate catabolic process	5
GO:0046294	0.038196	0.640963	formaldehyde catabolic process	5
GO:0046316	0.013999	0.330234	gluconokinase activity	2
GO:0046429	0.039996	0.645717	4-hydroxy-3-methylbut-2-en-1-yl diphosphate synthase activity	2
GO:0046513	0.017898	0.394988	ceramide biosynthetic process	5
GO:0046686	0.006599	0.196295	response to cadmium ion	7
GO:0046777	1.00E-04	0.007497	protein autophosphorylation	58
GO:0046835	0.041296	0.657012	carbohydrate phosphorylation	9
GO:0046872	0.001	0.043432	metal ion binding	371
GO:0046910	0.007299	0.210257	pectinesterase inhibitor activity	9
GO:0046912	0.0014	0.057175	acyltransferase, acyl groups converted into alkyl on transfer	7
GO:0047372	0.049295	0.731143	acylglycerol lipase activity	3
GO:0047560	0.006699	0.197126	3-dehydrosphinganine reductase activity	2
GO:0047780	0.010299	0.25738	citrate dehydratase activity	4
GO:0048017	0.035596	0.618474	inositol lipid-mediated signaling	2
GO:0048046	0.0005	0.025103	apoplast	35
GO:0048531	0.048395	0.730156	beta-1,3-galactosyltransferase activity	2
GO:0048544	1.00E-04	0.007497	recognition of pollen	39
GO:0050017	0.017798	0.394988	L-3-cyanoalanine synthase activity	2
GO:0050105	0.026097	0.523191	L-gulonolactone oxidase activity	3
GO:0050302	0.038196	0.640963	indole-3-acetaldehyde oxidase activity	2
GO:0050660	0.009699	0.250608	flavin adenine dinucleotide binding	30
GO:0050661	0.017698	0.394988	NADP binding	19
GO:0050664	0.0027	0.094716	oxidoreductase activity	7
GO:0050793	0.029197	0.556779	regulation of developmental process	2
GO:0050992	0.0018	0.068884	dimethylallyl diphosphate biosynthetic process	4
GO:0051119	0.017698	0.394988	sugar transmembrane transporter activity	7
GO:0051156	0.038796	0.644497	glucose 6-phosphate metabolic process	5
GO:0051213	0.0002	0.012727	dioxygenase activity	40
GO:0051300	1.00E-04	0.007497	spindle pole body organization	8
GO:0051560	0.049095	0.730156	mitochondrial calcium ion homeostasis	3
GO:0051762	0.026697	0.5294	sesquiterpene biosynthetic process	2
GO:0051903	0.022798	0.470837	S-(hydroxymethyl)glutathione dehydrogenase activity	5
GO:0051938	0.030897	0.577027	L-glutamate import	2
GO:0052381	0.0017	0.06598	tRNA dimethylallyltransferase activity	4

GO:0055085	1.00E-04	0.007497	transmembrane transport	161
GO:0061408	0.0038	0.123049	positive regulation of transcription from RNA polymerase II	10
GO:0070413	0.032597	0.589476	trehalose metabolism in response to stress	5
GO:0071398	0.027197	0.53161	cellular response to fatty acid	4
GO:0071732	0.032997	0.589476	cellular response to nitric oxide	4
GO:0071949	0.017698	0.394988	FAD binding	19
GO:0080030	0.014299	0.335863	methyl indole-3-acetate esterase activity	5
GO:0080031	0.033497	0.589476	methyl salicylate esterase activity	4
GO:0080032	0.033497	0.589476	methyl jasmonate esterase activity	4
GO:0080043	1.00E-04	0.007497	quercetin 3-O-glucosyltransferase activity	27
GO:0080044	1.00E-04	0.007497	quercetin 7-O-glucosyltransferase activity	27
GO:0080163	1.00E-04	0.007497	regulation of protein serine/threonine phosphatase activity	14
GO:0080183	0.010499	0.261185	response to photooxidative stress	3
GO:0098542	0.0024	0.088147	defense response to other organism	13
GO:0098869	1.00E-04	0.007497	cellular oxidant detoxification	46
GO:0102128	0.0002	0.012727	chalcone synthase activity	8
GO:0102229	0.0012	0.04975	amylopectin maltohydrolase activity	7
GO:0106310	1.00E-04	0.007497	protein serine kinase activity	58
GO:0120029	0.026597	0.5294	proton export across plasma membrane	6
GO:0140326	0.0016	0.062542	ATPase-coupled intramembrane lipid transporter activity	9
GO:0140359	0.012099	0.291703	ABC-type transporter activity	25
GO:1900027	0.039496	0.644968	regulation of ruffle assembly	2
GO:1901564	0.034297	0.597787	organonitrogen compound metabolic process	4
GO:1902000	0.032797	0.589476	homogentisate catabolic process	2
GO:1990246	0.049095	0.730156	uniplex complex	3
GO:1990542	0.009899	0.250821	mitochondrial transmembrane transport	3
GO:2000031	0.0025	0.090007	regulation of salicylic acid mediated signaling pathway	8

Appendix G - Differentially expressed and significantly up-enriched gene ontology (GO) term associated gene numbers represented between ascorbic acid pre-treated MP-inoculated treatment with the non-pre-treated MP-inoculated treatment in susceptible genotype (Pharaoh).

GO	*p*-value	*q*-value	Term	Gene No.
GO:0000166	0.0006	0.022173	nucleotide binding	40
GO:0000272	0.0042	0.105375	polysaccharide catabolic process	1
GO:0000981	1.00E-04	0.004883	DNA-binding transcription factor activity	2
GO:0003677	1.00E-04	0.004883	DNA binding	35
GO:0004028	0.0013	0.039283	3-chloroallyl aldehyde dehydrogenase activity	1
GO:0004029	0.0015	0.043639	aldehyde dehydrogenase (NAD+) activity	1
GO:0004553	1.00E-04	0.004883	hydrolase activity, hydrolyzing O-glycosyl compounds	5
GO:0004568	0.0004	0.015407	chitinase activity	2
GO:0004620	0.005499	0.127466	phospholipase activity	1
GO:0004672	0.012799	0.233363	protein kinase activity	44
GO:0004675	0.021798	0.351723	protein serine/threonine kinase activity	7
GO:0005524	1.00E-04	0.004883	ATP binding	52
GO:0005576	1.00E-04	0.004883	extracellular region	9
GO:0005618	1.00E-04	0.004883	cell wall	2
GO:0005634	1.00E-04	0.004883	nucleus	55
GO:0005773	0.0013	0.039283	vacuole	4
GO:0005774	0.006899	0.15279	vacuolar membrane	3
GO:0005794	0.032897	0.466179	Golgi apparatus	1
GO:0005886	1.00E-04	0.004883	plasma membrane	53
GO:0005975	1.00E-04	0.004883	carbohydrate metabolic process	10
GO:0006032	0.010399	0.209126	chitin catabolic process	1
GO:0006081	0.0013	0.039283	cellular aldehyde metabolic process	1
GO:0006351	1.00E-04	0.004883	transcription, DNA-templated	1
GO:0006355	1.00E-04	0.004883	regulation of transcription, DNA-templated	41
GO:0006468	0.0002	0.008103	protein phosphorylation	44
GO:0006629	1.00E-04	0.004883	lipid metabolic process	7
GO:0006631	1.00E-04	0.004883	fatty acid metabolic process	1
GO:0006633	1.00E-04	0.004883	fatty acid biosynthetic process	1
GO:0008061	0.011699	0.226122	chitin binding	1
GO:0008152	1.00E-04	0.004883	metabolic process	7
GO:0008171	0.015898	0.270917	O-methyltransferase activity	3

GO:0008271	0.030297	0.439587	sulfate transmembrane transporter activity	1
GO:0008289	1.00E-04	0.004883	lipid binding	1
GO:0009505	1.00E-04	0.004883	plant-type cell wall	5
GO:0009506	1.00E-04	0.004883	plasmodesma	9
GO:0009664	1.00E-04	0.004883	plant-type cell wall organization	1
GO:0009734	0.0024	0.064984	auxin-activated signaling pathway	3
GO:0009813	0.005099	0.120754	flavonoid biosynthetic process	1
GO:0010333	0.0033	0.087194	terpene synthase activity	3
GO:0010951	1.00E-04	0.004883	negative regulation of endopeptidase activity	1
GO:0015297	0.012999	0.236222	antiporter activity	2
GO:0015301	0.030297	0.439587	anion:anion antiporter activity	1
GO:0015333	0.035196	0.483316	peptide:proton symporter activity	3
GO:0016102	0.012399	0.232545	diterpenoid biosynthetic process	3
GO:0016298	0.041396	0.536577	lipase activity	1
GO:0016702	0.0002	0.008103	oxidoreductase activity, acting on single donors	1
GO:0016709	0.038696	0.508817	oxidoreductase activity, acting on paired donors	7
GO:0016717	1.00E-04	0.004883	oxidoreductase activity, acting on paired donors	1
GO:0016747	1.00E-04	0.004883	acyltransferase activity	2
GO:0016787	0.022798	0.36251	hydrolase activity	23
GO:0016788	1.00E-04	0.004883	hydrolase activity, acting on ester bonds	2
GO:0016798	1.00E-04	0.004883	hydrolase activity, acting on glycosyl bonds	7
GO:0016829	0.028097	0.41756	lyase activity	3
GO:0016887	1.00E-04	0.004883	ATP hydrolysis activity	3
GO:0016998	0.012499	0.232545	cell wall macromolecule catabolic process	1
GO:0019438	0.002	0.055247	aromatic compound biosynthetic process	3
GO:0020037	0.017998	0.300153	heme binding	14
GO:0030001	0.030897	0.444753	metal ion transport	10
GO:0030154	1.00E-04	0.004883	cell differentiation	1
GO:0030599	0.027797	0.41756	pectinesterase activity	1
GO:0031047	0.029297	0.429638	gene silencing by RNA	1
GO:0031225	1.00E-04	0.004883	anchored component of membrane	1
GO:0031408	1.00E-04	0.004883	oxylipin biosynthetic process	1
GO:0034440	1.00E-04	0.004883	lipid oxidation	1
GO:0042545	0.008999	0.183676	cell wall modification	1
GO:0042626	0.0005	0.018604	ATPase-coupled transmembrane transporter activity	4
GO:0043565	1.00E-04	0.004883	sequence-specific DNA binding	28
GO:0045330	0.008999	0.183676	aspartyl esterase activity	1

GO:0045490	0.0014	0.04139	pectin catabolic process	1
GO:0045735	0.046295	0.593058	nutrient reservoir activity	1
GO:0046658	1.00E-04	0.004883	anchored component of plasma membrane	3
GO:0046983	0.0005	0.018604	protein dimerization activity	5
GO:0047372	0.012799	0.233363	acylglycerol lipase activity	1
GO:0048046	1.00E-04	0.004883	apoplast	2
GO:0050660	0.045795	0.58803	flavin adenine dinucleotide binding	3
GO:0050790	0.007999	0.170255	regulation of catalytic activity	1
GO:0051213	0.0002	0.008103	dioxygenase activity	6
GO:0051607	0.0012	0.037292	defense response to virus	1
GO:0055085	0.008599	0.178172	transmembrane transport	28
GO:0071555	1.00E-04	0.004883	cell wall organization	1
GO:0140359	1.00E-04	0.004883	ABC-type transporter activity	4

Appendix H - Differentially expressed and significantly down-enriched gene ontology (GO) term associated gene numbers represented between ascorbic acid pre-treated MP-inoculated treatment with the non-pre-treated MP-inoculated treatment in susceptible genotype (Pharaoh).

GO	*p*-value	*q*-value	Term	Gene No.
GO:0000079	1.00E-04	0.004447	protein serine/threonine kinase activity	38
GO:0000082	0.019198	0.324116	G1/S transition of mitotic cell cycle	5
GO:0000166	1.00E-04	0.004447	nucleotide binding	552
GO:0000226	0.006299	0.141801	microtubule cytoskeleton organization	22
GO:0000254	0.009999	0.208758	C-4 methylsterol oxidase activity	5
GO:0000272	0.0023	0.061365	polysaccharide catabolic process	17
GO:0000278	1.00E-04	0.004447	mitotic cell cycle	53
GO:0000280	0.019698	0.324902	nuclear division	2
GO:0000307	1.00E-04	0.004447	cyclin-dependent protein kinase holoenzyme complex	45
GO:0000347	1.00E-04	0.004447	THO complex	11
GO:0000727	1.00E-04	0.004447	double-strand break repair via break-induced replication	14
GO:0000776	0.031497	0.448666	kinetochore	9
GO:0000779	0.0022	0.059568	condensed chromosome, centromeric region	4
GO:0000786	1.00E-04	0.004447	nucleosome	57
GO:0000796	0.0004	0.014299	condensin complex	7
GO:0000819	0.021698	0.344779	sister chromatid segregation	5
GO:0000822	0.023698	0.367213	inositol hexakisphosphate binding	5
GO:0000914	0.019198	0.324116	phragmoplast assembly	2
GO:0000976	0.014399	0.275372	transcription cis-regulatory region binding	49
GO:0000981	0.0003	0.011162	DNA-binding transcription factor activity	78
GO:0001676	0.043996	0.5785	long-chain fatty acid metabolic process	7
GO:0002229	0.021998	0.344779	defense response to oomycetes	13
GO:0003677	1.00E-04	0.004447	DNA binding	487
GO:0003678	0.027697	0.407268	DNA helicase activity	12
GO:0003688	0.014499	0.275372	DNA replication origin binding	7
GO:0003700	1.00E-04	0.004447	DNA-binding transcription factor activity	327
GO:0003774	1.00E-04	0.004447	cytoskeletal motor activity	65
GO:0003777	1.00E-04	0.004447	microtubule motor activity	62
GO:0003886	0.0005	0.016777	DNA (cytosine-5-)-methyltransferase activity	5
GO:0004028	0.0002	0.008043	3-chloroallyl aldehyde dehydrogenase activity	7
GO:0004029	0.0009	0.028454	aldehyde dehydrogenase (NAD+) activity	13

GO:0004084	0.039996	0.544224	branched-chain-amino-acid transaminase activity	4
GO:0004097	0.0002	0.008043	catechol oxidase activity	9
GO:0004170	0.018898	0.324116	dUTP diphosphatase activity	2
GO:0004180	0.0005	0.016777	carboxypeptidase activity	19
GO:0004185	0.0005	0.016777	serine-type carboxypeptidase activity	20
GO:0004351	0.0011	0.033424	glutamate decarboxylase activity	6
GO:0004367	0.024798	0.376785	glycerol-3-phosphate dehydrogenase [NAD+] activity	5
GO:0004467	0.017198	0.308441	long-chain fatty acid-CoA ligase activity	7
GO:0004497	1.00E-04	0.004447	monooxygenase activity	84
GO:0004553	1.00E-04	0.004447	hydrolase activity, hydrolyzing O-glycosyl compounds	114
GO:0004564	1.00E-04	0.004447	beta-fructofuranosidase activity	9
GO:0004565	0.0008	0.025588	beta-galactosidase activity	13
GO:0004568	1.00E-04	0.004447	chitinase activity	15
GO:0004575	1.00E-04	0.004447	sucrose alpha-glucosidase activity	9
GO:0004601	0.0005	0.016777	peroxidase activity	40
GO:0004611	0.0002	0.008043	phosphoenolpyruvate carboxykinase activity	5
GO:0004612	0.0002	0.008043	phosphoenolpyruvate carboxykinase (ATP) activity	5
GO:0004620	0.0003	0.011162	phospholipase activity	12
GO:0004657	0.019898	0.324902	proline dehydrogenase activity	3
GO:0004672	1.00E-04	0.004447	protein kinase activity	441
GO:0004674	1.00E-04	0.004447	protein serine/threonine kinase activity	257
GO:0004675	0.0009	0.028454	receptor protein serine/threonine kinase activity	58
GO:0004748	0.0028	0.0709	ribonucleoside-diphosphate reductase activity	3
GO:0004866	1.00E-04	0.004447	endopeptidase inhibitor activity	15
GO:0005094	0.011199	0.221148	Rho GDP-dissociation inhibitor activity	5
GO:0005179	1.00E-04	0.004447	hormone activity	8
GO:0005200	0.0024	0.062807	structural constituent of cytoskeleton	15
GO:0005313	0.037696	0.523346	L-glutamate transmembrane transporter activity	4
GO:0005366	0.028797	0.418937	myo-inositol:proton symporter activity	4
GO:0005506	1.00E-04	0.004447	iron ion binding	95
GO:0005507	1.00E-04	0.004447	copper ion binding	40
GO:0005524	1.00E-04	0.004447	ATP binding	679
GO:0005576	1.00E-04	0.004447	extracellular region	227
GO:0005618	1.00E-04	0.004447	cell wall	67
GO:0005634	0.0017	0.049458	nucleus	998
GO:0005658	0.016998	0.305858	alpha DNA polymerase:primase complex	4
GO:0005694	1.00E-04	0.004447	chromosome	56

GO:0005773	1.00E-04	0.004447	vacuole	49
GO:0005775	0.0002	0.008043	vacuolar lumen	5
GO:0005819	0.0006	0.019889	spindle	16
GO:0005856	0.0004	0.014299	cytoskeleton	44
GO:0005871	1.00E-04	0.004447	kinesin complex	53
GO:0005874	1.00E-04	0.004447	microtubule	103
GO:0005875	0.036796	0.517419	microtubule associated complex	3
GO:0005880	1.00E-04	0.004447	nuclear microtubule	13
GO:0005881	0.0048	0.110308	cytoplasmic microtubule	6
GO:0005886	1.00E-04	0.004447	plasma membrane	542
GO:0005971	0.0028	0.0709	ribonucleoside-diphosphate reductase complex	3
GO:0005975	1.00E-04	0.004447	carbohydrate metabolic process	166
GO:0005987	0.027397	0.403943	sucrose catabolic process	4
GO:0005992	0.0026	0.066763	trehalose biosynthetic process	11
GO:0006032	0.0003	0.011162	chitin catabolic process	10
GO:0006072	0.035696	0.504546	glycerol-3-phosphate metabolic process	5
GO:0006073	0.040296	0.544244	cellular glucan metabolic process	12
GO:0006081	0.0002	0.008043	cellular aldehyde metabolic process	7
GO:0006253	0.021998	0.344779	dCTP catabolic process	3
GO:0006260	0.0003	0.011162	DNA replication	35
GO:0006268	0.0031	0.076721	DNA unwinding involved in DNA replication	10
GO:0006270	1.00E-04	0.004447	DNA replication initiation	18
GO:0006271	0.0011	0.033424	DNA strand elongation involved in DNA replication	6
GO:0006334	1.00E-04	0.004447	nucleosome assembly	46
GO:0006351	1.00E-04	0.004447	transcription, DNA-templated	145
GO:0006355	1.00E-04	0.004447	regulation of transcription, DNA-templated	486
GO:0006468	1.00E-04	0.004447	protein phosphorylation	471
GO:0006536	0.0014	0.041843	glutamate metabolic process	7
GO:0006538	0.0008	0.025588	glutamate catabolic process	8
GO:0006560	0.019898	0.324902	proline metabolic process	3
GO:0006562	0.019898	0.324902	proline catabolic process	3
GO:0006629	1.00E-04	0.004447	lipid metabolic process	99
GO:0006631	1.00E-04	0.004447	fatty acid metabolic process	40
GO:0006633	1.00E-04	0.004447	fatty acid biosynthetic process	58
GO:0006817	0.031997	0.454604	phosphate ion transport	7
GO:0006855	0.0037	0.089544	xenobiotic transmembrane transport	17
GO:0006865	0.014599	0.276311	amino acid transport	27

GO:0006869	0.009399	0.200831	lipid transport	20
GO:0006950	0.038196	0.528945	response to stress	17
GO:0006979	0.0027	0.069007	response to oxidative stress	40
GO:0007017	1.00E-04	0.004447	microtubule-based process	21
GO:0007018	1.00E-04	0.004447	microtubule-based movement	62
GO:0007019	0.026397	0.39131	microtubule depolymerization	4
GO:0007049	1.00E-04	0.004447	cell cycle	68
GO:0007052	0.0015	0.044347	mitotic spindle organization	9
GO:0007076	1.00E-04	0.004447	mitotic chromosome condensation	9
GO:0007088	1.00E-04	0.004447	regulation of mitotic nuclear division	30
GO:0007094	0.0004	0.014299	mitotic spindle assembly checkpoint signaling	10
GO:0007142	0.0019	0.052221	male meiosis II	7
GO:0007178	0.014699	0.277245	receptor protein serine/threonine kinase signaling pathway	15
GO:0007266	0.012299	0.23941	Rho protein signal transduction	9
GO:0008017	1.00E-04	0.004447	microtubule binding	100
GO:0008061	0.0003	0.011162	chitin binding	10
GO:0008152	1.00E-04	0.004447	metabolic process	146
GO:0008171	0.0018	0.050487	O-methyltransferase activity	15
GO:0008194	0.023698	0.367213	UDP-glycosyltransferase activity	39
GO:0008271	0.010099	0.209248	sulfate transmembrane transporter activity	9
GO:0008272	0.010899	0.216004	sulfate transport	10
GO:0008283	0.015398	0.287473	cell population proliferation	7
GO:0008284	1.00E-04	0.004447	positive regulation of cell population proliferation	30
GO:0008289	1.00E-04	0.004447	lipid binding	51
GO:0008356	0.010699	0.214371	asymmetric cell division	6
GO:0008422	0.0008	0.025588	beta-glucosidase activity	20
GO:0008574	1.00E-04	0.004447	plus-end-directed microtubule motor activity	19
GO:0008725	0.0012	0.036262	DNA-3-methyladenine glycosylase activity	8
GO:0008810	0.012599	0.243516	cellulase activity	9
GO:0008970	0.0019	0.052221	phospholipase A1 activity	6
GO:0009044	0.0018	0.050487	xylan 1,4-beta-xylosidase activity	7
GO:0009055	0.031497	0.448666	electron transfer activity	42
GO:0009081	0.0042	0.099016	branched-chain amino acid metabolic process	4
GO:0009263	0.008499	0.185961	deoxyribonucleotide biosynthetic process	4
GO:0009331	0.024798	0.376785	glycerol-3-phosphate dehydrogenase complex	5
GO:0009360	0.016098	0.297494	DNA polymerase III complex	4
GO:0009414	0.0002	0.008043	response to water deprivation	14

GO:0009505	1.00E-04	0.004447	plant-type cell wall	38
GO:0009506	1.00E-04	0.004447	plasmodesma	134
GO:0009574	0.017898	0.31279	preprophase band	2
GO:0009607	0.048395	0.631794	response to biotic stimulus	11
GO:0009610	0.038696	0.531829	response to symbiotic fungus	11
GO:0009611	0.0025	0.064498	response to wounding	14
GO:0009639	0.049195	0.631969	response to red or far red light	7
GO:0009651	0.025897	0.389173	response to salt stress	21
GO:0009652	0.0018	0.050487	thigmotropism	4
GO:0009662	0.019898	0.324902	etioplast organization	2
GO:0009664	1.00E-04	0.004447	plant-type cell wall organization	24
GO:0009668	0.0023	0.061365	plastid membrane organization	3
GO:0009725	0.009899	0.20826	response to hormone	17
GO:0009734	0.008699	0.188826	auxin-activated signaling pathway	77
GO:0009753	0.0048	0.110308	response to jasmonic acid	5
GO:0009755	0.0005	0.016777	hormone-mediated signaling pathway	16
GO:0009832	0.005899	0.13502	plant-type cell wall biogenesis	9
GO:0009833	1.00E-04	0.004447	plant-type primary cell wall biogenesis	21
GO:0009834	1.00E-04	0.004447	plant-type secondary cell wall biogenesis	38
GO:0009873	0.0032	0.078485	ethylene-activated signaling pathway	23
GO:0009944	0.0024	0.062807	polarity specification of adaxial/abaxial axis	5
GO:0009956	0.0024	0.062807	radial pattern formation	5
GO:0009965	0.036396	0.513114	leaf morphogenesis	4
GO:0010023	0.0031	0.076721	proanthocyanidin biosynthetic process	3
GO:0010025	0.0004	0.014299	wax biosynthetic process	7
GO:0010037	0.018198	0.317019	response to carbon dioxide	4
GO:0010052	0.001	0.030727	guard cell differentiation	10
GO:0010119	0.0004	0.014299	regulation of stomatal movement	11
GO:0010133	0.016898	0.305858	proline catabolic process to glutamate	4
GO:0010143	1.00E-04	0.004447	cutin biosynthetic process	17
GO:0010154	0.0023	0.061365	fruit development	4
GO:0010158	1.00E-04	0.004447	abaxial cell fate specification	12
GO:0010183	0.049995	0.633039	pollen tube guidance	2
GO:0010197	0.022398	0.350045	polar nucleus fusion	3
GO:0010200	0.048195	0.630688	response to chitin	9
GO:0010215	0.001	0.030727	cellulose microfibril organization	8
GO:0010216	1.00E-04	0.004447	maintenance of DNA methylation	7

GO:0010330	0.041796	0.553551	cellulose synthase complex	3
GO:0010333	0.0017	0.049458	terpene synthase activity	8
GO:0010345	0.026297	0.390888	suberin biosynthetic process	4
GO:0010374	0.001	0.030727	stomatal complex development	10
GO:0010389	0.019198	0.324116	regulation of G2/M transition of mitotic cell cycle	5
GO:0010411	0.013899	0.266756	xyloglucan metabolic process	17
GO:0010424	0.0004	0.014299	DNA methylation on cytosine within a CG sequence	4
GO:0010493	0.021198	0.339042	Lewis a epitope biosynthetic process	2
GO:0010951	1.00E-04	0.004447	negative regulation of endopeptidase activity	21
GO:0010997	0.024798	0.376785	anaphase-promoting complex binding	5
GO:0015114	0.015598	0.290216	phosphate ion transmembrane transporter activity	5
GO:0015116	0.010899	0.216004	sulfate transmembrane transporter activity	10
GO:0015137	0.019698	0.324902	citrate transmembrane transporter activity	2
GO:0015189	0.037696	0.523346	L-lysine transmembrane transporter activity	4
GO:0015248	0.031497	0.448666	sterol transporter activity	7
GO:0015293	0.019498	0.324902	symporter activity	27
GO:0015301	0.010099	0.209248	anion:anion antiporter activity	9
GO:0015333	0.011899	0.232452	peptide:proton symporter activity	16
GO:0015746	0.019698	0.324902	citrate transport	2
GO:0015798	0.028797	0.418937	myo-inositol transport	4
GO:0015813	0.037696	0.523346	L-glutamate transmembrane transport	4
GO:0015976	0.042596	0.561443	carbon utilization	4
GO:0015996	0.039296	0.536034	chlorophyll catabolic process	4
GO:0016020	0.0014	0.041843	membrane	1480
GO:0016021	0.0025	0.064498	integral component of membrane	1329
GO:0016094	0.037096	0.520299	polyprenol biosynthetic process	3
GO:0016102	0.007699	0.169818	diterpenoid biosynthetic process	7
GO:0016126	0.019198	0.324116	sterol biosynthetic process	13
GO:0016174	0.0048	0.110308	NAD(P)H oxidase H2O2-forming activity	7
GO:0016298	1.00E-04	0.004447	lipase activity	24
GO:0016301	1.00E-04	0.004447	kinase activity	321
GO:0016310	1.00E-04	0.004447	phosphorylation	324
GO:0016413	0.011299	0.222319	O-acetyltransferase activity	22
GO:0016491	1.00E-04	0.004447	oxidoreductase activity	415
GO:0016538	1.00E-04	0.004447	protein serine/threonine kinase regulator activity	35
GO:0016584	0.040096	0.544231	nucleosome positioning	7
GO:0016614	0.017498	0.308533	oxidoreductase activity, acting on CH-OH group of donors	9

GO:0016616	0.025397	0.382711	oxidoreductase activity, acting on CH-OH group of donors	35
GO:0016620	0.031197	0.447892	oxidoreductase activity	18
GO:0016702	0.0002	0.008043	oxidoreductase activity, acting on single donors	23
GO:0016705	1.00E-04	0.004447	oxidoreductase activity, acting on paired donors	81
GO:0016709	1.00E-04	0.004447	oxidoreductase activity, acting on paired donors	56
GO:0016717	0.0003	0.011162	oxidoreductase activity, acting on paired donors	10
GO:0016722	1.00E-04	0.004447	oxidoreductase activity, acting on metal ions	31
GO:0016740	1.00E-04	0.004447	transferase activity	603
GO:0016746	1.00E-04	0.004447	acyltransferase activity	68
GO:0016747	1.00E-04	0.004447	acyltransferase activity	65
GO:0016759	0.0002	0.008043	cellulose synthase activity	17
GO:0016760	1.00E-04	0.004447	cellulose synthase (UDP-forming) activity	21
GO:0016762	0.040296	0.544244	xyloglucan:xyloglucosyl transferase activity	12
GO:0016788	1.00E-04	0.004447	hydrolase activity, acting on ester bonds	70
GO:0016798	1.00E-04	0.004447	hydrolase activity, acting on glycosyl bonds	135
GO:0016829	0.020398	0.331089	lyase activity	56
GO:0016830	0.014499	0.275372	carbon-carbon lyase activity	8
GO:0016998	1.00E-04	0.004447	cell wall macromolecule catabolic process	9
GO:0017076	1.00E-04	0.004447	purine nucleotide binding	6
GO:0017077	0.040696	0.546945	oxidative phosphorylation uncoupler activity	3
GO:0017116	1.00E-04	0.004447	single-stranded DNA helicase activity	12
GO:0018812	0.049795	0.631969	3-hydroxyacyl-CoA dehydratase activity	2
GO:0019199	0.0016	0.047049	transmembrane receptor protein kinase activity	6
GO:0019237	0.017398	0.308533	centromeric DNA binding	2
GO:0019310	0.0029	0.072759	inositol catabolic process	4
GO:0019438	0.0003	0.011162	aromatic compound biosynthetic process	13
GO:0019762	1.00E-04	0.004447	glucosinolate catabolic process	12
GO:0019901	1.00E-04	0.004447	protein kinase binding	40
GO:0020037	1.00E-04	0.004447	heme binding	118
GO:0022857	0.0005	0.016777	transmembrane transporter activity	109
GO:0030001	0.020598	0.332362	metal ion transport	33
GO:0030154	1.00E-04	0.004447	cell differentiation	66
GO:0030198	0.029397	0.424279	extracellular matrix organization	6
GO:0030244	1.00E-04	0.004447	cellulose biosynthetic process	21
GO:0030245	0.012599	0.243516	cellulose catabolic process	9
GO:0030246	0.0035	0.08508	carbohydrate binding	39
GO:0030247	0.0025	0.064498	polysaccharide binding	21

GO:0030261	0.0005	0.016777	chromosome condensation	13
GO:0030295	0.0015	0.044347	protein kinase activator activity	9
GO:0030332	0.028497	0.417907	cyclin binding	5
GO:0030337	0.017598	0.308533	DNA polymerase processivity factor activity	2
GO:0030570	0.006599	0.146741	pectate lyase activity	8
GO:0030574	0.029397	0.424279	collagen catabolic process	6
GO:0030599	0.003	0.074924	pectinesterase activity	17
GO:0031012	0.029397	0.424279	extracellular matrix	6
GO:0031222	0.0018	0.050487	arabinan catabolic process	7
GO:0031225	1.00E-04	0.004447	anchored component of membrane	23
GO:0031408	1.00E-04	0.004447	oxylipin biosynthetic process	20
GO:0031492	1.00E-04	0.004447	nucleosomal DNA binding	19
GO:0031616	0.019098	0.324116	spindle pole centrosome	2
GO:0031625	0.024498	0.376409	ubiquitin protein ligase binding	26
GO:0032051	0.016898	0.305858	clathrin light chain binding	4
GO:0032147	0.047095	0.617773	activation of protein kinase activity	18
GO:0032502	1.00E-04	0.004447	developmental process	33
GO:0033612	0.0005	0.016777	receptor serine/threonine kinase binding	9
GO:0033926	0.027397	0.403943	glycopeptide alpha-N-acetylgalactosaminidase activity	4
GO:0034090	0.009699	0.204841	maintenance of meiotic sister chromatid cohesion	3
GO:0034440	1.00E-04	0.004447	lipid oxidation	19
GO:0035336	0.026297	0.390888	long-chain fatty-acyl-CoA metabolic process	4
GO:0035371	0.010199	0.209731	microtubule plus-end	4
GO:0035372	0.0018	0.050487	protein localization to microtubule	4
GO:0035435	0.025397	0.382711	phosphate ion transmembrane transport	8
GO:0035673	0.0032	0.078485	oligopeptide transmembrane transporter activity	22
GO:0036033	0.016598	0.3057	mediator complex binding	2
GO:0038023	0.041496	0.553551	signaling receptor activity	16
GO:0042262	0.021998	0.344779	DNA protection	3
GO:0042343	0.024698	0.376785	indole glucosinolate metabolic process	8
GO:0042545	0.001	0.030727	cell wall modification	17
GO:0042555	1.00E-04	0.004447	MCM complex	12
GO:0042626	0.0002	0.008043	ATPase-coupled transmembrane transporter activity	41
GO:0042742	0.0003	0.011162	defense response to bacterium	29
GO:0042744	0.0045	0.105182	hydrogen peroxide catabolic process	31
GO:0042910	0.010599	0.213148	xenobiotic transmembrane transporter activity	20
GO:0042973	1.00E-04	0.004447	glucan endo-1,3-beta-D-glucosidase activity	28

GO:0043565	1.00E-04	0.004447	sequence-specific DNA binding	251
GO:0043626	0.017598	0.308533	PCNA complex	2
GO:0044547	0.049695	0.631969	DNA topoisomerase binding	2
GO:0044772	1.00E-04	0.004447	mitotic cell cycle phase transition	34
GO:0044774	0.017498	0.308533	mitotic DNA integrity checkpoint signaling	2
GO:0045017	0.038796	0.531867	glycerolipid biosynthetic process	4
GO:0045087	1.00E-04	0.004447	innate immune response	11
GO:0045132	0.041696	0.553551	meiotic chromosome segregation	4
GO:0045144	0.009699	0.204841	meiotic sister chromatid segregation	3
GO:0045165	1.00E-04	0.004447	cell fate commitment	11
GO:0045330	0.001	0.030727	aspartyl esterase activity	17
GO:0045431	0.019398	0.324902	flavonol synthase activity	2
GO:0045486	0.018498	0.321222	naringenin 3-dioxygenase activity	2
GO:0045490	1.00E-04	0.004447	pectin catabolic process	26
GO:0045491	0.004	0.095955	xylan metabolic process	7
GO:0045492	1.00E-04	0.004447	xylan biosynthetic process	14
GO:0045493	0.0018	0.050487	xylan catabolic process	7
GO:0045547	0.022898	0.356839	dehydrodolichyl diphosphate synthase activity	3
GO:0045735	0.008999	0.1938	nutrient reservoir activity	15
GO:0045787	1.00E-04	0.004447	positive regulation of cell cycle	30
GO:0045893	0.013799	0.265769	positive regulation of transcription, DNA-templated	47
GO:0045910	0.024198	0.3739	negative regulation of DNA recombination	8
GO:0045930	0.039196	0.536006	negative regulation of mitotic cell cycle	3
GO:0045962	0.007199	0.159433	positive regulation of development, heterochronic	4
GO:0046081	0.018898	0.324116	dUTP catabolic process	2
GO:0046148	0.0005	0.016777	pigment biosynthetic process	8
GO:0046168	0.016998	0.305858	glycerol-3-phosphate catabolic process	5
GO:0046274	1.00E-04	0.004447	lignin catabolic process	23
GO:0046556	0.0006	0.019889	alpha-L-arabinofuranosidase activity	9
GO:0046658	1.00E-04	0.004447	anchored component of plasma membrane	64
GO:0046686	0.048795	0.631969	response to cadmium ion	6
GO:0046777	1.00E-04	0.004447	protein autophosphorylation	85
GO:0046910	0.006599	0.146741	pectinesterase inhibitor activity	13
GO:0046982	1.00E-04	0.004447	protein heterodimerization activity	54
GO:0046983	1.00E-04	0.004447	protein dimerization activity	87
GO:0047196	0.025297	0.382711	long-chain-alcohol O-fatty-acyltransferase activity	4
GO:0047372	1.00E-04	0.004447	acylglycerol lipase activity	8

GO:0047746	0.038496	0.530413	chlorophyllase activity	3
GO:0047840	0.021998	0.344779	dCTP diphosphatase activity	3
GO:0047952	0.016898	0.305858	glycerol-3-phosphate dehydrogenase [NAD(P)+] activity	4
GO:0048046	1.00E-04	0.004447	apoplast	68
GO:0048364	0.014799	0.278171	root development	12
GO:0048448	0.019198	0.324116	stamen morphogenesis	2
GO:0048544	1.00E-04	0.004447	recognition of pollen	39
GO:0048653	0.019198	0.324116	anther development	2
GO:0048658	0.020798	0.334602	anther wall tapetum development	2
GO:0048731	0.020598	0.332362	system development	6
GO:0048831	0.0022	0.059568	regulation of shoot system development	5
GO:0050113	0.0029	0.072759	inositol oxygenase activity	4
GO:0050660	0.0008	0.025588	flavin adenine dinucleotide binding	42
GO:0050664	0.008299	0.182315	oxidoreductase activity, acting on NAD(P)H	7
GO:0050793	0.010299	0.210994	regulation of developmental process	3
GO:0051010	0.010199	0.209731	microtubule plus-end binding	4
GO:0051211	0.041796	0.553551	anisotropic cell growth	3
GO:0051213	1.00E-04	0.004447	dioxygenase activity	64
GO:0051225	0.035196	0.498769	spindle assembly	12
GO:0051233	0.0003	0.011162	spindle midzone	6
GO:0051295	0.016998	0.305858	establishment of meiotic spindle localization	2
GO:0051301	1.00E-04	0.004447	cell division	58
GO:0051307	0.0022	0.059568	meiotic chromosome separation	3
GO:0051453	0.041096	0.550967	regulation of intracellular pH	10
GO:0051455	0.017398	0.308533	monopolar spindle attachment to meiosis I kinetochore	2
GO:0051513	1.00E-04	0.004447	regulation of monopolar cell growth	9
GO:0051603	0.038296	0.52899	proteolysis involved in cellular protein catabolic process	26
GO:0051753	0.0003	0.011162	mannan synthase activity	14
GO:0051754	1.00E-04	0.004447	meiotic sister chromatid cohesion, centromeric	5
GO:0051777	0.021298	0.339648	ent-kaurenoate oxidase activity	2
GO:0051783	0.049095	0.631969	regulation of nuclear division	2
GO:0052324	0.006499	0.145703	plant-type cell wall cellulose biosynthetic process	6
GO:0052654	0.0042	0.099016	L-leucine transaminase activity	4
GO:0052655	0.0042	0.099016	L-valine transaminase activity	4
GO:0052656	0.0042	0.099016	L-isoleucine transaminase activity	4
GO:0052716	1.00E-04	0.004447	hydroquinone:oxygen oxidoreductase activity	23
GO:0055085	1.00E-04	0.004447	transmembrane transport	246

GO:0060236	0.0002	0.008043	regulation of mitotic spindle organization	9
GO:0060918	0.015298	0.286584	auxin transport	7
GO:0070413	0.0048	0.110308	trehalose metabolism in response to stress	7
GO:0071439	0.016898	0.305858	clathrin complex	4
GO:0071554	0.004	0.095955	cell wall organization or biogenesis	7
GO:0071555	1.00E-04	0.004447	cell wall organization	74
GO:0072587	0.049695	0.631969	DNA topoisomerase type II ctivator activity	2
GO:0072686	0.0002	0.008043	mitotic spindle	11
GO:0080019	0.026297	0.390888	fatty-acyl-CoA reductase (alcohol-forming) activity	4
GO:0080043	0.006299	0.141801	quercetin 3-O-glucosyltransferase activity	28
GO:0080044	0.006299	0.141801	quercetin 7-O-glucosyltransferase activity	28
GO:0090116	0.0005	0.016777	C-5 methylation of cytosine	5
GO:0090307	0.0033	0.080577	mitotic spindle assembly	9
GO:0090447	1.00E-04	0.004447	glycerol-3-phosphate 2-O-acyltransferase activity	11
GO:0097027	0.010499	0.211916	ubiquitin-protein transferase activator activity	5
GO:0097502	0.008699	0.188826	mannosylation	15
GO:0097573	0.028797	0.418937	glutathione oxidoreductase activity	17
GO:0098542	0.0019	0.052221	defense response to other organism	18
GO:0098656	0.016098	0.297494	anion transmembrane transport	16
GO:0098813	0.019698	0.324902	nuclear chromosome segregation	2
GO:0098869	0.0024	0.062807	cellular oxidant detoxification	45
GO:0099402	1.00E-04	0.004447	plant organ development	28
GO:0102158	0.049795	0.631969	very-long-chain 3-hydroxyacyl-CoA dehydratase activity	2
GO:0102293	0.009099	0.195184	pheophytinase b activity	3
GO:0102343	0.049795	0.631969	3-hydroxy-arachidoyl-CoA dehydratase activity	2
GO:0102344	0.049795	0.631969	3-hydroxy-behenoyl-CoA dehydratase activity	2
GO:0102345	0.049795	0.631969	3-hydroxy-lignoceroyl-CoA dehydratase activity	2
GO:0102756	1.00E-04	0.004447	very-long-chain 3-ketoacyl-CoA synthase activity	19
GO:0102965	0.026297	0.390888	alcohol-forming fatty acyl-CoA reductase activity	4
GO:0106310	1.00E-04	0.004447	protein serine kinase activity	61
GO:0120029	0.041896	0.553551	proton export across plasma membrane	6
GO:0140359	1.00E-04	0.004447	ABC-type transporter activity	46
GO:0140575	0.009999	0.208758	transmembrane monodehydroascorbate reductase activity	4
GO:1901371	1.00E-04	0.004447	regulation of leaf morphogenesis	8
GO:1901673	0.021798	0.344779	regulation of mitotic spindle assembly	2
GO:1902025	1.00E-04	0.004447	nitrate import	8
GO:1902183	0.0007	0.022926	regulation of shoot apical meristem development	4

GO:1902358	0.010899	0.216004	sulfate transmembrane transport	10
GO:1902975	0.0002	0.008043	mitotic DNA replication initiation	7
GO:1903401	0.037696	0.523346	L-lysine transmembrane transport	4
GO:1904667	0.049095	0.631969	negative regulation of ubiquitin protein ligase activity	2
GO:1904668	0.010499	0.211916	positive regulation of ubiquitin protein ligase activity	5
GO:1904680	0.011899	0.232452	peptide transmembrane transporter activity	16
GO:1904825	0.0018	0.050487	protein localization to microtubule plus-end	4
GO:1905775	0.019998	0.325563	negative regulation of DNA helicase activity	2
GO:1990542	0.040696	0.546945	mitochondrial transmembrane transport	3
GO:1990757	0.010499	0.211916	ubiquitin ligase activator activity	5
GO:1990961	0.006099	0.139015	xenobiotic detoxification by transmembrane export	18
GO:2000024	0.0019	0.052221	regulation of leaf development	4
GO:2000032	1.00E-04	0.004447	regulation of secondary shoot formation	11
GO:2000280	1.00E-04	0.004447	regulation of root development	10
GO:2001006	0.041796	0.553551	regulation of cellulose biosynthetic process	3